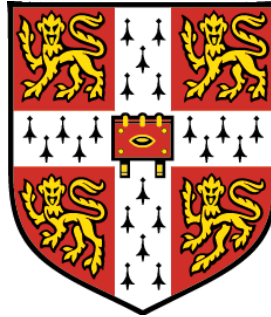


# Humoral alloimmunity in cardiac allograft rejection



**Jawaher Alsughayyir**

**Darwin College**

**Department of Surgery**

**University of Cambridge**

**This dissertation is submitted for the degree of Doctor of Philosophy July 2018**

## **Declaration**

This dissertation is the result of my own work and includes nothing which is the outcome of work done in collaboration except where declared in the text. It has not been submitted in whole or part for a degree at any university.

The length of this thesis does not exceed the 60,000 word limit

**Dissertation title: Humoral alloimmunity in cardiac allograft rejection**

**Student name: Jawaher Alsughayyir**

## Abstract

Although the short-term outcomes of solid allograft survival have improved substantially over the last few decades, there has been no significant improvement in long-term survival of solid allografts. This thesis presents the initial characterisation of alloantibody mediated rejection in a murine heart transplant model, with particular focus on the impact of the different phases of the humoral alloimmune response (follicular or germinal centre) on graft rejection. The key findings of this work are:

- 1) The precursor frequency of allospecific CD4 T cells determines the magnitude of the alloantibody response, with a relatively high frequency of CD4 T cells eliciting strong extrafollicular responses, while a high frequency of B cells promotes slowly-developing germinal centre responses.
- 2) Strong extrafollicular antibody response can mediate acute heart allograft rejection in the absence of CD8 T cells alloresponses.
- 3) Germinal centre humoral immunity mediates chronic antibody-mediated rejection.
- 4) Recipient memory, but not naïve, CD4 T cells that recognise one graft alloantigen can provide 'unlinked' help to allospecific B cells that recognise a different graft alloantigen for generating germinal centre alloantibody responses.

## ACKNOWLEDGEMENTS

To my dearest family, friends, and colleagues. Thank you for all of your support!

## CONTRIBUTIONS OF COLLABORATORS

The following section details individual collaborators and their role in this thesis.

- All surgical procedures were performed by Mr. Reza Motallebzadeh and Mr. Saeed Qureshi.
- Prof. Robert Brink (Garvan Institute of Medical Research, Australia) provided HEL<sup>3x</sup> recombinant protein, anti-HEL<sup>3x</sup> hyperimmune serum, and SW<sub>HEL</sub> mice.
- NIH tetramer core facility (Emory University, Atlanta, GA) for providing H2-K<sup>d</sup> tetramers.
- Thank you for Dr. Katherine Stott, Hannah Copley and Ashley Priddey for teaching me the principals of BLI and discussing my results.
- Breeding and genotyping of the mouse colonies were kindly performed by Mrs Jackie Higgins and Mrs Sylvia Rehakova.
- Special thanks to Mrs. Marg Negus for teaching me most of the laboratory techniques.
- Mrs. Faye Hills for her endless assistance and friendship during my time in the laboratory.

My sincere gratitude to my supervisor Mr. Gavin Pettigrew and to Mr. Reza Motallebzadeh for their continuous support and mentorship

# Abbreviations

2ME	2 - Mercaptoethanol
7-AAD	7 – Aminoactinomycin D
Ab	antibody
Ag	antigen
ADCC	antibody dependent cell-mediated cytotoxicity
AMR	antibody-mediated rejection
APC	antigen presenting cell
AUC	area under the curve
BCR	B cell receptor
BM	bone marrow
BLI	bio-layer interferometry
BSA	bovine serum albumin
CD	cluster of differentiation
CMV	cytomegalovirus
CSR	class-switch recombination
CTL	effector cytotoxic killer cells
DC	dendritic cell
ELISA	enzyme-linked immunosorbent assay
ELISPOT	enzyme-linked immunosorbent spot
EVG	elastin van Gieson
Fc	fragment crystallizable region of immunoglobulin
FCS	foetal calf serum
FITC	flourexcein isothiocyanate
GC	germinal centre
HEL	Hen egg lysozyme
HLA	human leukocyte antigen
ICOS	inducible T cell co-stimulator

IEL	internal elastic lamina
IFN $\gamma$	interferon gamma
Ig	immunoglobulin
Ip	intraperitoneal
Iv	intravenous
LLPC	long-lived plasma cell
MACS	magnetic-activated cell sorting
MHC	major Histocompatibility Complex
MST	mean survival time
MZ	marginal zone
NK	natural killer
PBS	phosphate buffered saline
PE	phycoerythrin
Rag	recombinase activating gene
Rpm	revolutions per minute
RPMI	Roswell Park memorial institute medium
SD	standard deviation
SEM	standard error of the mean
SHM	somatic hypermutation
SLO	secondary lymphoid organ
TCR	T cell receptor
TCR <sup>-/-</sup>	T cell receptor knock out
WT	wild type

# Table of contents

Abstract .....	ii
ACKNOWLEDGEMENTS.....	iii
CONTRIBUTIONS OF COLLABORATORS .....	iv
Abbreviations.....	v
Table of contents.....	vii
List of Figures.....	xii
List of Tables .....	xiv
Chapter 1 .....	1
1. Introduction.....	2
1.2 Allograft rejection Pathogenesis .....	2
1.2.1 The Major Histocompatibility Complex (MHC) .....	3
1.2.2 Allorecognition mechanisms by CD4 T cells.....	9
1.2.3 Cellular-mediated rejection.....	11
1.2.4 Antibody-mediated rejection .....	12
1.3 Mechanisms underlying AMR pathogenesis .....	13
1.3.1 Complement activation .....	14
1.3.2 Endothelial cell activation .....	14
1.3.3 Antibody-dependent cell mediated cytotoxicity (ADCC) .....	15
1.4 Histopathological and Immunopathological features of chronic AMR.....	16
1.4.1 Histopathological features of chronic AMR .....	16
1.4.2 Immunopathological features of AMR .....	17
1.5 AMR management and therapy .....	20
1.6 Structure and function of secondary lymphoid organs.....	20
1.6.1 Lymph node structure .....	21

1.6.2 Splenic structure .....	22
1.7 Mechanisms of antibody formation .....	24
1.7.1 B cell activation and priming .....	24
1.7.2 Extrafollicular humoral response .....	27
1.7.3 Germinal centre humoral response .....	27
1.7.4 Allogenic B cell activation by unlinked CD4 T cell help .....	33
1.7.5 T-dependent responses and allograft rejection .....	33
1.7.6 The potential of alloantibody affinity on allograft damage .....	35
1.8 Project objectives .....	36
Chapter 2 .....	37
2. Materials and methods.....	37
2.1 Animals .....	37
2.2 Animal related techniques .....	40
2.2.1 Skin and heterotopic heart transplantation.....	40
2.2.1.1 Skin transplantation .....	40
2.2.1.2 Heterotopic heart transplantation .....	40
2.2.2 Adoptive cell transfer and immunisation.....	41
2.2.2.1 Adoptive cell transfer .....	41
2.2.2.2 Immunisation.....	41
2.2.2.3 Conjugation of HEL to sheep RBCs .....	41
2.2.3 Collection of blood samples and sera preparation .....	41
2.2.4 Organs harvest and storage .....	42
2.2.5 Generation of bone-marrow chimera .....	42
2.3 Tissue and cell related techniques .....	44
2.3.1 Single cell suspensions from spleens and bone marrow.....	44
2.3.2 Single cell suspension from the heart .....	44
2.3.3 Cell culture and maintenance.....	45

2.4 In vitro cellular assays.....	45
2.4.1 Endothelial cell migration.....	45
2.4.2 Western blot.....	46
2.5 General Flow cytometry protocol .....	46
2.5.1 Magnetic-activated cell sorting (MACS).....	47
2.5.2 Trucount™ analysis for cell quantification.....	47
2.6 Assay of humoral alloimmunity .....	51
2.6.1 Enzyme Linked Immunosorbent Assay (ELISA).....	51
2.6.2 B cell ELISPOT.....	54
2.7 Bio-layer interferometry for affinity measurement:.....	55
2.7.1 Principle overview: .....	55
2.7.2 MHC-I and HEL proteins biotinylation, purification, and validation .....	57
2.7.3 BLI protocol.....	57
2.7.4 Processing kinetics data .....	57
2.8 Histology.....	60
2.8.1 Evaluation of allograft vasculopathy and parenchymal damage .....	60
2.8.2 Immunohistochemistry and immunofluorescence .....	61
2.9 Statistical analysis.....	63
Chapter 3: Development and characterisation of murine AMR model* .....	64
3.1 Introduction:.....	65
3.1.1 The number of precursor alloantigen-specific CD4 T cells correlate with rejection kinetics.....	65
3.1.2 How antibody production pathway is relevant to clinical transplantation?.....	67
3.1.3 Current murine AMR heart transplant models and their limitations .....	68
3.1.4 Designing a murine model of chronic humoral heart graft rejection .....	71
3.2 Aims .....	72
3.3 Results.....	73

3.3.1 Rejection kinetics.....	73
3.3.2 Histology of explanted allografts.....	75
3.3.3 Humoral response characterisation .....	80
3.3.4 Investigating the significance of GC development in mediating AMR.....	84
3.4 Discussion: .....	94
Chapter 4: Initial precursor frequency of antigen-specific CD4 T cells and T-dependent antibody responses .....	98
4.1. Introduction:.....	98
4.1.1 Transgenic B and CD4 T cells .....	98
4.2 Aim.....	100
4.3 Results.....	101
4.3.1 Development of adaptive transfer model .....	101
4.3.2 The size of the extrafollicular and GC response is highly influenced by the precursor frequency of helper T cells and antigen specific B cells, respectively .....	102
4.4 Discussion .....	106
Chapter 5: Role of antibody affinity maturation in allograft vasculopathy progression .....	107
5.1 Introduction.....	107
5.1.1 Relevance of alloantibody affinity to AMR pathogenesis .....	107
5.1.2. The Ig knock-in mouse strain SW <sub>HEL</sub> .....	108
5.1.3 HEL <sup>WT</sup> and HEL <sup>3x</sup> proteins as membrane-bound alloantigens.....	108
5.1.4 TCR-transgenic strain 'TCR7' as a source for CD4 T cells .....	109
5.2 Aims .....	111
5.3 Results.....	112
5.3.1 The SW <sub>HEL</sub> heart transplant model .....	112
5.3.2 Rejection kinetics.....	114
5.3.3 Histology of explanted allografts.....	114
5.3.4 Humoral response characterisation .....	117

5.3.5 Affinity maturation assessment in a competitive HEL-specific B cells environment .....	125
5.4 Discussion .....	134
Chapter 6: Characterising the humoral alloresponse mediated by ‘un-linked’ helper CD4 T cells .....	139
6.1 Introduction .....	140
6.2 Aims .....	142
6.3 Results.....	143
6.3.1 Development of murine un-linked B cell activation model .....	143
6.3.2 Delivery of early memory (but not naïve) CD4 T cells with specificity for second graft alloantigen mediated rapid graft rejection and graft parenchymal damage .....	145
6.3.4 B cells activated via un-linked help by early memory TCR75 CD4 T cells elicit persistent humoral response .....	150
6.3.5 GCs establishment via unlinked-help provided from early memory but not naïve CD4 T cells.....	155
6.4 Discussion: .....	158
Chapter 7: Overall discussion and future plan .....	163
Recommendations and future plan.....	169
References .....	170

## List of Figures

Figure 1. MHC class I and II structures..	6
Figure 2. T cells recognize alloantigen by three different pathways.	10
Figure 3. Lymph node and spleen structures.	23
Figure 4. Schematic presentation of the T-dependent humoral response.	26
Figure 5. Early memory TCR75 CD4 T cells generation.	43
Figure 6. Calculation of relative antibody serum titres.	53
Figure 7. Schematic representation of BLI principle.	56
Figure 8. Schematic presentation of sample distribution in 96-well format.	59
Figure 9. Representative micrograph of heart vasculopathy stained with EVG.	60
Figure 10. Non-linear relationship between the number of transferred TCR75 CD4 T cells and survival of BL/6.K <sup>d</sup> heart allograft in BL/6 recipients.	66
Figure 11. Antigen specificity of TCR75 CD4 T cells.	Error! Bookmark not defined.
Figure 12. Rejection kinetics of donor heart grafts in AMR murine model.	74
Figure 13. Histopathological features of murine AMR model.	76
Figure 14. C4d and IgG immunofluorescent staining of allografts.	77
Figure 15. Vasculopathy development in heart allografts.	79
Figure 16. Characterization of the humoral response in murine AMR heart transplant model	83
Figure 17. AMR kinetics in the absence of GC formation.	86
Figure 18. GC response is essential in mediated chronic AMR in murine model.	87
Figure 19. GC-derived alloantibodies mediate endothelial activation.	90
Figure 20. Ranking anti-H2K <sup>d</sup> alloantibodies dissociation constants.	93
Figure 21. Schematic representation of the experimental model.	101
Figure 22. Anti-HEL effector response following the transfer of variable numbers of cognate T and B cells in CFA-HEL challenged animals.	104
Figure 23. Transfer of high numbers of CD4 T cells correlated with strong extrafollicular response.	105
Figure 24. HEL protein structure and expression.	110
Figure 25. Schematic study plan for heart transplantation model designed to investigate the development of affinity matured alloantibodies and their contribution to graft vascular disease and histopathological changes.	113

Figure 26. Graft survival and CAV development in $SW_{HEL}$ recipients of $mHEL^{WT}$ or $mHEL^{3x}$ heart grafts.....	115
Figure 27. Histology assessment of $mHEL^{WT}$ or $mHEL^{3x}$ heart grafts in $SW_{HEL}$ recipients. ...	116
Figure 28. GC activity in $SW_{HEL}$ recipients of $mHEL$ -expressing heart allografts.. ..	118
Figure 29. Antibody response analysis in $SW_{HEL}$ recipients of $mHEL$ -expressing allografts	120
Figure 30. HEL-specific IgG isotypes distribution in response to $mHEL^{WT}$ or $mHEL^{3x}$ allografts in $SW_{HEL}$ recipients. ....	122
Figure 31. Distribution of HEL-specific B cells in spleens of $SW_{HEL}$ recipients.. ..	124
Figure 32. Heart grafts survival and histopathological assessment in BL/6 recipients of $mHEL$ donors.. ..	128
Figure 33. Heart grafts assessment from $mHEL$ -expressing donors in BL/6 recipients. .	Error! Bookmark not defined.
Figure 34. GC and long-lived plasma cells assessment in BL/6 recipients of $mHEL$ -expressing grafts.....	130
Figure 35. Germinal center activation assessment.. ..	Error! Bookmark not defined.
Figure 36. Anti-HEL humoral response assessment by ELISA.....	133
Figure 37. HEL-specific IgG isotypes distribution in response to $mHEL^{WT}$ or $mHEL^{3x}$ allografts in BL/6 recipients.....	134
Figure 38. Simplified diagram of proposed un-linked recognition pathway in murine heart transplant model. ....	141
Figure 39. Schematic presentation of study plan of humoral response triggered by un-linked CD4 T cell help.....	144
Figure 40. Allograft rejection kinetics induced by un-linked CD4 T cell help signals. ....	146
Figure 41. Development of allograft vasculopathy in $Rag^{-/-}$ . $SW_{HEL}$ recipients reconstituted with naïve or memory TCR75 CD4 T cells. ....	147
Figure 42. Immunofluorescence staining of sections obtained from donor hearts stained for C4d and the lymphocyte CD4 T cells and B cells markers. ....	149
Figure 43. Humoral responses against $mHEL^{WT}.K^d$ and $mHEL^{3x}.K^d$ graft recipients reconstituted with naïve or early memory CD4 T cells. ....	153
Figure 44. Characterizing antibody specificity and off-rate of IgG sera obtained from $Rag2^{-/-}$ $SW_{HEL}$ recipients of $mHEL^{3x}.K^d$ or $mHEL^{WT}.K^d$ hearts.....	154
Figure 45. Naïve un-unlinked CD4 T cells help provide exclusive extrafollicular humoral response. ....	156

## List of Tables

<b>Table 1. AMR grading and nomenclature, adapted and modified from [112].</b> .....	19
<b>Table 2. Immunopathologic features of AMR, adapted and modified from [112].</b> .....	19
<b>Table 3. Key transcription factors and protein receptors involved in control of GC B cells versus plasma cell fate.</b> .....	32
<b>Table 4. Strains and MHC haplotypes of mice used in this study</b> .....	39
<b>Table 5. Antibodies used in this work</b> .....	49
<b>Table 6. Murine heart transplant models</b> .....	70

# Chapter 1

## Overview

Organ transplantation enhances the length and quality of life in patients with end-stage organ failure. Both the introduction of immunosuppressive therapy, and a better understanding of rejection pathology have improved short-term outcomes. However, chronic rejection remains a major obstacle to long-term graft survival. Chronic rejection is the process of slow decline in graft function over a period of months to years. In cardiac transplantation, chronic rejection is mostly associated with the development of chronic allograft vasculopathy (CAV), a concentric intimal and smooth muscle hyperplasia which ultimately leads to graft ischemia [1]. The incidence of CAV in heart transplantation is approximately 30% five years following-transplantation; increasing to 50% by ten years [2]. Once CAV develops, prognosis is poor and re-transplantation remains the only definitive therapy.

Graft rejection mediated by antibodies specific to the donor major histocompatibility complex (MHC) has only become recognized as a distinct form of rejection within the last decade, partly due to the availability of improved immunopathological and serological techniques [3]. 'Allospecific' plasma cells that secrete 'alloantibody' directed against donor MHC antigen can be generated from extrafollicular (EF) or germinal centre (GC) reactions. The relative contribution of these reactions to allograft rejection has not been addressed previously, and their relationship to the histopathological features described in clinical cardiac transplantation is not clear. Because defining the interplay between human immune cell networks and target antigen on donor organs can be a daunting task, murine cardiac transplantation models were employed to better examine fundamental aspects of humoral alloimmunity and to determine its contribution to acute and chronic rejection. My research had the following aims:

1. To examine the relative roles of extrafollicular-and germinal centre-humoral alloimmune responses in mediating antibody-mediated rejection (AMR).
2. To investigate the contribution of germinal centre, somatic hypermutation to the progression of chronic AMR.
3. To characterise the germinal center response generated by 'un-linked' memory CD4 T cells that recognize minor histocompatibility antigens.

# 1. Introduction

## 1.2 Allograft rejection Pathogenesis

The pathophysiology of graft rejection can be attributed to non-immune and immune factors. Non-immune factors include ischemic-reperfusion injury [1], cytomegalovirus infection [4], and age of the donor/recipient [5]. Although these factors can affect long-term graft survival, immune mechanisms are thought to be more relevant to the development of chronic rejection. Immune recognition was first identified as the mediator of allograft rejection more than 60 years ago by Sir Peter Medawar and colleagues [6], [7]. Their work introduced the concept that rejection occurs as a result of the antigenic disparity between donor and recipient (designated H-2 in mice), and that once a recipient rejected a graft of a particular H-2 type, a subsequent graft bearing the same donor H-2 molecule would be rejected more rapidly—so-called ‘second-set’ phenomenon. Classically, three types of rejection have been described based on time-course of their development: hyperacute, acute, and chronic. Hyperacute rejection develops within minutes to hours after transplantation, and occurs mainly in vascularised grafts [8]. It is caused by pre-sensitization of the recipient to donor tissue; typically after pregnancy or previous blood transfusion; and is mediated by binding of pre-existing alloantibodies to antigens on donor vascular endothelium [8]. The role of complement activation in mediating hyperacute graft rejection was first established from early study of xenotransplantation [9]. Widespread thrombosis and IgG deposition on graft vascular endothelium are frequent features in patients with hyperacute rejection [10].

Acute rejection develops from a few days to several months following transplantation and is a consequence of antigen-specific T cells and/or B cell alloreactivity [11]. In a 10-year follow up study performed on kidney transplant recipients, improvements in immunosuppressive treatments reduced the incidence of acute rejection from 51% to 13% [12]. Similar to acute rejection, chronic rejection is also considered to be mediated by B and T cell alloimmunity, but it develops over months to years (reviewed in [13]).

In the past decades, improvements in donor organ preservation and immunosuppressive regimes have resulted in longer survival times for transplanted organs. However, the development of AMR continues to impair long-term graft function and survival [14]. Early

allograft failure and the requirement for re-transplantation places further pressure on demand for organs, lengthening overall waiting times for transplantation.

This section will highlight the complex interplay between immune cells and endothelial cell proteins that are involved in mediating AMR pathogenesis.

## **1.2.1 The Major Histocompatibility Complex (MHC)**

### **1.2.1.1 MHC Structure**

The major histocompatibility complex molecules (known as human leukocyte antigen (HLA) in humans, and the H-2 antigen in mice) can be divided into three classes: Class I, II and III. Classes I and II are involved in antigen presentation and are central to allorecognition (detailed in section 1.2.2). Genes encoding Class III involve secretory proteins with immune functions such as the second and fourth components of the complement system (C2 and C4) which are synthesized in the liver [15].

In humans, HLA class I is encoded by three genes: HLA-A, B, and C. Similarly, HLA class II is encoded by three genes HLA-DR, DP, and DQ. All HLA class I and class II genes are located in chromosome six, while in mice MHC class I (H-2K, H-2D, and H-2L) and class II (I-A and I-E) are located in chromosome 17 [16]. The structure of both MHC class I and class II is comprised of two subunits that fold into immunoglobulin domains. The MHC class I molecule consists of a heavy polypeptide alpha chain ( $\alpha$ ) with a molecular weight of approximately 44 kDa. The extracellular region of the MHC class I molecule comprises three alpha domains:  $\alpha_1$ ,  $\alpha_2$ , and  $\alpha_3$  that are anchored to the cell membrane by a hydrophobic region, and terminate in the cytoplasm with a short hydrophilic C-terminus domain [17] (figure 1A). The  $\alpha$  chain is non-covalently linked to a  $\beta_2$ -microglobulin unit of approximately 12 kDa. This is a highly preserved structure and is encoded by a non-polymorphic gene located external to the MHC locus (at chromosome 15 in humans, and chromosome 2 in mice) [17].

MHC class II, on the other hand, lacks the  $\beta_2$ -microglobulin subunit and consists of two transmembrane glycoprotein chains  $\alpha$  (34 kDa) and  $\beta$  (29 kDa). These are non-covalently associated with one another. Each chain is composed of several domains, with the  $\alpha_1$  and  $\beta_1$  domains distal to the cell membrane. The  $\alpha_2$  and  $\beta_2$  domains are proximal, are tethered to

the cell membrane by a transmembrane domain, which then terminates intra-cellularly with a cytoplasmic domain [16], [17] (figure 1A).

Although MHC class I and class II share some structural homology (in particular at the membrane distal portion where peptide presentation and T cell recognition occur), there are some crucial differences. In the class I molecule both  $\alpha 1$  and  $\alpha 2$  domains are arranged in parallel to one another and are surrounded underneath by a  $\beta$ -pleated sheet to create a groove where a peptide can be loaded and held in position [18]. The peptide (typically 8-10 amino acid residues) is held in position due to the presence of conserved anchor residues in the peptide sequence (typically 2 residues), and the groove is closed at both ends. In the class II molecule, an open-ended groove is formed by the junction of  $\alpha 1$  and  $\beta 1$  domains allowing the accommodation of 10-13 amino acid residues, with peptide held into the MHC groove through the preferential binding to anchor residues at allele-specific pockets (typically 3 to 4 anchor residues) [18]. The amino acid sequence of the peptide other than the anchor residues may vary, resulting in one MHC molecule binding to a large number of peptides of variable sequences (figure 1B).

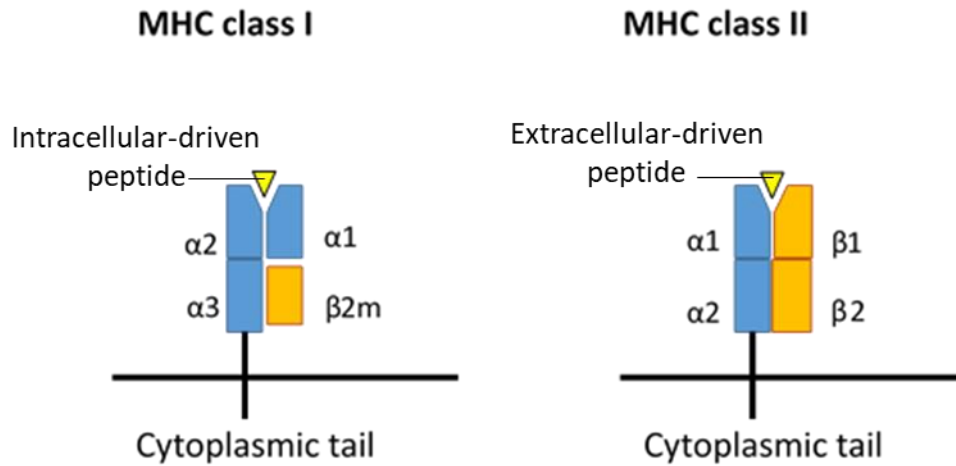
### **1.2.1.2 MHC Function**

MHC molecules are fundamental to the immune system, because their ability to bind and present peptide enables the immune system to distinguish between self and foreign proteins. MHC class I molecules mainly present peptides generated from intracellular proteins, such as self- or virus-derived peptides [19], and are typically restricted for presentation to CD8 T cells. If the presented peptide is of self-origin, it will generally be ignored by CD8 T cells. In contrast, if the presented peptide is of non-self origin, a naïve CD8 T cell will engage via its T-cell receptor (TCR) with the MHC-peptide complex. This binding is stabilised by the engagement of CD8 to a conserved region on the  $\alpha 3$  domain of the MHC class I. Naïve CD8 T cells are primed in draining lymphatic tissues upon encounter of APCs presenting the non-self peptide in the context of MHC class I [20]. Primed CD8 T cells then undergo proliferation and differentiation into effector cytotoxic killer cells (CTLs) and are recruited to the sites of inflammation to clear cells expressing the same non-self peptide presented on MHC class I molecule. The target cells are then killed by apoptosis as a consequence of the release of cytotoxic granular proteins such as perforins and granzymes

(detailed in section 1.2.3) [21], [22], [23]. Once the target cell has been eliminated, the majority of CD8 T cells die and cell residues are cleared by phagocytosis, while a fraction of cells will differentiate into memory CD8 T cells [24]. MHC class I molecules also contribute to the interaction with the innate arm of the immune system by acting as a ligand for the inhibitory killer cell immunoglobulin-like receptors (KIRs) expressed on natural killer cells (NK cells) to regulate their cytotoxicity through sophisticated mechanisms that have been extensively reviewed elsewhere [25], [26]. Briefly, the interaction between MHC class I on normal cells with KIR receptors prevent NK cell-mediated cytotoxicity. Cells that lose MHC class I expression (e.g., compromised due to viral infection or tumour) become prone to NK cell-mediated killing.

MHC class II molecules are expressed mainly on professional antigen presenting cells (APCs), such as dendritic cells, B cells, and macrophages. MHC class II can present non-immunogenic peptides that are derived from intracellular self-proteins [27], or peptides of extracellular origin to CD4 T helper cells [18]. The peptide-MHC class II complex is recognised by the TCR/CD3 complex on the CD4 T cell surface to provide the first activation signal (signal 1) [28]. In addition, CD4 binding to the  $\beta 2$  domain of MHC class II molecule augments the sensitivity of CD4 T cell to its ligand and initiates a number of intracellular kinases that results in priming of the CD4 T cell. This signal is followed by a co-stimulatory signal between CD28 on a T cell and either CD80 or CD86 that is expressed alongside the MHC class II complex on the APC (signal 2) [29]. Additional co-stimulatory molecules that are crucial for T cells activation include inducible T cell co-stimulator (ICOS), CD27, CD40 and OX40 which are upregulated on activated T cells, and likewise their ligands ICOSL, CD70, CD40L and OX40L respectively, which are expressed on the encountered APC [30]. Activated CD4 T cells proliferate and release IL-2, and also upregulate IL-2 receptor (IL-2R) expression; thus, IL-2 acts in an autocrine manner leading to potent clonal expansion on the same cell, and also on surrounding cells [31]. Activated CD4 T cells play a major role in shaping the adaptive immune response. Those responses particularly relevant to transplantation are described in section 1.2.2.

A)



B)

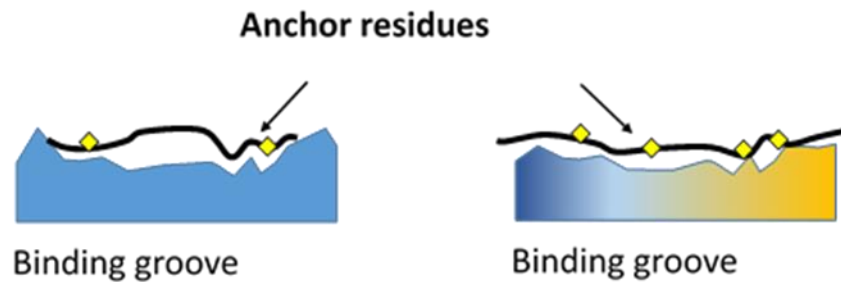


**Figure 1. MHC class I and II structures.** A) MHC class I molecules consist of an  $\alpha$  heavy chain made up of three polypeptide domains ( $\alpha 1$ ,  $\alpha 2$ ,  $\alpha 3$ ) and a noncovalently associated  $\beta 2$  microglobulin molecule. MHC class II are heterodimers consisting of  $\alpha$  chain and  $\beta$  chain. B) Anchor residues on presented peptide bind to complementary pockets within the MHC groove. Amino acid sequence and number between anchor peptides can vary.

### **1.2.1.3 Polymorphism**

MHC molecules contain highly polymorphic amino acid residues that line the peptide-binding groove. This polymorphism broadens the range of peptides that can be bound and presented by a single MHC molecule. However, as mentioned earlier, amino acid sequences of the presented peptide can vary for a single MHC molecule as long as the anchor residues (typically two amino acids) are compatible with the complementary pockets in the MHC groove [18]. It is also important to stress that the choice of peptide loading into the MHC molecule is not only dependent on peptide size and amino acid sequences, but also on other factors such as protease activity, chaperones availability, and peptide editors (or catalysts) that are specific for each MHC class (reviewed [18]).

The existence of over 200 alleles of some human MHC class I and class II genes, and the co-dominant expression nature of MHC genes (i.e., equal expression of two alleles at one locus in heterozygotes) both contribute to MHC diversity in the human population [32], [33]. All MHC loci possess allelic diversity (with the exception of DR $\alpha$  in humans and E $\alpha$  in mice of MHC class II) [34]. The  $\alpha$  chain of MHC class I is highly polymorphic, with HLA-B being the most polymorphic, followed by HLA-A and HLA-C [35]. Similarly, the  $\beta$  chain of the MHC class II antigen is highly polymorphic, whereas the  $\alpha$  chain displays limited polymorphism. In transplantation, polymorphism presents a major barrier to graft survival, because mismatched MHC molecules between donor and recipient are a critical target for lymphocyte activation. In particular, HLA-DR matching is beneficial for long-term graft survival and function [36]. The serological and DNA-based methods available today for MHC class I and class II typing enable extensive HLA mapping of prospective transplant donors and recipients, and thus help to minimize the overall antigenic disparity between recipient and donor tissues [37].

### **1.2.1.4 MHC class I-related genes**

Non-HLA antigens have also been associated with allograft pathology. These include MHC class I-related genes (MIC) and minor histocompatibility antigens (minor H antigens). MIC comprises of a group of genes encoding molecules that possess similar conformational structure to HLA class I and were first described in 1994 [38]. There are two MIC genes that

have been identified, namely MICA and MICB which are polymorphic but to a lesser extent than MHC class I genes. Both MICA and MICB function as ligands for NKG2D receptor on NK cells,  $\gamma\delta$  T cells, and CD8<sup>+</sup> T cells, leading to their activation to promote cytotoxicity, or cytokine production (reviewed [39], [40]). MICA and MICB molecules share sequence homology with HLA class I, in that both contain three  $\alpha$  domains that terminate with a short cytoplasmic domain. The  $\alpha$  chain does not, however, associate with a  $\beta$ 2 microglobulin molecule [41]. In addition, both MICA and MICB do not bind or present peptides for T cell recognition [41]. Unlike MHC class I, MIC molecules have a limited tissue distribution which include epithelial cells (especially that of the gastrointestinal tract) [42], endothelial cells, fibroblasts, dendritic cells [43], and on activated, but not resting lymphocytes, under certain conditions [44].

Humoral responses against MIC antigens have been associated with reduced graft survival and increased risk of acute and chronic rejection following kidney and heart transplantation [45], [46]. Zou et al. demonstrated that MICA can be a target of complement-dependent cytotoxicity [47]. In addition, a 10-year retrospective study performed by Mizutani et al. demonstrated that concurrent development of HLA and MICA antibodies in kidney recipients was correlated with more frequent rejection episodes, as compared to patients not developing either antibody [48]. Although a correlation exists, the definitive role of anti MIC antibodies and how they contribute to graft rejection is not clear. Anti-MICA antibodies have been reported following transplantation of solid organs and approximately 10% of patients on the waiting list for kidney transplantation are positive for MICA antibodies [49], [50].

Minor H antigens were first recognised clinically after a female patient who received a bone marrow transplant from an HLA-identical male sibling demonstrated a strong cytotoxic lymphocyte response that was specific to the male donor [51], [52]. Theoretically, any non-MHC genes that encode proteins that, after processing, load into MHC class I or class II molecules and induce CD4 and CD8 T cell responses, can be considered as minor histocompatibility antigens [53]. Both CD8 T cells [54], [55] and CD4 T cells [56] have been isolated from humans and rodents with specificity for minor antigens, and up to 54 minor H antigens have been identified [57]. While two cohort studies did not identify a role for responses against minor H antigens in kidney transplant rejection [58], [59], a retrospective study reported a correlation between H-Y mismatch and kidney graft outcome [60].

### 1.2.2 Allorecognition mechanisms by CD4 T cells

Allorecognition can be defined as the ability of immune cells to recognize incompatible antigens (mainly MHC class I or II) between genetically disparate individuals within the same species [61], [62]. MHC class I molecules are expressed on the surface of all nucleated cells, whereas expression of MHC class II is mainly limited to the surface of APCs. In humans, some non-immune cells (e.g., endothelial cells) can express MHC class II, depending on the stimuli that they have been exposed to: for example, following activation by interferon- $\gamma$  [63]. To date, three allorecognition pathways have been described: the direct, indirect, and semi-direct pathways (figure 2). In the direct pathway, recipient CD4 T cells recognize intact MHC molecules expressed on donor APCs [64]. Direct-pathway CD4 T cell allorecognition is thought to be short-lived, reflecting the rapid killing of MHC-class II expressing passenger donor APCs by the recipient [65], and hence is generally considered to mediate early acute rejection [66], [67].

Indirect allorecognition refers to the presentation of processed donor peptide alloantigen by self-MHC on the recipient's APCs. The indirect allorecognition pathway appears to be the principle mechanism mediating chronic rejection [64], [68], partly as a consequence of decay of direct allorecognition secondary to death of passenger donor APCs [65]. The semi-direct pathway has only been described recently [69], and involves the acquisition of intact allogeneic MHC-peptide complex from donor cells by recipient APCs and their presentation to recipient T cells. The clinical significance of this pathway to transplant rejection has not been established.

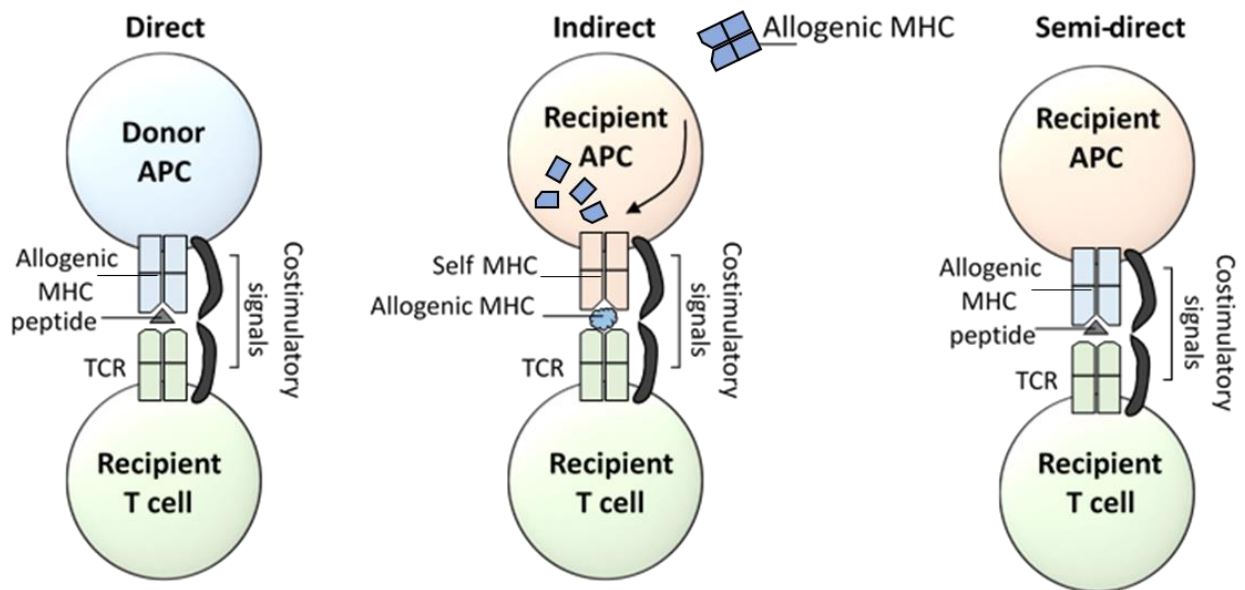


**Figure 2. T cells recognize alloantigen by three different pathways.** *Left:* In direct allorecognition, recipient T cells recognise donor MHC:peptide complex expressed on the surface of donor APC. *Middle:* In indirect allorecognition, recipient CD4 T cells recognise donor MHC after it has been processed and loaded as a linear peptide in the context of recipient MHC II on the surface of recipient APCs. *Right:* In semi-direct allorecognition, recipient T cells recognize intact donor MHC:peptide complex that was acquired and then re-presented as a whole, intact complex on the surface of recipient APCs.

### 1.2.3 Cellular-mediated rejection

Acute cellular rejection is characterised histologically by inflammatory infiltrates - comprising mainly T cells and macrophages - with accompanying myocyte damage [3]. Cytotoxic CD8 T cell responses that are directed against MHC class I alloantigens have long been considered the major effector mechanism in acute allograft rejection [70]. In 1975, Strom and colleagues isolated donor-specific CD8 T cells from rejecting human renal allografts [71]. Rosenberg et al, subsequently demonstrated that adoptive transfer of CD8 effector T cells was sufficient to induce skin rejection in MHC class-I mismatched murine model [72]. Naïve recipient CD8 T cells were generally considered to be activated by direct allorecognition of donor MHC class I antigen presented on donor passenger APCs [73]. However, Kreisel et al have proposed, based on *in vitro* observations, that MHC class I-expressing donor endothelial cells can also directly activate CD8 T cells [74]. After 1-3 days of CD8 T cell activation, effector CD8 CTLs migrate to the allograft where they identify target MHC class I alloantigen expressed on graft parenchymal cells via the direct pathway. Specific interactions between the TCR and CD8 on recipient CTL and MHC class I on donor parenchymal cells results in the release of granules containing cytotoxic molecules (such as perforin and granzyme B) and secretion of soluble mediators such as TNF- $\alpha$  [75]. The perforin and granzymes released into the target cell cytoplasm culminates in apoptosis [70].

Differentiation of naïve CD8 T cells to cytotoxic effectors also requires help from primed CD4 T cells, but exactly how this help is provided for an alloreactive response is not clearly understood. Based on how CD4 T cell help is provided for cytotoxic CD8 T cell responses against conventional, non-transplant antigens [76], it is likely that donor APC are first 'licensed' by interaction with recipient CD4 T cells with direct allospecificity that recognise MHC class II alloantigen on the surface of the donor APC. This licensing enables the donor APC to interact productively with alloreactive recipient CD8 T cells, leading to full differentiation into cytotoxic killers [77], [78]. In addition, Valujskikh and Heeger reported that CD8 T cells can reject skin allografts via the indirect allorecognition [79]. Similarly, recipient CD4 T cells can also be primed via the indirect allorecognition pathway in order to activate recipient CD8 T cells [80], [81]. The different allorecognition pathways of CD4 and CD8 T cells and their interrelationships have been reviewed recently [82].

Current immunosuppression therapy is generally successful at preventing acute cellular rejection. Such therapies aim mainly to inhibit T-cell responses by targeting principal signalling molecules required for T cell activation, or by direct depletion of the alloreactive T cell populations. However, whether the frequency or severity of acute cellular rejection correlate with longer-term development of CAV remains to be determined [83]. It is important to note that cellular and humoral rejection can occur concurrently in up to 25% of acute rejection episodes [84], [85].

#### **1.2.4 Antibody-mediated rejection**

In AMR, antibodies specific to donor MHC class I or class II molecules are generated and are termed donor-specific antibodies (DSAs). DSAs may either be present prior to transplantation (e.g., previous transplantation, pregnancy, or blood transfusion) or arise following transplantation (*de novo*) [86], [87], [88]. The generation of *de novo* DSAs in non-sensitized patients is associated with worse graft outcomes and early graft failure [89], [90], [91]. Patients who have received more than one transplant frequently develop alloantibodies against multiple different HLA antigens, which further reduces their probability of finding a suitable matching donor. Indeed, one third of wait-listed kidney transplant recipients are sensitized recipients with pre-formed DSAs [92], [93].

DSAs can also be generated against ABO blood group antigens, or minor histocompatibility antigens [49] [94], and non-MHC related polymorphic proteins [95]. Although the significance of these antibodies are unclear, it has been suggested that they are associated with an increased risk for chronic rejection [96], or long-term cardiac allograft dysfunction [97].

One of the most important targets of DSAs is the endothelium lining donor graft vessels. Anti-endothelial antibodies may mediate endothelial cell activation, apoptosis and cell injury [98]. Both acute and chronic AMR have been observed clinically in solid organ transplantation; however, although chronic AMR is recognized as a distinct entity in renal transplantation [99], it has not yet been defined precisely for other vascularised organs.

The development of progressive vasculopathy, a hallmark of chronic rejection, manifests differently in different organs (detailed in 1.4.1.1). Although studies have reported poorer

outcomes for cardiac allograft survival in patients developing donor specific antibody, the exact mechanism by which DSAs contribute to the development of vasculopathy has not been clarified. AMR is poorly defined in the heart making its diagnosis difficult. It was first described by Herskowitz et al. in 1987, as a subset of heart transplant recipients with arteriolar vasculitis and poor outcomes [100]. Two years later, Hammond et al. demonstrated that rejection was associated with antibody deposition and complement activation [101]. In 2005, AMR was recognized as a pathological entity, and although a consensus on standard AMR diagnostic guidelines is still lacking, the International Society for Heart and Lung Transplantation (ISHLT) have recently published and agreed upon AMR diagnostic guidelines [3].

Fine and colleagues [102] performed a retrospective study on 329 heart transplant recipients, with the aim of investigating the role of DSA development in acute allograft dysfunction. The study reported that in the absence of cellular rejection, patients can be grouped into three major categories: 1) patients who are DSA positive and with AMR features following endomyocardial biopsy assessment; 2) patients who are DSA negative but with AMR features evident on endomyocardial biopsy; and 3) patients who are DSA negative and with no AMR features [102]. Subsequently, Nair et al. proposed that AMR pathogenesis is a “clinical-pathological continuum”, where AMR begins as a latent DSA response that progresses through a silent phase with no clinical or histological manifestations (but that involves complement deposition); to a subclinical (i.e., histological features on biopsy, but no clinical symptoms); and then to symptomatic AMR [14]. This proposal may explain why some DSA-positive patients do not suffer from clinical manifestations. In addition, Loupy et al detected subclinical AMR in almost one third of DSA-positive patients at 3 months following transplantation, and associated DSA positivity with worse glomerular filtration rate at 1 year [103]. Because work presented in this thesis is directly related to AMR, the next section will discuss AMR pathogenesis in more detail.

### **1.3 Mechanisms underlying AMR pathogenesis**

AMR pathogenesis is complex and involves the contribution of innate and adaptive immune system components. After alloreactive B cells are activated in a T-cell dependent manner,

they result in alloantibody response that can last for the life-time of the recipient (detailed in section 1.7). The overall result of AMR is graft endothelial cell integrity loss, leading to unregulated activation of coagulation factors and immune cells which contribute to vascular thrombosis, and parenchymal loss. The critical components of the innate and adaptive immune systems and their relevance to AMR are described below.

### **1.3.1 Complement activation**

Certain subclasses of antibodies are capable of activating the classical complement pathway upon binding to graft endothelium, namely, IgG1 and IgG3 in humans[104]; and IgG2b in mice [105]. Complement-fixing DSAs are linked with poorer kidney transplant outcomes [106]. The complement system comprises a set of plasma proteins that are sequentially activated in an enzymatic cascade [93] [107]. Once activated, the interaction of the first complement component C1q with the Fc portion of DSA triggers a series of amplified steps that culminates in formation of the membrane attack complex (MAC) (reviewed in [108]). The MAC complex consists of complement components (C5b-C6-C7-C8-C9), which result in target cell lysis. During complement activation, chemoattractant complement by-products C3a and C5a are generated, which activate endothelial cells that express C3a and C5a receptors to, in turn, release pro-inflammatory molecules (i.e., cytokines, adhesion molecules, and growth factors). This results in increased vascular permeability [109]–[111]. Macrophages and NK cells also express C3a and C5a receptors, thereby recruiting macrophages and neutrophils to enhance the local inflammatory response [108], [112]. The two complement split products, C4d and C3d, are formed during complement activation and bind covalently to endothelial cell targets. Because they bind to tissues longer than other complement system components, C4d and C3d have been used as surrogate markers for complement activation [113]. Finally, it is important to stress that endothelial cell lysis is not extensive in AMR, due to the existence of inhibitory receptors, such as decay accelerating factor (DAF) and CD59, on endothelial cells that counter MAC formation [114].

### **1.3.2 Endothelial cell activation**

At the early stages of an inflammatory insult, endothelial cells express variable adhesion molecules depending on the stimulant(s) [115]. Leukocytes travel to the sites of

inflammation by migrating across activated endothelial cells expressing adhesion molecules (e.g., ICAM-1 and VCAM-1) [116]. The complex mechanisms involved in leukocytes rolling, adhesion, diapedesis and migration have been extensively reviewed [117]–[120]. By enabling extravasation of pro-inflammatory cells from the vascular compartment into the graft, endothelial expression of adhesion molecules is thus extremely important for initiation of graft damage. The donor allograft endothelial cells are the first available target for graft damage by recipient's effector and inflammatory cells (e.g., CTLs, NK cells, macrophages, neutrophils). The different effector functions carried by each cell subset have been reviewed [107], [121].

Work by Yamakuchi et al. demonstrated that cross linking of MHC molecules expressed on vascular endothelial cells by alloantibody results in the exocytosis of von Willibrand factor (vWf) from Weibel-Palade storage granules and P-selectin, turning the endothelial layer into a pro-coagulant, adhesive and chemo-attractive surface [122]. Similarly, HLA class I cross linking can induce the exocytosis of prothrombotic mediators (e.g., serine protease thrombin) which are involved in cleaving fibrinogen (i.e., substrate of thrombin). The release of thrombin and vWF would enable endothelial cells to mediate platelet rolling and aggregation, potentiating thrombus formation [123]. Furthermore, endothelial cell activation has been associated with increased production of platelet-derived growth factor and fibroblast growth factor receptors that promote endothelial proliferation that may contribute to arterial vasculopathy development (CAV) [124]. The mechanism underlying this response is not immediately clear, but elegant studies by Reed and colleagues [125]–[127] suggest that, following MHC class I crosslinking, endothelial cells are activated via the PI3K/Akt/mTOR pathway. In support, Tible et al. have reported a correlation between mTOR signalling activation in cardiac transplant biopsy tissue and active clinical AMR [128].

### **1.3.3 Antibody-dependent cell mediated cytotoxicity (ADCC)**

DSA may contribute to the pathogenesis of graft rejection independently of complement activation via a mechanism known as antibody dependant cell mediated cytotoxicity (ADCC) [129]. In humans, activating (Fcγ RIIA, FcγIIC, FcγRIIIA and FcγRIIIB) and inhibitory (FcγRIIB) Fcγ receptors are expressed on effector cells such as macrophages (reviewed [130]). The type of expressed Fcγ receptors differ from one cell type to another [130]. Antibody binding to activating receptors via the Fc portion of IgG, and can directly stimulate phagocytosis and

release of inflammatory cytokines (e.g., tumour necrosis factor (TNF), IL-6, and IL-1 $\alpha$ ) [130]. Activating signals are counter balanced by the co-engagement of inhibitory receptors. Therefore, the magnitude of NK cell activation is governed by the relative level of expression of activating and inhibitory Fc $\gamma$ Rs and their co-engagement by antibodies [130]. In other words, the balance between activating and inhibitory receptors will influence the overall effector response of the alloantibody binding. Although there is no direct evidence that ADCC mediates damage in human organ allografts [13], [107], Hirohashi et al., have demonstrated a role for Fc-dependent NK-cell responses in CAV development and chronic cardiac rejection in a murine transplant model [131]. In addition, NK cell infiltrates and CAV development were observed following the passive transfer of non-complement fixing antibodies [132].

## **1.4 Histopathological and Immunopathological features of chronic AMR**

AMR diagnosis is not solely reliant upon clinical assessment, as even asymptomatic patients can be suffering from AMR [133]. Instead, in cardiac transplantation, routine endomyocardial biopsies are examined histologically. Standard histopathology is considered poor at diagnosing AMR, and thus, immunopathology is generally performed concurrently [134]. Histopathologic and immunopathological features are detailed in the following section.

### **1.4.1 Histopathological features of chronic AMR**

A hallmark histopathological feature of chronic AMR is the development of a progressive histological lesions which manifests differently in different organs. It is characterised by transplant glomerulopathy (duplication of the glomerular basement membrane) and arteriosclerosis in renal transplants [135], bronchiolitis obliterans syndrome (i.e., occlusion of small airways) in lung allografts [136], vanishing bile duct syndrome in liver transplants [137], and allograft vasculopathy in cardiac allografts [138].

The endothelial cell layer lining the graft blood vessels is the first site to be encountered by DSAs. Oedematous endothelial cells with enlarged nuclei are consistently seen in AMR biopsies, and are thought to reflect endothelial cell activation [113]. Histological analysis may also reveal myocardial injury and intravascular macrophage accumulation [113]. The presence of NK cell infiltrates through the endothelium into the vessel wall may be an

indicator of active humoral immunity [139]. In the heart, additional features include interstitial oedema and haemorrhage in severe cases; however, interpretation of these findings can be difficult due to the traumatic nature of the biopsy procedure [140], [141]. According to the revision of the 1990 grading system of the diagnosis of cardiac rejection (which was completed in 2005 [3], and refined in 2015 [113]), an agreement on AMR grading based on histological and immunopathological features was established (illustrated in table 1).

#### **1.4.1.1 Vasculopathy**

CAV develops sub-clinically, and is found in 8% of patients following 1 year, and 50% following 10 years after heart transplantation [142]. Although its development can result in serious sequelae, no serological markers have been identified to predict its development. CAV development induces a progressive, irreversible fibrosis and occlusion of the donor vasculature. It is distinct from atherosclerosis in that it is concentric rather than focal, and is characterised by fibromuscular intimal hyperplasia that affects only the arteries of the allografts [143]. Neointima formed in affected blood vessels is composed of smooth muscle cells, fibroblasts, macrophages, T cells, and extracellular matrix, with relatively intact internal and external elastic laminae. The progressive formation of neointimal lesions is an irreversible process and ultimately results in occlusion of the lumen and graft ischemia [138]. In the heart, CAV particularly affects both the epicardial and intramyocardial arteries [143]. Infiltrating macrophages and subendothelial lymphocytes can also be detected [144], [145]. Although CAV development is not included in the most recent ISHLT histopathological features for heart AMR [146], it is commonly reported following AMR episode in adult heart transplants [133], [143], [147], [148].

#### **1.4.2 Immunopathological features of AMR**

Improved immunological detection methods have led to the detection of a spectrum of immunological changes that have helped in AMR characterisation. C4d deposition in myocardial capillaries has a strong correlation with AMR [149]. Patients who develop DSAs after heart transplantation have poorer graft survival [147], [150], [151]. According to the 2015 ISHLT guidelines, the identification of C3d, C4d and/or C1q complement deposition within capillaries in combination with DSAs is predictive of AMR [113]. Additional

immunopathological features and their interpretation are illustrated in table 2. Although C4d deposition along myocardial capillaries is associated with AMR, and when detected alongside DSAs predicts a worsening prognosis, it is important to emphasize that such findings by themselves would not justify the initiation of AMR treatment in the absence of clinical manifestations [147]. In addition, neither DSA nor complement detection in graft biopsies are considered a consistent feature of AMR, probably due to the vast array of generated DSAs with variable affinities to target antigens, and their subclass differences (complement and non-complement fixing). In addition, not all described features of AMR may be present at a particular time-point, making AMR diagnosis challenging.

**Table 1. AMR grading and nomenclature, adapted and modified from [113].**

<b>AMR grade</b>	<b>Description</b>
<b>AMR 0: Negative for pathological AMR</b>	Both histological and immunopathological features are negative
<b>AMR 1: Histopathologic</b>	Histopathological findings present but immunopathologic findings are negative
<b>AMR 1: Immunopathologic</b>	Histopathological findings negative but immunopathologic findings are positive
<b>AMR 2: Pathological AMR</b>	Both histological and immunopathological features are present
<b>AMR 3: Severe pathological AMR</b>	Severe AMR with histopathologic findings of interstitial haemorrhage, capillary fragmentation, mixed inflammatory infiltrates, endothelial cell pyknosis, and marked oedema

**Table 2. Immunopathologic features of AMR, adapted and modified from [112].**

<b>Marker</b>	<b>Interpretation and Limitations</b>
<b>IgG/IgM</b>	Detect tissue-bound immunoglobulin (Ig), limitations are Ig can easily dissociate, short half-life (IgM), inter-observer variability
<b>C3, C1q</b>	To detect complement activation by immunofluorescence, relatively short half-life
<b>C3d/C4d</b>	Detect complement activation, the combination of both markers is more predicative of AMR than C4d alone
<b>CD68</b>	Focal/ diffuse intravascular macrophages, indicate monocytes differentiation into macrophages
<b>CD31, CD34</b>	Confirm endothelial integrity, and help delineating intravascular localization of macrophages

## 1.5 AMR management and therapy

Due to lack of consensus for AMR diagnosis, there is a considerable variation in practice between different transplant centres. Current AMR management includes: removal of circulating alloantibodies (e.g., plasmapheresis [152]); reducing production of additional alloantibodies (e.g., intravenous immunoglobulins [153]); suppressing T cell (calcineurin-inhibitor (CNI)) and B cell responses (e.g., corticosteroids, mycophenolate mofetil (MMF)); or total lymphocyte depletion by antibodies (e.g., Rituximab which targets CD20 on B cells [154] or Muromonab, which targets CD3 on T cells [155]). Splenectomy may reduce numbers of activated B cells, but plasma cells may persist in other tissues, such as lymph nodes and bone marrow; in addition, splenectomy raises concerns relating to increased infectious complications [156], [157]. The development of therapeutic agents that inhibit antibody effector functions are another active area of research. For instance, eculizumab (humanized anti-C5 antibody) has proven beneficial in the treatment of AMR. For instance, in kidney transplant recipients with positive crossmatch, the incidence of AMR was reduced to 7.7% in the group treated with eculizumab compared to 41.2% in the control group [158].

Collectively, there is no standardised therapy for AMR. In addition, chronic AMR is more difficult to treat than acute AMR due to the irreversible tissue damage, and most of the above therapies can be used simultaneously [159]. Due to their potent immunosuppressive effect on the number and function of all types of immune cells and endothelial cells, corticosteroids represent an essential component of the treatment regimen of either acute or chronic AMR [160]. The use of corticosteroids in combination with CNI have effectively reduced early graft loss with 93-98% of kidney transplants surviving beyond one year. In this regard, there is a growing interest in monitoring DSAs following transplantation as a supporting feature for AMR diagnosis, albeit the optimal monitoring of DSA quantification and binding strength have not been elucidated [161].

## 1.6 Structure and function of secondary lymphoid organs

Secondary lymphoid organs (SLOs) include the lymph nodes, tonsils, spleen, and the mucosa-associated lymphoid tissue (MALT). SLOs are highly organised tissues and are designed to trap foreign antigens and initiate an appropriate immune response. Naïve lymphocytes

recirculate through SLO tissues, to which antigens are carried from sites of infection mainly by antigen presenting cells. The structure of SLOs is broadly characterised by follicles comprising naïve B cells, separated by interfollicular regions. T cell-rich areas are found at the border of the follicles.

### **1.6.1 Lymph node structure**

Lymph nodes are bean-shaped encapsulated structures, with an indented region known as the hilum. Lymph from extracellular space enters the node through the afferent lymphatic vessels where they drain into the subcapsular sinus (figure 3A). From there, the lymph distributes in the lymph node mass. Lymph is drained out of the lymph node via channels called the cortical sinuses, which converge at the hilum and drain into the efferent lymphatic vessel. Similarly, the blood supply enters and leaves the lymph node at the hilum [162]. Circulating lymphocytes or free antigens can enter the lymph node by specialized blood vessels called high endothelial venules (HEVs) [163]. The lymph node structure can be divided into the cortex, paracortex and medulla. The cortex consist of densely packed B cell follicles, which also contain follicular dendritic cells (FDCs) clustered within the B-cell follicles, and are essential in the germinal centre response [164]. Adjacent to the follicles is the paracortex, where dendritic and T cells are diffusely distributed (also known as T cell zones), and it is in this area where HEVs supply and drain lymphocytes from the lymph node. In addition, a network of fibroblastic reticular cells (FRCs) are present in the paracortical T cell area, where they form reticular fibres and a stromal network that functions as a guidance path for lymphocytes and DCs. The medulla contains T cells, B cells, macrophages, and plasma cells which are organized into medullary cords [165]. If lymphocytes do not encounter their specific antigen, they leave the lymph node through medullary sinuses and exit through the efferent lymphatic vessels and return to the circulation via the thoracic duct [166].

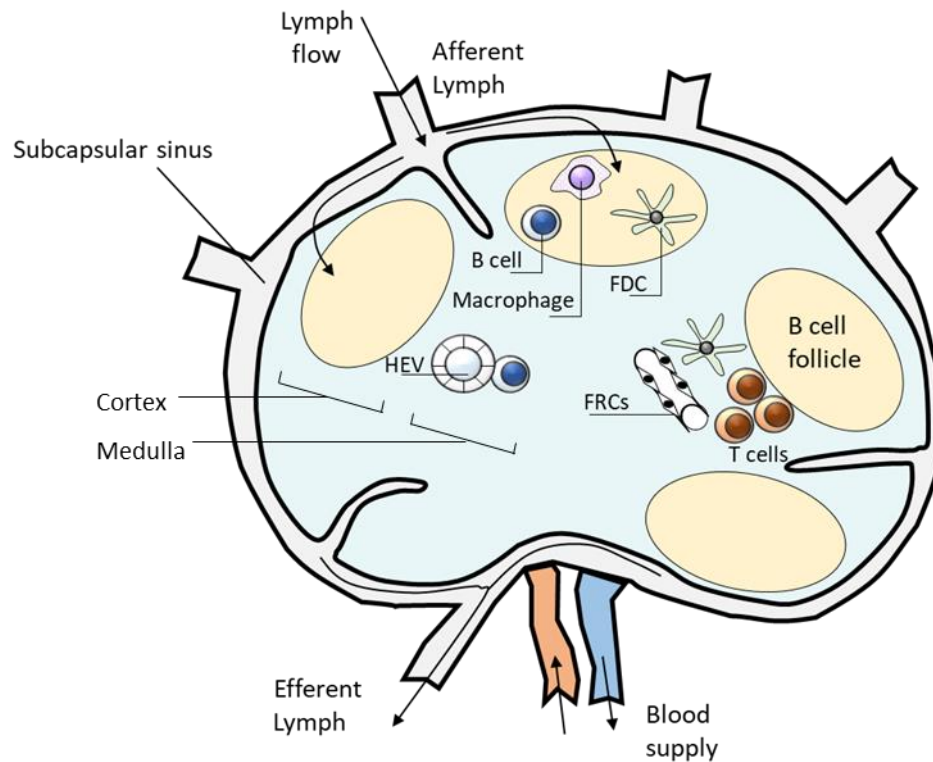
The location of B and T cells within the lymph node is dynamically regulated by chemokines and transcription factors [167]. Physiologically, naïve B and T cells extravasate through HEVs by a multistep adhesion cascade, using their main “homing receptor”, L-selectin, that binds to homeostatic chemokine gradients (intensively reviewed [168], [169]). T cells then migrate and localise to the T cell zone (located in the paracortex) under the influence of CC-chemokine ligand 21 (CCL21) and CCL19 gradient produced by FRCs in the T cell zone. B cells

enter the B cell follicle and localise at the cortex under the influence of CXC-chemokine ligand 13 (CXCL13) gradient produced by FDCs in the B-cell follicles. CXCL13 is the ligand for CXCR5 receptor on naïve B cells [166], [170]–[172].

### 1.6.2 Splenic structure

Unlike lymph nodes, the spleen is not divided into a cortex and medulla, but instead, is divided into a red pulp (the site of red blood cell destruction and iron storage [173]) and the white pulp (or B cell corona), which contains leukocyte clusters and plays a major role in protection against blood-borne antigens (figure 3B). The white pulp is composed of three adjacent compartments: the periarteriolar lymphoid sheath (PALS), B cell follicles, and the marginal zone (MZ). Each white pulp cluster is supplied by blood carrying both lymphocytes and antigen through the central arteriole [174]. Surrounding the central arteriole is the PALS area which comprises a dense population of T cells, mainly CD4<sup>+</sup> T cells and a smaller population of CD8<sup>+</sup> T cells, and dendritic cells [175]. B cells accumulate in clusters to form follicles adjacent to the PALS area. The follicle homes recirculating B cells (CD21<sup>int</sup> CD23<sup>+</sup> IgD<sup>high</sup> IgM<sup>low</sup>), and upon binding to their cognate antigen displayed on FDCs, they arrest within the follicle and proliferate to give rise to a germinal centre [164]. Such follicles are termed secondary follicles. In rodents, the white pulp is surrounded by the marginal zone which separates it from the red pulp, and consist of T cells, dendritic cells, macrophages, and a population of resident non-circulating B cells (CD21<sup>high</sup> CD23<sup>low</sup> IgD<sup>low</sup> IgM<sup>high</sup>) that are involved in rapid T-independent antibody responses to blood borne antigens, and also participate in T-dependent antibody responses [176], [177]. In contrast, the human white pulp has inner and an outer marginal zone (MZ) areas, that are both surrounded by a larger perifollicular zone [174]. MZ B cells comprise mainly of a mixture of non-recirculating naïve and memory cells. Memory B cells express higher levels of IgM and less IgD, and the costimulatory molecules (CD80 and CD86) than that of recirculating B cells [178].

A)



B)

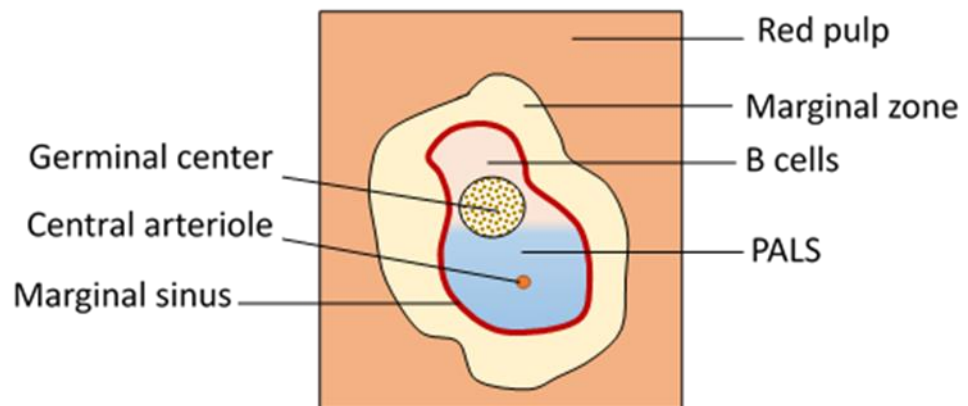


**Figure 3. Lymph node and spleen structures.** A) Schematic diagram of lymph node. The lymph node consists of an outermost cortex and an inner medulla. The cortex is composed of B cell follicles and is separated by paracortical areas rich with T cells. The medulla consists of strings of macrophages and plasma cells known as the medullary cords. Circulating lymphocytes and free antigen enter the lymph node through the high endothelial venules (HEV). B) The red pulp of the spleen serves as the site of red blood cells destruction. The white pulp which contains organized zones of B cells and T cells. The central arteriole found in the B cell follicle is surrounded by a T cell rich area referred to as the PALS. The marginal zone contains macrophages, dendritic cells, and non-recirculating B cells.

## 1.7 Mechanisms of antibody formation

B cell maturation and differentiation into plasma cells is either T cell-dependent (mainly responses against protein antigens) or T cell-independent (mainly triggered against mitogenic or polysaccharide antigens) [179]. T cell-dependent antibody responses require the degradation of protein antigen and its presentation on MHC class II molecules for cognate recognition by CD4 T cells. Circulating alloantibodies are believed to be the product of T-dependent antibody responses [68].

### 1.7.1 B cell activation and priming

B cells comprise of the two lineages; B1 and B2; based on their origin, self-renewal, and anatomical distribution (reviewed [180]). B1 cells mainly reside in the peritoneal and pleural cavities and can be identified by CD5 expression and other distinctive markers (IgM<sup>hi</sup>, IgD<sup>lo</sup>, CD45<sup>lo</sup>, CD23<sup>lo/-</sup>, and CD43<sup>+</sup>) [181]. They are involved in host protection during the primary humoral response with provide fundamental housekeeping functions, such as the removal of damaged apoptotic cells [182].

Both follicular and MZ B cells belong to the B2 lineage, and are generated in the bone marrow. Following B cell receptor (BCR) editing and central selection, mature B cells continuously circulate through secondary lymphoid organs until they encounter their specific target. The humoral response is initiated by antigen binding to the BCR which activates a cascade of downstream events of members of the Src family of protein tyrosine kinases and transcriptional programs (reviewed in [183], [184]). BCR cross-linking to the target antigen not only provides activation signals, but also mediates internalization and processing of the bound antigen into peptides that are returned into the cell surface complexed with MHC II molecules. At this stage, B cells also upregulate the expression of co-stimulatory molecules such as CD86 [185]. Cognate T-helper cells recognizing the peptide-MHC II complex can deliver activating signals to the B cell. The interaction between CD28 on T cells and CD80 (B7.1) and CD86 (B7.2) on B cells [186]–[188], and that between CD40 on T cells and CD40L on B cells contribute an essential part for B cell survival and differentiation into antibody secreting plasma cells [189]. It is important to emphasize that naïve T helper cells need to be primed prior to providing cognate B cell help for humoral immunity [190]. This is achieved by naïve T cell interaction with its cognate peptide presented by a dendritic cell in the T cell-rich regions (or T cell zone) of secondary lymphoid organs.

Several changes take place in SLOs during the initial phase of a T-dependent humoral response. Upregulation of cell adhesion molecule expression (such as P-selectin and E-selectin) on HEVs, in response to pro-inflammatory cytokines release [191], facilitates egression of high numbers of lymphocytes into peripheral lymphoid tissues. Antigen-bound B cells increase their expression of CCR7 and are attracted by a gradient of CCL19/CCL21 to the B cell-T cell zone border released by perifollicular stromal cells [192]. This follicular exclusion of antigen-binding B cells promotes encounter with antigen-specific T helper cells [185]. Similarly, upregulation of CXCR5 and downregulation of CCR7 promotes migration of primed T cells to the B cell-T cell zone border [193] [185]. At this stage, engagement of the MHC-peptide complex on B cells with the T cell receptor, in conjunction with costimulatory molecule interactions (e.g., CD86-CD28, CD40L-CD40, and FasL-Fas), leads to the formation of an immunological synapse (figure 4). Following 3-4 days of the initial phase of a T cell-dependent response, proliferating B cell blasts undergo differentiation into either extrafollicular plasmablasts or initiate a GC response. The mechanisms that determine the B cell fate and whether it undergo plasmablast or GC differentiation remain to be fully elucidated.

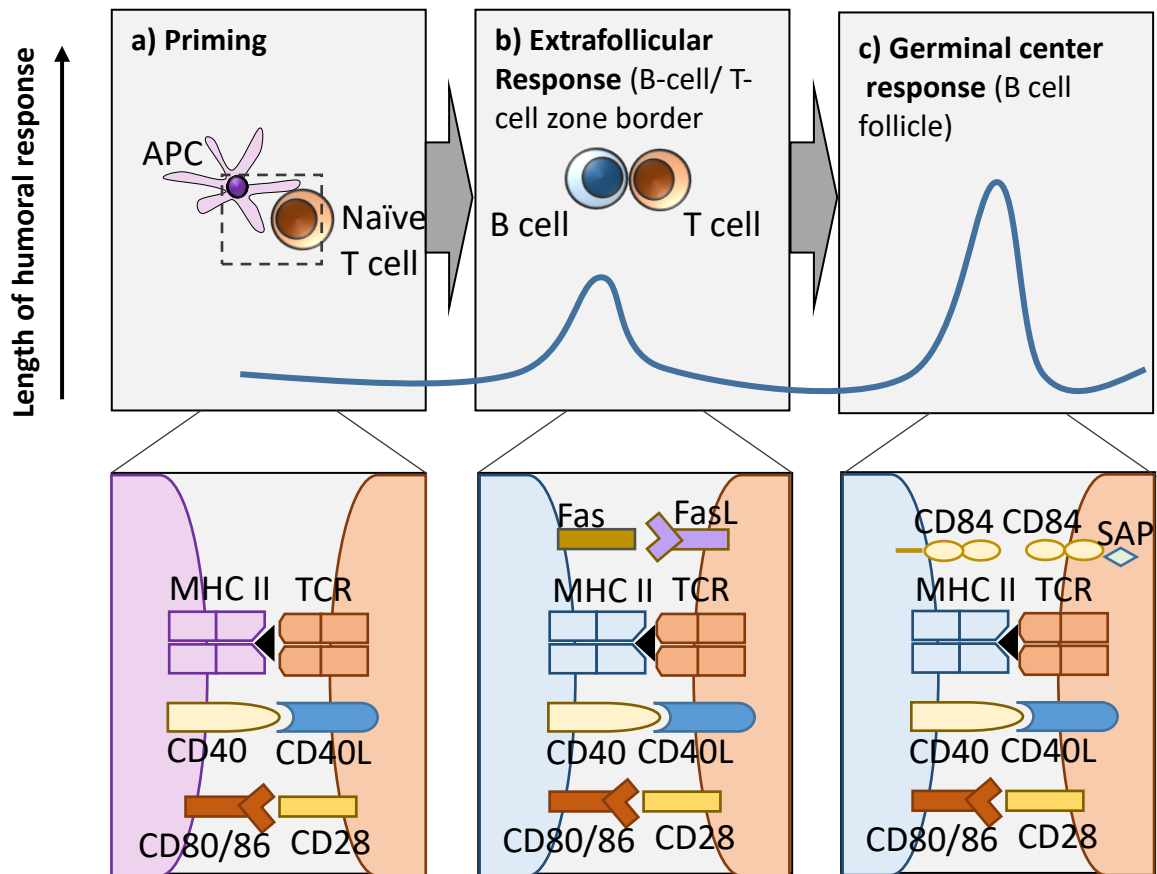


**Figure 4. Schematic presentation of the T-dependent humoral response.** a) Naïve T cells are primed following contact with APCs in the peripheral lymphoid tissues. b) Cognate interaction between primed T-B cells result in the proliferation and differentiation of B cells into plasmablasts which are short-lived and capable of secreting class switched antibodies, c) Few B cells migrate to the B cell follicle to initiate GC structure resulting in the generation of LLPCs and memory B cells. Key signaling molecules at each stage are illustrated in the lower panel.

### 1.7.2 Extrafollicular humoral response

Extrafollicular plasma cell precursors migrate to the border between the T-cell zone and the red pulp (i.e., the bridging channel in the spleen or the medullary cords of the lymph nodes) to form a foci of short-lived plasmablasts [194]. This migration is guided by the upregulation of the transcription factor B-lymphocyte induced maturation protein1 (Blimp-1) and maintaining orphan G-protein-coupled receptor called Epstein-Barr-virus-induced molecule 2 (EBI-2), and loss of CXCR5 and CCR7 [195]. Generated plasmablasts provide an early wave of antibodies that are generally of modest affinity, but can be critical for early control of infection [196]. Extrafollicular plasma cells can undergo class switching, survive for approximately 3 days before undergoing apoptosis [197], [198], and were conventionally considered to be less likely to differentiate into memory B cells. However, a number of recent studies have demonstrated that a fraction of extrafollicular plasma cells may survive for longer periods and that class switched memory B cells can be generated independently of GC formation; in these cases, BCR and CD40 engagement seems to be sufficient to drive memory B cell differentiation [199], [200], [201].

### 1.7.3 Germinal centre humoral response

GCs are highly specialised structures found within B cell follicles of secondary lymphoid organs. They are the main sites where antigen-specific B cells produce high affinity antibodies and generate memory B cells. Following the initial B cell activation, antigen-specific B cells migrate to the T cell zone border where antigen-specific B and T cells form long-lived cognate interactions that are necessary for B cell activation under the influence of chemokine gradients as described in the above section [202], [203]. At this stage, T:B cellular interaction is stabilised by the homotypic interactions between CD84 and Ly108 (both are SLAM family members), which are expressed by T and B cells, in addition to ICOS/ICOSL interactions. The SLAM-associated protein (SAP) is an adaptor molecule with a Src homology 2 (SH2) domain, which binds to the cytoplasmic domain of SLAM family receptors. SAP acts as a facilitator in balancing negative signals from Ly108 with positive signals from CD84, thus enabling the formation of stable T:B cellular interactions. Deletion of SAP corresponding gene (*Sh2d1a*) results in shorter B cell-T cell adhesion, and abrogates GC formation [204], [205].

Following 2-3 days of prolonged B-T cell interaction, a subset of activated B cells will seed the follicle for GC formation, and, under the influence of the upregulation of the transcription factor Bcl-6, proliferate rapidly to form a mature GC [190]. Histologically, mature GCs comprise two distinct regions: the dark zone, and the light zone [206]. While the dark zone consists mainly of a dense population of mitotically active B cells (known as centroblasts), the light zone is composed of non-dividing B cells (known as centrocytes), and a network of FDCs and T follicular helper cells ( $T_{FH}$ ) cells, which are essential cellular components for the maintenance of the GC reaction (reviewed in [207]). FDCs express interleukin-6 (IL-6), B cell-activating factor (BAFF), and several adhesion molecules which contribute to their interaction with B cells, and promote their survival within the GC [208], [209]. More importantly, FDCs can retain intact antigens as immune complexes on their surface for prolonged periods (even after termination of the response [210]).

### **1.7.3.1 Clonal selection**

In the germinal centre, B cells undergo a highly regulated multistep process that involves activation and regulation. Centroblasts in the dark zone of the GC undergo proliferation and somatic hypermutation (SHM), where random base-pair changes are introduced into the immunoglobulin variable region of the heavy and light chains of the BCR [164]. The enzyme activation induced cytidine deaminase (AID) initiates DNA damage into the immunoglobulin genes. The DNA damage is repaired by a set of DNA repair enzymes resulting in mutations (reviewed in [210]). During the process of SHM, GC B cells must up-regulate Bcl-6 to overcome the DNA damage and tolerate a high mutation rate. Bcl-6 is a transcription repressor, and once upregulated it mediates repression of the ATR (ataxia telangiectasia and Rad3 related), TP53 and p21 genes [211]–[213]. ATR is a master regulator of genomic damage during cell replication, and its suppression permits GC B cell survival during their synthesis phase [214]. SHM generates in B cells with a broad range of affinities to target antigen. Because the process is random, it may also generate some centroblasts with unfavourable antibodies (i.e., binding with low affinity, or not binding at all, or autoreactive). In such case, B cells undergo apoptosis due to the lack of a BCR-mediated survival signal and/or  $T_{FH}$  helper signals [215]–[217].

After centroblasts divide and mutate in the dark zone, they differentiate into centrocytes and move to the light zone of the GC for selection.  $T_{FH}$  cells reside alongside FDCs in the light zone, and one of two proposed mechanisms select centrocytes with improved affinity. Traditionally, it was thought that selection of high-affinity clones occurs by competitive binding of centrocytes to antigen deposited on the surface of FDCs, such that centrocytes with higher BCR affinity outcompete centrocytes of lower affinities for available antigen. Those low affinity centrocytes subsequently undergo apoptosis due to insufficient BCR survival signals. In this proposed model,  $T_{FH}$  cells would play an accessory role by either providing survival or differentiation signals to selected cells [218]. More recent evidence instead suggests that within the light zone, centrocytes bearing BCRs with higher affinity capture more antigen from FDCs to be processed, and presented on their surface [219], [220]. Thus, clones with higher affinity bear denser peptide:MHC II complexes on their surface, and thereby receive more efficient help and survival signals from  $T_{FH}$  cells [221], [222]. In addition, Gitlin et al. reported that the amount of antigen presented by GC B cells to  $T_{FHs}$  in the LZ is proportionate to the number of subsequent cell divisions and hypermutation occurring in the DZ [223]. Similarly, Victora and colleagues [224] have proposed a model wherein an intrinsic molecular circuit in GC B cells (regulated mainly by mTOR complex 1 kinase (mTORC1)) is activated upon positive selection by  $T_{FHs}$  in the LZ. The study further demonstrated that mTORC1 triggered several intracellular anabolic programs responsible for mediating cell growth, which in turn contributed to clonal expansion of the selected B cell clones in the DZ.

Continual inter-zonal cycles of centroblast division and hypermutation in the dark zone is followed by selection in the light zone and are a hallmark feature of affinity-matured humoral responses. In addition to selection, B cells undergo immunoglobulin class-switch recombination (CSR) in the light zone, which is an irreversible mechanism whereby B cells can switch the heavy chain class of the antibody [225]. Light zone B cells may undergo CSR directly, while others can switch following recirculation through the light and dark zones [226]. GC B cells eventually differentiate into either memory B cells, which express high-affinity BCRs that can quickly differentiate into plasma cells upon antigen encounter, or to long-lived plasma cells (LLPCs) that persist for years [227]. LLPC migration to the bone marrow is dependent on the expression of both CXCR4 by the plasma cell, and its ligand CXCL12 by bone marrow stroma. Bone marrow stroma supports plasma cells survival, and provides the necessary microenvironment for plasma cells to secrete antibody [192], [228].

Generated LLPCs and memory B cells persist for years or the life-time of the individual, and their survival is independent of each other [229].

Lastly, it is important to emphasize that other transcription factors and cytokines present in the surrounding microenvironment are detrimental to B cell activation and differentiation. For instance, Bcl-6 and the interferon regulatory factors Irf4 and Irf8, govern the fate of activated B cells into either the GC or extra-follicular pathway. The upregulation of Irf4 on B cells leads to the upregulation of B-lymphocyte induced maturation protein1 (Blimp1) and the plasma cell differentiation [230], [231]. In contrast, upregulation of Irf8 leads to Bcl-6 expression which is required for GC formation [197]. Additional transcription factors and protein receptors are illustrated in table 3.

### **1.7.3.2 T<sub>FH</sub> cells differentiation**

The T<sub>FH</sub> cell subset represents an essential compartment for establishing germinal centres. Although FDCs were first described in 1965 [232], T<sub>FH</sub> cells were not recognised until 2009, when the transcriptional factor Bcl-6 was identified for its role in directing T<sub>FH</sub> cell lineage commitment [233]–[235]. T<sub>FH</sub> differentiation involves multiple signals and is regulated under the influence of positive and negative mediators comprising interleukins, cell receptors, and transcription factors. The complex multifactorial differentiation pathways between positive and negative mediators were reviewed recently [236], [237]. Briefly, after CD4 T cell priming by follicular dendritic cells, CD4 T cells undergo fate decision between differentiation into pre-T<sub>FH</sub> or other effector CD4 T cell subsets (e.g., Th1, Th2, or Th17) [238]. The earliest regulator that influences pre-T<sub>FH</sub> cell differentiation is IL-6, which is abundantly secreted by FDCs [235]. IL-6 signalling induces Bcl-6 expression on pre-T<sub>FHs</sub> [234]. The expression of Bcl-6 is essential for the early CXCR5 expression on pre-T<sub>FHs</sub> and subsequent localisation to the B cell follicle [235]. ICOS/ICOSL signalling between pre-T<sub>FH</sub> and the FDC is also critical at this early stage [238]. Tubo et al. demonstrated that the strength of antigen recognition via TCR can also regulate the likelihood of T cells differentiation into T<sub>FH</sub> cells, but in a non-linear relationship [239]. The differentiation of early T<sub>FHs</sub> is also regulated by signals provided by the expression of positive regulators (e.g., LEF-1, TCF-1 transcription factors) [240], and negative regulators (e.g., IL-2, IL-7, CTLA-4, PD-1, CCR7 and Blimp-1) [236]. Studies using knockout mice have revealed that IL-6, IL-21 and Bcl-6 are essential for the early stages of

T<sub>FH</sub> differentiation [241]. In humans, however, IL-12 and activin A signalling are found to be essential [236], [237].

After two days, DC-primed T<sub>FH</sub> cells become extremely dependent on B cells for their complete differentiation, and localise at the interfollicular zone (i.e., T-B cell border) under the influence of CXCR5 expression, and downregulation of CCR7 and P-selectin glycoprotein ligand 1 (PSGL1) (which otherwise would anchor T cells to the T cell zone). Continuous antigen presentation by responding B cells is essential for T<sub>FH</sub> differentiation and maintenance. Deenick et al. [242] demonstrated that T<sub>FH</sub> differentiation was completely blocked when T-B cell interactions were compromised. In addition, B cells provide an abundant source for ICOSL; a requisite for full T<sub>FH</sub> cell differentiation. At the interfollicular zone, stable prolonged interactions between B and T cells take place through SAP/SLAM signalling, which is essential for T<sub>FH</sub> cell differentiation [243]. The SAP/SLAM signalling also regulates ICOS expression, thought to be important for maintaining expression of CXCR5 on differentiated T<sub>FHs</sub> [240].

Differentiated T<sub>FH</sub> cells are confined to the B cell follicle under the influence of CXCR5 expression and contribute to B cell clonal selection (as detailed in section 1.7.3). Most differentiated GC T<sub>FH</sub> cells are CXCR5<sup>hi</sup>PD1<sup>hi</sup>Bcl6<sup>hi</sup>SAP<sup>hi</sup> and PSGL1<sup>lo</sup>CD200<sup>+</sup>BTLA<sup>hi</sup>CCR7<sup>lo</sup>. In addition, T<sub>FH</sub> cells do not express Epstein-Barr virus-induced G-protein coupled receptor 2 (EBI2), because its oxysterol ligand is present in the B cell follicle, rather than within the GC environment, and the loss of EBI2 expression is essential for both GC B cells and T<sub>FH</sub> cells to localise into the GC active area [244]. Finally, while GC B cells are strictly confined to a single active GC within the B cell follicle, T<sub>FHs</sub> cells can transit to neighbouring B cells follicles [245] and join a different GC, or downregulate Bcl-6 expression and develop into a memory T<sub>FH</sub> cells [245].

**Table 3. Key transcription factors and protein receptors involved in control of GC B cells versus plasma cell fate**

<b>Marker</b>	<b>Nature</b>	<b>Effect</b>
<b>CCR7</b> [185]	Protein receptor	Migration to CCL19/CCL21 areas
<b>CXCR5</b> [185]	Protein receptor	Migration to B cell follicles area
<b>EBI-2</b> [185]	Transcription factor	Migration to splenic bridging channels or lymph nodes medullary cords
<b>ICOS</b> [246]	Protein receptor	Sustain long T-B cell interaction
<b>SAP</b> [185]	Adaptor molecule	Sustain long T-B cell interaction
<b>PD-1</b> [216]	Protein receptor	Activation marker
<b>CXCR4</b> [247]	Protein receptor	Plasma cell survival
<b>CXCL12</b> [247]	Protein receptor	Plasma cell survival, migration and survival in bone marrow niche
<b>Bcl-6</b> [247]	Transcription factor	Master regulator of TFH lineage (proposed to repress <i>Blimp1</i> )
<b>Irf4</b> [247]	Transcription factor	Plasma cell differentiation and survival (by repressing <i>Bcl-6</i> )
<b>Irf8</b> [247]	Transcription factor	Involved in GC B cell differentiation (by sustaining <i>Bcl-6</i> upregulation)
<b>Blimp1</b> [247]	Transcription factor	Plasma cell differentiation (by repressing <i>Bcl-6</i> )

#### **1.7.4 Allogenic B cells activation by unlinked CD4 T cell help**

In addition to the conventional T-dependent antibody response described earlier, “unlinked help” has been described in the context of organ transplantation [248]. This refers to the ability of CD4 T cells that are specific for one graft alloantigen to provide help to B cells that are specific for another alloantigen on the graft. B cells that are activated via this un-linked pathway can generate class-switched allospecific antibodies, provided that the antigen recognized by CD4 T cells - ‘the helper antigen’ - and the BCR-specific antigen are expressed on the same donor cell. It has been proposed that upon BCR-mediated internalisation of the target B cell antigen, the B cell also acquires the second ‘helper antigen’. The internalised helper antigen will be processed and re-presented as allopeptide in the context of MHC class II on the B cell surface. The unlinked help signals are then delivered by interaction between MHC class II/peptide complex on the B cell with TCR on CD4 T cell, regardless of the BCR specificity. The contribution of allospecific B cells activated via unlinked-help in the generation of alloantibody responses have been described in murine cardiac transplant models [248].

#### **1.7.5 T-dependent responses and allograft rejection**

The outcome of a T-cell dependent antibody response is the generation of DSAs capable of recruiting effector cells and activating the classical pathway of complement. This contributes to poorer graft survival and potentiates the development of CAV [249]. It is now established that DSA represents a substantial barrier to transplantation, and sensitised patients have low transplant rates [87]. With the availability of pre-operative cross-matching and precise, solid-phase immunophenotyping assays, hyperacute AMR is virtually no longer seen. However, chronic AMR continues to impair long-term graft survival. Teraski et al. showed in a large multi-centre study that renal graft failure at 4 years was approximately three times more frequent in patients who developed DSA than in those who did not [89]. Furthermore, in a retrospective study performed by Kfoury and colleagues on 665 cardiac transplant patients, the occurrence of acute AMR episodes (three or more) was statistically associated with increased cardiovascular mortality, whereas cellular rejection episodes did not increase risk [250].

Recent research has focused on elucidating the role of T<sub>FH</sub> cells in rejection of solid organ transplants, with the aim of identifying key ligands / signalling proteins that mediate T<sub>FH</sub>-B cell interaction and that may be targeted to prevent AMR development (reviewed [251], [252]). Experiments performed by our group have established that only CD4 T cells with indirect allospecificity can acquire the T<sub>FH</sub> cell phenotype that is crucial for sustaining GC humoral alloimmunity [68].

Although plasmapheresis and intravenous immunoglobulin treatment can reduce anti-HLA titers, depletion of LLPCs (the source of antibodies) with rituximab (anti-CD20) is ineffective, because terminally differentiated antibody producing B cells do not express CD20, and their bone marrow residence makes them less accessible to circulating monoclonal antibody [113]. B cell depletion by anti-CD19 offers an alternative to anti-CD20, as CD19 is expressed on a broader range of developing B cells, including a subset of plasma cells [253], and has been associated with depletion of up to 80% of bone marrow CD138+ plasma cells in a murine model of kidney transplantation [254]. In contrast to CD20, treatment with anti-CD19 significantly reduced the frequencies of IgG-expressing B cells in the peripheral blood in murine acute cardiac model [254]. Although anti-CD19 therapy has shown promising results in the treatment of autoimmune diseases and lymphomas, no reports are available on its clinical application in solid organ transplantation [255], [256]. Specific targeting of LLPCs can theoretically be achieved using the proteasome inhibitor Bortezomib, as has recently been described in recipients of kidney [257], heart [258]–[260], and lung grafts [227], [228]. Bortezomib prevents the degradation of misfolded proteins manufactured by plasma cells, and the resulting excessive endoplasmic reticulum stress eventually leads to plasma cell apoptosis [257], [261]. However, the administration of Bortezomib as the sole desensitisation agent does not reduce DSA titer [262], [263], and the beneficial effect of Bortezomib was mostly evident when administered in conjunction with steroids, or when administered early after transplantation and during the context of rising DSA during acute AMR [264], [265].

Collectively, humoral T-cell dependent responses generate LLPCs capable of producing class-switched antibodies of high affinity, which persist long-term in the bone marrow, as well as memory B cells, which differentiate to LLPCs upon re-encountering cognate antigen, making treatment and re-transplantation for those patients more challenging. Hence, it is likely that alloreactive GCs contribute to chronic AMR by generating LLPCs that can secrete

alloantibody indefinitely. This, however, has not been confirmed experimentally. Thus, dissecting the T-dependent humoral alloimmune response would improve our understanding of the contribution of the extrafollicular and GC pathways to AMR, and would likely inform the design of more efficient immunosuppressive therapy.

### **1.7.6 The potential of alloantibody affinity on allograft damage**

The relative expression levels of HLA on the vascular walls of a transplanted organ may vary among different HLA loci [127]. For instance, HLA-C has been reported to be expressed at a lesser extent than HLA-A and HLA-B [266] which may partly explain the lower sensitization frequency to HLA-C compared to that reported for HLA-A and HLA-B [267]. Although antigen abundance can increase immunogenicity, the influence of alloantibody affinity to donor-specific HLA antigens on allograft damage has not been thoroughly investigated. Recent work by Daga and colleagues [268] reported affinity constants in real time for human alloantibodies against different HLA molecules. The study demonstrated that the two anti-HLA-A2 human monoclonal antibodies SN230G6 (i.e., generated following HLA-A2 or HLA-B57 immunization) and SN607D8 (i.e., generated following HLA-A2 immunization) bound to HLA-A2 at different affinities. The binding affinity of SN230G6 to HLA-A2 was 20-folds greater than that of SN607D8. Work by Kushihata et al. [269] showed that the complement-dependent cytotoxicity activity of SN230G6 antibody was ten-times greater than that of SN607D8 when performed on lymphocytes obtained from the same human donor cells. These results suggest that effector functions of alloantibodies are influenced by affinity to the target antigen.

To conclude, HLA mismatched allografts can generate alloantibodies that vary in pathogenicity due to the overall effect of their specificity and titer [268]. Every HLA antigen carries a unique combination of epitopes, and some epitopes are shared between different HLA antigens. The humoral response in recipients of multiple HLA mismatched donors usually generate an alloantibody response that is directed against 1 or 2 immunodominant epitopes that are shared by the different unmatched HLA antigens [270], [271]. So far, only one study has investigated human alloantibody affinity to HLA. The study suggested a potential correlation between the antibody binding affinity and its efficacy at eliciting complement cytotoxicity. If correlation exist, the ability of estimating the “average” antibody

affinity in recipient sera may provide a beneficial parameter before considering drug regimen alteration or for predicting prognosis.

## 1.8 Project objectives

My project aims to improve our understanding of B cell activation during AMR and to clarify the contribution of extrafollicular and germinal centre humoral alloimmunity to CAV development. Thus, the project focuses on the following objectives:

1. Distinguish the influence of GC from that of extrafollicular humoral alloimmunity in mediating AMR.
2. Determine the contribution of alloantibody in mediating CAV development.
3. Characterise alloantibody responses that develop when T cell help is restricted to naïve or early memory recognition of second, 'un-linked' alloantigen.

## Chapter 2

### 2. Materials and methods

#### 2.1 Animals

C57BL/6 (H-2<sup>b</sup>; BL/6) [wild-type (WT)] and BALB/c mice (H-2<sup>d</sup>) were purchased from Charles River Laboratories (Margate, UK). T cell receptor-deficient mice (H-2<sup>b</sup>, hereafter TCR<sup>-/-</sup>) B6.129P2-*Tcrb*<sup>tm1Mom</sup>*Tcrd*<sup>tm1Mom</sup>/J were purchased from the Jackson Laboratory (Bar Harbor, ME).

C57BL/6 *Rag2*<sup>-/-</sup> mice (H-2<sup>b</sup>) lacking both B and T cells were gifted by Prof T. Rabbitts (Laboratory of Molecular Biology, Cambridge, UK). TCR-transgenic *Rag1*<sup>-/-</sup> TCR75 mice (H-2<sup>b</sup>) [hereafter, WT.TCR75 T cells], specific for I-A<sup>b</sup>-restricted H-2K<sup>d</sup><sub>54-68</sub> peptide, and C57BL/6-Tg(K<sup>d</sup>)RPB (hereafter BL/6.K<sup>d</sup>) mice, which express the full H-2K<sup>d</sup> sequence [272], were gifted by Prof. P. Bucy (University of Alabama, Birmingham, AL).

BCR-transgenic SW<sub>HEL</sub> (VH10<sub>tar</sub><sup>+/-</sup> x LC2) mice (H-2<sup>b</sup>) specific for Hen Egg Lysozyme (HEL) protein [273] and BL/6.mHEL mice (H-2<sup>b</sup>, KLK3 Tg) that express membrane bound HEL<sup>WT</sup> or HEL<sup>3x</sup> [274], were gifted by Prof R. Brink (Garvan Institute of Medical Research, Darlinghurst, Australia). SW<sub>HEL</sub> mice were crossed with BL/6.*Rag2*<sup>-/-</sup> to provide BL/6.*Rag2*<sup>-/-</sup>.SW<sub>HEL</sub> (hereafter *Rag2*<sup>-/-</sup>.SW<sub>HEL</sub>) strain, which lack all T cells, but retain a monoclonal population of B cells with high-affinity to HEL<sup>WT</sup> antigen. *Rag2*<sup>-/-</sup>.SW<sub>HEL</sub> mice were routinely checked for the lack of CD3 T cells, and for availability of HEL-specific B cells by flow cytometry on samples obtained from tail bleeds.

Mice expressing mHEL<sup>WT</sup> or mHEL<sup>3x</sup> in conjunction with full-length K<sup>d</sup> protein were generated in house by crossing B6.mHEL<sup>WT</sup> or B6mHEL<sup>3x</sup> mice with BL/6.K<sup>d</sup>. The gene constructs of mHEL<sup>WT</sup> and mHEL<sup>3x</sup> strains were designed to express the HEL protein under the human ubiquitin C promoter (UBC) while being anchored to the cell membrane by a short transmembrane segment and a cytoplasmic domain of the H-2K<sup>b</sup> or H-2K<sup>k</sup> MHC class I molecule.

*Sh2d1a*<sup>-/-</sup> TCR-transgenic *Rag1*<sup>-/-</sup> TCR75 (hereafter TCR75.SAP<sup>-/-</sup>) mice, which contain a monoclonal population of CD4 T cells that is deficient to SLAM-associated protein (SAP) were

generated in house by crossing male WT.TCR75 mice with heterozygous SAP<sup>+/-</sup> females. Female offspring that are SAP<sup>+/-</sup>. TCR75<sup>+/-</sup>. Rag<sup>+/-</sup> were back-crossed with male TCR75<sup>+/-</sup>.Rag<sup>-/-</sup>.SAP<sup>+/+</sup>. To confirm phenotype, TCR75 CD4 T cells were determined by flow cytometry using anti-Vβ 8.3 antibody, and anti-CD4 antibody and the absence of B cells (negative staining by anti-CD19 antibody).

TCR-transgenic mice (TCR7.Ly5.1, H-2<sup>b</sup>), comprised of > 80% CD4+ splenic or inguinal lymph node T cells are I-A<sup>b</sup>- restricted for the (HEL<sub>74-88</sub>) peptide [275] was gifted by Dr. M Linterman (Laboratory of Lymphocyte Signalling and Development, Babraham Institute, Cambridge, UK).

A summary of animals used in this work is presented in table 4. All animals were bred and maintained in specific pathogen-free facilities at Central Biomedical Services, University of Cambridge. All experiments were approved by the UK Home Office Animal (Scientific Procedures) Act 1986.

**Table 4. Strains and MHC haplotypes of mice used in this study**

Mouse Strain	Description	MHC Haplotype			
		H2-K	H-2D	I-A	I-E
<b>C57BL/6</b>	H-2 <sup>b</sup> wild-type	<i>b</i>	<i>b</i>	<i>b</i>	Null
<b>BALB/c</b>	H-2 <sup>d</sup> wild-type	<i>d</i>	<i>d</i>	<i>d</i>	<i>D</i>
<b>Tcrbd<sup>-/-</sup></b>	TCR deficient C57BL/6 (wild-type B cells, deficient for CD4 and CD8 T cells)	<i>b</i>	<i>b</i>	<i>b</i>	Null
<b>Rag2<sup>-/-</sup></b>	B and T cell deficient C57BL/6	<i>b</i>	<i>b</i>	<i>b</i>	Null
<b>WT.TCR75</b>	<i>Rag1</i> <sup>-/-</sup> TCR transgenic specific to K <sup>d</sup> peptide presented on I-A <sup>b</sup> . Deficient for CD8 T cells and B cells.	<i>b</i>	<i>b</i>	<i>b</i>	Null
<b>SAP<sup>-/-</sup>.TCR75</b>	<i>Rag1</i> <sup>-/-</sup> mice with TCR transgenic CD4 T cells specific to K <sup>d</sup> peptide presented on I-A <sup>b</sup> . This strain is deficient for SAP protein and CD4 T cells cannot differentiate to T <sub>FHs</sub>	<i>b</i>	<i>b</i>	<i>b</i>	Null
<b>BL/6.K<sup>d</sup></b>	C57BL/6 with K <sup>d</sup> transgene. Wild-type B and T cells.	<i>bd</i>	<i>b</i>	<i>b</i>	Null
<b>BL/6.mHEL<sup>WT</sup></b>	C57BL/6 with membrane bound HEL <sup>WT</sup> protein	<i>b</i>	<i>b</i>	<i>b</i>	Null
<b>BL/6.mHEL<sup>3x</sup></b>	C57BL/6 with membrane bound HEL <sup>3x</sup> protein	<i>b</i>	<i>b</i>	<i>b</i>	Null
<b>BL/6.mHEL<sup>WT</sup>.K<sup>d</sup></b>	C57BL/6 with K <sup>d</sup> transgene crossed with BL/6.mHEL mice. Express both K <sup>d</sup> and membrane-bound HEL.	<i>bd</i>	<i>b</i>	<i>b</i>	Null
<b>SW<sub>HEL</sub></b>	(VH10 <sub>tar</sub> <sup>+/-</sup> x LC2) mice with BCR transgenic B cells specific to HEL protein. Consist of wild-type CD4 and CD8 populations, and some non-HEL binding B cells	<i>b</i>	<i>b</i>	<i>b</i>	Null

<b>Rag2<sup>-/-</sup>.SW<sub>HEL</sub></b>	<i>Rag2<sup>-/-</sup></i> BCR transgenic specific to HEL protein. Consist of HEL-specific B cells, deficient for CD4 and CD8 T cells.	<i>b</i>	<i>b</i>	<i>b</i>	Null
<b>TCR7</b>	<i>Tcrbd<sup>-/-</sup></i> TCR transgenic specific to HEL <sub>74-88</sub> restricted I-A <sup>b</sup> . Wild-type B cells, and CD8 T cells deficient.	<i>b</i>	<i>b</i>	<i>b</i>	Null

## 2.2 Animal related techniques

### 2.2.1 Skin and heterotopic heart transplantation

All surgical procedures were carried under 10-40x magnifications using a light microscope (Carl Zeiss OPM11-FC Thornwood, NY). Anaesthesia was induced and maintained by 1-2 % isoflurane inhalation (Abott Laboratories Ltd, UK). Sterile conditions were observed throughout the procedures. All surgeries were kindly performed by Mr. R. Motallebzadeh or Mr. M. Qureshi.

#### 2.2.1.1 Skin transplantation

During the procedure the animals were placed on a warmed (37°C) operating heat board and received subcutaneous analgesia (Temgesic). Full-thickness tail skin obtained from donor animals was sutured as 1 cm<sup>2</sup> grafts onto the recipients' back. The animals were allowed to fully recover by being placed in 28°C incubator. Rejection was defined as loss of skin grafts three days post transplantation; loss of skin graft within 48 hours of surgery was defined as a technical failure.

#### 2.2.1.2 Heterotopic heart transplantation

Vascularized cardiac grafts were transplanted intra-abdominally according to the procedure described by Corry et al. [276]. Briefly, donor ascending aorta was anastomosed to the recipient abdominal aorta. The donor pulmonary artery was anastomosed to the recipient inferior vena cava. The transplanted hearts function do not contribute to the cardiac output of the recipient, but rather produce aorto-caval shunts.

Heart grafts were assessed by weekly abdominal palpation. Cessation of myocardial contractions was termed as rejection of the grafts and confirmed at the time of explanation of grafts. Grafts were explanted at a predetermined time points after transplantation.

## 2.2.2 Adoptive cell transfer and immunisation

### 2.2.2.1 Adoptive cell transfer

Recipients were warmed for a minimum of 10 minutes at 37 °C prior reconstitution with required populations and numbers of lymphocytes. Cells were suspended in normal saline and injected intravenously (i.v.) via the tail vein.

### 2.2.2.2 Immunisation

Where required, mice were immunised subcutaneously with 50 µg Hen Egg Lysozyme (HEL) purified protein (Sigma-Aldrich Inc.) or 50 µg MHC class I (K<sup>d</sup>) purified protein emulsified in complete Freund's adjuvant (CFA, Sigma-Aldrich Inc.) as a 1:1 dilution, in volume of 200 µl/injection. In some experiments, mice were immunised with BALB/c splenocytes (10<sup>7</sup>) injected subcutaneously.

### 2.2.2.3 Conjugation of HEL to sheep RBCs

HEL antigen was covalently conjugated to sheep RBCs (sRBC) with 1-ethyl-3-(3-dimethylaminopropyl) carbodiimide hydrochloride (EDCI) (Sigma). Briefly, sRBCs cell suspension adjusted to 8-9 x10<sup>9</sup> cells/ mL in PBS was aliquoted into 1 mL volumes and washed twice in 30 mL PBS by centrifugation at 2,300 rpm for 4 minutes at 4°C. After the second wash sRBCs were resuspended in conjugation buffer (0.35 M D-Mannitol, 0.01 M sodium chloride). HEL protein (20 µg) was added to the sRBCs cell suspension and incubated on ice for 10 minutes on a platform rocker. Next, 100 µL of 100 mg/mL EDCI was added and incubated for additional 30 minutes. SRBCs were washed in PBS for four times as described above and re-adjusted to 8-9 x10<sup>9</sup> cells/ mL in PBS.

## 2.2.3 Collection of blood samples and sera preparation

Animals were warmed at 37 °C for a minimum of 10 minutes to dilate the tail veins, and 20-30 µL of blood was collected from the tail vein of each animal using a 25-gauge needle into microvette (Sarstedt). At explant, up to 1 mL of blood was collected from animals by direct cardiac puncture under terminal anaesthesia. Blood was refrigerated overnight at 4°C to allow for clot formation. Blood samples were then centrifuged at 13,000 rpm for 7 minutes, and separated serum was collected by pipetting. Serum complement was heat-inactivated

by incubating the serum in water bath at 56°C for 30 minutes and stored at -20°C until analysis.

## 2.2.4 Organs harvest and storage

Explanted hearts were cut longitudinally, and half embedded in OCT compound (VWR International, Lutterworth, UK), flash-frozen in dry ice, and stored at -80°C. The other half was fixed in 10% formal saline. Spleens were collected in Roswell Park Memorial Institute 1640 tissue culture medium (RPMI, Gibco, Invitrogen, Paisley, UK). In some experiments, the spleens were cut transversally, half a spleen was embedded in OCT compound (VWR international, Lutterworth, UK), flash-frozen in dry-ice and stored at -80°C, while the other half was transferred to RPMI medium for flow cytometry processing.

## 2.2.5 Generation of bone-marrow chimera

For the generation of memory TCR75 CD4 T cells, *Rag2*<sup>-/-</sup> SW<sub>HEL</sub> mice were sub-lethally irradiated (4 Gy) and reconstituted on the same day with TCR75 bone marrow cells to generate *Rag2*<sup>-/-</sup> SW<sub>HEL</sub> x TCR75 mice (figure 5). Chimerism was confirmed four weeks after the transfer of TCR75 bone marrow cells by flow cytometry analysis. Chimeric mice were immunised twice one week apart with 5µg K<sup>d</sup> protein emulsified in CFA at 1:1 ratio subcutaneously and CD4 memory was confirmed by flow cytometry 2 weeks later. TCR75 CD4 T cells (10<sup>3</sup>) were isolated by autoMACS and transferred to *Rag2*<sup>-/-</sup> SW<sub>HEL</sub> recipients of mHEL.K<sup>d</sup> hearts. During a typical CD4 T cell response different subpopulations of CD4 T cells may generate during different overlapping phases. Therefore, CD4 T cells isolated one week after the second challenge may contain a heterogeneous population of effector and early memory CD4 T cells [277], [278]. Thus, TCR75 CD4 T cells isolated by MACS will be referred to as 'early memory' CD4 T cells for the remainder of this thesis.

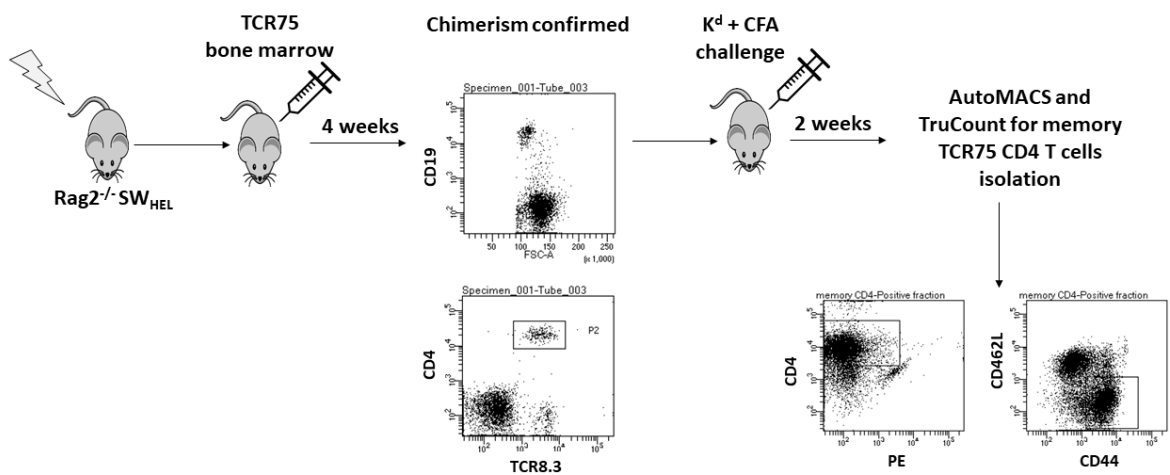


**Figure 5. Early memory TCR75 CD4 T cells generation.** *Rag2*<sup>-/-</sup>.SW<sub>HEL</sub> mice were irradiated 4 Gy and reconstituted on the same day with  $1.5 \times 10^7$  TCR75 bone marrow cells. Following 4 weeks chimerism was confirmed by flow cytometry for the detection of both SW<sub>HEL</sub> B cells (FITC), and TCR75 CD4 T cells (CD4 APC, TCR 8.3 PE), after which mice were challenged with K<sup>d</sup> protein emulsified in CFA intraperitoneally. Two weeks later, CD4 T cells were purified by autoMACs using anti-CD4 beads, and numbers of early memory CD4 T cells were labelled with antibodies specific to CD44 and CD62L and frequencies were determined by TruCount flow cytometry.

## 2.3 Tissue and cell related techniques

### 2.3.1 Single cell suspensions from spleens and bone marrow

Spleens were mashed using the rubber end of a 1 mL syringe plunger and teased through a 40 µm cell strainer (BD Biosciences). Splenocytes were re-suspended as a single cell suspension in 10 mL of Hank's Balanced Salt Solution (HBBS) (Gibco®, Life Technologies Ltd.) enriched with 2% Foetal Calf Serum (FCS) (Sigma-Aldrich Inc.). For bone marrow processing, tibias and femurs of sacrificed animals were flushed out with HBBS using a needle and a syringe. Isolated cells were teased through a 40 µm cell strainer (as above) and re-suspended as a single cell suspension in 10 mL HBBS (Gibco®) enriched with 2% FCS.

All isolation and preparation of cells were performed in Microflow SE laminar flow hood (Bioquell, Andover, Hampshire, UK). All centrifugation steps were performed in a Howe 6K10 Centrifuge (Sigma Laboratory Centrifuges GmbH, Osterode am Harz, Germany) at 1200 revolutions per minute (rpm) for 7 minutes at 4°C, unless otherwise specified.

### 2.3.2 Single cell suspension from the heart

Hearts obtained from 9 – 14 days old neonatal mice were rinsed with HEPES buffered Dulbecco modified Eagle medium (DMEM) (Gibco®) in order to wash blood clots. Hearts were minced into 1-2mm pieces using a sterile scalpel, and transferred into a bijoux tube containing collagenase digestion mix (1 mg/mL collagenase A [Roche], 1 mg/mL DNase1 [Roche] and 2% FCS [Sigma] in DMEM) and incubated for 30 minutes in a 37°C water bath. Next, the digested tissue was sieved through a 40 µm strainer and incubated for a further 15 minutes. Collagenase reaction was stopped by adding ice-cold working medium (100 IU/mL penicillin-streptomycin [Sigma-Aldrich Inc.], 2mM L-Glutamine [Sigma-Aldrich Inc.], 0.05 mM 2-mercaptoethanol, and 10% FCS in DMEM) and the cell suspension was centrifuged. Supernatant was discarded, and cell pellet was further digested by adding 3 mL of Trypsin (0.5 g/mL)/ EDTA (0.2 g/mL) solution (Sigma-Aldrich Inc.) and incubating cell suspension for 10 minutes in a 37°C water bath. The digestion was stopped by adding ice-cold working medium, centrifuged, and resuspended in 1 mL of MACS buffer for endothelial cells separation as described section 2.5.1.

### **2.3.3 Cell culture and maintenance**

Endothelial cells derived from neonatal hearts were isolated as described above and resuspended in a growth medium (HEPES buffered DMEM supplemented with 10% FCS, 100 IU/mL penicillin/Stretomycin, 2mM L-Glutamine, 1mM sodium pyruvate (Sigma-Aldrich Inc.), 1/1000 non-essential aminoacids (Sigma-Aldrich Inc.), and endothelial cell growth factor [Sigma-Aldrich Inc.]), and transferred to a tissue culture flask (Nunc™, Thermo Scientific Ltd.) pre-coated with 1% Gelatin (Sigma-Aldrich Inc.) in PBS. Cell culture was incubated overnight in humidified tissue culture incubator at 37°C supplemented with 5% CO<sub>2</sub>. The next day, non-adherent cells were removed, and medium was changed every 2 days. Once the culture reaches 80-90% confluency, cells were detached by rinsing the cells in sterile PBS, and adding 3 mL of Trypsin-EDTA solution (Sigma-Aldrich Inc.) and incubated at 37°C for a maximal of 3 minutes. The digestion is stopped by adding excess growth medium, and centrifugation. The cell pellet was then resuspended in growth medium and passaged in a fresh 1% Gelatin pre-coated flask. Endothelial cells were passaged a maximum of 3 times.

## **2.4 In vitro cellular assays**

All in vitro cellular assays were performed on 80-90% confluent endothelial cells (passage 3). Cells were starved for 16 – 19 hours in DMEM medium containing 0.2% FCS and lacking growth factor before performing the designated assay. All incubation steps were done in humidified incubator at 37°C, supplied with 5% CO<sub>2</sub>. Sterile techniques were maintained throughout.

### **2.4.1 Endothelial cell migration**

Endothelial cells were seeded in 6-well plate culture dishes pre-coated with 1% gelatin following the third passage. After reaching ~90% confluence, cells were starved for 24 hours (as described above). A rectangular lesion was made across the well diameter using a 1 mL sterile pipette tip, and cellular monolayer was washed once in starving medium and serum of interest was added in a dilution of 1:100 in starved medium and incubated for further 24 hours. Cells were then washed with PBS and fixed with paraformaldehyde (Cytofix kit, BD Biosciences) for 30 minutes at room temperature. Cells were then washed twice in PBS, and stained with Crystal Violet 0.05% for 1 minute, rinsed twice with PBS, and allowed to dry. Five fields were analysed for each well at 4x magnification, and images were photographed

using an ORCA-ER digital camera (Hamamatsu Photonics, Japan) and the scratch area covered with cells was measured using CellSens imaging software (Olympus, Japan).

#### **2.4.2 Western blot**

Endothelial cells were grown to ~90% confluency in 8 cm diameter Petri dishes pre-coated with 1% gelatin. Following cells starvation for 24 hours (as described above), serum of interest (diluted 1:100 in starving medium) was added to designated wells, and cells were incubated for 30 minutes in humidified incubator at 37°C. The supernatant was removed, and cells were washed once with PBS and lysed with CelLytic M reagent (Sigma) containing 1X protease inhibitor cocktail (Roche) for 15 minutes at room temperature. Harvested cells were heated for 10 minutes at 100°C in SDS loading buffer, electrophoresed on 20% polyacrylamide gel (approximately 10 ug of cell lysate per lane quantified using the protein quantification kit-rapid as described by the manufacturer (Fluka, Dorset, UK)), and transferred to a polyvinylidene difluoride membrane. The membrane was blocked in 5% non-fat dry milk in PBS containing 0.1% Tween 20 (hereafter blocking buffer) for 1 hour at room temperature, the membrane was cut into stripes corresponding to protein size of interest. The membrane stripes were incubated overnight at 4°C with phosphorylated-Akt (Ser473) mouse mAb (Cell Signalling Technology) diluted to 1:1000 in blocking buffer, and mouse anti-GADPH (Abcam) diluted to 1:1000 as a loading control. Membranes were washed with PBS containing 2.5% Tween 20 followed by incubation in polyclonal HRP-conjugated rabbit anti-mouse IgG (Abcam) for 1 hour at 37°C. The blots were subsequently washed as before, developed and enhanced by chemiluminescence (ECL, Amersham Pharmacia).

#### **2.5 General Flow cytometry protocol**

Flow cytometry was performed on single cell suspension of lymphocytes in 96-well U-bottomed plates (BD, Franklin Lakes, NJ). All incubation steps were done in the dark for 30 min at 4°C. Cells were blocked with 1/200 anti-mouse CD16/CD32 (table 5) in FACS buffer (PBS + 1% BSA + 0.1% azide) for 30 minutes at 4°C. All washing steps were done with 150 µl/well of FACS buffer, and dead cells were stained with either exclusion dye 7-AAD (BD Pharmingen, San Diego, CA) or Fixable Viability Dye (eFluor® 780, eBiosciences). Primary and subsequent secondary monoclonal antibodies (mAbs) were added according to dilutions in table 5.

Prior to analysis, cells were transferred to flow cytometry tubes (BD Falcon, Franklin Lakes, NJ) and Labeled cells were identified on a FACSCanto II flow cytometer. Data was analysed using FLOWJo software (Tree 19 Star Inc., Ashland, OR).

### **2.5.1 Magnetic-activated cell sorting (MACS)**

For endothelial cell isolation, single cell suspensions derived from the organ of interest were resuspended in 1 mL of MACS buffer (Miltenyi Biotec) and Fc gamma receptors were blocked for 30 minutes on ice. Depending on the cell population of interest, suitable antibodies (table 5) were diluted in MACS buffer and added to the suspension and incubated in the dark for 30 minutes on ice (for endothelial cell isolation a mixture of biotinylated antibodies specific to CD31, CD105, and isolectin B4 were added; for K<sup>d</sup>-specific splenocytes 50  $\mu$ L cells were incubated with K<sup>d</sup> tetramers labelled with either APC or FITC and incubated for 30 minutes, followed by incubation with both anti-APC and anti-FITC magnetically labelled microbeads (Miltenyi Biotec). The use of K<sup>d</sup> tetramers bound to two different fluorochromes provides a higher degree of specificity and binding efficiency [279]. For CD4 T cells isolation cells were incubated with CD4 magnetic beads (Miltenyi Biotec)). In cases where biotinylated antibodies were used, 20  $\mu$ L of anti-biotin magnetic beads (Miltenyi Biotec) was added per  $10^7$  of cells suspension and incubated for 15 minutes at 4°C in the dark. Cells were washed in MACS buffer as before and separated by autoMACS Column machine (Miltenyi Biotec) using Possel program and the positive fraction was collected.

### **2.5.2 Trucount™ analysis for cell quantification**

When the absolute number of a cell subset is required, a 20 $\mu$ L aliquot of single cell suspension was stained to label the populations of interest with corresponding antibodies after blocking with purified anti-CD16/32 mAb and dead cell exclusion dye 7-AAD (BD Pharmingen). Prior acquiring on the flow cytometer, the cells were transferred from 96-well plate to a Trucount™ tube (BD Biosciences) containing known number of fluorescent beads. Cell populations of interest were enumerated by Trucount™ analysis according to manufacturer's instructions (BD Biosciences, San Jose, CA).

The absolute number of cells of interest was calculated according to manufacturer instructions using the following formula:

$$\text{Number of cells per } \mu\text{L in original cell suspension} = \frac{\text{Number of gated cells of interest}}{\text{Number of Trucount™ beads recorded}} \times \frac{\text{Number of Trucount™ beads in tube}}{\text{Volume } (\mu\text{L}) \text{ obtained from original sample}}$$

To calculate the percentage of H-2K<sup>d</sup>-specific B cells with GC phenotype the following formula was utilised:

$$\% \text{ H-2K}^{\text{d}}\text{-allospecific GC B cells} = \frac{\text{Number of H-2K}^{\text{d}}\text{-allospecific GC B cells}}{\text{Number of H-2K}^{\text{d}}\text{-allospecific B cells}} \times 100$$

**Table 5. Antibodies used in this work**

Primary antibody			Secondary antibody		
Antibody (clone), source	Dilution	Conjugate	Antibody, Source	Dilution	Use
Anti-C4d (16D2), Abcam Inc., Cambridge, Massachusetts	1:100	-	Biotinylated rabbit polyclonal anti-rat IgG, Abcam	1:500	IHC
Rat anti-mouse CD68 (ER-HR3), Abcam	1:20	-	Biotinylated rabbit polyclonal anti-rat IgG, Abcam	1:500	IHC
Anti-NK1.1 (PK136), in house	1:100	-	Mouse on mouse polymer kit (ab127055), Abcam		IHC
Rat anti-B220 (RA3-6B2), BD Pharmingen™	1:200	APC	-	-	Confocal microscopy
Rat anti-B220 (RA3-6B2), BD Pharmingen™		-	Cy3 goat anti-rat IgG, Jackson Labs	1:500	IF
PNA, Vector laboratories Inc	1:200	FITC	-	-	IF
Anti-mouse H-2K <sup>d</sup>	1:50	Biotin	Streptavidin TRITC	1:300	IF
Rat anti-GL7 (GL7), BD Pharmingen™	1:100	FITC	-	-	IF, confocal microscopy
Rat anti-MAdCAM-1 (MECA-367), Abcam	1:100	Biotin	Streptavidin Alexa Fluor-555	1:500	Confocal microscopy
Rat anti-CD4, (GK1.5) BD Pharmingen™	1:200	Biotin	Streptavidin Alexa Fluor-555	1:500	Confocal microscopy
Goat anti-mouse IgG (F9006), Sigma-Aldrich	1:500	FITC	-	-	Confocal microscopy
Anti-CD31, BD, Pharmingen™	1:100	Biotin	-	-	MACS
Anti-CD105, eBioscience	1:200	Biotin	-	-	MACS
Anti-isolectin B4 (B-1205), Vector	1:25	Biotin	-	-	MACS
Rat anti-mouse CD16/CD32, (2.4G2), BD Pharmingen™	1:200	-	-	-	Fc receptor block
Rat anti-CD19, Miltenyi	1:10	PerCP-Vio700	-	-	Flow cytometry
Rat anti-GL7 (GL7), BioLegend	1:1000	PE	-	-	Flow cytometry
Rat anti-FAS (Jo2), BD Pharmingen™	1:200	PE-CY7	-	-	Flow cytometry
Rat anti-B220, BD Pharmingen™	1:200	FITC	-	-	Flow cytometry

<b>Anti CD4, BD Pharmingen™</b>	1:100	V500	-	-	Flow cytometry
<b>Anti-PD1, BD Pharmingen™</b>	1:200	BV421	-	-	Flow cytometry
<b>Anti-CXCR5, BioLegend</b>	1:200	PE-Dazzle	-	-	Flow cytometry
<b>Anti-CD44, BioLegend</b>	1:200	APC-Cy7	-	-	Flow cytometry
<b>Anti-CD62L, BioLegend</b>	1:200	Cy5.5	-	-	Flow cytometry
<b>Protein, source</b>					
<b>HEL protein (produced in house)</b>	1:1000	Biotin	Streptavidin Alexa Fluor-555	1:300	Confocal microscopy
			Streptavidin APC (Thermo Fisher Scientific)	1:500	Flow cytometry
<b>K<sup>d</sup> tetramer, NIH Core Tetramer facility, Atalanta, GA</b>		APC or FITC or purified	-	-	Flow cytometry

## 2.6 Assay of humoral alloimmunity

### 2.6.1 Enzyme Linked Immunosorbent Assay (ELISA)

Serum samples were collected from experimental mice at weekly intervals and analysed for binding to H-2K<sup>d</sup> or HEL proteins. To do so, flat-bottomed 96-well ELISA plates (Immulon 4HBX, Thermo, Milford, MA) were coated with antigen (H-2K<sup>d</sup> (produced in house), HEL<sup>WT</sup> (Sigma-Aldrich) or HEL<sup>3x</sup> (gifted by Prof. Brink)) at 0.5 µg/mL diluted in bicarbonate buffer Na<sub>2</sub>CO<sub>3</sub>-NaHCO<sub>3</sub> [pH 9.6]) was distributed at 50 µL per well and incubated overnight at 4°C. The next day, plates were washed (x6) with 0.05% tween in PBS (Sigma, Poole, UK) (hereafter referred to as 'wash buffer') and was dried by blotting against clean tissue. Non-specific binding sites were blocked by adding 200 µl/well 5% Marvel dried skimmed milk powder in PBS (blocking buffer), Premier International Foods, UK) for 2 hours at 37°C. Serum samples were diluted 1:9 in blocking buffer and added as 50 µL/well. Serial 1/3 dilution was carried out down the 8 rows of the plate, and incubated for one hour at 37°C. Next, biotinylated rabbit F(ab')<sub>2</sub> anti-mouse IgG (diluted 1/1000 in block; STAR11B; AbD Serotec, Oxford, U.K.) was added and incubated for 1 hour at 37°C. Bound IgG was detected by the addition of ExtrAvidin Peroxidase conjugate (diluted 1/1000 in block; Sigma, Poole, U.K.). In order to generate a colorimetric signal, Sure Blue substrate (KPL, Gaithersburg, MD) was added to each well and reaction was stopped by the addition of 0.2 M H<sub>2</sub>SO<sub>4</sub>. Plates were read in FLUOstar OPTIMA plate reader (BMG Labtech, Aylesbury, U.K.) at 450nm.

In experiments aiming at detecting antibody isotypes, ELISA was performed as described above, however serum antibodies bound to coated proteins were first incubated with biotinylated isotype specific monoclonal antibodies (diluted 1/1000, Abcam) in block, followed by incubation with ExtrAvidin Peroxidase conjugate as described earlier.

For each sample, an absorbance vs. dilution curve was plotted, and the area under the curve (AUC) was calculated [280]. Results were expressed as the percentage of positive control serum which was assigned an arbitrary value of 100% (sera pooled from BL/6 animals transplanted with BALB/c skin or heart grafts collected 5 weeks post-transplantation). Pooled sera from naïve BL/6 or TCR<sup>-/-</sup> animals were used as a negative control (figure 6). For experiments where anti-HEL IgG response was investigated, 1/1000 HyHEL10 anti-HEL IgG monoclonal antibody was used as a positive control (Absolute Antibody, Oxford, UK) (for

HEL<sup>WT</sup> antigen), or hyperimmune serum obtained from mice immunised with HEL<sup>3x</sup> protein (for HEL<sup>3x</sup> antigen) gifted by Prof. Brink's group.

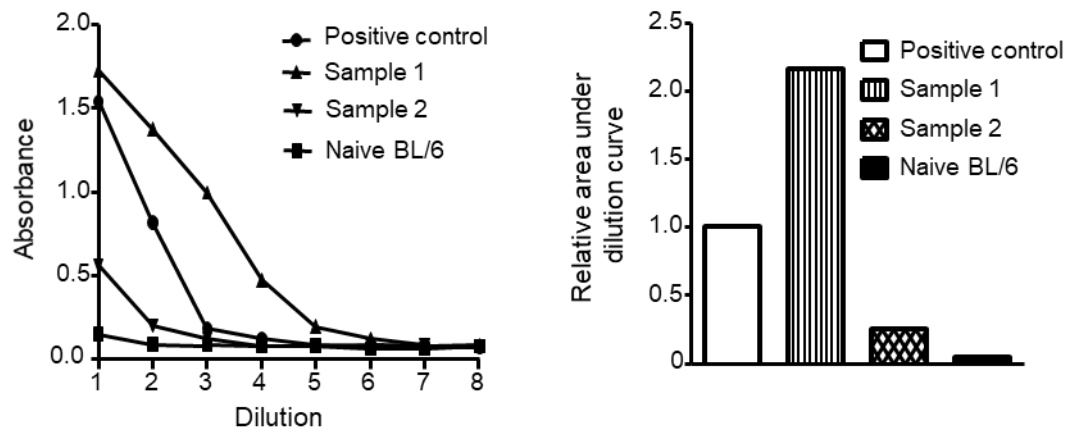


**Figure 6. Calculation of relative antibody serum titres.** Typical absorbance versus dilution curves obtained from anti-H-2K<sup>d</sup> IgG ELISA assay of serum samples read at 450 nm (left). Area under the curve of antibodies were plotted in comparison to positive control serum which was assigned an arbitrary valued of 100 (right).

## 2.6.2 B cell ELISPOT

MultiScreen 96-well Filter Plates (Millipore, Billerica, MA, USA) were coated with 100  $\mu\text{L}$ /well of purified 5  $\mu\text{g}/\text{mL}$  K<sup>d</sup> (produced in house), HEL<sup>WT</sup>, or HEL<sup>3x</sup> 5  $\mu\text{g}/\text{mL}$  (Sigma-Aldrich) diluted in sterile bicarbonate buffer Na<sub>2</sub>CO<sub>3</sub>-NaHCO<sub>3</sub> [pH 9.6], and incubated for 2 hours at 37°C, 5% CO<sub>2</sub>. Excess Ag was washed 5 times with sterile PBS + 0.5% BSA (PBS buffer), and 200  $\mu\text{L}$ /well of full medium (RPMI culture medium + 10% FCS, 1% penicillin-streptomycin [Sigma, Poole, UK] + 1% L-Glutamine 200mM [Sigma] and + 0.1% 50mM 2mercaptoethanol [2ME; Sigma]) was added. Single cell suspensions from spleen and BM were prepared as previously described and resuspended at 1 x 10<sup>7</sup>/mL in full medium and added to the plate in triplicates of 1x10<sup>6</sup>, 1x10<sup>5</sup> and 1x10<sup>4</sup> cells per well. The plates were incubated for 18 hours at 37°C, 5% CO<sub>2</sub>, ensuring the plate was not moved during this time. On the next day, plates were washed and Biotinylated Rabbit (ab')<sub>2</sub> anti-mouse IgG (STAR11B, AbD Serotec, Oxford, UK) was diluted to 1  $\mu\text{L}/\text{mL}$  in in PBS buffer, and 100  $\mu\text{L}$  of that dilution was added per plate for 2 hours at 37°C. Next, excess antibody was washed (x6) with wash buffer, blotted against clean tissue, and the plate was incubated with 100  $\mu\text{L}/\text{well}$  ExtrAvidin Peroxidase conjugate (Sigma, Poole, UK) 1  $\mu\text{L}/\text{mL}$  in PBS buffer for 2 hours at RT. During incubation time, developing solution was prepared by adding 1 tablet of 3-amino-9-ethyl-carbazole (AEC; Sigma, Poole, UK) to 2.5ml dimethylformamide (DMF; Sigma, Poole, UK), mixed well, and 1 mL of the resulting solution was transferred to 19 mL acetate buffer, filtered through a 0.2 $\mu\text{m}$  filter (Sartorius Stedim, Surry, UK) and 10  $\mu\text{L}$  of 30% hydrogen peroxide solution (Sigma, Poole, UK), prepared in distilled water. The plate was washed (x6) and spots were developed by incubation with 100  $\mu\text{L}/\text{well}$  of the above developing solution in the dark at RT till spots appeared. The plate was washed (x3) with distilled water and left overnight in the dark to dry, and the plates was read on an AID<sup>TM</sup> Elispot Reader version 3.5 (Autoimmun Diagnostika, Strasberg, Germany).

## 2.7 Bio-layer interferometry for affinity measurement:

### 2.7.1 Principle overview:

Biolayer interferometry (BLI) is a novel label-free technology for quantifying macromolecules, and studying molecular kinetics [281]. In this technology, a layer of molecules is attached to the extremity of a biosensor tip (i.e., ligand), the sensor is then exposed to a test sample containing macromolecules of interest (i.e., analyte, figure 7). BLI is equipped with a white light source emitting down the sensor and reflects back to a spectrometer to record the spectral shift ( $\Delta\lambda$ ) resulting from the accumulation of bound analyte at the biosensor tip. Emitted white light is reflected from two surfaces: at the optical fibre tip (i.e., internal reference layer), and at the buffer (Figure 7). The spectral shift generated from the increased number of bound molecules to the biomolecular layer is interpreted by an analysis software and molecular kinetics can be determined from generated binding curves [281].

BLI technology offers a number of advantages over conventional kinetic systems. For instance, the sensors are moved and dipped into 384- or 96-wells plate format without requiring a microfluidics system; and thus, different samples can be studied simultaneously [282]. Furthermore, the unique feature of having an internal reference layer, and because spectral shift depends only on the amount of binding /or decaying of molecules bound on the optical fiber, it allows the study of molecular interactions in crude samples regardless of the surrounding medium [283].

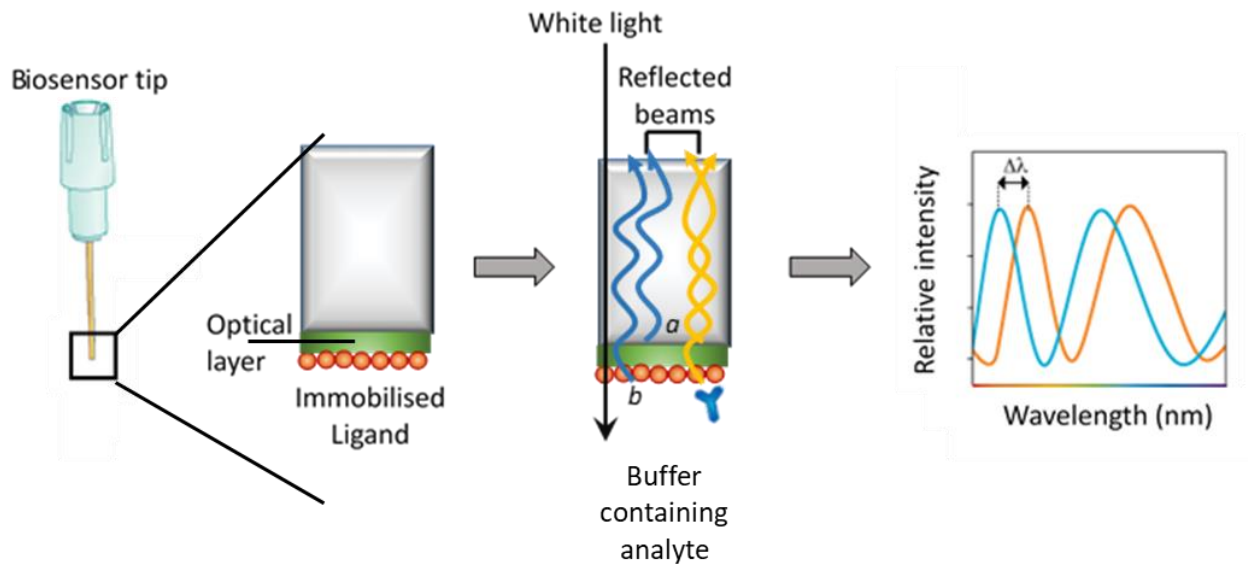


**Figure 7. Schematic representation of BLI principle.** White light beam travel through the optical fibre and is reflected at two surfaces: at the fibre and biomolecular layer (*a*), and at the biomolecular layer and buffer interface (*b*). The resulting spectral shift ( $\Delta\lambda$ ) is then recorded and binding kinetics are interpreted. (Reproduced from [368] et al., with permission from Elsevier).

### 2.7.2 MHC-I and HEL proteins biotinylation, purification, and validation

Purified MHC-I ( $K^d$ ), HEL<sup>WT</sup>, and HEL<sup>3x</sup> proteins were biotinylated using EZ-Link Sulfo-NHS-LC-Biotinylation Kit (Thermo Scientific, Rockford, IL) in PBS following the manufacturer's recommendations. Excess labelling reagent was removed by 7 kDa Zeba spin desalting columns (Thermo Scientific). The concentration of the biotinylated proteins were determined using HABA/avidin assay (Thermo Scientific) and absorbance was determined at 500 nm using Helios-alpha spectrophotometer (Unicam LTD, UK). The ratio of biotin:protein was 3:1 for  $K^d$ , and 2:1 for HEL<sup>WT</sup> and HEL<sup>3x</sup> proteins.

### 2.7.3 BLI protocol

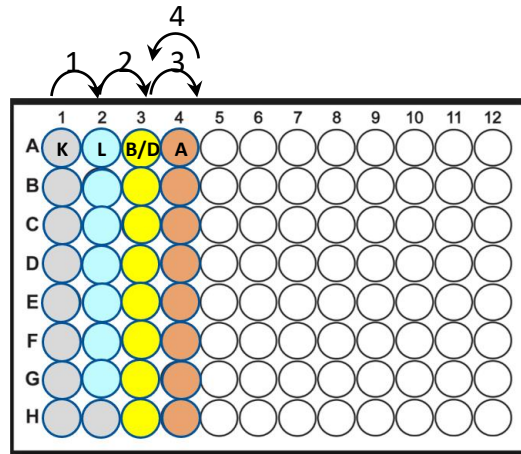
Off-rate screening was performed on RED96-platform instrument ForteBio (Menlo Park, CA, USA). All experiments included pre-equilibration step where streptavidin coated biosensors (ForteBio) were dipped in 1× PBS buffer containing 0.1% BSA, 0.02% Tween-20, and 0.02% NaN<sub>3</sub> (pH 7.4); hereafter referred to as 'kinetics buffer' for 10 minutes (figure 8A). In all experiments data were collected at 27°C with agitation at 1000 rpm. Biotinylated MHC class I  $K^d$  antigen (1.25 µg/mL) was captured on biosensors at a maximal threshold of 1.5 nm in kinetics buffer. After ligand capture, sensors were blocked for 60 seconds in wells containing naive serum obtained from BL/6 mice or *Rag2*<sup>-/-</sup>.SW<sub>HEL</sub> mice at 1:20 or 1:40 dilutions. After blocking, sensors were transferred to corresponding wells containing immune serum diluted in kinetics buffer for association over 1000 seconds, followed by transfer to dissociation wells containing diluted naive serum over a period of 1000 seconds. Each biological sample was tested at two dilutions: 1:20 and 1:40. Typical kinetics curves and sample distribution are illustrated in figure 8. It is worth mentioning that in this experiment it was not practical to load serum-derived antibody (as ligand). This is because recipients of BALB/c heart transplantation may have generated non- $K^d$  IgG antibodies and therefore, the exact concentration  $K^d$ -antibody will remain difficult to achieve. Therefore, two dilutions of test sera were used following sensor blocking in naive serum as described above.

### 2.7.4 Processing kinetics data

Dissociation rate constants for each sample were calculated by applying a 1:1 interaction model (specifications: global fitting). The sensograms were double referenced with both reference biosensor (no biotinylated MHC class I  $K^d$  antigen loading) and sample reference (naive BL/6 serum, figure 8B). In experiments where multiple analyte concentrations are

being tested, dissociation curves that did not perfectly match the 1:1 model were excluded (i.e.,  $R^2$  value less than 0.95).  $R^2$  is defined as the coefficient of determination, and is an estimate to indicate how well the model and experimental data are correlated, a value close to 1.0 is considered a perfect fit [284]. All data analyses were performed on ForteBio Data analysis 7.0.1.5 (ForteBio).

A)



B)

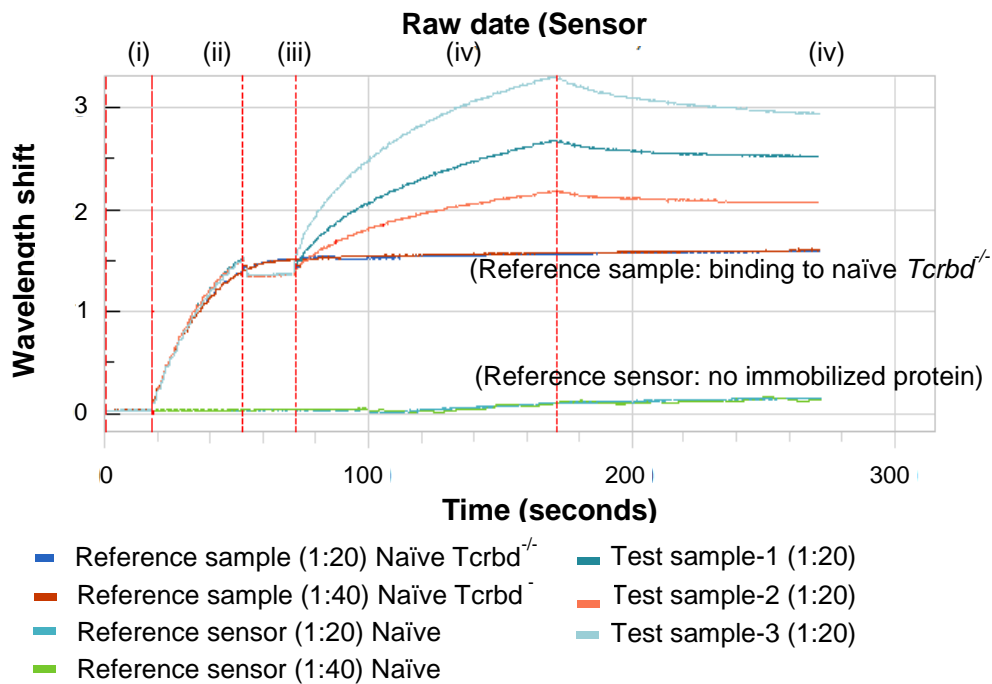


**Figure 8. Schematic presentation of sample distribution in 96-well format.** A) Kinetics buffer (K) containing wells were used for sensor pre-equilibration, followed by loading (L) streptavidin sensors with designated proteins. Sensors were then blocked in either 1/20 or 1/40 naïve serum (B) before being transferred to the association wells (A) containing 1/20 or 1/40 test serum. Antibody dissociation (D) was enabled by immersing the biosensors back again in the blocking wells. The direction of arrows indicated biosensor movement throughout the plate. B) Representative raw data of binding kinetics of test sera. i) sensor pre-equilibration, ii) loading with biotinylated protein, iii) blocking with naïve serum (diluted at 1:20 or 1:40), iv) association with test serum (diluted at 1:20 or 1:40), and v) dissociation in naïve serum at a dilution equivalent to test serum. Sonograms were corrected for inter-step alignment on Y-axis, and baseline drift was corrected by subtracting the average value obtained from reference sample (protein loaded sensor exposed no naïve serum) and reference sensor (un-loaded sensor exposed to naïve serum).

## 2.8 Histology

### 2.8.1 Evaluation of allograft vasculopathy and parenchymal damage

Paraffin fixed sections were stained by the Department of Pathology, Papworth Hospital, Cambridge, UK with either Haematoxylin and Eosin (H&E) or elastin van Gieson (EVG). The severity of parenchymal allograft damage was scored on H&E paraffin sections by a cardiac histopathologist, blinded to the study groups. The ISHLT graft damage severity scale was employed as a reference [3] where: 0, no parenchymal damage; 1, <30% parenchymal damage; 2, 30-60% parenchymal damage; 3, >60% parenchymal damage. Degree of luminal stenosis was assessed on EVG paraffin sections by morphometric analysis, using digital imaging software (Cell®, Olympus, Japan). All elastin-positive vessels in each section were evaluated, with approximately 10 vessels/heart were analysed (figure 9).

Luminal stenosis was calculated as follows:

$$\text{Percentage cross-sectional area luminal stenosis} = \frac{\text{Area within internal elastic lamina (IEL) - area of lumen} \times 100}{\text{Area of IEL}}$$

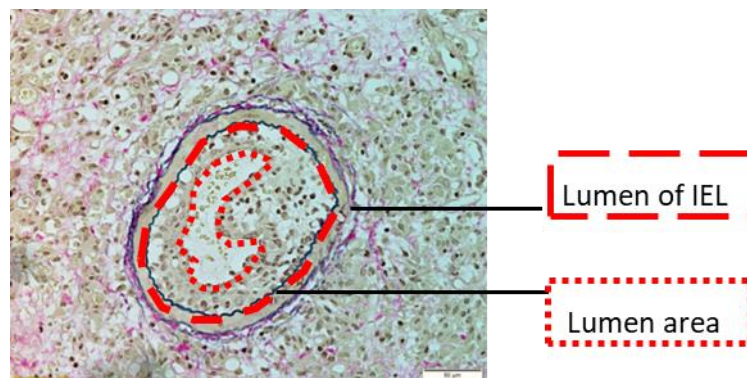


**Figure 9. Representative micrograph of heart vasculopathy stained with EVG.**

## **2.8.2 Immunohistochemistry and immunofluorescence**

Frozen tissues were cut into 7µm serial sections and placed onto Poly-L-Lysine coated slides (Sigma Aldrich Inc.), and fixed in chilled acetone for 10 minutes. Sections were then air dried for 30 minutes and stored at -80°C. Prior to staining, slides were rehydrated for 10 minutes in 1%PBS, and if biotinylated antibodies are applied, endogenous biotin and avidin were blocked by incubating tissue sections with avidin and biotin blocking kit solutions (Vector Laboratories Inc.), each for 15 min and washed in between with 1% PBS for 5 minutes. All washing steps were done with 1%PBS three times, each for 5 minutes. Primary and secondary antibodies used for staining are illustrated in table 5.

### **2.8.2.1 Immunohistochemistry staining**

Complement C4d deposition was assessed on heart frozen sections using purified rat anti-mouse C4d monoclonal antibody for 1 hour at room temperature. After washing excess antibody, secondary biotinylated-polyclonal rabbit anti-Rat antibody was incubated for 1 hour at room temperature. Sections were visualized using chromogen 3,3-diaminobenzidine (Sigma-Aldrich, St Louis, Missouri) and counterstained with Harris hematoxylin (BDH, London, United Kingdom). NK1.1 cells deposition was detected using unconjugated mouse anti-mouse PK136 (produced in house) and the staining was developed using mouse on mouse polymer IHC kit (ab127055, Abcam) following manufacturer's protocol.

Formalin-fixed sections were used to detect macrophages using anti CD68 because of excellent tissue morphology. Briefly, antigen retrieval (including de-paraffinization) was performed using DAKO Target retrieval solution Low pH (DAKO Corporation, Carpinteria, CA). Using Dako PT link system (DAKO), temperature ramps up from 20°C to 96°C for 20 mins, then cooled down to 65°C. Following quenching with endogenous peroxidase, the slides were washed in PBS, blocked for 20 minutes, followed by standard procedures of avidin / biotin blocking as described above. After incubating the primary anti-CD68 for 1 hour at room temperature, excess antibody was washed three times with 1% PBS, each for 5 minutes, and secondary biotinylated antibody was added. The sections were then incubated in VECTASTAIN elite ABC reagent (Vector Laboratories) for 30 minutes and visualized by DAB

using standard procedures. Finally, the sections were counterstained with Harris hematoxylin (BDH).

### **2.8.2.2 Immunofluorescence staining**

In order to determine GC structures, frozen spleen sections were incubated with two primary antibodies (anti-GL7-FITC and purified anti-B220, or anti-PNA-FITC and purified anti-B220) for one hour in a dark humidified chamber. After washing excess antibody, secondary goat anti-rat IgG-Cy3 was added and incubated for one hour in the dark. Sections were washed, counterstained with 20% Harris' haematoxylin for 20 seconds, and mounted in FluorSave™ reagent (Calbiochem®, Merck-Millipore). Sections were viewed using an IX81 microscope with a 20X0, 70 UplanApo Lense (Olympus, Japan). Images were acquired with CellR 2.6 software (Olympus Imaging Solutions, Germany).

Co-localization of T cells within GCs was determined by incubating the primary antibodies anti-CD4 biotin and anti-B220-APC overnight at 4°C. The next day, excess antibody was washed, and secondary streptavidin-AF-555 was incubated for 1 hour at room temperature in humidified chamber. After washing excess antibody, a third antibody (rat anti-mouse GL7-FITC) was added and incubated for 1 hour at room temperature in humidified chamber. After washing excess antibody, sections were counterstained and mounted with Vectashield's hard set mounting medium with 4', 6- diamidino-2-phenylindole (DAPI) (Vector Laboratories Inc.). Class-switched IgG<sup>pos</sup> extrafollicular response was visualized using triple antibody procedure using the antibodies anti-MadCam-1-biotin, anti-B220-APC, anti-mouse IgG-FITC and the secondary antibody streptavidin-AF-555. Confocal microscopy was performed using a Leica TCS SP5 immunofluorescence microscope (Leica Microsystem, Mannheim, Germany). Separate images were collected for each fluorochrome and overlaid to obtain a multicolour image using a Leica SP5 confocal microscope using LAS AF software, version 2.7.2.9586 (Leica Microsystems, Wetzlar, Germany).

### **2.8.2.3 Quantification of germinal centres**

The presence of germinal centres in the spleens was quantified by staining with B220 and PNA or B220 and GL7. Minimal number of total follicles counted per spleen was 20 – 25

follicles. The percentage of follicles with GCs was calculated according to the following formula:

Percentage of GCs =

$$\frac{\text{Number of PNA}^+ \text{ or GL7}^+ \text{ GCs}}{\text{Total number of B220}^+ \text{ follicles}} \times 100$$

## 2.9 Statistical analysis

Mann-Whitney U test was used for analysis of non-parametric data and log-rank test for analysis of Kaplan-Meier survival curves. Student t-test was used to analyse parametric data. Two-way ANOVA was used to compare antibody titers depicted as area under the curve. Statistical analyses were performed using GraphPad Prism version 5.02 (GraphPad Software Inc., San Diego, CA, USA). *P* values less than 0.05 were considered statistically significant.

## Chapter 3: Development and characterisation of murine AMR model\*

\*Additional control groups performed during the development of the murine model were performed by a colleague (M. Chabra) and are detailed in a manuscript (submitted for reviewing) where I am a joint first author. All results presented in this thesis are the author's own experimental work. Reproduced data from control groups used for comparison purposes were noted in text.

### 3.1 Introduction:

#### 3.1.1 The number of precursor alloantigen-specific CD4 T cells correlate with rejection kinetics

The generation of murine TCR-transgenic CD4 T cells with defined alloreactivity have helped in investigating different aspects of the alloimmune response *in vivo*. Bucy and colleagues [285] showed that naive BL/6 mice that were adoptively transferred with allospecific TCR75 CD4 T cells (specific for H-2K<sup>d</sup><sub>54-68</sub> epitope presented by MHC class II I-A<sup>b</sup>, figure 10) rejected heart allografts that expressed H-2K<sup>d</sup> MHC-I antigen (BL/6.K<sup>d</sup>), with the speed of rejection dependent upon number of TCR75 T cells transferred (Figure 11). Bucy's experiments did not assess humoral alloimmunity, but because TCR75 CD4 T cell recognise donor MHC class I alloantigen via the indirect pathway, one would anticipate that the transferred cells would have acted as helpers for production of alloantibody.

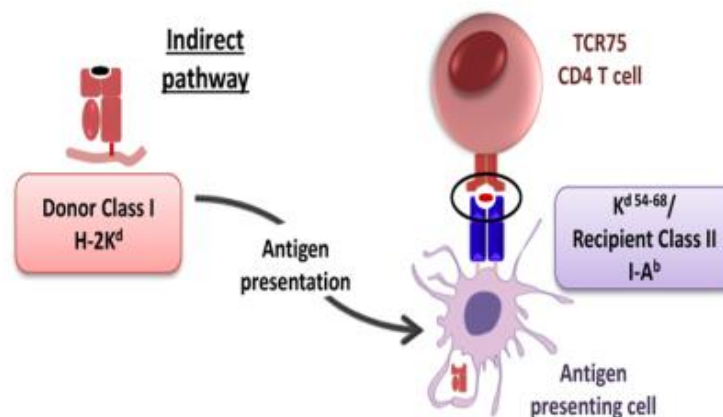


**Figure 10. Antigen specificity of TCR75 CD4 T cells.** TCR75 CD4 T cells are capable of the indirect allorecognition of a dominant allopeptide derived from H-2K<sup>d</sup> (amino acids 54-68, K<sup>d</sup><sub>54-68</sub>) after being processed and presented in the context of recipient MHC class II I-A<sup>b</sup> on the surface of recipient antigen presenting cells.

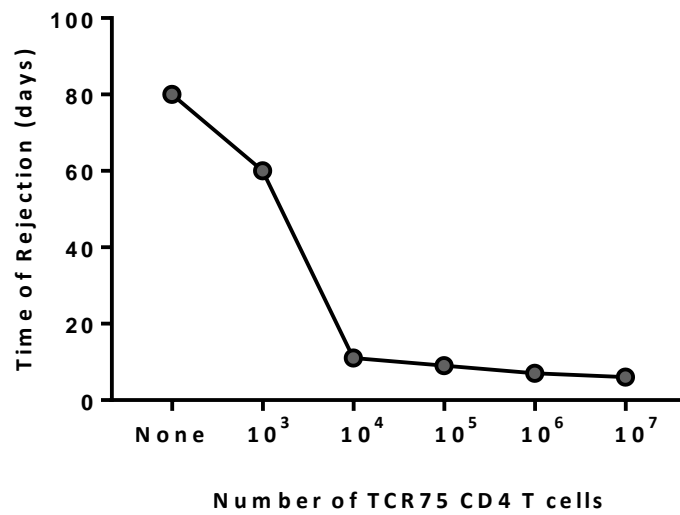


**Figure 11. Non-linear relationship between the number of transferred TCR75 CD4 T cells and survival of BL/6.K<sup>d</sup> heart allograft in BL/6 recipients.** Each circle represents the median survival time of a group of animals receiving the indicated number of TCR75 CD4 T cells. Figure reproduced with permission from [285].

### 3.1.2 How is antibody production pathway relevant to clinical transplantation?

Work by Nussenzweig and colleagues reported that adoptive transfer of high numbers of ovalbumin-specific OT-II CD4 T cells result in increased proliferation and activation of antigen-specific B cells, even before establishment of the GC response [286]. This observation suggests that the precursor frequency of antigen-specific CD4 T cells is a limiting factor for development of the initial extrafollicular response [164]. The extrafollicular humoral response produces an initial wave of antibodies that are short-lived, with minimal somatic hypermutation, and therefore, of low affinity for target antigen. On the other hand, the GC response is associated with the generation of long-lived plasma cells, affinity-matured antibodies and memory B cells. Although the pathogenesis of AMR has been studied extensively, a comprehensive analysis of the relative contribution of the extrafollicular and germinal centre reactions to CAV has not been performed.

An interesting pattern of *de novo* donor-specific antibody development was observed in the clinical setting of kidney transplantation. Dörje et al. conducted a retrospective study that assessed potential risk factors associated with early (<3 months after transplantation) versus late (>3 months after transplantation) acute AMR in kidney transplantation [287]. Although more recipients were pre-sensitised to human HLA at the time of transplantation in the early acute AMR group (55%) as opposed to the late acute group (15%), graft survival in the latter group was significantly poorer. The late acute group were perceived as low-risk at time of transplantation, but their poor graft outcome was associated with increased occurrence of *de novo* DSA and suboptimal responses to immunosuppression. The differences in graft survival in the two groups may therefore reflect fundamental differences in the nature of the alloantibody responses that were observed. Late developing DSAs (that are persistent and unresponsiveness to immunosuppression therapy) are likely products of bone-marrow resident LLPCs, and thus reliant on germinal centres for their deposition.

### 3.1.3 Current murine AMR heart transplant models and their limitations

Since the acknowledgment of AMR as a distinct entity of graft rejection, several groups have developed murine models of acute AMR. In contrast, models of chronic AMR are lacking, possibly reflecting a lack of consensus on the definition of chronic AMR. Current research on AMR models have focused on understanding the mechanisms underlying graft injury mediated by alloantibodies. The mechanisms include: complement activation and generation of membrane-attack-complex; ADCC responses, and activation of allograft endothelial cells (summarised in table 6).

Two decades ago, Hancock et al. demonstrated clearly the contribution of alloantibodies in the development of allograft arterial disease by passive transfer experiments [288]. In addition, Wasowska and colleagues demonstrated that passive transfer of monoclonal allospecific antibody into B-cell deficient recipients provoked acute cardiac allograft histological features (11 days after transplantation). On the other hand, heart grafts in the control group treated with isotype control monoclonal antibody were well-functioning at this time point [289]. In addition, the mRNA levels of IL-1 $\alpha$ , IL-12, TNF- $\alpha$ , IL-2, IFN- $\gamma$ , IL-4 were equivalent in donor endothelial cells obtained from both wild type and B-cell deficient recipients 8-10 days after transplantation, indicating intact macrophage- and T cell-dependent immune responses in the B-cell deficient recipients. The work was expanded by investigating different IgG subclasses and their role in mediating endothelial cell activation and graft rejection, and the authors reported that while complement-fixing antibodies (IgG2b) alone were effective at mediating acute rejection, non-complement fixing antibodies (IgG1) could only induce endothelial cell activation by acting in synergy with IgG2b to induce endothelial cell activation. This, in turn, stimulated production of monocyte chemoattractant protein 1 (MCP-1) and neutrophil chemoattractant growth-related oncogene  $\alpha$ , which promoted recruitment of neutrophils and monocytes to the graft [290]. Although these models provide critical insights into humoral rejection of vascularised allografts, the recipient mice harboured normal endogenous T cell population; hence interpretation of results may be confounded by simultaneous cytotoxic T cell activation and cellular rejection. Another model of acute AMR was developed by Nozaki and colleagues, in which the recipients were lacking T and B cells (*Rag1*<sup>-/-</sup> recipients (H-2<sup>b</sup>) [291]). Adoptive transfer of sera containing high titer of donor-specific alloantibodies into these recipients resulted in rejection of A/J H-2<sup>a</sup> heart grafts within 12 days. Rejection was associated with histological

features of innate immune cells infiltration (mainly neutrophil and macrophage); a characteristic feature of acute AMR. Rejection was abrogated when test sera were diluted 15-fold, indicating the direct correlation between alloantibody titer and AMR.

In addition to alloantibodies, allografts can provoke humoral autoimmune responses where antibodies directed against self-antigen can be generated (reviewed [292]). Recent studies have demonstrated a possible association between autoantibody development and graft failure [293]. Exactly how humoral autoimmunity mediates allograft damage remains unclear.

Although not yet validated experimentally or clinically, it seems likely that chronic AMR is mediated by bone marrow LLPCs, and as such, is a facet of an allospecific GC response. Consequently, allospecific T<sub>FH</sub> cells may be indispensable for the development of chronic AMR. The role of the allospecific T<sub>FH</sub> cell in allograft rejection have not been researched in detail. For instance, Kwun et al. [294] investigated the effect of T cells depletion (CD4 and CD8) in the development of AMR in a fully mismatched heart transplant model. The study demonstrated that T cell depletion resulted in long-term graft survival; however, >50% of recipients showed CAV development and perivascular C3d deposition at day 100 after transplantation. CAV development in this group correlated with DSA generation. Flow cytometric analysis revealed a population of allospecific B cells with GC B cell phenotype. However, assessment of the T cell compartment in DSA-positive mice for IFN- $\gamma$ -producing T effector cells did not reveal augmented anti-donor reactivity. This is possibly because the T cell response was polarised towards a Th2, rather than a Th1, response.

**Table 6. Murine heart transplant models**

Donor/recipient	Special treatment	Key findings	Reference
<b>Acute AMR</b>			
<b>H-2<sup>a</sup>/ H2<sup>b</sup>Ig- knock out recipient</b>	Delayed passive transfer of anti-MHC class I monoclonal antibody	Transfer of IgG2b, but not IgG1 was sufficient to induce acute AMR in IgKO recipients 11-12 days after transplantation	[289]
<b>H-2<sup>a</sup>/ Rag-1<sup>-/-</sup> recipient</b>	Passive transfer of immune serum from sensitised CCR5 <sup>-/-</sup> recipients	High alloantibody titer produced in CCR5 <sup>-/-</sup> is sufficient to mediate graft rejection within 14 days	[291]
<b>H-2<sup>k</sup>/ pre- sensitised H-2<sup>d</sup> recipient</b>	Anti-C5 administration, cyclosporine and cyclophosphamide	Terminal complement blockage improved graft survival and prevented AMR formation	[295]
<b>Chronic AMR</b>			
<b>H-2<sup>a</sup>/H-2<sup>k</sup></b>	Repeated passive transfer of anti-MHC class I antibodies over 28 days	Donor grafts developed vasculopathy following the passive transfer of immune serum in a dose-dependent manner.	[296]
<b>H-2<sup>b</sup>/H-2<sup>k</sup></b>	Recipients subjected to <i>in vivo</i> T cell depletion (both CD4 and CD8)	Depletion of T cells prevented acute rejection and prolonged graft survival. It suppressed alloantibody production at early time points, but late ( $\geq 7$ weeks) alloantibody responses were generated in $\sim 50\%$ of recipients and were associated with development of allograft vasculopathy.	[294]
<b>H-2<sup>d</sup>/H-2<sup>b</sup></b>	IgH <sup>-/-</sup> heart transplant recipients (treated with anti-CD4 antibody) were subject to the passive transfer of immune serum from wild type recipients treated with anti-CD4 antibody	Heart grafts in immunoglobulin-deficient recipients developed allograft vasculopathy following the passive transfer of antibody only when the antibody transfer was performed during the lack protective genes expression by the graft vascular cells	[288]

### 3.1.4 Designing a murine model of chronic humoral heart graft rejection

Given the complexity of the humoral response, with its fundamental division into extrafollicular and GC components, it seems likely that certain aspects of the response are much more critical for determining transplant outcome. However, a major limitation with existing chronic AMR rejection models (especially those involving passive transfer of antibodies [288], [297]) is that they do not provide the opportunity of correlating cellular events occurring within the allospecific B cell population (such as GC formation, LLPCs deposition and memory deposition) with graft outcome. In order to investigate the ability of T-dependent humoral alloimmunity to mediate heart graft rejection, a murine heart transplant model was developed that incorporated (H-2<sup>b</sup>) C56BL/6 recipients devoid of T cells (CD4 and CD8 T cells; hereafter TCR<sup>-/-</sup>). The helper CD4 T cell population was restored in these recipients by adoptive transfer of ( $10^3$  or  $5 \times 10^5$ ) (TCR)-transgenic TCR75 CD4 T cells the day after transplantation with a MHC-mismatched BALB/c heart graft. The BALB/c graft expresses the H-2K<sup>d</sup> MHC class I antigen that is recognised *indirectly* by the TCR75 CD4 T cell population in the recipient. Hence, we anticipated that the TCR75 CD4 T cells would provide essential help for development of alloantibody in the recipient directed against the H-2K<sup>d</sup> alloantigen.

## 3.2 Aims

The aims of the work presented in this chapter are:

1. To develop and characterise a pure murine model of AMR, with minimal contribution from cellular rejection.
2. To investigate the contribution of the extrafollicular and GC alloresponses on the kinetics and morphology of allograft rejection.
3. To investigate the role of the  $T_{FH}$  cell subset in mediating AMR.

## 3.3 Results

### 3.3.1 Rejection kinetics

Reconstitution of TCR<sup>-/-</sup> recipients with relatively large number of T cells ( $5 \times 10^5$  WT.TCR75 CD4 T cells) resulted in rapid rejection of BALB/c heart allografts, with a median survival time (MST) of 9 days (figure 12). On the other hand, limiting T cell help by the transfer of  $10^3$  WT.TCR75 CD4 T cells resulted in slower allograft rejection (MST of 50 days). Control, un-reconstituted TCR<sup>-/-</sup> recipients of BALB/c allografts did not reject, and grafts were beating strongly at the day of sacrifice (day 100). To examine whether the transferred CD4 T cells effected rejection autonomously (by, for example, developing cytotoxic killing potential) or through providing help for effector alloantibody production, two additional control groups were established. In the first control group, T and B cell deficient *Rag2<sup>-/-</sup>* C57BL/6 mice were transplanted with BALB/c hearts and reconstituted with large ( $5 \times 10^5$ ) or small ( $10^3$ ) numbers of WT.TCR75 CD4 T cells. Heart allografts transplanted in the *Rag2<sup>-/-</sup>* recipients continued to beat until explant (day 50 or day 100 for recipients reconstituted with  $5 \times 10^5$  or  $10^3$  TCR75 CD4 T cells, respectively). In the second control group, an effector role of alloantibodies in mediating rejection was confirmed by passive transfer experiments wherein sera from graft recipients reconstituted with  $5 \times 10^5$  TCR75 CD4 T cells were transferred to *Rag2<sup>-/-</sup>* recipients of BALB/c heart allografts. In such recipients, the grafts rejected rapidly (MST = 20 days), whereas recipients receiving equivalent amounts of control serum obtained from unmodified *Rag2<sup>-/-</sup>* recipients of BALB/c hearts did not prompt rejection up to day 30 when the experiment was terminated [298]\*.

\* Courtesy of Manu Chhabra.

A)

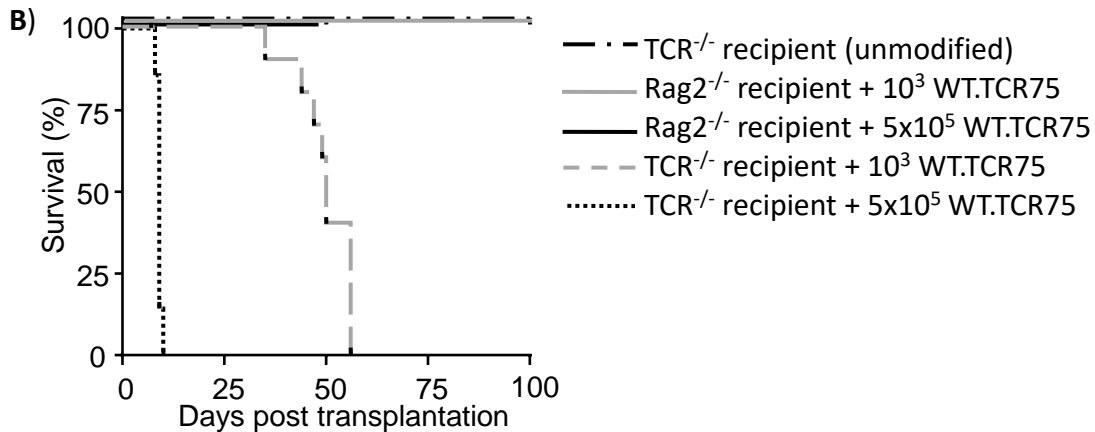
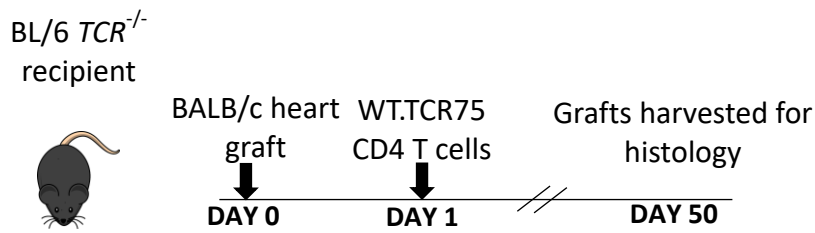


**Figure 12. Rejection kinetics of donor heart grafts in AMR murine model.** A) BL/6  $TCR^{-/-}$  recipients of BALB/c heart allograft were reconstituted with low ( $10^3$ ) or high ( $5 \times 10^5$ ) dose of WT.TCR75 CD4 T cells, which recognize H-2K<sup>d</sup><sub>54-68</sub> peptide in the context of MHC II (I-A<sup>b</sup>) by the indirect pathway. B) Reconstitution of  $TCR^{-/-}$  recipients with low dose of WT.TCR75 T cells resulted in gradual allograft failure (MST=50 days; n=10), whereas heart grafts rejected acutely in recipients receiving high dose (MST=9 days, n=10,  $P < 0.001$ , log rank test).  $Rag2^{-/-}$  recipients reconstituted with either low or high dose of TCR75 CD4 T cells (n=10 each) did not reject heart allografts up to the day of explant.

### 3.3.2 Histology of explanted allografts

#### 3.3.2.1 Haematoxylin and eosin assessment

Paraffin-embedded allografts stained with haematoxylin and eosin (H&E) were assessed by a senior pathologist blinded to the study groups. Stained sections obtained at day 5 from TCR<sup>-/-</sup> recipients that received  $5 \times 10^5$  WT.TCR75 T cells displayed myocyte loss, haemorrhage, oedema, and plumping of the endothelium (figure 13A). Grafts obtained at day 9 from this group were difficult to assess due to severe parenchymal damage / destruction. Explanted grafts from TCR<sup>-/-</sup> recipients that rejected chronically (reconstituted with  $10^3$  WT.TCR75 T cells, at day 50) displayed parenchymal injury, with diffuse myocyte loss and replacement fibrosis. Sections obtained from both acutely or chronically rejecting groups displayed inflammatory infiltrates consisting of neutrophils, few plasma cells, and macrophages [3] (figure 13B). Donor hearts in control TCR<sup>-/-</sup> recipient groups (unmodified) remained disease-free (explanted at day 100) (figure 13A).

#### 3.3.2.2 Immunohistopathology assessment

Explanted heart allografts were assessed for AMR histopathological features, based on the Banff 2013 meeting report [299]. Immunohistochemistry staining was performed for the complement split-product C4d, macrophage marker CD68, NK cell marker NK1.1, and class switched IgG deposition on graft endothelium, as described in the methods section (see section 2.8.2). Acutely rejecting grafts displayed diffuse parenchymal distribution for C4d as well as CD68 macrophages, and NK cells (figure 13A), which possibly reflect acute myocyte death, a feature that is consistent with severe AMR, grade 3 (table 1). Chronically rejecting grafts also displayed strong endothelial C4d deposition, widespread CD68 macrophage distribution, and perivascular accumulation of NK cells. Unmodified TCR<sup>-/-</sup> recipients displayed relatively minimal CD68 distribution, and were negative for C4d deposition, and did not contain NK cells. Interestingly, IgG deposition in the chronically rejecting grafts was not evident in BALB/c allografts explanted at day 14, but was wide-spread by day 50, regardless of comparable C4d deposition at both time points (figure 14). Collectively, the lack of a cytotoxic CD8 T cell alloresponse in this model, and the histopathological features observed in the acutely rejecting allografts are compatible with the histological picture of AMR.

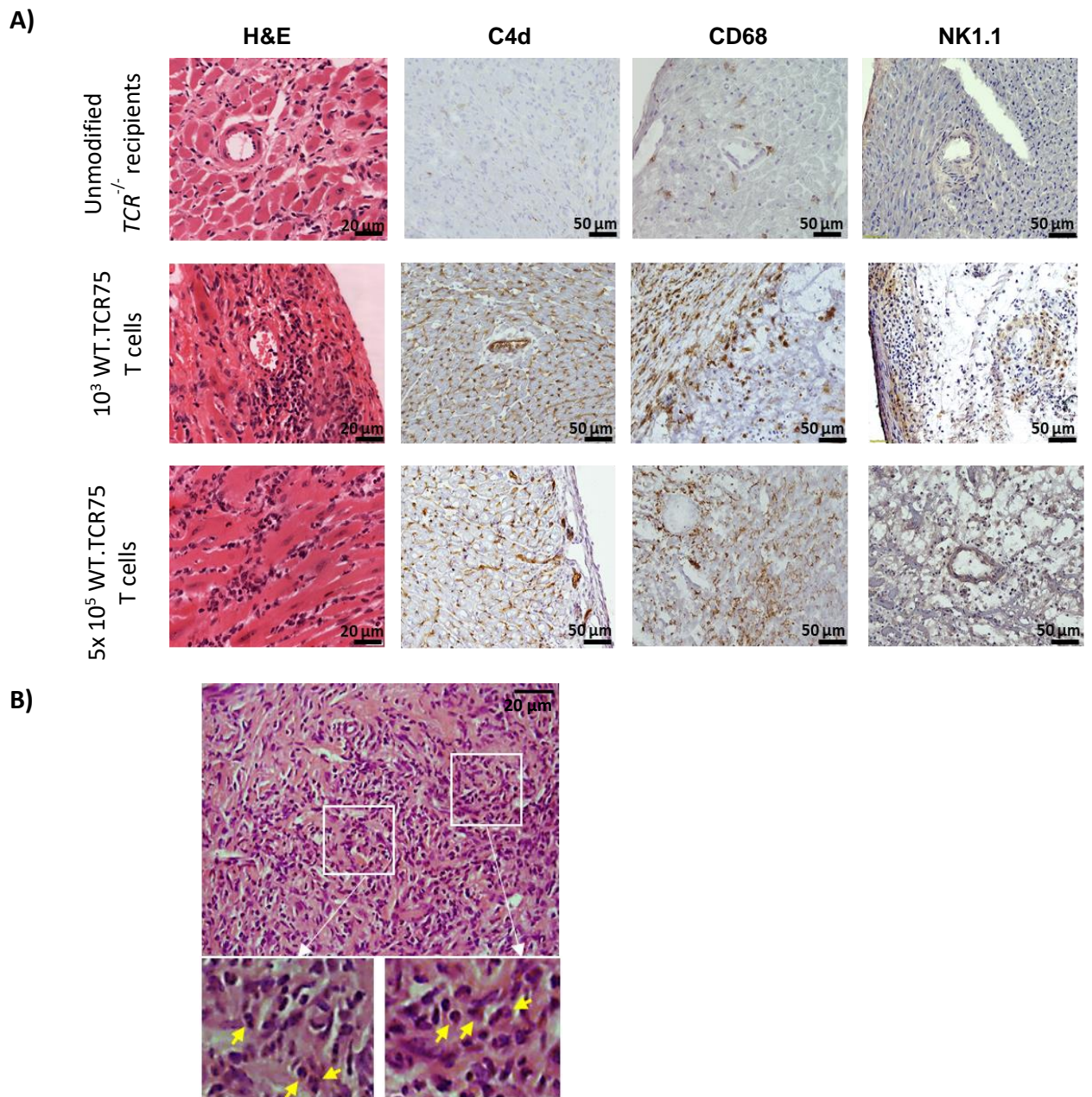


**Figure 13. Histopathological features of murine AMR model.** A) Representative photomicrographs of BALB/c allografts from *TCR*<sup>-/-</sup> recipients reconstituted with 10<sup>3</sup> WT.TCR75 (day 50) or 5x10<sup>5</sup> WT.TCR75 T cells (day 5). Both groups demonstrated positive C4d deposition, diffuse distribution of CD68+ macrophages, and focal distribution of NK cells. The histology was compared to that of *TCR*<sup>-/-</sup> recipients of BALB/c allografts that were not reconstituted with T cells (unmodified). Photomicrograph magnifications are depicted. B) Inflammatory infiltrates observed in chronically rejecting recipients consisted of polymorphs (inset left) and occasional plasma cells (inset right).

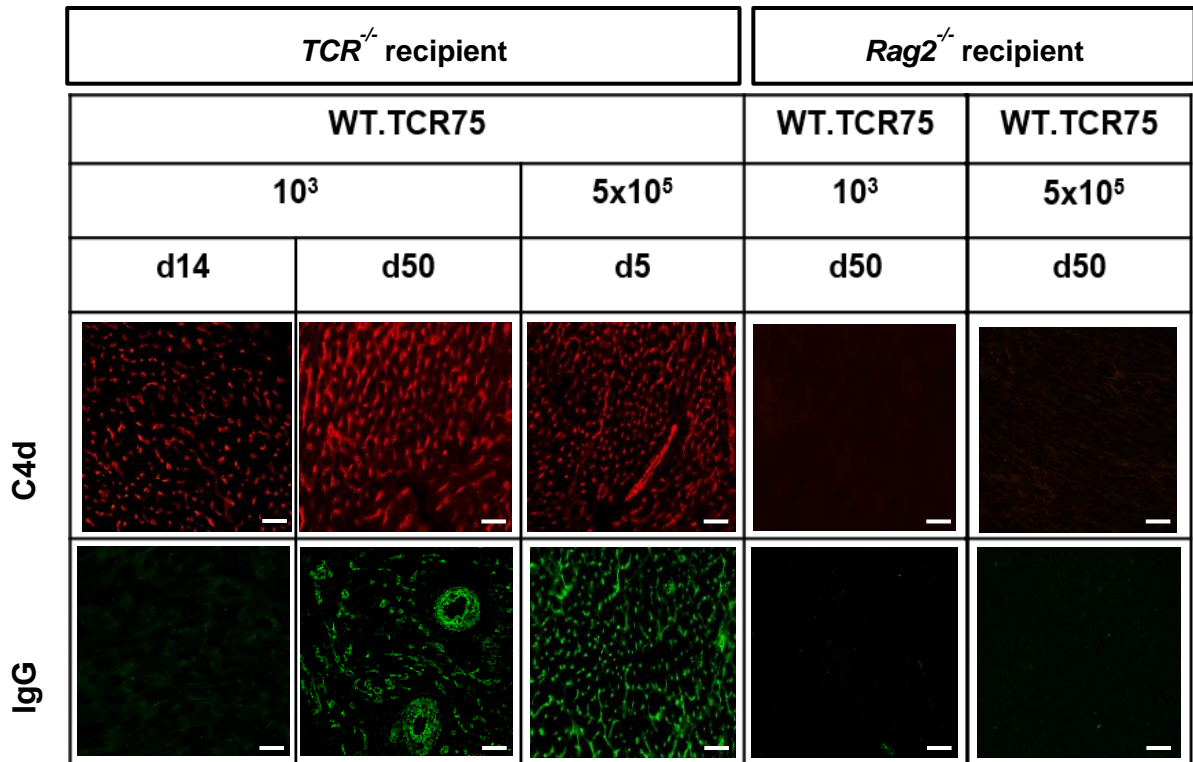


**Figure 14. C4d and IgG immunofluorescent staining of allografts.** Representative photomicrographs of immunofluorescence staining showing interstitial capillary staining for C4d (red, *top row*) and IgG deposition (green, *bottom row*) in BALB/c cardiac allografts explanted at different time points from *TCR<sup>-/-</sup>* or control *Rag2<sup>-/-</sup>* recipients reconstituted with variable numbers of WT.TCR75 CD4 T cells as depicted. Scale bar in all captured images is equivalent to 50  $\mu$ m.

### 3.3.2.3 Severity of allograft vasculopathy

Grafts obtained at day 50 from TCR<sup>-/-</sup> recipients reconstituted with 10<sup>3</sup> WT.TCR75 T cells displayed concentric vascular lesions that had progressed significantly when compared to allografts explanted 14 days after transplant (figure 15A). The mean vasculopathy score in TCR<sup>-/-</sup> recipients reconstituted with 10<sup>3</sup> WT.TCR75 T cells at day 50 was 3-folds higher than that observed in control TCR<sup>-/-</sup> unmodified recipients of BALB/c allografts (figure 15B). The vascular lesions were observed mainly in the small and medium intra-myocardial arteries. TCR<sup>-/-</sup> recipients of BALB/c hearts reconstituted with 5x10<sup>5</sup> WT.TCR75 T cells were fibrous and scarred by day 50 and difficult to assess. Graft vasculopathy in *Rag2*<sup>-/-</sup>, unmodified (TCR<sup>-/-</sup>) and syngeneic recipients (BL/6 graft to BL/6 recipient) was minimal.

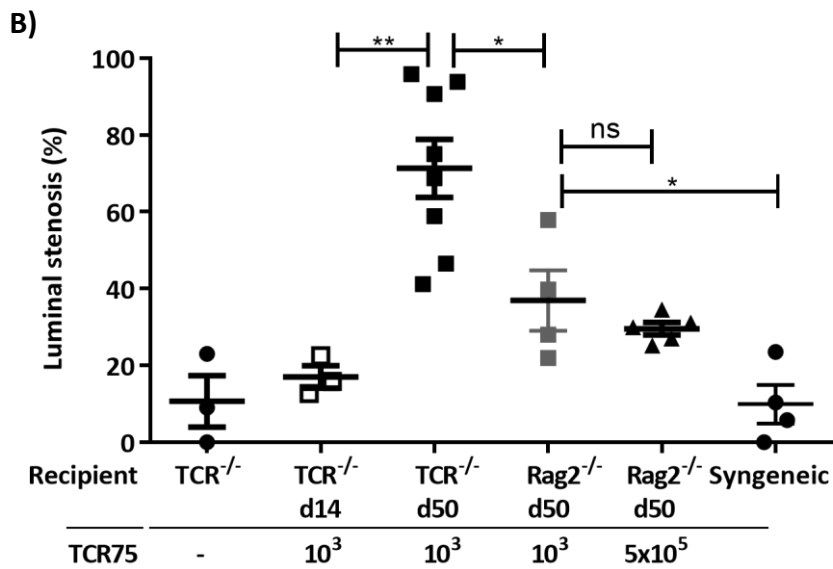
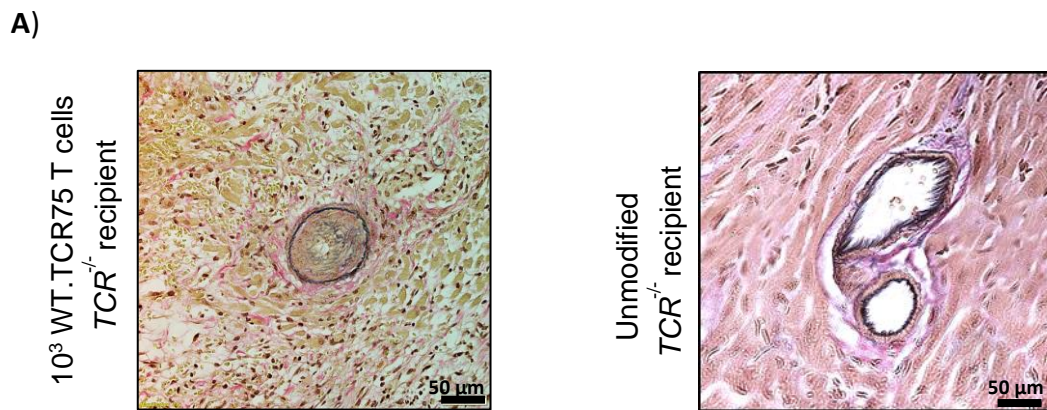


**Figure 15. Vasculopathy development in heart allografts.** A) Representative EVG stained paraffin sections of grafts explanted at day 50 from the chronically rejecting group reconstituted with 10<sup>3</sup> WT.TCR75 CD4 T cells depicting typical fibroproliferative arterial intimal thickening (*left*), compared to disease-free vessels observed in hearts from the unmodified control group (*right*). Images obtained at x20 magnification. B) Severity of vasculopathy in heart grafts explanted at days 14 (n=3) and 50 (n=8) from chronically rejecting group were compared to similarly reconstituted *Rag2*<sup>-/-</sup> (n=4 for recipients reconstituted with 10<sup>3</sup> TCR75 CD4 T cells, and n=6 for recipients of 5x10<sup>5</sup> TCR75 CD4 T cells) unmodified TCR<sup>-/-</sup> (n=3) and syngeneic (n=4) recipients. Results expressed as mean ± SEM, each dot represent one biological replicate, two-tailed Mann-Whitney test: \*\**P* < 0.002, \**P* < 0.02, ns: non-significant.

### **3.3.3 Characterisation of the humoral alloresponse**

Alloantibody titers, splenic GC activity, and numbers of donor-specific GC B cells were compared in TCR<sup>-/-</sup> recipients of BALB/c heart grafts reconstituted with either small (help limited) or relatively large (help unlimited) numbers of WT.TCR75 CD4 T cells.

#### **3.3.3.1 The magnitude of the alloantibody response is influenced by frequency of allospecific helper T cells**

Reconstitution of TCR<sup>-/-</sup> mice with either small or relatively large numbers of WT.TCR75 T cells provoked long-lasting class-switched alloantibody responses (7 weeks post transplantation) directed against the mismatched H-2K<sup>d</sup> alloantigen. The magnitude of antibody titre was markedly higher and developed more rapidly in the group receiving greater numbers of CD4 T cells (Figure 16A). In particular, the response was particularly strong at week one in the help-unlimited group, by which time all BALB/c heart grafts had rejected (figure 16A). Control unmodified recipients of BALB/c hearts did not develop anti-K<sup>d</sup> antibodies.

#### **3.3.3.2 Extrafollicular and GC components of the alloantibody response**

The magnitude of the anti-K<sup>d</sup> alloantibody responses observed in the acute and chronically rejecting groups was mirrored in the number of splenic H-2K<sup>d</sup>-specific plasma cells (as demonstrated by K<sup>d</sup> ELISPOT). Specifically, numbers of splenic K<sup>d</sup>-specific plasma cells were substantially greater in the acutely rejecting group, compared to that observed in the chronically rejecting group (figure 16B). Interestingly, the number of K<sup>d</sup> specific B cells in the recipients' bone marrow was comparable between the two groups. Bone marrow LLPC deposition is considered a hallmark feature of the GC response, suggesting that despite the early augmented response in the group reconstituted with  $5 \times 10^5$  TCR75 CD4 T cells, at late time points the GC response was similar in strength in the two groups. Indeed, immunohistochemical staining of splenic sections for GC-B cells (follicular B cells that express B220 and GL7) at day 50 following transplantation revealed similar GC activity in the two groups (figure 16C).

Interestingly, GC activity at day 9 of the acutely rejecting group was barely above that observed in naïve control spleen (Figure 16C), suggesting that circulating alloantibody present at the time of rejection was principally a consequence of an extrafollicular response. In support, confocal imaging confirmed the presence of class-switched IgG-positive B cells in the extrafollicular space of the acutely rejecting group at day 10 (figure 16E, left and middle), while class-switched IgG-positive B cells were located within the B cell follicle in both groups at day 50 (figure 16E, right). These results thus suggest that the extrafollicular alloantibody response was responsible for the acute rejection observed in the group receiving  $5 \times 10^5$  TCR75 CD4 T cells.

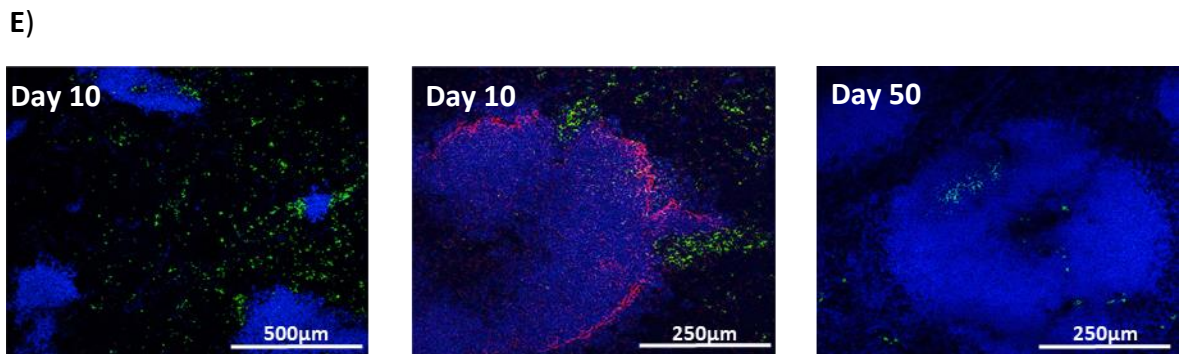
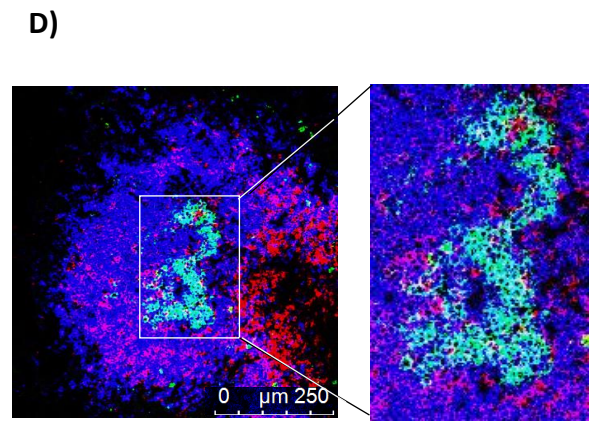
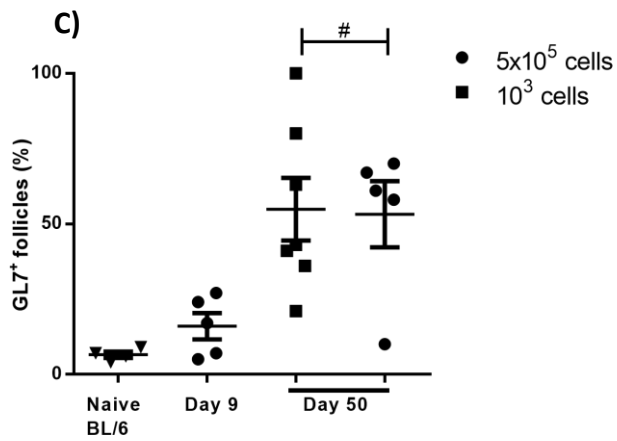
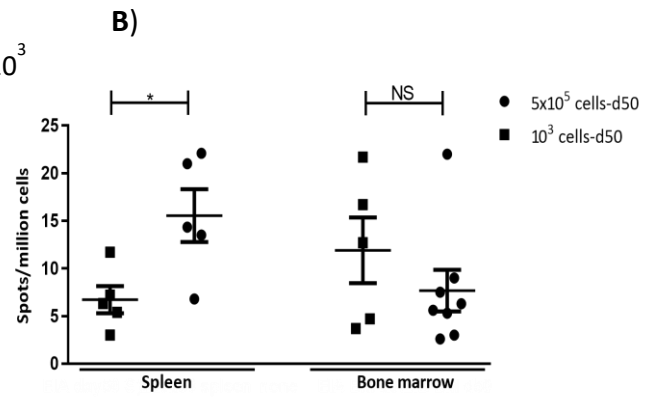
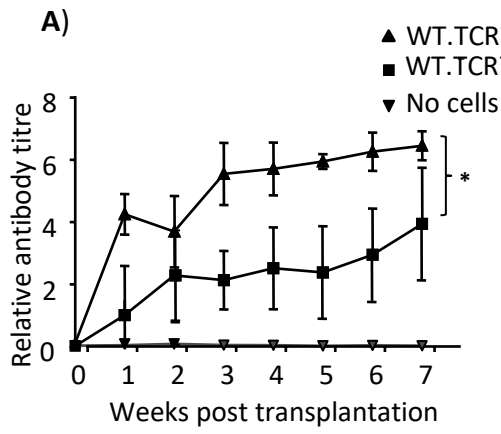


**Figure 16. Characterization of the humoral response in murine AMR heart transplant model.** A) BL/6 TCR<sup>-/-</sup> recipients developed anti-H2K<sup>d</sup> IgG antibodies in a magnitude that is proportionate to the transferred numbers of WT.TCR75 T cells (data represent mean ± S.D. of n=5 mice per group, \*P<0.05 two-way ANOVA). B) ELISPOT assay showed more anti-K<sup>d</sup> IgG secreting cells from the spleens 50 days post-transplantation in the acutely rejecting model (n=5 spleens, n=8 bone marrow) as opposed to the chronically rejecting model (n=5), but both demonstrated comparable numbers of anti-K<sup>d</sup> IgG secreting cells from bone marrow samples. Data represents mean ± SEM \*P<0.05, NS: non-significant (P= 0.52); two-tailed Mann-Whitney. C) GCs developed in the spleens expressed as a percentage of total follicles depicting similar percentage of activated GCs at day 50 post transplantation. Data displayed as mean ± SEM, two-tailed Mann-Whitney test #= non significant. D) Representative confocal triple immunofluorescence photomicrographs of a spleen obtained from chronically rejecting TCR<sup>-/-</sup> recipient reconstituted with low dose of WT.TCR75 T cells. The section was stained with antibodies against: B220 (B cells, blue); GL7 (GC B cells, green); and CD4 (T cells, red), the staining displayed a typical secondary follicle with T<sub>FH</sub> cells present within the follicle (inset). E) Representative confocal imaging of splenic sections obtained from the acutely rejecting model at day 10 (left, centre) demonstrating the localization of IgG-switched B cells (green) in the extrafollicular space (follicles labelled with B220; blue), close to the marginal sinus (MadCAM-1; red), while IgG class-switched B cells were localised within the B cell follicles on day 50 (right).

### 3.3.4 The contribution of GC humoral alloimmunity to chronic AMR

In order to confirm that GC activity is essential for mediating chronic alloantibody rejection, TCR<sup>-/-</sup> recipients of BALB/c allografts were reconstituted with either relatively large ( $5 \times 10^5$ ) or small ( $10^3$ ) numbers of TCR75 CD4 T cells that are deficient for SAP adaptive molecule (hereafter, SAP<sup>-/-</sup>.TCR75). SAP is essential for the prolonged interaction between the B cell and helper T cell that leads to T<sub>FH</sub> cell differentiation and thus SAP<sup>-/-</sup> T cells cannot provide help for formation of a germinal centre reaction [300]. However, SAP<sup>-/-</sup> T cells can still provide help for extrafollicular responses.

#### 3.3.4.1 Rejection kinetics in the absence of GC response

TCR<sup>-/-</sup> mice reconstituted with relatively large frequencies ( $5 \times 10^5$ ) SAP<sup>-/-</sup>.TCR75 CD4 T cells rejected BALB/c heart allografts rapidly (MST =13 days) [figure 17A, left]. Explanted hearts displayed histological findings similar to those observed following transfer of large frequencies WT.TCR75 T cells, including: wide-spread C4d endothelial deposition; intravascular CD68<sup>pos</sup> macrophage infiltration; and, to a lesser extent, NK1.1 cell interstitial distribution (figure 17B, left). In contrast, heart grafts of TCR<sup>-/-</sup> mice receiving small dose ( $10^3$ ) SAP<sup>-/-</sup> TCR75 T cells survived up to the date of experiment termination (day 60) [figure 17A, left], with no evidence of C4d endothelial deposition, nor macrophage nor NK cells intra-graft infiltration (figure 17B, left).

#### 3.3.4.2 Humoral response following the delivery of SAP<sup>-/-</sup>.TCR75 T cells

Anti-K<sup>d</sup> antibody titers were substantially lower in the recipient group reconstituted with  $10^3$  SAP<sup>-/-</sup>.TCR75 CD4 T cells than observed in the group reconstituted with  $5 \times 10^5$  SAP<sup>-/-</sup>.TCR75 T cells (Figure 17). In the latter, robust alloantibody responses were detectable at weeks 1 and 2 post-transplant, but unlike following reconstitution with WT CD4 T cells, these responses then declined gradually (figure 17A, right). As expected, GCs were not detectable by immunofluorescence staining on splenic frozen sections obtained from either the group receiving small dose ( $10^3$ ) or relatively large dose ( $5 \times 10^5$ ) SAP<sup>-/-</sup>.TCR75 T cells.

To specifically identify responding H-2K<sup>d</sup>-specific B cells in this model, alloreactive B cells were tracked by staining with H-2K<sup>d</sup> tetramers fluorescently labelled with APC or FITC (figure 18, left panel). The dual labelling approach was utilised to avoid contamination from non-

antigen specific binding of the B cell to the fluorochrome / tetramer construct; only those B cells that bind both tetramer / fluorochrome constructs are alloantigen (H-2K<sup>d</sup>) specific [279]. After the exclusion of dead cells and doublets, allospecific B cells within the CD19<sup>+</sup> B cell population were identified on the basis of binding to both tetramer constructs (i.e., H-2K<sup>d</sup>-APC<sup>+</sup> and H-2K<sup>d</sup>-FITC<sup>+</sup>), and further characterised for GC surface phenotype (GL7<sup>+</sup> and FAS<sup>+</sup>). H-2K<sup>d</sup>-specific B cells were not found in naïve un-transplanted TCR<sup>-/-</sup> animals, but were evident in small numbers in cardiac allograft recipients reconstituted with 10<sup>3</sup> WT.TCR75 T cells from two weeks after transplantation, but with a dramatic expansion evident by seven weeks (figure 18). The proportion of allospecific B cells expressing GC phenotype progressively increased over the same period (13% at week 2; 53%, week seven). In contrast, H-2K<sup>d</sup>-specific B cells were barely detectable at day 50 in recipients reconstituted with 10<sup>3</sup> SAP<sup>-/-</sup>.TCR75 T cells, and although an expanded population was present at day 50 in recipients reconstituted with 5x10<sup>5</sup> SAP<sup>-/-</sup>.TCR75 T cells, numbers were still less than observed in the group reconstituted with 10<sup>3</sup> WT.TCR75 CD4 T cells (Figure 18). As anticipated, allospecific B cells did not develop GC phenotype in recipients of 10<sup>3</sup> or 5x10<sup>5</sup> SAP<sup>-/-</sup>.TCR75 T cells, confirming that the alloantibody response observed in SAP<sup>-/-</sup>.TCR75 T cell reconstituted group was exclusively from an extrafollicular focus. Together, these results strongly suggest that acute AMR can be mediated by an extrafollicular response alone, whereas chronic AMR (that did not develop in recipients of small dose SAP<sup>-/-</sup>.TCR75) is dependent upon establishment of a GC reaction for its progression.

A)

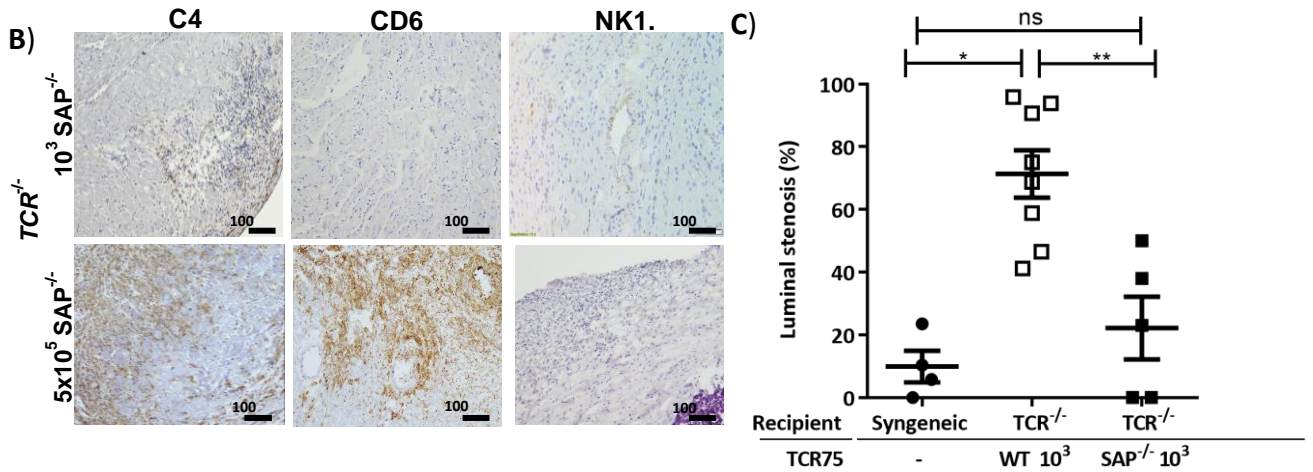
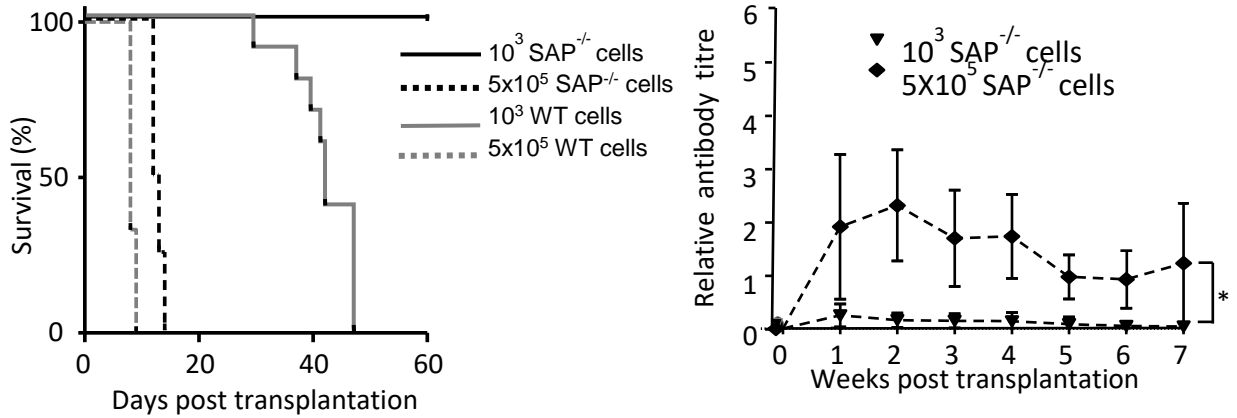


**Figure 17. AMR kinetics in the absence of GC formation.** A) left: BL/6 TCR<sup>-/-</sup> recipients of BALB/c heart grafts reconstituted with 10<sup>3</sup> SAP<sup>-/-</sup> TCR75 T cells survived long term (n=5) up to day 60, on the other hand recipients reconstituted with 5x10<sup>5</sup> SAP<sup>-/-</sup> TCR75 T cells rejected acutely (n=4). BL/6 TCR<sup>-/-</sup> recipients of BALB/c allografts reconstituted with 10<sup>3</sup> or 5x10<sup>5</sup> WT.TCR75 T cells were imposed from figure 16A for comparison. Right: DSA titre of recipients receiving 10<sup>3</sup> SAP<sup>-/-</sup> TCR75 T cells was (n=5) markedly low at all time points, while DSA titre was relatively higher at earlier time points and gradually declined afterwards in recipients of 5x10<sup>5</sup> SAP<sup>-/-</sup> TCR75 T cells (n=4). \**P*<0.001; two-way ANOVA. B) BALB/c heart allografts explanted from recipients reconstituted with 10<sup>3</sup> SAP<sup>-/-</sup> TCR75 T cells showed no evidence of complement (C4d), macrophage, nor NK cells deposition. C) TCR<sup>-/-</sup> recipients of BALB/c allografts reconstituted with low numbers of SAP<sup>-/-</sup> TCR75 CD4 T cells (n=5) developed minimal CAV that was comparable to background levels observed in syngeneic mice (n=4). Data represents mean ± SEM. \**P*<0.003, \*\**P*<0.002, ns: non-significant ;two-tailed Mann-Whitney test.

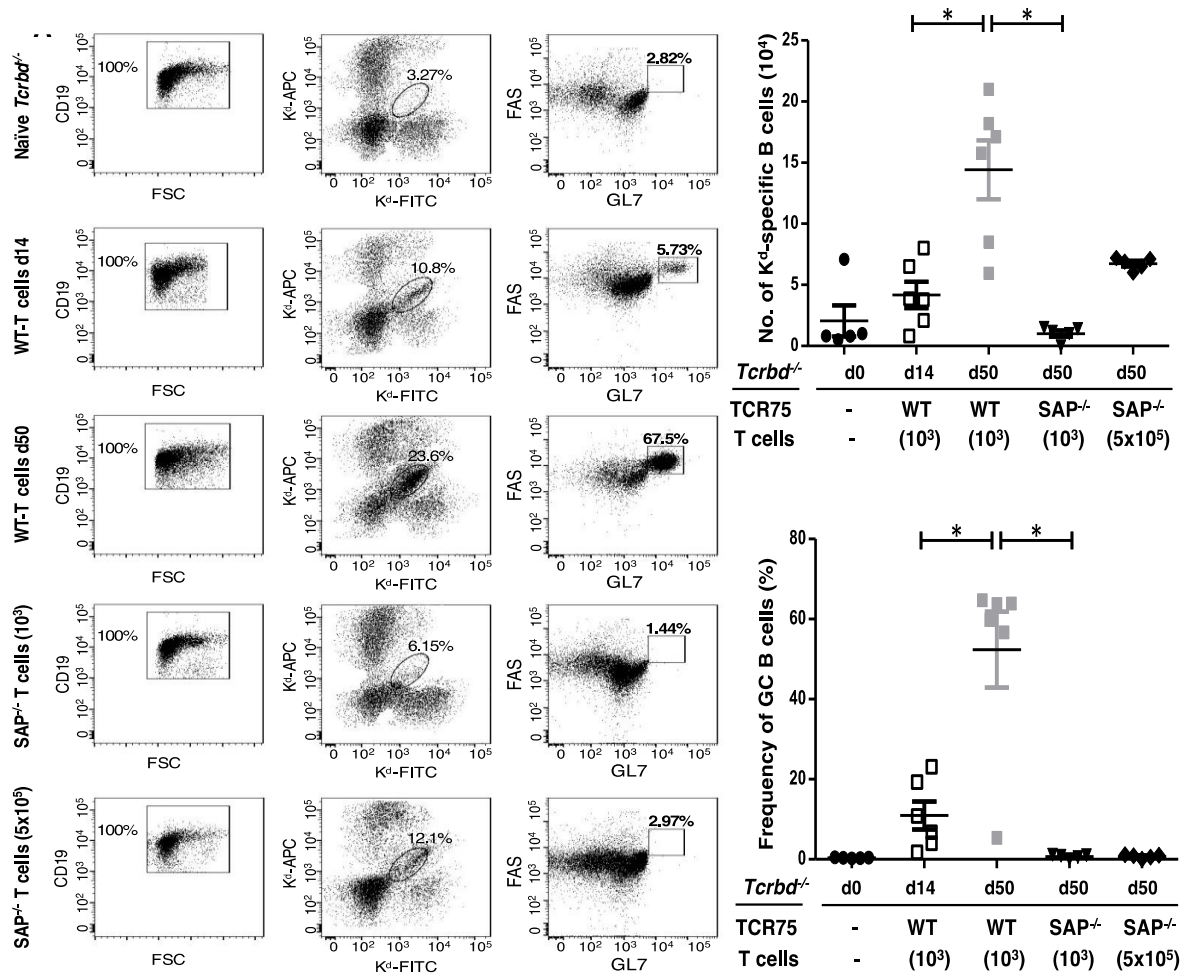


**Figure 18. GC response is essential in mediating chronic AMR in murine model.** Representative flow cytometry dot plot profiles of K<sup>d</sup>-specific splenocytes obtained from naïve BL/6 *TCR*<sup>-/-</sup> mice, or BL/6 *TCR*<sup>-/-</sup> recipients of BALB/c hearts 50 days following reconstitution<sup>3.4</sup> with variable numbers of SAP<sup>-/-</sup> *TCR*75 T cells, or WT.*TCR*75 T cells as depicted. Lymphocytes were first gated by a combination of forward scatter (FSC) and side scatter (SSC), dead cells were excluded, and B cells were selected based on CD19 expression. K<sup>d</sup>-specific B cells were identified by dual labelling of the B cells with a mixture of synthetic H-2K<sup>d</sup> tetramers labelled with either APC or FITC. B cells that proof positive for both flourochromes were gated, and plotted against GC markers FAS and GL7 (right panel). Absolute numbers of splenic H-2K<sup>d</sup>-specific B cells (x10<sup>4</sup> cells per mouse) (top); Percentage of H-2K<sup>d</sup>-specific B cells expressing FAS<sup>+</sup>GL7<sup>high</sup> germinal center phenotype (bottom) (right panel). Data represents mean ± SEM \**P*<0.05, two-tailed Mann-Whitney test.

### 3.3.4.3 Assessing the effector role of alloantibodies in activating endothelial cells *in vitro*

In TCR<sup>-/-</sup> recipients reconstituted with 10<sup>3</sup> WT.TCR75 CD4 T cells, the alloantibody response persisted for many weeks, and the continual presence of alloantibody presumably mediates the progression of allograft vasculopathy and eventual graft failure at about 7-8 weeks. Notably, alloantibody levels had plateaued by week 2, raising the question whether some other aspect of the response, such as affinity for target antigen, altered with time. In order to investigate changes in the 'quality' of the alloantibody produced, the ability of test sera - sampled at various times after transplant - to activate allograft endothelial cells was assessed *in vitro*.

Following inflammatory insult, endothelial cells upregulate the expression of chemokines and adhesion molecules in order to mediate the recruitment of immune cells to the site of inflammation [107]. Although the mechanisms underlying CAV development are still unclear [301], different groups have shown that MHC class I crosslinking on graft endothelium by alloantibody can trigger intracellular signalling that result in dynamic endothelial cell proliferation and migration [302]–[304]. The ability of DSAs to activate endothelial cells was assessed *in vitro* by scratch wound migration assay [305] as described in the methods (section 2.4.1). In this experiment, BALB/c or BL/6 endothelial cells were incubated overnight in minimal culture medium with week 2 and week 7 sera from the chronically rejecting TCR<sup>-/-</sup> group (that received 10<sup>3</sup> WT.TCR75 CD4 T cells). Photomicrographs demonstrated that week 7 serum induced substantially more cell migration in BALB/c endothelial cells than serum sampled from week 2, and the migration observed at week 2 was no greater than with control, naïve serum. Similarly, no migration was elicited by addition of sera sampled at week 7 from recipients reconstituted with 10<sup>3</sup> SAP<sup>-/-</sup>.TCR75 CD4 T cells (figure 19A). No migration was observed upon addition of test sera to control, cultured syngeneic (C57BL/6) endothelium.

We hypothesised that the endothelial cell migration observed relates to signalling via the phosphoinositide 3-kinase (PI3K)/Akt pathway [305]. In support, the expression of phosphorylated Akt Ser<sup>473</sup> in cultured BALB/c endothelial cells upon addition of test sera revealed similar patterns to those observed in the endothelial migration assay (Figure 19B). Strong Akt signalling was triggered by addition of sera obtained at week 7 from the group

receiving  $10^3$  WT.TCR75, and indeed, greater than observed in the positive control (sera obtained from BL/6 recipient of a BALB/c skin graft (SG)). In comparison, little or no signalling was detected upon addition of either week 2 sera from group  $10^3$  WT.TCR75 or at day 50 from the group receiving  $10^3$  SAP<sup>-/-</sup>.TCR75 (figure 19B)

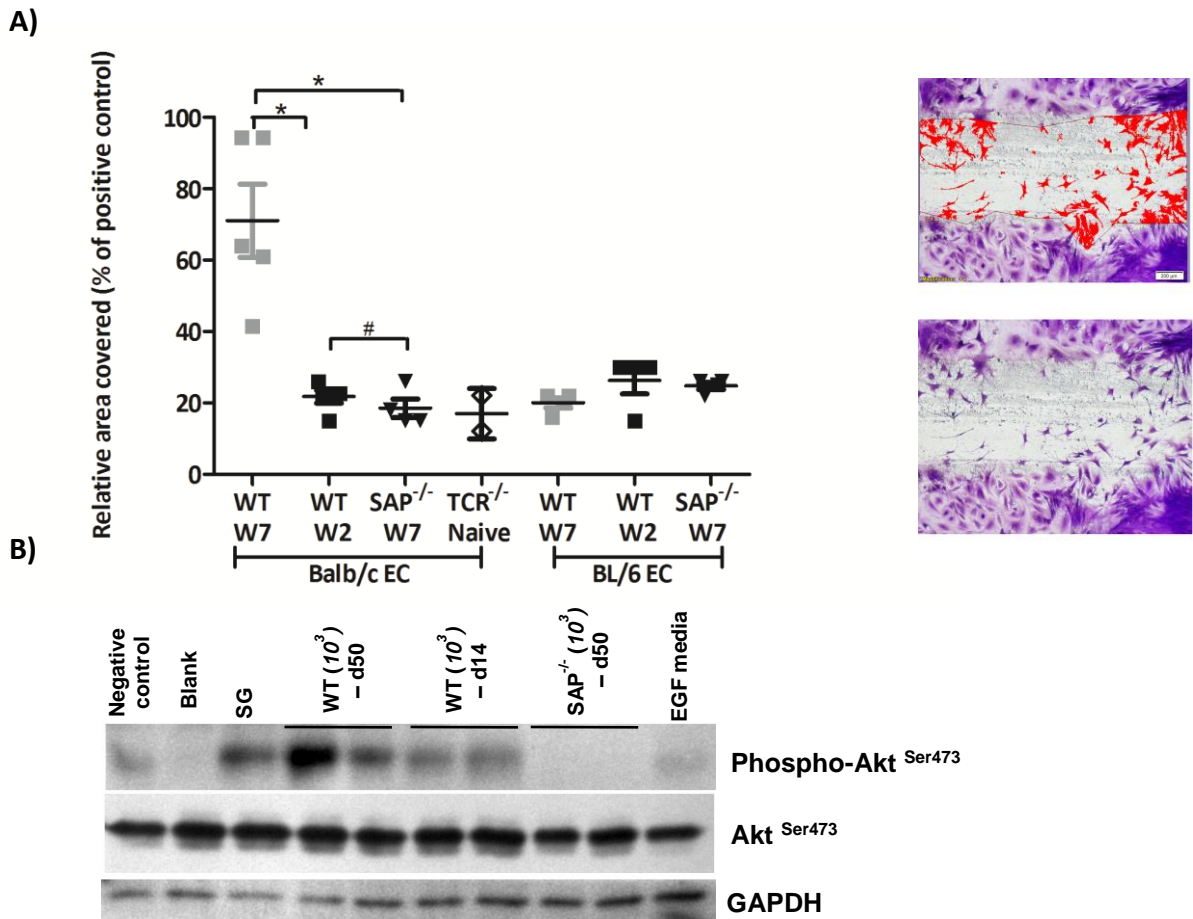


**Figure 19. GC-derived alloantibodies mediate endothelial activation.**

**A)** left: Scratch-wound assay demonstrated enhanced migration of BALB/c endothelial cells upon incubation with day 50 serum sampled from TCR<sup>-/-</sup> recipients reconstituted with 10<sup>3</sup> WT.TCR75 CD4 T cells (WT, W7) as opposed to cells incubated with serum obtained at week 2 (WT,W2) or at week 7 of the equivalently reconstituted group with 10<sup>3</sup> SAP<sup>-/-</sup>.TCR75 CD4 T cells (SAP<sup>-/-</sup>, W7). BL/6 endothelial cells migration following incubation with the aforementioned groups was low and comparable among all tested groups. Data displayed as mean ± SEM, with each dot representing an average of six fields treated with the same serum sample (right), analysed per biological replicate (magnification x4); \*P<0.01, #P non-significant, two-tailed Mann-Whitney test). **B)** Quiescent BALB/c endothelial cells were stimulated with sera from recipients of 10<sup>3</sup> WT.TCR75 CD4 T cells at day 14, or day 50, and recipients of 10<sup>3</sup> SAP<sup>-/-</sup> TCR75 CD4 T cells at day 50. Controls involved serum obtained from naïve BL/6 animals (negative control), pooled hyperimmune anti-H-2K<sup>d</sup> IgG serum (from BALB/c skin graft on BL/6 (SG) as positive control), and with media containing epidermal growth factor (EGF). Cell lysates were separated by gel electrophoresis and immunoblotted with anti-phospho-AktSer<sup>473</sup> monoclonal antibody and GAPDH (housekeeping control) antibody. Displayed Western blot represents at least two independent experiments of test sera.

### 3.3.4.4 Affinity maturation of the humoral alloimmune response

The endothelial cell migration assay indicated that endothelial cell responses were induced by addition of sera sampled from the chronically rejecting group ( $10^3$  WT.TCR75 CD4 T cells) at late time points (week 7), but not by sera sampled earlier (week 2), despite the approximately equivalent antibody titers at the two time points (see figure 16A). To examine affinity maturation of the alloantibody response, binding of test sera to target MHC class I H-2K<sup>d</sup> molecule was assessed using bio-layer interferometry (BLI).

Because the precise concentration of H-2K<sup>d</sup>-specific allantibody in collected sera was not known, antigen-antibody binding affinity cannot be estimated, as the affinity constant formula requires knowledge of analyte (i.e., alloantibody) molar concentration in the serum sample [284]. Therefore, affinity maturation was assessed more crudely by quantifying alloantibody dissociation rates from target antigen – so called “off-rate ranking”. The kinetic rate of dissociation is concentration independent, and it measures how rapidly a complex is decaying, regardless of the analyte concentration, with slow decay of the complex indicating stronger analyte/ligand binding [284].

Dissociation rates for sera obtained from TCR<sup>-/-</sup> recipients reconstituted with  $10^3$  WT.TCR75 T cells at weeks 2 and 7 following heart transplantation were compared. In keeping with a GC response, the dissociation rates at week 2 were more rapid than that at week 7, indicating that alloantibodies from week 7 bound more strongly to H-2K<sup>d</sup> alloantigen (apparent by the significantly lower dissociation constant “K<sub>off</sub>”) (figure 20). The low alloantibody titer in recipients reconstituted with  $10^3$  SAP<sup>-/-</sup> TCR75 CD4 T cells did not permit analysis of dissociation constants for this group. However, kinetics were analysed for recipients reconstituted with  $5 \times 10^5$  SAP<sup>-/-</sup> TCR75 CD4 T cells and demonstrated that sera sampled at late time points (day 50) dissociated less rapidly than sera sampled at week 2 in recipients of  $10^3$  WT.TCR75. This might reflect either preferential selection of naturally-occurring (non-mutated) high affinity variants [306], or a degree of affinity maturation occurring solely within extrafollicular foci [307]. The analysis of sera from recipients reconstituted with  $5 \times 10^5$  WT.TCR75 CD4 T cells at day 50 was not performed as the serum contained a pool of GC-derived and extrafollicular alloantibodies.

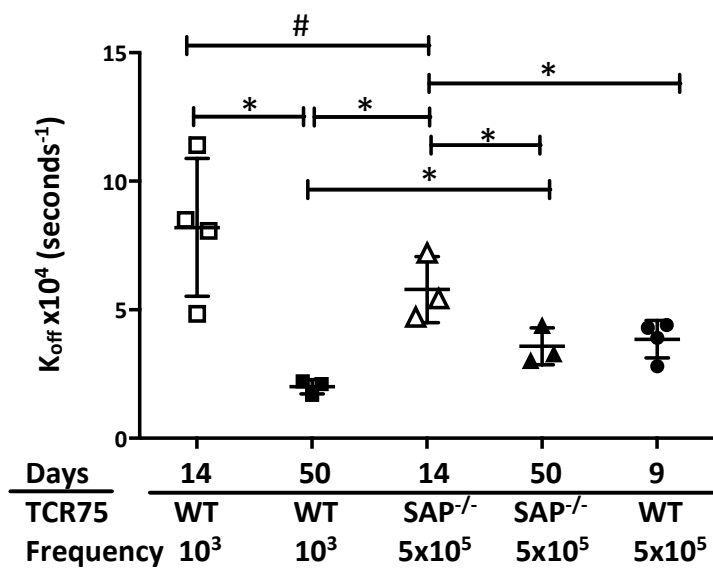
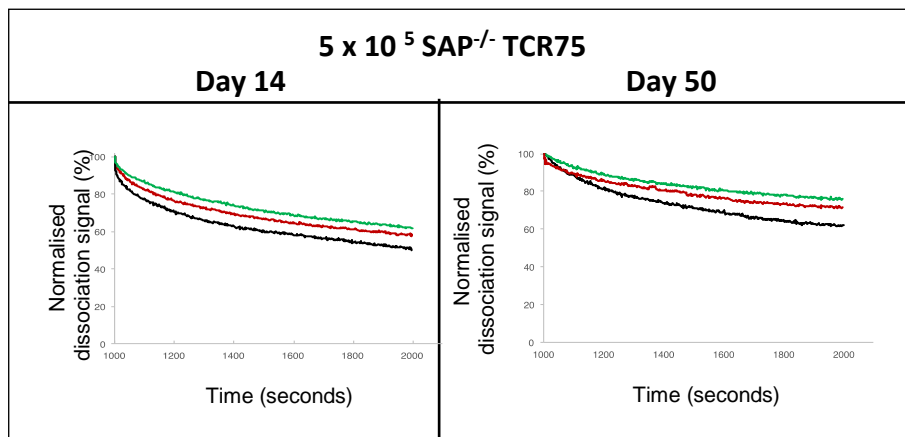
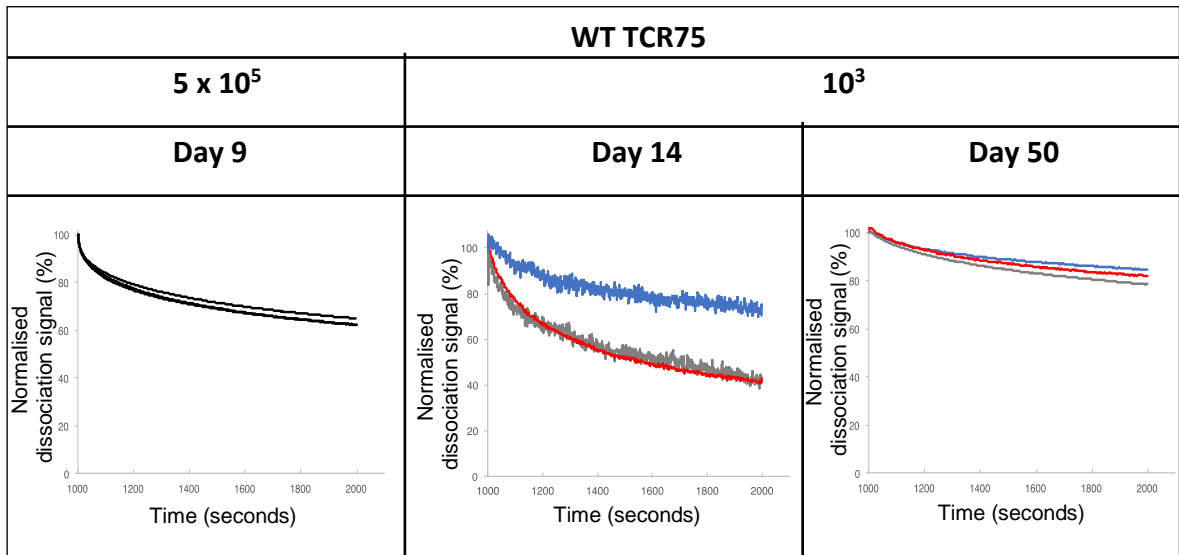


**Figure 20. Ranking anti-H2K<sup>d</sup> alloantibodies dissociation constants.** Top: graphs depict sensograms of anti-H-2K<sup>d</sup> antibody dissociation rates in sera obtained from TCR<sup>-/-</sup> recipients of BALB/c hearts reconstituted with either WT or SAP<sup>-/-</sup> TCR75 CD4 T cells at variable frequencies and time points as depicted. Each curve representing individual recipient mouse. Same colour indicating the same recipient mouse at two different time-points. *Bottom:* dot plot histogram comparing anti-H-2K<sup>d</sup> alloantibody dissociation constants ( $K_{off}$ ) among, TCR<sup>-/-</sup> recipients of BALB/c hearts reconstituted with either WT or SAP<sup>-/-</sup> TCR75 CD4 T cells (at day 9 (n=4), week 2 (n=4) and 7 (n=3) as depicted). Each value represents the  $K_{off}$  after global fit of two serum dilutions (at 1:20 and 1:40) of the same biological replicate. Values are presented as mean  $\pm$ SEM. \* $P < 0.05$ , # $P = N.S.$ , two-tailed Mann-Whitney test.

### 3.4 Discussion:

The humoral immune response is undoubtedly complex, but the key anatomical division into extrafollicular and germinal centre foci has been appreciated for several decades, and it is perhaps surprising that the contribution of the two phases to transplant rejection has not been previously addressed. Experimental work performed in this chapter involved the development and characterisation of a murine AMR heart transplant model that would enable assessment of the contribution of the extrafollicular and germinal centre phases of the alloantibody response to allograft rejection. This model incorporated recipients lacking all T cell types in order to exclude the potential contribution from cytotoxic CD8 T cell alloimmunity.

Although histopathological criteria have been established for diagnosing chronic AMR in kidney allografts, this is not the case for clinical heart transplantation [146]. In my model, histopathological assessment of the acutely rejecting heart grafts demonstrated endothelial plumping, neutrophil infiltration, complement deposition, and widespread myocyte death. This matches the histological features that define acute AMR in humans [299]. Given the absence of cytotoxic cellular alloimmunity in this model, these pathological changes are most likely mediated by the alloantibody response. This is further supported by the C4d deposition observed in small and intermediate graft vessels in the chronically rejecting group; such deposition did not occur when recipients were reconstituted with small frequencies of T cells that were SAP-deficient.

The essential role of GC response in mediating chronic AMR was evident in experiments involving the transfer of small dose WT.TCR75 CD4 T cells. In these experiments, the alloantibody response developed gradually, and having peaked at week 2, was present at similar titres for the duration of the experiment (7 weeks). Labelling of the allospecific B cell population with dual MHC class I tetramer-fluorochrome constructs confirmed that the transfer of allospecific helper CD4 T cells was associated with marked expansion of the allospecific B cell population, with approximately half expressing GC phenotype. When the GC response was prevented by the transfer of  $10^3$  TCR75 CD4 T cells that lacked SAP expression, the degree of allograft vasculopathy was equivalent to that of syngeneic recipients and all hearts were beating upon sacrifice (day 60). The proportion of splenic B cell follicles that exhibited secondary, activated phenotype was greater at week 7 than at week 2 in graft recipients of  $10^3$  WT.TCR75 T cells, suggesting the ongoing delivery of help

from T<sub>FH</sub> cells in sustaining the GC response. In support, confocal imaging of spleens obtained from the chronically rejecting group confirmed CD4 T cell localisation within secondary follicles seven weeks after transplant. Persistent GC activity is not seen in primary responses against model protein antigens (e.g., nucleoprotein, which typically resolve after three weeks [308], [309]). To what extent these late GC-derived alloantibodies contribute to graft rejection is, however, not clear. Alloantibody may simply impact in a time-dependent manner, whereby persisting low alloantibody titer (that does not change in character) mediates the development of vasculopathy by eliciting minor, but continual, damage. On the other hand, although LLPCs deposited early in the bone marrow express BCRs of higher affinity than other B cells generated contemporaneously during the GC response [310], LLPCs generated at later time points (with high affinity BCRs) would be expected to outcompete those LLPCs generated at earlier time point and displace them from the limited bone marrow niches [311]. If so, then alloantibody titer and GC-mediated alloantibody affinity are both likely to influence the progression of allograft vasculopathy. High affinity alloantibodies will more readily resist physiological blood flow shear and more effectively transduce the endothelial activating signals thought to underpin progression of allograft vasculopathy. Although not addressed experimentally in this chapter, the BLI experiments demonstrated that serum obtained from the chronically rejecting group reconstituted with WT.TCR75 CD4 T cells showed lower dissociation constants to H2-K<sup>d</sup> antigen at week 7 than at week 2. In addition, an effector role for late-generated alloantibody was demonstrated by the strong migration and phospho-Akt signalling upon treating endothelial cells with week 7 serum obtained from recipients reconstituted with 10<sup>3</sup> WT.TCR75 T cells. Neither migration nor phospho-Akt signalling were observed in donor endothelial cells treated with serum obtained at week 2 from the same recipient group, suggesting that affinity maturation may be required to trigger endothelial cell responses.

Comparing the rejection kinetics and humoral response in recipients reconstituted with small frequencies of WT or SAP<sup>-/-</sup> TCR75 CD4 T cells suggest that chronic pathological changes are likely to be dependent on the establishment of a GC reaction. It also highlights the crucial role of T<sub>FHs</sub> in maintaining humoral alloimmunity. Thus, development of therapeutic strategies aimed at specifically targeting CD4 T<sub>FH</sub> cells as a mean of preventing late AMR may be beneficial. Because T<sub>FH</sub> cells are a relatively small, and specialised, subset of the endogenous CD4 T cell pool, specific targeting of this population offers the advantage of abrogating the GC response, without compromising the recipient's immune system. Kim

et al., [312] have shown in a nonhuman primate kidney transplant model that combining T cell (belatacept) and B cell co-stimulation blocker (anti-CD40) to inhibit T-dependent antibody production was successful at suppressing GC development. In addition, the treatment resulted in profound suppression of alloantibody production and improved graft function. However, the proposed therapy is not clinically translatable due to its association with severe weight loss and poor prognosis.

Another interesting observation was that the kinetics of rejection can be shifted from acute to chronic, depending on the number of allospecific CD4 T cells delivered. The number of transferred allospecific CD4 T cells correlated with the magnitude of the early alloantibody response (but not with the titre at late time points). This relates to the particularly strong extrafollicular response generated following transfer of relatively large frequencies allospecific T helper cells, and it was notable that large numbers of SAP<sup>-/-</sup>.TCR75 CD4 T cells (that only provoke extrafollicular responses) still provoked strong early germinal centre responses that resulted in acute AMR. Grafts did not undergo rejection following transfer of an equivalent number of WT.TCR75 CD4 T cells to Rag2<sup>-/-</sup> recipients, indicating that the transferred CD4 T cells are, by themselves, incapable of effecting rejection in this model. However, inflammatory injury mediated by infiltrating T cells and macrophages may influence long-term graft survival beyond 50 days.

The exact mechanisms by which the early extrafollicular alloantibody response mediates acute rejection were not examined in detail, but it seems likely that complement fixation, with generation of membrane attack complex and widespread intra-allograft thrombosis, was responsible -there was strikingly little cellular infiltrate in the acutely rejecting grafts in our model. Pober et al. [313] suggested that terminal complement proteins C5b-9 can initiate endothelial cells activation via non-canonical NF- $\kappa$ B signalling pathway. This activation would mediate the expression of pro-inflammatory receptors on the surface of allograft endothelial cells; thus, enhancing its capacity for recruiting and activating allogeneic host T cells [314], [315]. This cellular infiltration to the graft tissue can exacerbate T cell-mediated changes (e.g., local production of INF $\gamma$ ) into the vessel's wall, and enhance the formation of CAV lesions. In addition, allospecific antibodies deposition on the allograft can recruit macrophages and increase the local release of inflammatory cytokines which may contribute to the allograft parenchymal damage [105], [113], (reviewed [107]).

These findings in the mouse are consistent with some aspects of clinical kidney transplantation. For instance, a cohort study performed by Everly and colleagues examined the effect of rejection therapy on de novo DSA levels in acute cellular rejection. The study demonstrated that acute cellular rejection was treated successfully with >50% of patients showing high graft survival rates when de novo DSA levels were reduced within the first 14 days post transplantation [316]. This may imply that suppressing the alloimmune response at an early stage, before the establishment of GC response and deposition of LLPCs, may improve long-term graft survival.

## Chapter 4: Initial precursor frequency of antigen-specific CD4 T cells and T-dependent antibody responses

### 4.1. Introduction:

Nussenzweig et al. demonstrated that limiting T<sub>FH</sub> cell numbers is important for establishing a competitive GC environment that selects cycling centrocytes with higher affinity for target antigen [286]. Their work also showed that transfer of increased numbers of helper T cells resulted in rapid pre-GC B cell proliferation and activation. A correlation between excessive T<sub>FH</sub> cell numbers and impaired affinity maturation has been similarly reported by Priete *et al* [317]. The role of T<sub>FH</sub> cell numbers in executing an optimal GC reaction has been discussed recently [318].

In the AMR rejection model described in chapter 3, it was interesting that the transfer of either large or low numbers of WT.TCR75 CD4 T cells was associated with marked differences in kinetics and magnitude of the early alloantibody response, but germinal centre activity at week 7 appeared similar in the two groups (see figure 17C). Given that the two groups otherwise received an identical antigen challenge (a BALB/c heart allograft) this suggests that, whereas availability of T cell help is a limiting factor for development of the extrafollicular arm, some other factor determines the relative 'strength' of the germinal centre reactions. We hypothesised that this other factor may be the relative number of antigen-specific B cells. To investigate how frequencies of antigen-specific B and T cells can shape the magnitude of T-dependent antibody responses, I developed a model wherein numbers of B and T cells responding to a model protein antigen (Hen Egg Lysozyme, HEL) could be manipulated independently.

#### 4.1.1 Transgenic B and CD4 T cells

The study of antigen-receptor transgenic mice has provided valuable insights into how T-dependent antibody responses develop [319], and how humoral autoimmunity is avoided [320], [321]. Antigen-receptor transgenic mice express a transgene encoding a BCR or TCR with defined antigen specificity, and transgenic mice can be back-crossed onto different

backgrounds in order to obtain mice with desired characteristics. In this chapter, two transgenic mouse strains were used as a source for adoptively-transferred B and CD4 T cells.

#### **4.1.1.1 SW<sub>HEL</sub> strain as a source of B cells**

The SW<sub>HEL</sub> strain was generated by Brink and colleagues [273] to investigate different aspects of the early T-dependent antibody responses [322]. The SW<sub>HEL</sub> strain carries a rearranged variable region gene of the heavy chain (V<sub>H</sub>) that is specific to HEL antigen, and the encoded amino acid sequence is known precisely [9]. The Ig knock-in strain was generated by targeting DNA coding the V<sub>H</sub> of HyHEL-10 (i.e., obtained from high affinity anti-HEL monoclonal antibody-secreting hybridoma [325]) to the endogenous BL/6 Ig heavy chain locus to generate V<sub>H</sub>10<sub>tar</sub> mice. Heterozygous (V<sub>H</sub>10<sub>tar</sub><sup>+/-</sup>) mice were crossed with the transgenic strain LC2 which carry the anti-HyHEL V<sub>K</sub>10<sub>K</sub> light chain specific to HEL to create the SW<sub>HEL</sub> (V<sub>H</sub>10<sub>tar</sub><sup>+/-</sup> x LC2) mice which are heterozygous for both the heavy chain V<sub>H</sub>10<sub>tar</sub> and the light chain V<sub>K</sub>10-K alleles [273]. SW<sub>HEL</sub> mice were shown to generate HEL-binding and non-HEL binding B cells. Among the HEL-specific population (40 - 60% of the entire B cell population [273]), 10 – 20% of the B cells retained HyHEL-10 specificity [322]. The SW<sub>HEL</sub> strain was maintained on a C57BL/6 (H-2<sup>b</sup>) background.

SW<sub>HEL</sub> B cells are capable of switching to all classes of immunoglobulins, and can undergo somatic hypermutation. The strain has been widely used to study cell fate decisions, and commitment into extrafollicular or GC B cell compartments [306], [319].

#### **4.1.1.2 TCR7 strain as a source for CD4 T cells**

The TCR7 transgenic strain was developed by Neighbors and colleagues originally to investigate the immunoregulatory checkpoints of differentiated T helper cells in a diabetic mouse model [275]. The strain carries the TCR V $\alpha$ 11 and V $\beta$  chain genes of HEL-specific T cell hybridoma. TCR7 CD4 T cells are specific for the non-cryptic HEL<sub>74-88</sub> epitope presented in the context of MHC class II (I-A<sup>b</sup>).

## 4.2 Aim

To investigate how the relative frequencies of antigen-specific B and T cells shape the magnitude of GC activity in T-dependent antibody response.

## 4.3 Results

### 4.3.1 Development of adoptive transfer model

To assess how the germinal centre reaction is shaped by the frequencies of antigen-specific B and CD4 T cells, an adoptive transfer model was developed. In this model, monoclonal populations of purified SW<sub>HEL</sub> B cells ( $10^4$  or  $10^6$ ) were co-transferred with TCR7 T cells ( $10^3$  or  $10^5$ ) into TCR<sup>-/-</sup> recipient mice were simultaneously immunised subcutaneously with HEL emulsified in CFA. Animals were sacrificed one or three weeks after-immunisation (figure 21).

The anti-HEL response in the C57BL/6 strain is considered weak, due to a relative lack of endogenous HEL-reactive CD4 T cells [326]. Thus adoptively transferred TCR7 CD4 T cells would provide essential help for anti-HEL antibody responses that was otherwise not provided by the endogenous C57BL/6 CD4 T cell population. This permits ready examination of the impact of the precursor frequency of antigen-specific T helper cells on the magnitude and kinetics of the subsequent antibody response.

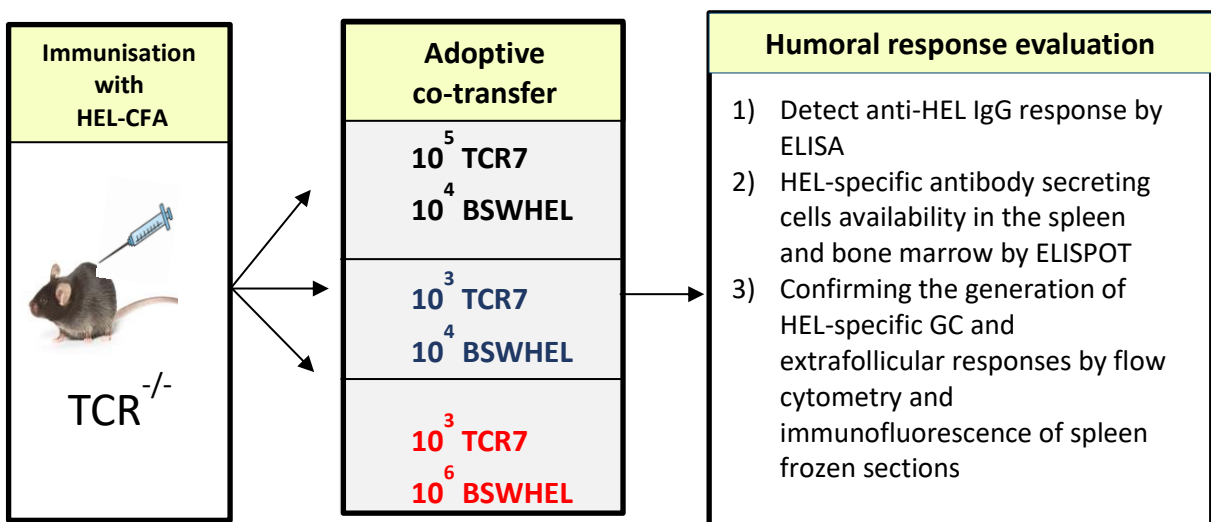


**Figure 21. Schematic representation of the experimental model.** Following subcutaneous immunization of TCR<sup>-/-</sup> mice with HEL-CFA, they were placed into three groups based on the ratios of delivered T and B cells as depicted. Series of experiments were carried in order to investigate how different T:B cell ratios can shape the humoral response.

### **4.3.2 The respective strengths of the extrafollicular and GC responses is influenced by the proportions of antigen specific B cells to T cells.**

Analysis of sera obtained 1 week after immunisation demonstrated that recipients of  $10^3$  TCR7 CD4 T cells generated low levels of HEL-specific IgG, regardless of the number of transferred SW<sub>HEL</sub> B cells (i.e., either intermediate ( $10^4$ ) or high ( $10^6$ )). Conversely, transfer of higher numbers of TCR7 T cells ( $10^5$ ) resulted in robust anti-HEL IgG responses (figure 22A). Anti-HEL antibodies generated during the first week of immunisation were likely the product of an extrafollicular response, because GL7+, GC B cells were not detectable in the spleen at that stage (figure 22B).

The weak anti-HEL IgG response at week 1 in mice receiving  $10^3$  TCR7 T cells was consistent with numbers of HEL-specific plasma cells in the spleen, as determined by HEL-specific ELISPOT assay. Appreciable numbers of anti-HEL antibody secreting cells were detected only in the group receiving  $10^5$  TCR7 CD4 T cells ( $43 \pm 18$ ; mean  $\pm$  SEM) and not, notably, in the group receiving greater numbers ( $10^6$ ) of SW<sub>HEL</sub> B cells, yet low numbers of TCR7 CD4 T cells ( $11 \pm 4$ , and  $5 \pm 0.2$ ; mean  $\pm$  SEM) (figure 22C, left). Numbers of HEL-specific plasma cells in the bone marrow were low in all groups, suggesting that bone marrow plasma cell deposition had not yet occurred (figure 22C).

Flow cytometry analysis confirmed the presence of splenic HEL-specific B cells (B220+ HEL+) in all groups one week after challenge. Although the total number of HEL-specific B cells appeared higher in the group receiving greater number of TCR7 T cells ( $10^5$ ), sample numbers were too small to permit accurate statistical comparison. HEL-specific B cells did not express GC markers (GL7 and FAS) after one week of immunisation (figure 23A and C). In addition, immunofluorescence staining of splenic frozen sections obtained one week after immunisation confirmed that class-switched B cells were located exclusively within the extrafollicular foci (figure 23D, top panel).

Three weeks after challenge, anti-HEL IgG responses were detectable and comparable in magnitude in all three groups (figure 22A), whereas GC activity was substantially greater in the group that received greater numbers of HEL-specific B cells ( $10^6$ ) and relatively low numbers ( $10^3$ ) of HEL-specific T cells (figure 22B). In addition, confocal microscopy demonstrated that class switched IgG B cells were now localised within B cell follicles (figure 23D, lower panel). ELISPOT showed comparable pattern of antibody secreting cells within

the spleen and bone marrow at both weeks 1 and 3 post challenge (figure 22C).

Nevertheless, flow cytometry analysis showed that a greater proportion of HEL-specific B cells developed GC phenotype in the group co-transferred with  $10^3$  TCR7 and  $10^6$  SW<sub>HEL</sub> B cells (figure 23B).

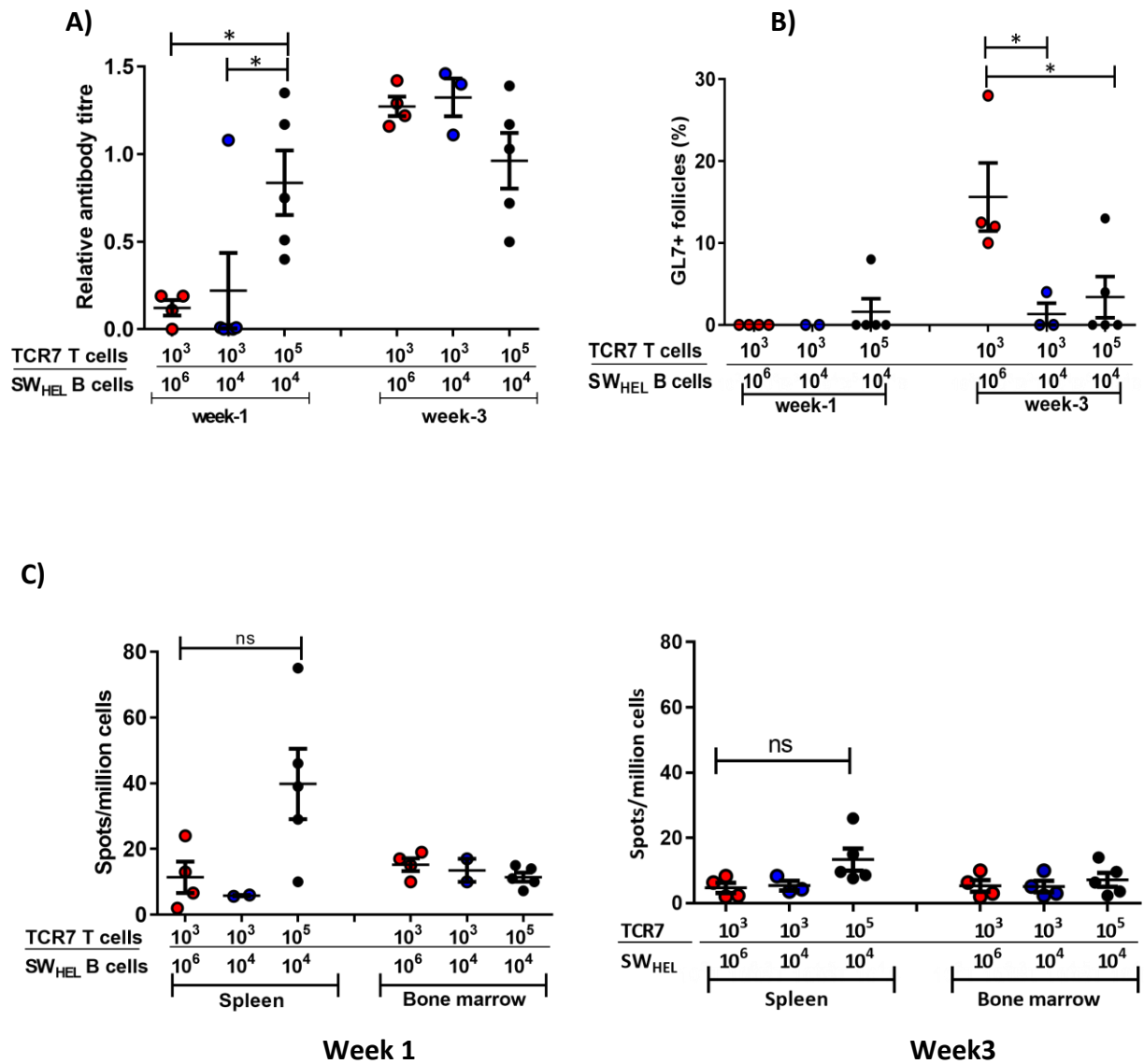


**Figure 22. Anti-HEL effector response following the transfer of variable numbers of cognate T and B cells in CFA-HEL challenged animals.** A) Anti-HEL IgG ELISA one and three weeks following CFA-HEL immunisation. Data represent mean  $\pm$  SEM ( $n=4$  in all groups except TCR7  $10^3$  and SW<sub>HEL</sub>  $10^4$  at week 1 ( $n=2$ ) and at week 3 ( $n=3$ ),  $*P<0.05$ , student two-tailed Mann-Whitney test. B) HEL-specific GL7+ GCs as determined by immunofluorescence staining expressed as a percentage of total B cell follicles within TCR<sup>-/-</sup> recipients.  $*P<0.05$ . C) ELISPOT assay of splenic and bone marrow anti-HEL IgG secreting cells following 1 or 3 weeks of challenge. Each dot represents the average of one biological replicate, mean  $\pm$  SEM; Mann-Whitney test, ns: non-significant.

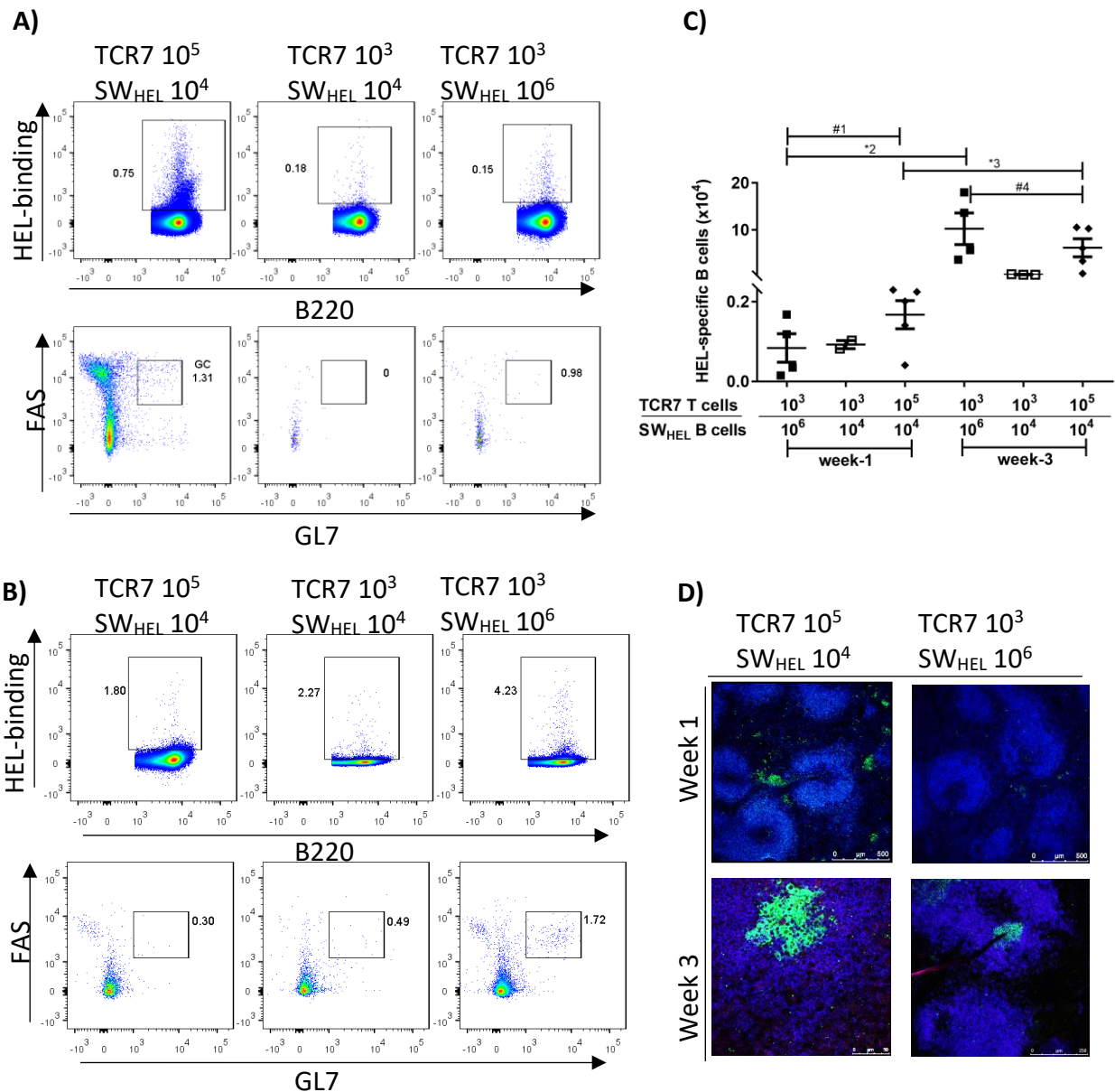


**Figure 23. Transfer of high numbers of CD4 T cells correlated with strong extrafollicular response.** Pseudocolour plots of a representative splenocytes flow cytometry obtained following 1 week (A) or 3 weeks (B) of HEL-CFA challenge. HEL-specific B cells were gated based on binding to HEL (top row) [positive for B220 and HEL], GC-derived B cells were gated based on FAS and GL7 expression (lower row). Numbers indicate percentages of gated cells. C) Absolute numbers (mean  $\pm$  SEM) of HEL-specific B cells as determined in (A) and (B) are shown. Two-tailed Mann-Whitney test. ( $n=4$  in all groups except TCR7  $10^3$  and SW<sub>HEL</sub>  $10^4$  at week 1 ( $n=2$ ) and at week 3 ( $n=3$ ). 1# = 0.1464, 2\* = 0.0233, 3\* = 0.0138, 4# = 0.3069. D) Histological analysis of spleen 1 week (top panel) or 3 weeks (lower panel) after co-transfer of SW<sub>HEL</sub> B cells and TCR7 CD4 T cells following challenge with CFA-HEL. Follicles are stained with B220 (blue), class switched B cells are stained with anti-mouse IgG-FITC (green).

## 4.4 Discussion

In order to explore how the relative precursor frequency of antigen-specific B and T cell populations impacts upon differentiation to either an extrafollicular or germinal centre B cell, I developed a model that incorporated adoptive transfer of antigen-receptor transgenic T and B cells.

The experiments performed using this model demonstrated that transfer of monoclonal populations of HEL-specific T and B cells at different ratios to one another shaped the ensuing humoral response. The extrafollicular response was particularly influenced by the availability of antigen-specific CD4 T cell help, in that increased numbers of HEL-specific CD4 T cells resulted in skewing towards a strong extrafollicular response. In contrast, transfer of small numbers of TCR7 CD4 T cells resulted in weak, barely perceptible extrafollicular responses, even if the group simultaneously transferred with large numbers of HEL-specific B cells. Work by Okada et al. [327] demonstrated that following HEL-adjuvant challenge, HEL-specific Ig-transgenic B cells paired with cognate TCR7 CD4<sup>+</sup> T cells at the border between the B cell follicle and the T- cell zone for prolonged periods (10 – 60 minutes). They further noted that a single HEL-specific B cell interacted with more than one TCR7 T cell simultaneously (conversely, single TCR7 T cell did not form stable interaction with multiple B cells). Therefore, it is possible that in an environment with relative excess of antigen-specific CD4 T cells, the chance of synapse formation between cognate T and B cells is increased, allowing multiple T cells to bind to a single cognate B cell. This may result in a help signal that somehow favours either preferential seeding to the extrafollicular foci, or greater survival and differentiation of B cells upon arrival at the extrafollicular sites. The latter is probably more likely, because the ELISPOT analysis (Figure 22C) revealed higher numbers of splenic HEL-specific plasma cells at week 1 in the group receiving relatively few SW<sub>HEL</sub> B cells (but large number of TCR7 CD4 T cells) than in the groups receiving greater numbers of B cells, and relatively few CD4 T cells.

# Chapter 5: Role of antibody affinity maturation in allograft vasculopathy progression

## 5.1 Introduction

The experimental work presented in chapter 3 suggested that GC humoral alloimmunity is critical for progression of chronic AMR. The GC response uniquely generates antibody with progressively greater affinity for target antigen; a process driven by SHM. This chapter will investigate the role of GC-mediated SHM in the progression of allograft vasculopathy. In this model, donor hearts expressing HEL antigen (as a surrogate alloantigen) were transplanted into the immunoglobulin-transgenic mouse strain SW<sub>HEL</sub> that contain a predominant B cell population specific for HEL antigen. Donor and recipient strains were maintained on H2-K<sup>b</sup> backgrounds, to avoid confounding responses against strongly immunogenic mismatched MHC antigen. The structures of HEL antigen and HEL antibody have been extensively studied. Similarly, the amino acid substitutions in the heavy chain of HyHEL-10 that are associated with increased affinity for HEL antigen have been identified (detailed in 5.1.2).

### 5.1.1 Relevance of alloantibody affinity to AMR pathogenesis

'Sensitised' individuals with anti-MHC alloantibody generally wait longer for organ transplants, and may never receive a transplant [328]. Cell based technologies (e.g., complement dependent cytotoxicity and flow cytometry) and solid phase immunoassays (e.g., ELISA and Luminex) are available for DSA screening and detection (reviewed in [329]). However, a reliable method for quantitating DSA affinity to donor antigens is still lacking. Serum obtained from human organ recipients has been reported to present a complex mixture of antibodies, comprising anti-HLA (class I, and class II) [330], autoantibodies [331], and non-HLA antibodies [332]. Furthermore, circulating alloantibodies are the product of a heterogenic pool of reactive allospecific B cells (estimated as a mean of 2,880 antibody-secreting cells per 10<sup>6</sup> B cells eight weeks after renal transplantation in non-sensitised recipients [333]). Therefore, generated alloantibodies may vary in titer and affinity from one patient to another.

Interrelated antibody effector mechanisms (reviewed [107]) can contribute to graft injury. The differences between murine and human immune systems potentially limit our ability to translate results obtained from murine studies into the clinical setting. Nevertheless, affinity

maturation is thought to proceed similarly in both species. Hence, investigating binding affinity of antibodies isolated from murine transplant models can provide the first insight into the role of alloantibody affinity maturation in the progression of allograft vasculopathy.

### **5.1.2. The Ig knock-in mouse strain SW<sub>HEL</sub>**

The SW<sub>HEL</sub> strain was developed by Professor Robert Brink's group (detailed in [273], and described earlier in section 4.1.1.1). SW<sub>HEL</sub> mice contain a trackable population of BCR-transgenic, HEL-specific B cells, but unlike the earlier MD4 strains, the Ig heavy chain is 'knocked-in'. This enables the SW<sub>HEL</sub> B cells to undergo class switch recombination and somatic hypermutation [319].

### **5.1.3 HEL<sup>WT</sup> and HEL<sup>3x</sup> proteins as membrane-bound alloantigens**

The antibody response to HEL, as a model protein antigen, has been well characterised [324]. Due to the ease of crystallizing the HEL protein, it has been an attractive model for protein structural studies [334]. However, the HEL<sup>WT</sup> protein binds so strongly to the HyHEL-10 Ig heavy chain of the SW<sub>HEL</sub> B cell that further affinity maturation is essentially not possible. Hence, Brink and colleagues [306] have further introduced three amino-acid substitutions (i.e., R21Q, R73E, and D101R, figure 24A) on the HEL<sup>WT</sup> protein at locations overlaying the binding site of HyHEL-10 antibody to create the mutated protein HEL<sup>3x</sup>. The resulting HEL<sup>3x</sup> protein binds with ~300-fold lower affinity to HyHEL-10, as determined by competitive ELISA [306]. Chan et al. have shown that reconstitution of WT BL/6 mice with SW<sub>HEL</sub> B cells and challenge with HEL<sup>3x</sup>-sRBC resulted in strong class-switched responses [335]. In addition, DNA sequencing of sorted HEL-specific GC B cells in those challenged mice confirmed that antibodies underwent affinity maturation to HEL<sup>3x</sup>. This maturation was associated with acquisition of predictable V<sub>H</sub> chain amino acid mutations (e.g., canonical somatic mutation encoding for Y53D substitution) [335], [13].

In this chapter, two heart donor strains, maintained on BL/6 (H-2<sup>b</sup>) background and that expressed either mHEL<sup>WT</sup> [274] or mHEL<sup>3x</sup> [336], were incorporated into a transplant model. The gene constructs of mHEL<sup>WT</sup> and mHEL<sup>3x</sup> strains were designed to express the HEL protein while being anchored to the cell membrane by a transmembrane linker amino acid sequence

and cytoplasmic domains of the H-2K<sup>b</sup> [336] or H-2K<sup>k</sup> [274] class I MHC molecules, respectively (figure 24B). The presence of mHEL gene was confirmed by PCR from ear notched mice, and the phenotype was confirmed by flow cytometry on tail bleeds and staining B cells for using anti-CD19 and anti-HEL antibodies.

#### **5.1.4 TCR-transgenic strain 'TCR7' as a source for CD4 T cells**

The TCR7 transgenic strain was detailed previously (4.1.1.2). Briefly, the strain comprises a large proportion (> 80%) of CD4 T cells that is specific to HEL<sub>74-88</sub> epitope presented in the context of MHC class II (I-A<sup>b</sup>) [275]. The HEL<sub>74-88</sub> sequence is conserved in both the HEL<sup>WT</sup> and HEL<sup>3x</sup> variants.

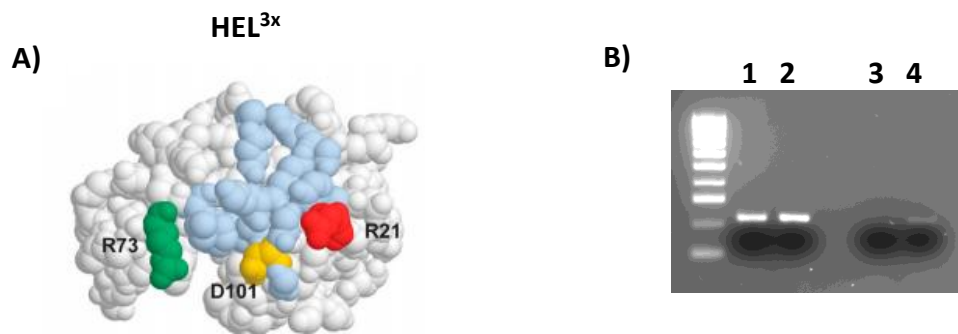


**Figure 24. HEL protein structure and expression.** A) Rasmol space-filling model of the HEL<sup>3x</sup> mutant protein with mutated residues displayed in colour against the HyHEL10-binding site (light blue). Mutations are arginine 21 to glutamine (R21, red), arginine 73 to glutamate (R73 green), and aspartate 101 to arginine (D101, yellow). Figure obtained with permission from Brink et al., 2007. B) Both mHEL<sup>WT</sup> and mHEL<sup>3x</sup> are homozygous for HEL gene (lanes 1 and 2, respectively), and travelled through the 1% agarose gel at an equivalent size to that of the positive control obtained from breeder mHEL<sup>WT</sup> or mHEL<sup>3x</sup> parent (lane 4). No bands were shown in the negative control (lane 3, master mix with no DNA), courtesy of Mrs. Sylvia Rehakova.

## 5.2 Aims

To develop and characterise a heart transplant model in SW<sub>HEL</sub> recipients that will permit study of the contribution of affinity maturation to progression of allograft vasculopathy.

## 5.3 Results

### 5.3.1 The SW<sub>HEL</sub> heart transplant model

Hearts from BL/6 (H-2<sup>b</sup>) mice expressing either membrane bound mHEL<sup>WT</sup> (high affinity) [274] or mHEL<sup>3x</sup> protein (low affinity) [336] were grafted into SW<sub>HEL</sub> recipients [319]. In some experiments, recipients of mHEL<sup>3x</sup> hearts were additionally reconstituted with 5x10<sup>5</sup> TCR-transgenic TCR7 CD4 T cells that recognize I-A<sup>b</sup>-restricted HEL<sub>74-88</sub> peptide; CD4 T cell responses to HEL protein in the C57BL/6 strain are generally weak, and we reasoned that the transferred TCR7 cells may deliver essential helper function not otherwise provided by the endogenous C57BL/6 CD4 T cell population [275] (figure 25). I anticipated that in this model, the mHEL<sup>3x</sup> heart graft would trigger an anti-HEL germinal centre response, in which SW<sub>HEL</sub> B cell would initially bind to the mHEL<sup>3x</sup> graft with low affinity. In the GC dark zone, SW<sub>HEL</sub> B cells would be subject SHM, and, after several rounds of proliferation and selection in the light zone, B cells with affinity-matured BCRs to HEL<sup>3x</sup> would leave the B cell follicle and differentiate into plasma cells that generated high affinity anti-HEL<sup>3x</sup> antibodies. The role of affinity maturation in the progression of allograft vasculopathy could then be investigated.

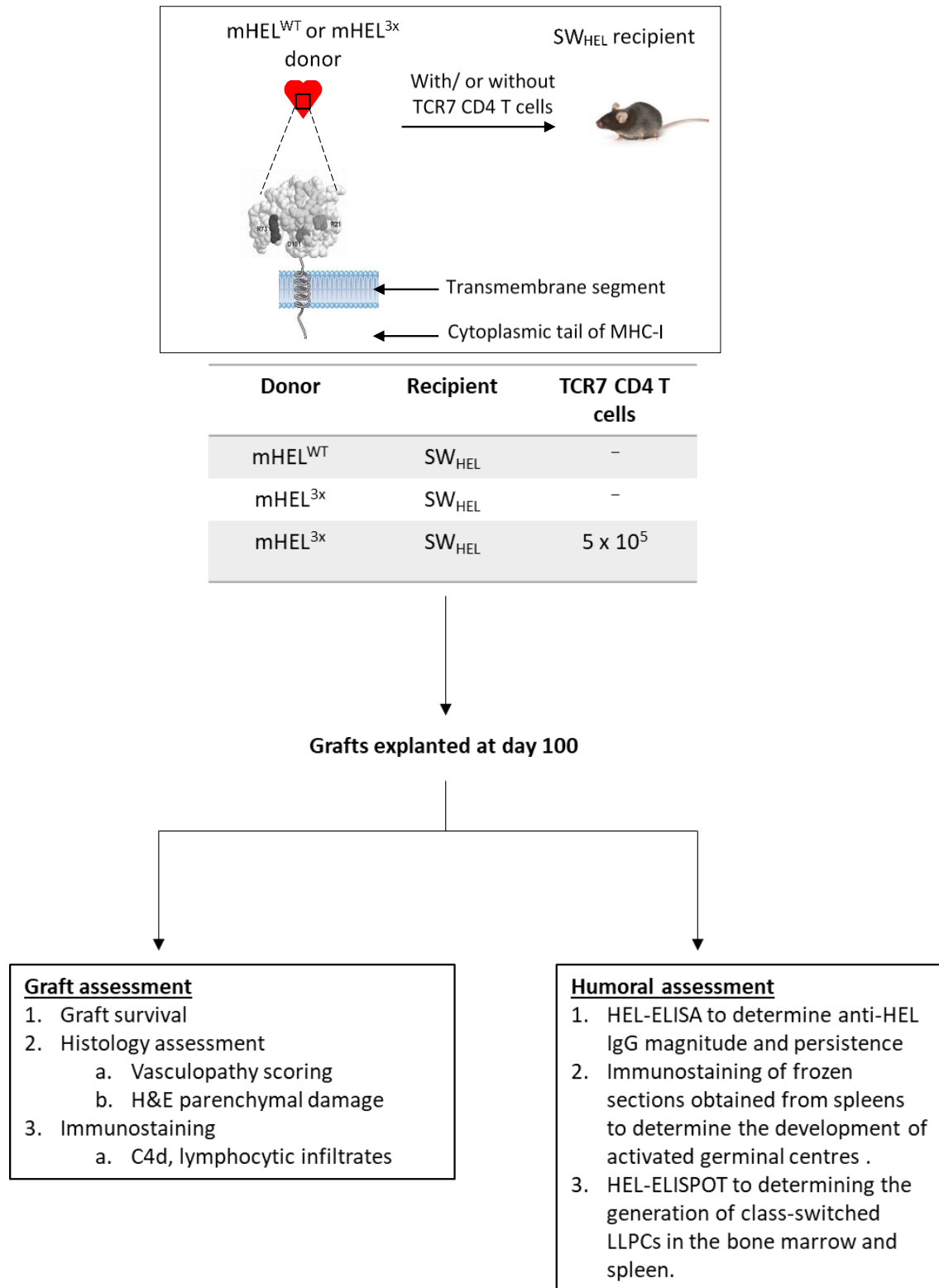


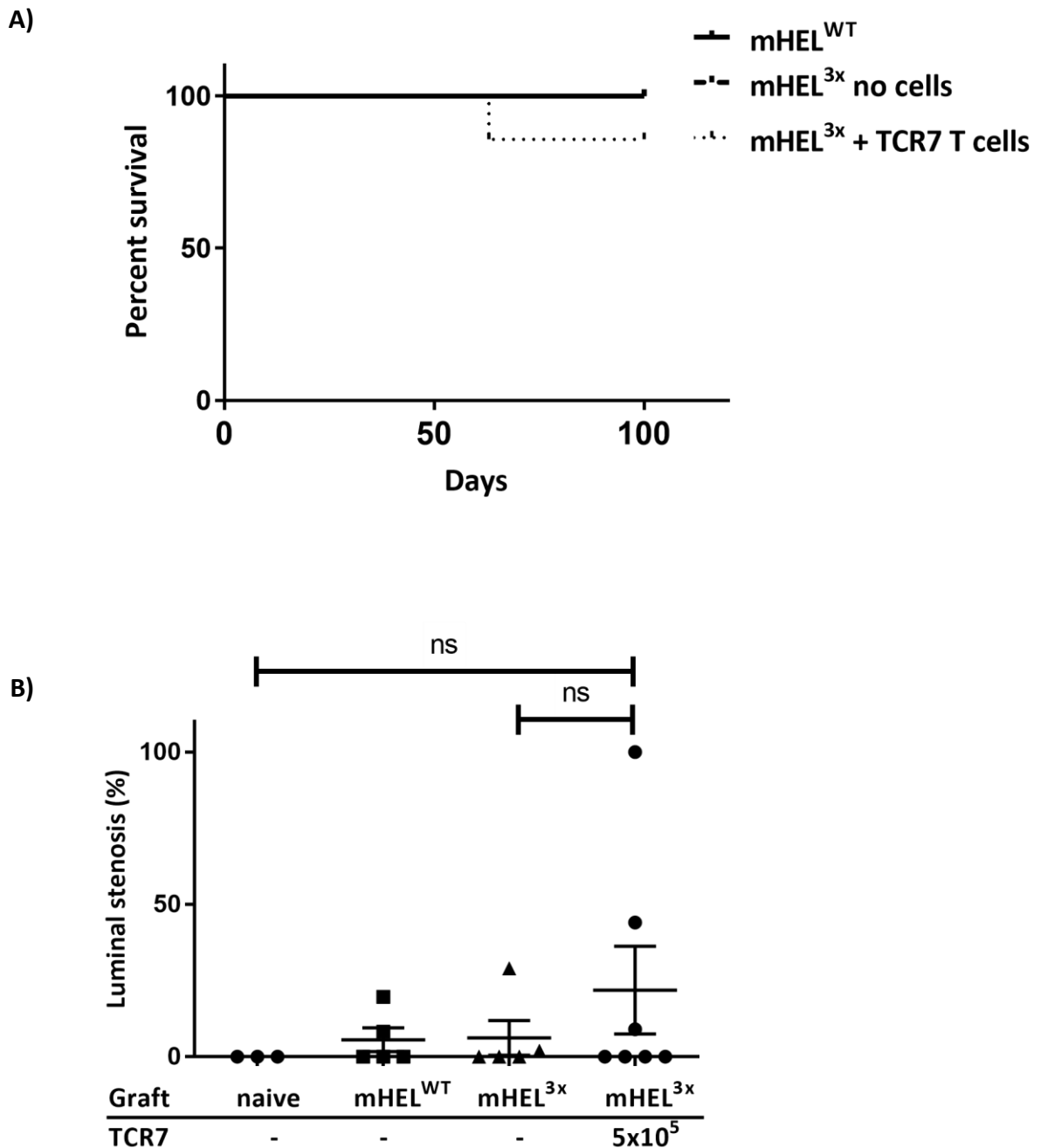
**Figure 25. Schematic study plan for heart transplantation model designed to investigate the development of affinity matured alloantibodies and their contribution to graft vascular disease and histopathological changes.**

### 5.3.2 Rejection kinetics

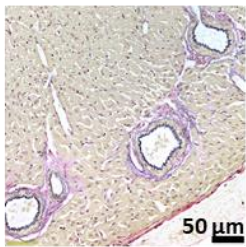
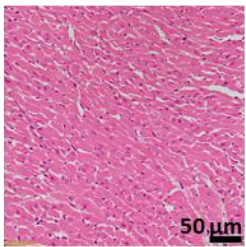
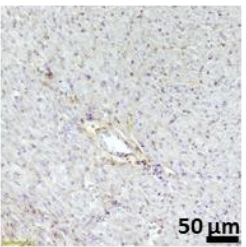
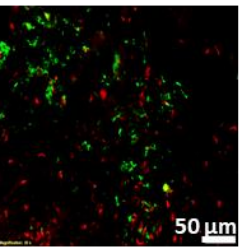
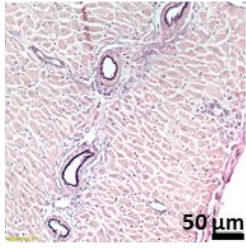
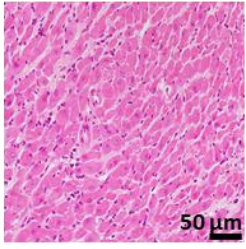
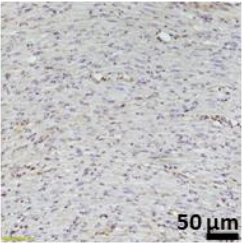
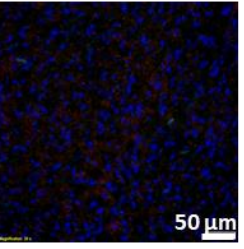
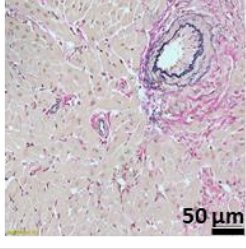
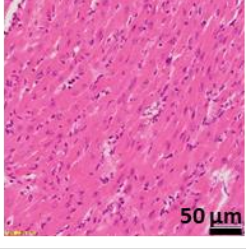
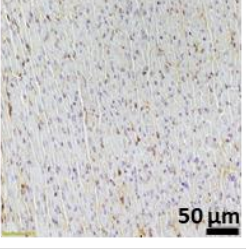
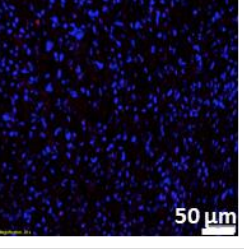
Hearts from mHEL<sup>WT</sup> (n = 5) donors were transplanted into SW<sub>HEL</sub> recipients, contractility of the heart was assessed by digital palpation weekly, and mice were sacrificed at a predetermined time point (day 100). Although it was expected that this model would elicit an immediate, and strong antibody response that would cause severe damage to the mHEL<sup>WT</sup>-expressing hearts, all grafts were beating upon sacrifice and did not reject. Similarly, mHEL<sup>3x</sup>-expressing grafts (n=5) and those receiving 5x10<sup>5</sup> TCR7 CD4 T cells (n=7) continued to beat until the day of graft retrieval, except for one heart which rejected at week 9 from mHEL<sup>3x</sup> recipient reconstituted with 5x10<sup>5</sup> TCR7 CD4 T cells (figure 26A).

### 5.3.3 Histology of explanted allografts

Paraffin-embedded heart grafts obtained from mHEL<sup>WT</sup> and mHEL<sup>3x</sup> donors demonstrated intact parenchymal tissue on H&E staining, no significant CAV development when compared to normal unmodified mHEL<sup>WT</sup> hearts (figure 26B), and were negative for the complement split-product C4d (figure 27). In order to investigate the graft-infiltrating lymphocyte populations, frozen sections obtained from heart allografts at explant were stained for B220+ B cells and CD4+ T cells by immunofluorescent-conjugated antibodies. This demonstrated minimal CD4 T cell or B cells infiltration (Figure 27). Lymphocyte deposition was not associated with obvious myocyte injury, and hence, according to the revised ISHLT cellular rejection grading system [11], there was no evidence of rejection (R0). However, histological examination of the one mHEL<sup>3x</sup> heart (from a recipient reconstituted with TCR7 CD4 T cells) that rejected at week 9 demonstrated widespread myocyte death, with all medium and large arteries developing CAV (figure 27). Immunofluorescence staining of heart grafts obtained from mHEL<sup>3x</sup> did not show any lymphocytic infiltrates.



**Figure 26. Graft survival and CAV development in SW<sub>HEL</sub> recipients of mHEL<sup>WT</sup> or mHEL<sup>3x</sup> heart grafts.** A) SW<sub>HEL</sub> recipients of mHEL<sup>WT</sup> and mHEL<sup>3x</sup> grafts survived up to the date of experiment termination. One graft rejected early (week 9) in a recipient of mHEL<sup>3x</sup> graft which was reconstituted with TCR7 CD4 T cells (n=5 in recipients of mHEL<sup>WT</sup> and mHEL<sup>3x</sup>; n=6 in recipients of mHEL<sup>3x</sup> and TCR7 T cells). B) Histogram demonstrating vasculopathy development scores in mHEL<sup>WT</sup> or mHEL<sup>3x</sup> grafts explanted at day 100 from SW<sub>HEL</sub> recipients. All grafts displayed comparable low levels of luminal stenosis that were not statistically significant from one another (naïve n=3, recipients of mHEL<sup>WT</sup> and mHEL<sup>3x</sup> n=5, and recipients of mHEL<sup>3x</sup> and TCR7 cells n=7). Data presented as mean ± SEM, Mann-Whitney unpaired two-tailed, ns: nonsignificant.

Donor/ cells	EBVG	H&E	C4d	CD4 and B220
mHEL <sup>WT</sup>	 50 $\mu$ m	 50 $\mu$ m	 50 $\mu$ m	 50 $\mu$ m
mHEL <sup>3x</sup> No cells	 50 $\mu$ m	 50 $\mu$ m	 50 $\mu$ m	 50 $\mu$ m
mHEL <sup>3x</sup> 5x10 <sup>5</sup> TCR7	 50 $\mu$ m	 50 $\mu$ m	 50 $\mu$ m	 50 $\mu$ m

**Figure 27. Histology assessment of mHEL<sup>WT</sup> or mHEL<sup>3x</sup> heart grafts in SW<sub>HEL</sub> recipients.**

Heart grafts obtained from mHEL<sup>WT</sup> or mHEL<sup>3x</sup> donors (whether receiving TCR7 CD4 T cells or not) developed low degree of vascular lesions as demonstrated by EBVG staining. H&E staining demonstrated intact parenchyma and few interstitial inflammatory infiltrates with no myocyte damage. Immunohistochemistry for donor hearts small arteries and capillaries did not show evidence of the complement split product C4d. Lymphatic deposition showed few scattered CD4 T cells and B cells in the mHEL<sup>WT</sup> donor hearts as demonstrated by CD4 (red) and B220 (green) immunofluorescence staining, while mHEL<sup>3x</sup> donor hearts showed no lymphocytic deposition (DAPI, blue). Scale bar is equivalent to 50  $\mu$ m.

### 5.3.4 Humoral response characterisation

Splenic GC activity (proportion of B cell follicles that exhibited secondary morphology (GL7<sup>+</sup>ve)) in unmodified SW<sub>HEL</sub> recipients of either mHEL<sup>WT</sup> or mHEL<sup>3x</sup> donors was similar, and slightly higher in TCR7 CD4 T cell-reconstituted recipients of mHEL<sup>3x</sup> heart, but this difference did not reach statistical significance (figure 28, A and B). GC activity in all recipient groups was similar, and comparable to that observed in control spleens obtained from SW<sub>HEL</sub> mice challenged with 2x10<sup>8</sup> sRBC-HEL<sup>WT</sup>. GC activity in control mice challenged with 2x10<sup>8</sup> sRBCs only (mock) was minimal. Despite the evidence of GC development in SW<sub>HEL</sub> recipients, numbers of HEL-specific long-lived class-switched plasma cells (considered an exclusive output of the GC response) were similar to those retrieved from naïve mice. Because this experiment detected class-switched plasma cells only in two graft recipients per group, accurate statistical comparisons cannot be obtained (figure 28C).

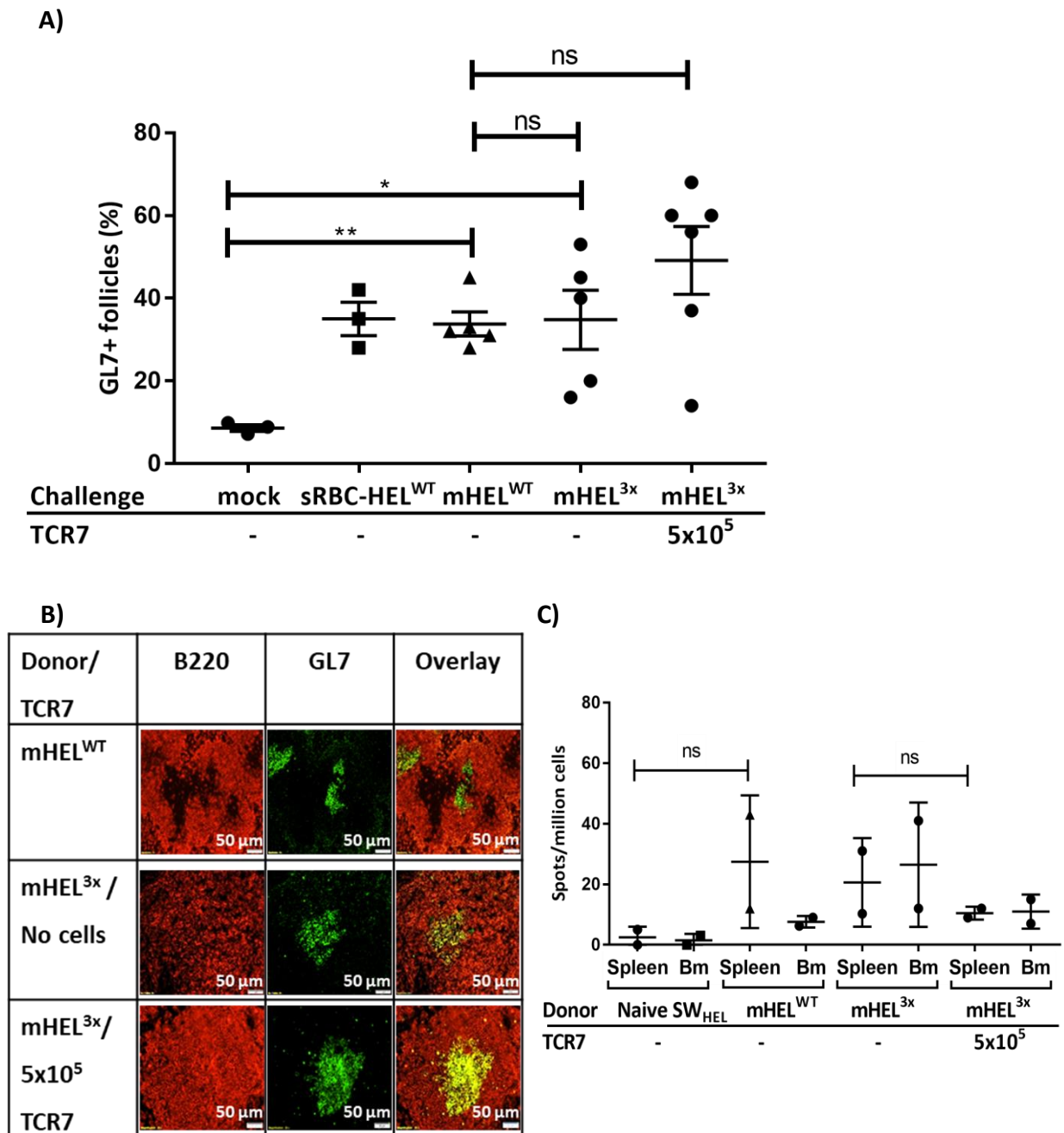


**Figure 28. GC activity in SW<sub>HEL</sub> recipients of mHEL-expressing heart allografts.** A) Histogram depicting frequency of secondary splenic follicles expressed as a percentage of total follicles within the spleen of SW<sub>HEL</sub> recipients of sRBCs only (mock n=3), HEL<sup>WT</sup> conjugated to sRBCs (sRBC-mHEL<sup>WT</sup> n=3), mHEL<sup>WT</sup>-expressing (mHEL<sup>WT</sup> n=5), mHEL<sup>3x</sup>-expressing heart grafts (n=5) and recipients of mHEL<sup>3x</sup> grafts and TCR7 T cells (n=7). Each dot represent one biological replicate. Data represents mean ± SEM, two-tailed Mann-Whitney test. \**P*=0.03, \*\**P*=0.0007, ns: nonsignificant (*P*>0.05). B) Immunofluorescence staining of spleens from recipients of mHEL-expressing grafts demonstrating activated B cells (GL7, green) within the secondary follicles (B220, red). Scale bar is equivalent to 50 μm. C) Numbers of IgG-switched HEL-specific B cells retrieved from bone marrow of SW<sub>HEL</sub> recipients was not different when compared to bone marrow retrieved from naïve SW<sub>HEL</sub>. Data presented as mean ± SEM, (n=2).

In order to estimate affinity maturation status, anti-HEL ELISA was performed. Serum samples from two and fourteen weeks after heart transplantation were assayed for binding to HEL<sup>WT</sup> or HEL<sup>3x</sup> recombinant proteins, in the expectation that little affinity maturation would have occurred by two weeks, but that by 14 weeks the response to the HEL<sup>3x</sup> challenge would have been subject to substantial SHM. As expected, recipients of mHEL<sup>WT</sup> donor hearts demonstrated strong binding to HEL<sup>WT</sup> protein at both early and late time points (figure 29A). This reflects the high proportion of the B cell population that expressed HyHEL-10 specificity (10 – 20% of naïve B cells); the early antibody response from this population was already of such high affinity against the HEL<sup>WT</sup> target that further mutation would be unproductive [273].

As anticipated, recipients of mHEL<sup>3x</sup> heart grafts which did not receive TCR7 CD4 T cells demonstrated strong binding to HEL<sup>WT</sup> protein at both early and late time points. Surprisingly, however, there was no apparent affinity maturation towards HEL<sup>3x</sup> antigen with time (figure 29B). A similar pattern was also observed following the transfer of TCR7 CD4 T cells, in that TCR7-reconstituted recipients of mHEL<sup>3x</sup> grafts demonstrated strong, and long lasting anti-HEL<sup>WT</sup> antibodies, but with no apparent increase in affinity towards the HEL<sup>3x</sup> protein at late time points (figure 29C).

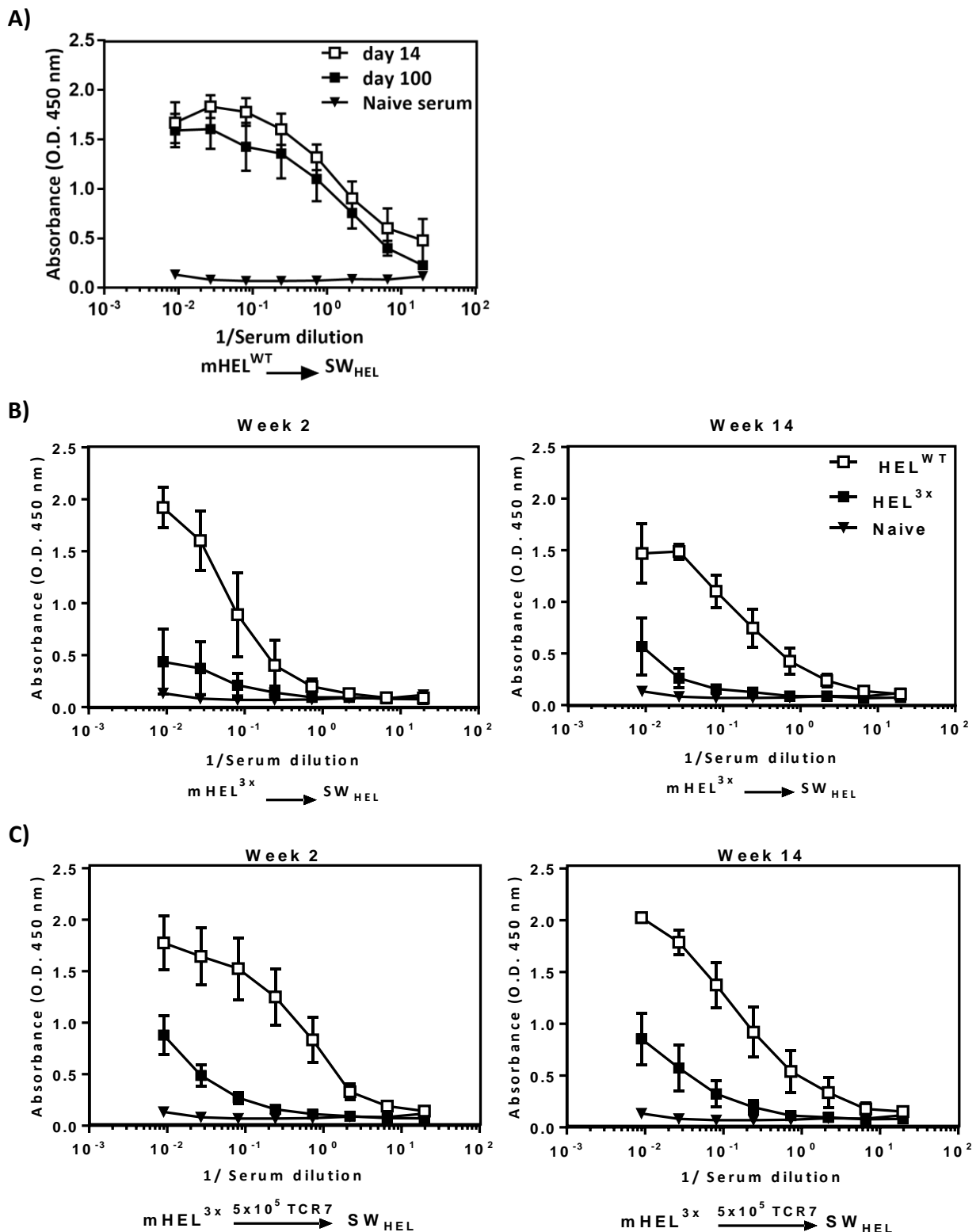


**Figure 29. Antibody response analysis in SW<sub>HEL</sub> recipients of mHEL-expressing allografts.**

A) Serum samples obtained from SW<sub>HEL</sub> recipients of mHEL<sup>WT</sup> heart grafts at an early time point (d14) were compared to those obtained at a late time point (day 100) for binding to HEL<sup>WT</sup> by ELISA (n=5, each dilution is represented as mean ± SEM). B) Triple serial dilution of serum samples obtained from recipients of HEL<sup>3x</sup> hearts not receiving (n=4), or C) receiving TCR7 CD4 T cells (n=6) at an early (week 2) or late time point (week 14) were plotted against absorbance (O.D. 450 nm) for binding HEL<sup>WT</sup> (white boxes) or mHEL<sup>3x</sup> (black boxes) protein by ELISA (each dilution is represented as mean ± SEM). Serum obtained from naive SW<sub>HEL</sub> mice was plotted for comparison.

The generation of IgG subclasses in response to mHEL-expressing grafts was determined by ELISA on serum samples obtained at week 14. Plates were coated with HEL<sup>WT</sup> antigen, and bound serum antibodies were detected using anti-isotype heavy chain-specific secondary antibodies as detailed in the methods section. The humoral anti-HEL response generated all IgG subclasses except for IgG1, which was generated at low levels. Notably, the production of IgG2a and IgG2b, which can fix complement in mice [337], were not associated with complement deposition in donor grafts (figure 30).

An interesting observation was that in splenic frozen sections retrieved from SW<sub>HEL</sub> recipients of either mHEL<sup>WT</sup> or mHEL<sup>3x</sup> donor grafts, HEL-specific B cells were localized in the B cell follicles (identified as HEL<sup>+</sup> IgD<sup>+</sup> B cells) (figure 31A). However, although formal enumeration was not performed, there appeared to be relatively lower frequencies of HEL-specific B cells within the GC area (GL7<sup>+</sup> HEL<sup>+</sup> B cells - figure 31B). This observation may indicate that HEL-specific B cells did not enter the secondary follicles as GC B cells, and instead accumulated outside the GC, resulting in ineffective affinity maturation (figure 31C).

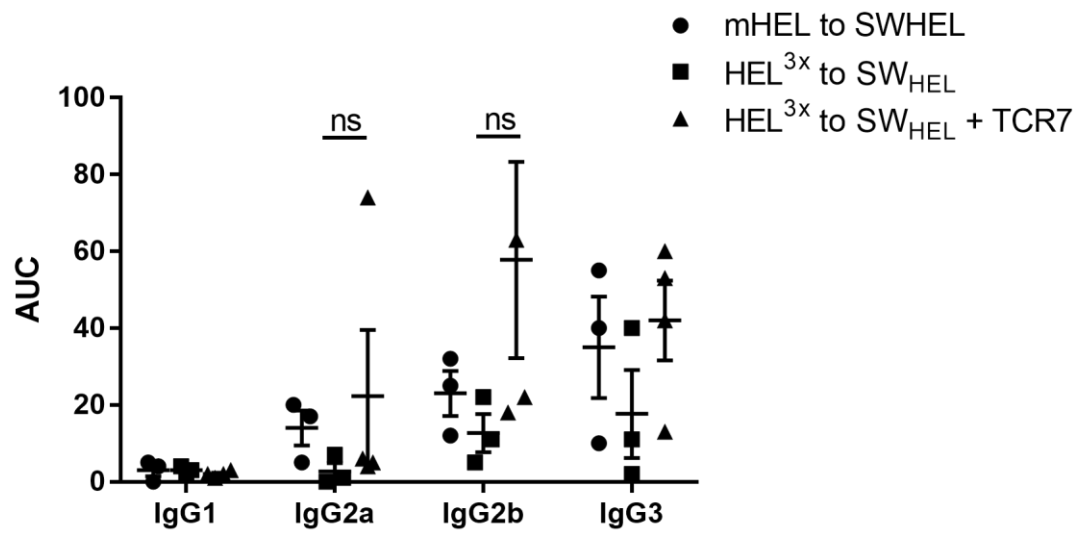
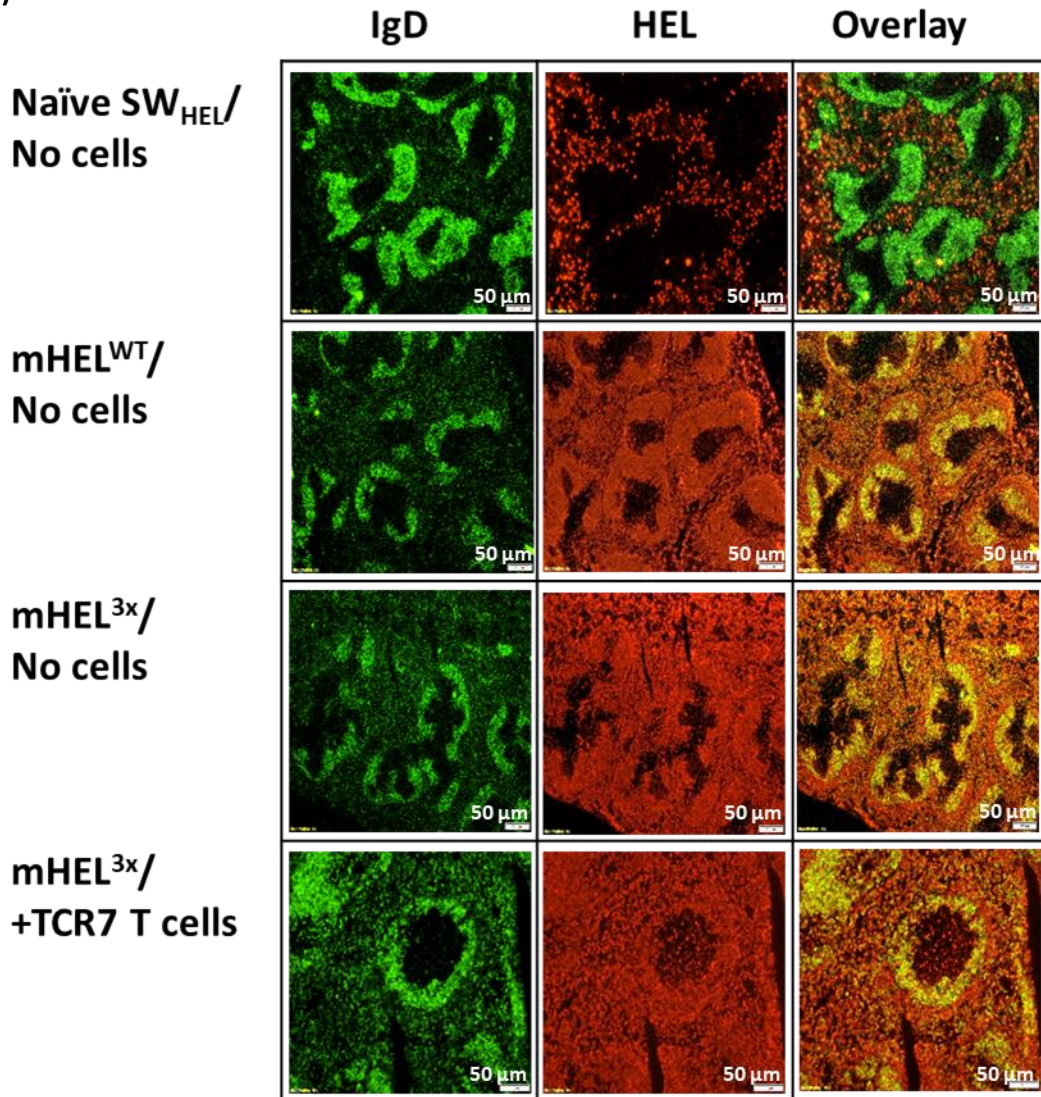
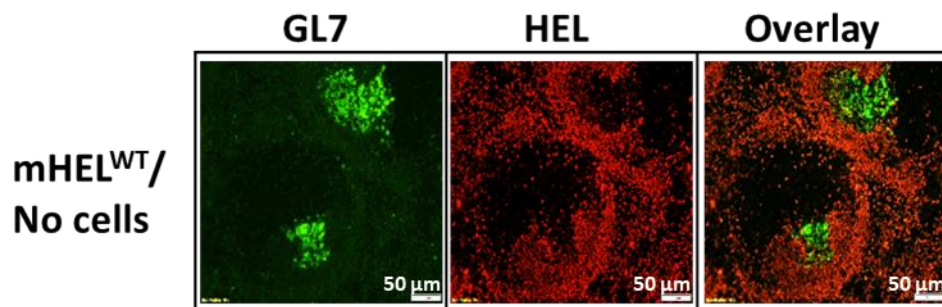


**Figure 30. HEL-specific IgG isotypes distribution in response to mHEL<sup>WT</sup> or mHEL<sup>3x</sup> allografts in SW<sub>HEL</sub> recipients.** Sera obtained from mHEL<sup>WT</sup> or mHEL<sup>3x</sup> graft recipients at day 100 post transplantation were tested for the presence of class switched IgG isotypes. Data represents mean  $\pm$  SEM, ns: nonsignificant, two-tailed Mann-Whitney test (n=3).

A)



B)



C)

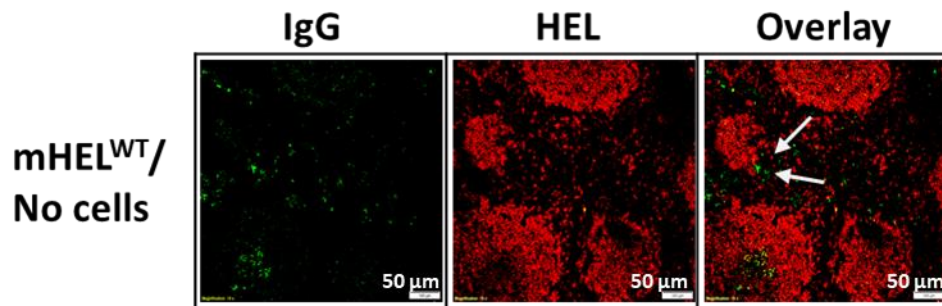


**Figure 31. Distribution of HEL-specific B cells in spleens of SW<sub>HEL</sub> recipients.** A) Spleens obtained from naïve (top row) or from SW<sub>HEL</sub> recipients of heart allografts (mHEL<sup>WT</sup> or mHEL<sup>3x</sup>) which either received no or 5x10<sup>5</sup> TCR7 CD4 T cells were collected at day 100 post-transplantation and double stained with anti-IgD (FITC, green) and HEL protein (detected by rabbit anti-HEL serum, and goat anti-rabbit Cy3, red) to identify the distribution of HEL-specific B cells. B) Representative immunofluorescence staining of recipient SW<sub>HEL</sub> mouse demonstrating relatively few HEL-specific B cells are getting access to GC area (GL7-FITC, green). C) Representative immunofluorescence staining of recipient SW<sub>HEL</sub> mouse of mHEL<sup>WT</sup> graft demonstrating class-switched IgG B cells (goat anti mouse IgG-FITC, green), and HEL-specific B cells (red). Scale bar equivalent to 50 μm.

### 5.3.5 Affinity maturation assessment in a competitive HEL-specific B cells environment

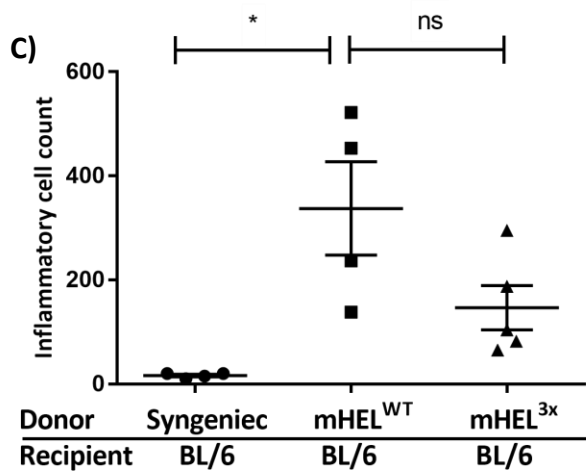
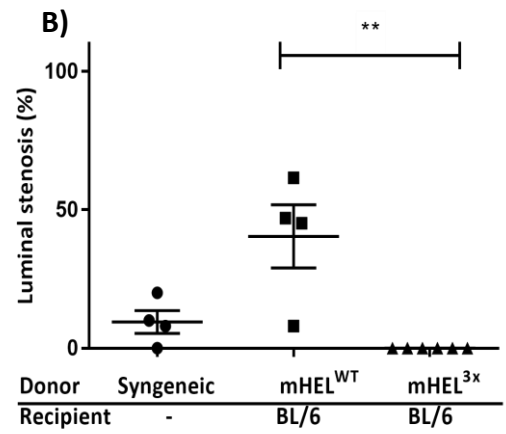
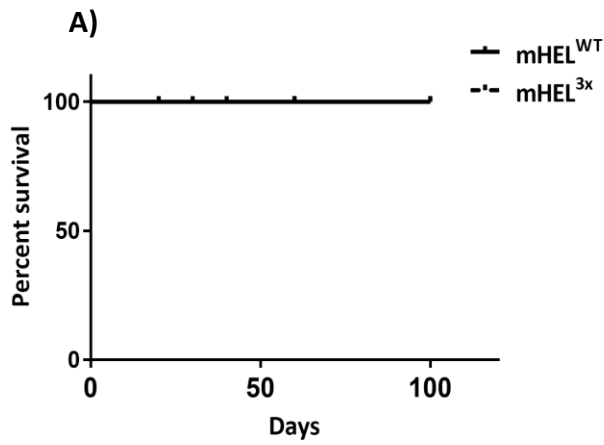
Because the previous heart transplant model in SW<sub>HEL</sub> recipients (described in 5.3.1) generated large amounts of activated HEL-specific B cells that might have affected the ability of tracking antibody affinity maturation by ELISA, the model was refined to mirror the low precursor frequencies that are typically seen in primary antibody responses. To do so, the BL/6 strain was utilized as a recipient for mHEL<sup>WT</sup> or mHEL<sup>3x</sup> heart allografts. In order to provide a pure population of HEL-specific B cells without nonHEL-specific B cells or T cells that can be otherwise present in the wild type SW<sub>HEL</sub> strain, the *Rag2*<sup>-/-</sup> SW<sub>HEL</sub> strain was developed. The wild type SW<sub>HEL</sub> strain [273] was crossed with BL/6.*Rag2*<sup>-/-</sup> mice to provide *Rag2*<sup>-/-</sup> SW<sub>HEL</sub> strain, which lack all T cells, but retain SW<sub>HEL</sub> B cells with high-affinity to HEL<sup>WT</sup> antigen – the rearranged VDJ variable region genes (i.e., encoding anti-HEL specificity) are already incorporated in the germline of the heavy- and light chain loci, and hence *Rag2* deficiency does not prevent BCR expression and SW<sub>HEL</sub> B cell survival. Similarly the *Rag2*<sup>-/-</sup>.SW<sub>HEL</sub> B cells can still undergo SHM and affinity maturation, because this is dependent, not on *Rag* enzymes, but upon expression of activation-induced cytidine deaminase (AID) [338]. However, in the absence of *Rag2* enzyme, endogenous (non-receptor-transgenic) B cells do not develop and *Rag2*<sup>-/-</sup>.SW<sub>HEL</sub> mice therefore only contain a monoclonal population of HEL-specific B cells.

This section explores whether the anti-HEL alloantibody response in BL/6 recipients of mHEL<sup>WT</sup> or mHEL<sup>3x</sup> heart allografts reconstituted with 10<sup>5</sup> *Rag2*<sup>-/-</sup> SW<sub>HEL</sub> B cells undergo affinity maturation, and if so, whether this results in accelerated rejection and development of allograft vasculopathy.

#### 5.3.5.1 Rejection kinetics in BL/6 recipients of mHEL<sup>WT</sup> and mHEL<sup>3x</sup> heart grafts

BL/6 recipients of either mHEL<sup>WT</sup> (n = 4) or mHEL<sup>3x</sup> (n = 6) heart grafts which received intravenous 10<sup>5</sup> *Rag2*<sup>-/-</sup> SW<sub>HEL</sub> B cells did not reject donor grafts up to the day of experiment termination (day 100) (figure 32A). While mHEL<sup>WT</sup> donor hearts developed some degree of vasculopathy (%40 ± 10; mean ± SEM), recipients of mHEL<sup>3x</sup> remained CAV-free (figure 32B).

In both groups, immunofluorescence analysis of heart frozen sections was negative for complement split product C4d (figure 32D). Histological evaluation of H&E-stained paraffin sections demonstrated that inflammatory infiltrates were more numerous in grafts obtained from mHEL<sup>WT</sup> donors as opposed to mHEL<sup>3x</sup> allografts, but this difference did not reach statistical significance (figure 32C, and 32D). Inflammatory infiltrates were mainly polymorphonuclear leukocytes, with no CD4 T cells detected, and only very sparse B cells, confirming the absence of cellular rejection.



**D)**

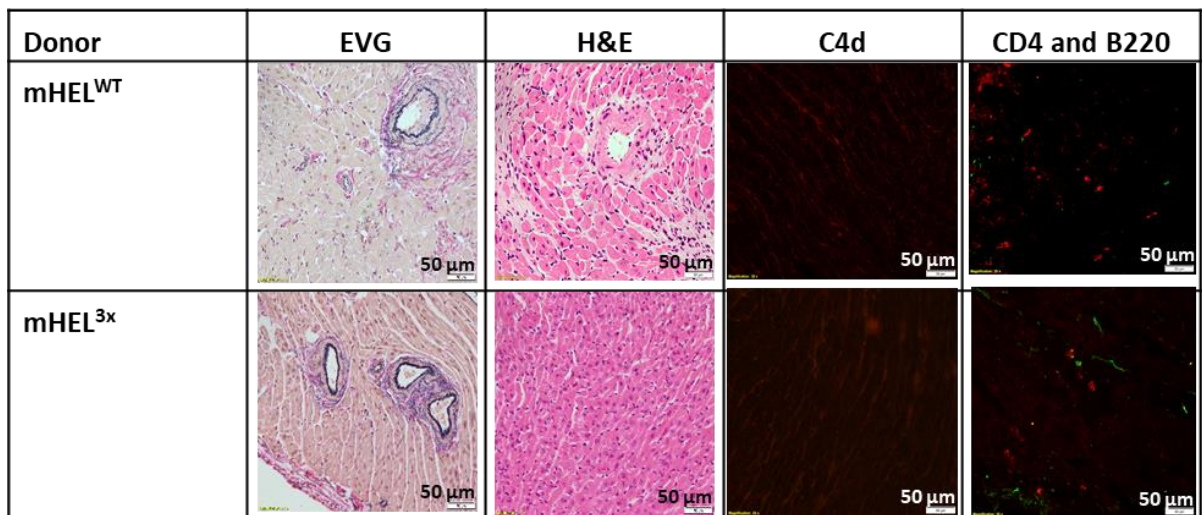


**Figure 32. Heart grafts survival and histopathological assessment in BL/6 recipients of mHEL donors.** A) All grafts from mHEL<sup>WT</sup> (n=4) or mHEL<sup>3x</sup> (n=6) donors survived long term in BL/6 recipients reconstituted with 10<sup>5</sup> *Rag2*<sup>-/-</sup> SW<sub>HEL</sub> B cells. B) Vasculopathy development was significantly higher in recipients of mHEL<sup>WT</sup> grafts (n=4) than in recipients of mHEL<sup>3x</sup> hearts (n=6) receiving SW<sub>HEL</sub> B cells. Syngeneic control (n= 4). Data displayed as mean ± SEM; \*\**P*<0.002, unpaired two-tailed Mann-Whitney test. C) Inflammatory cellular infiltrates (i.e., neutrophils) present in images taken at x20 of the graft tissue were counted and compared between different donor hearts. Each data point represents the average number of inflammatory cells present in 5 representative images of the same biological replicate. Data displayed as mean ± SEM; \**P*<0.01, ns: nonsignificant, unpaired, two-tailed Mann-Whitney test). D) Representative image of paraffin embedded heart sections stained with EVG demonstrating CAV development in mHEL<sup>WT</sup> donor grafts as opposed to mHEL<sup>3x</sup> donor grafts which remained CAV-free. H&E staining demonstrated intact parenchyma with more pronounced inflammatory infiltrates in mHEL<sup>WT</sup> grafts as opposed to minimal damage and inflammatory infiltrates in retrieved mHEL<sup>3x</sup> grafts. Frozen sections stained for complement deposition (C4d) were negative, with minimal B220<sup>+</sup> B cells (Red), and CD4<sup>+</sup> T cells (green). Scale bar is equivalent to 50 μm.

### 5.3.5.2 Humoral response in a competitive HEL-specific B cell environment

Splenic germinal centre activity was similar in BL/6 recipients of mHEL<sup>WT</sup> and mHEL<sup>3x</sup> grafts reconstituted with *Rag2*<sup>-/-</sup>.SW<sub>HEL</sub> B cells, and comparable to that observed in BL/6 mice challenged with HEL antigen (200µg) emulsified in CFA (figure 33A). In addition, HEL-specific B cells in challenged mice were concentrated within the active GC areas of B cell follicles or within the follicular marginal zone (figure 34A). The presence of such GCs at late time point suggests ongoing delivery of help from T<sub>FH</sub> cells – Crotty has suggested that this is required to maintain the GC response [243]. In support, CD4 T cells were identifiable within the splenic GC microenvironment on confocal imaging at late time-points (figure 34B). Despite the detectable GC activity in both recipient groups, the frequency of HEL-specific B cells obtained from the bone marrow (an exclusive output of the GC response) was limited and did not reach statistical significance when compared to HEL-specific class-switched B cells retrieved from naïve BL/6 mice (figure 33B).

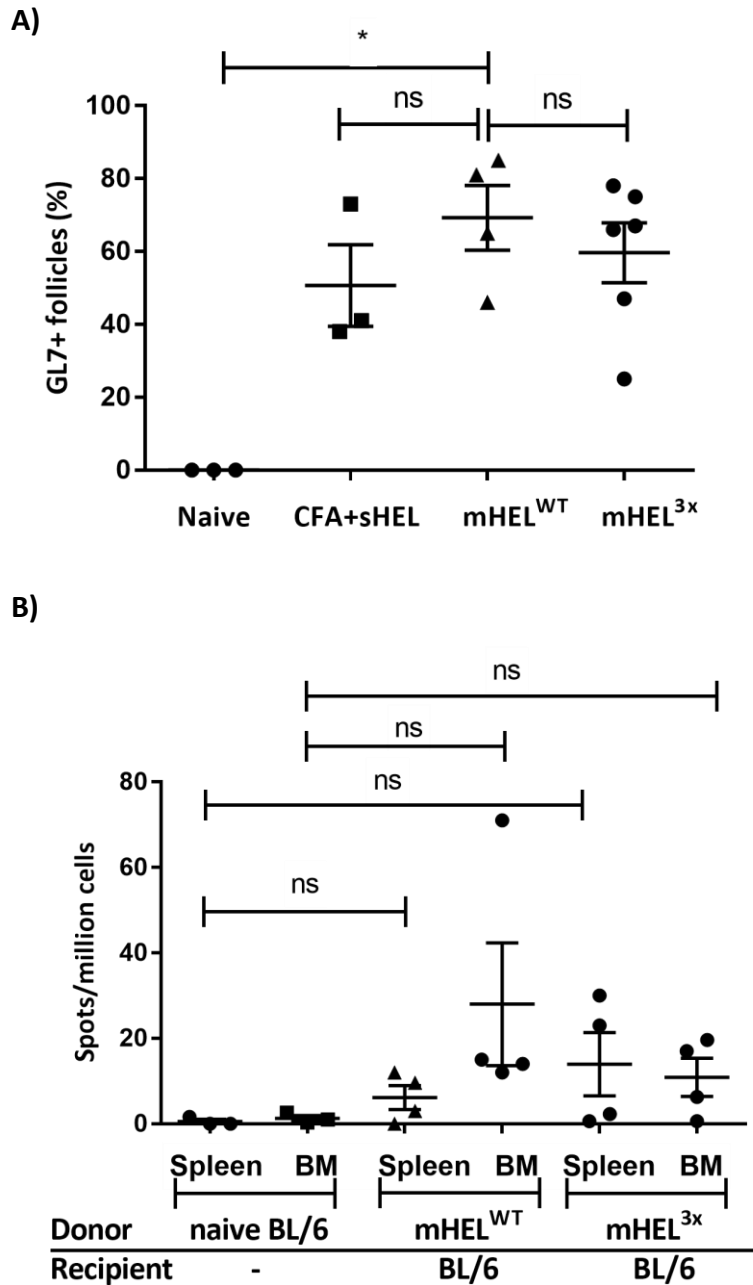
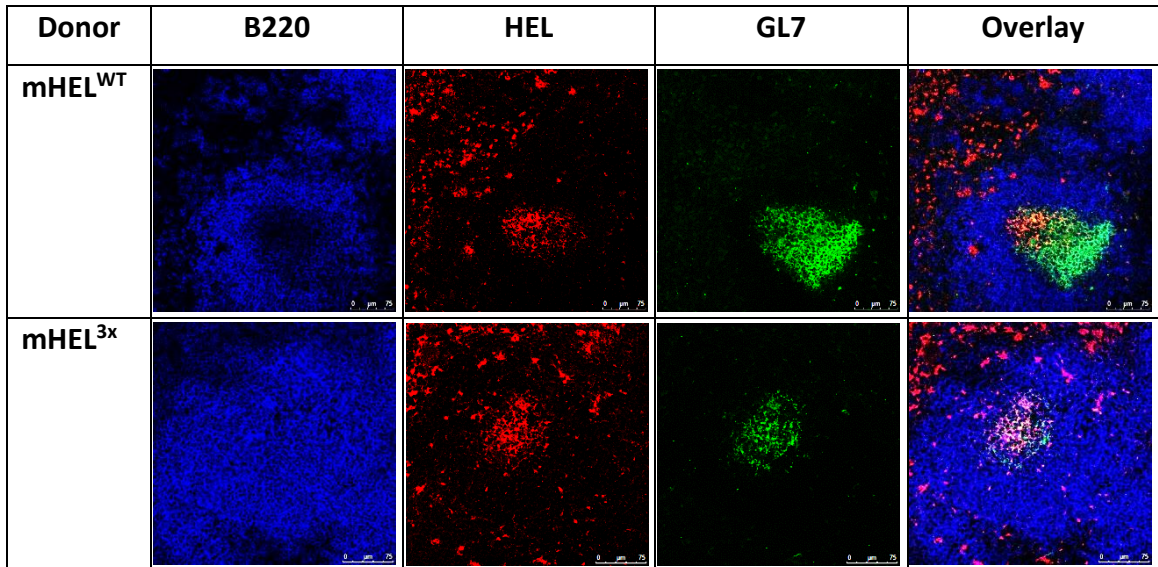


**Figure 33. GC and long-lived plasma cells assessment in BL/6 recipients of mHEL-expressing grafts.** A) BL/6 recipients of either mHEL<sup>WT</sup> (n=4) or mHEL<sup>3x</sup> heart grafts (n=6) reconstituted with 10<sup>5</sup> Rag2<sup>-/-</sup> SW<sub>HEL</sub> B cells developed similar degrees of activated secondary follicles to that of BL/6 recipients challenged with CFA-HEL emulsion (n=3). The percentage of HEL-specific GC activity in recipients of mHEL<sup>WT</sup> was statistically significant from the level of GC activity in naïve BL/6 mice (n=3). Data is represented as mean ± SEM; Mann-whitney, unpaired, two-tailed \*P=0.001, ns: non-significant. B) Both recipients of mHEL<sup>WT</sup> (n=4) or mHEL<sup>3x</sup> (n=4) allografts displayed low numbers of HEL-specific B cells retrieved from the spleens and bone marrow of recipient mice. Numbers of HEL-specific class-switched B cells were not statistically significant from naïve BL/6 (n=3). Data is represented as mean ± SEM; ns: non-significant, Mann-Whitney unpaired two-tailed.

A)



B)

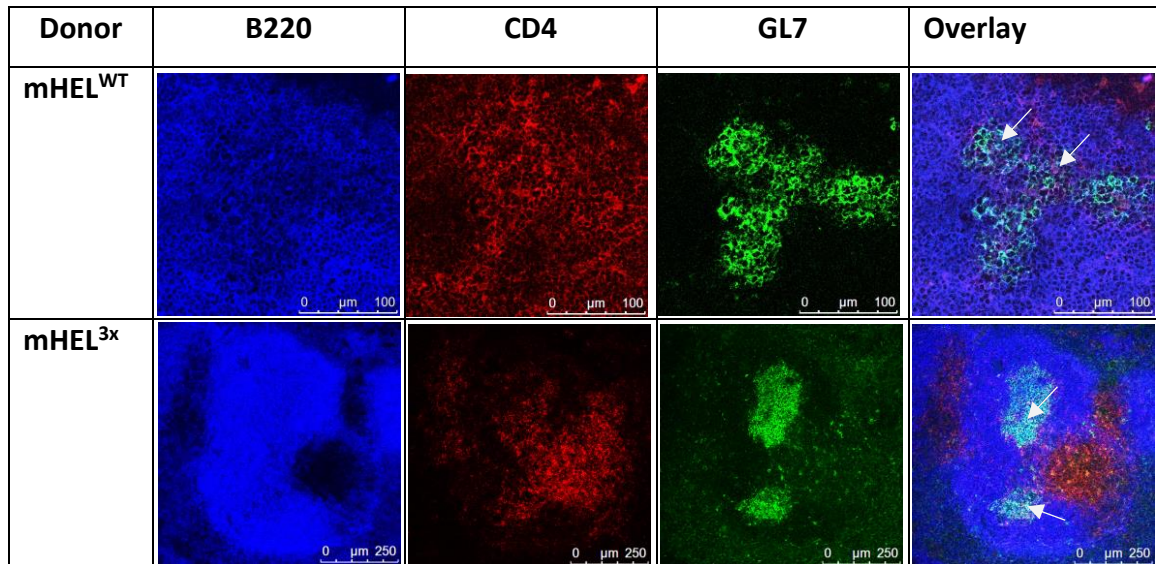


**Figure 34. Representative germinal center activation images in spleens obtained at day 100 post-transplantation from BL/6 recipients of mHEL<sup>WT</sup> or mHEL<sup>3x</sup> allografts and 10<sup>5</sup> *Rag2*<sup>-/-</sup> SW<sub>HEL</sub> B cells.** A) GC specificity towards HEL-antigen was confirmed in three colored confocal microscopy (B cells: B220-APC [blue], HEL was detected by anti-HEL rabbit-serum and goat anti-rabbit Cy3 secondary staining [red], and GC activity by GL7-FITC [green]). B) Formed GCs contained a population of T<sub>FH</sub> cells as demonstrated by three coloured confocal microscopy B220-APC [blue], CD4-biotin detected by SA-AF555 secondary staining [red], and GL7-FITC [green]). Arrows indicate areas where CD4 T cells overlapped with GL7+ B cells. A) GC specificity towards HEL-antigen was confirmed in three colored confocal microscopy (B cells: B220-APC [blue], HEL was detected by anti-HEL rabbit-serum and goat anti-rabbit Cy3 secondary staining [red], and GC activity by GL7-FITC [green]). B) Formed GCs contained a population of T<sub>FH</sub> cells as demonstrated by three coloured confocal microscopy B220-APC [blue], CD4-biotin detected by SA-AF555 secondary staining [red], and GL7-FITC [green]). Arrows indicate areas where CD4 T cells overlapped with GL7+ B cells.

Consistent with the severity of allograft vasculopathy, the anti-HEL antibody response was stronger in recipients of mHEL<sup>WT</sup> grafts than in recipients of mHEL<sup>3x</sup> grafts. Recipients of mHEL<sup>WT</sup> grafts mounted anti-HEL antibody responses that were still detectable in serum at week 14, albeit not as strong as the response observed at week 2 (Figure 35A). Anti-HEL titres were less at both time points in recipients of mHEL<sup>3x</sup> grafts (Figure 35B). Surprisingly, analysis of antibody binding to HEL<sup>WT</sup> and HEL<sup>3x</sup> proteins suggested that, if anything, the HEL response was stronger at early time points. Finally, all IgG isotypes (except for IgG1) were generated in response to mHEL allografts at variable degrees (figure 36). Similar to SW<sub>HEL</sub> recipients, the generation of complement fixing isotypes IgG2a and IgG2b were not associated with C4d deposition in either mHEL<sup>WT</sup> or mHEL<sup>3x</sup> heart grafts.

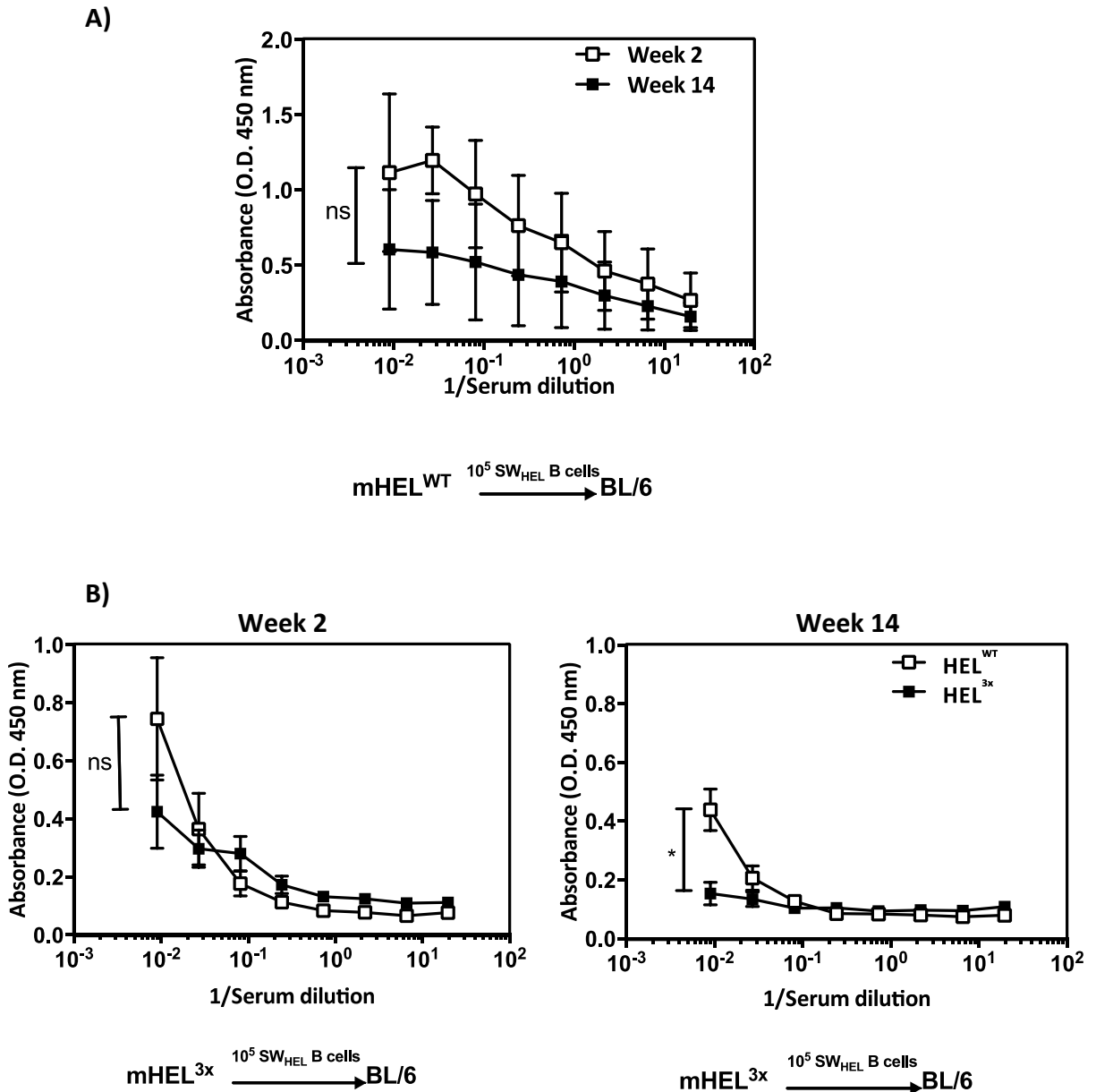


**Figure 35. Anti-HEL humoral response assessment by ELISA.** A) Serially diluted serum samples obtained from BL/6 recipients of mHEL<sup>WT</sup> grafts receiving  $10^5$  Rag.SW<sub>HEL</sub> B cells demonstrated higher anti-HEL antibody titers at week 2 than at week 14 post-transplant. A similar pattern was observed in BL/6 recipients of mHEL<sup>3x</sup> hearts receiving  $10^5$  SW<sub>HEL</sub> B cells in that both anti-HEL<sup>WT</sup> and anti-HEL<sup>3x</sup> antibody titers were higher initially at week 2, and both present at lower levels at week 14. Data represent mean  $\pm$  SEM, ns: non-significant, \* $P < 0.0001$  ANOVA.

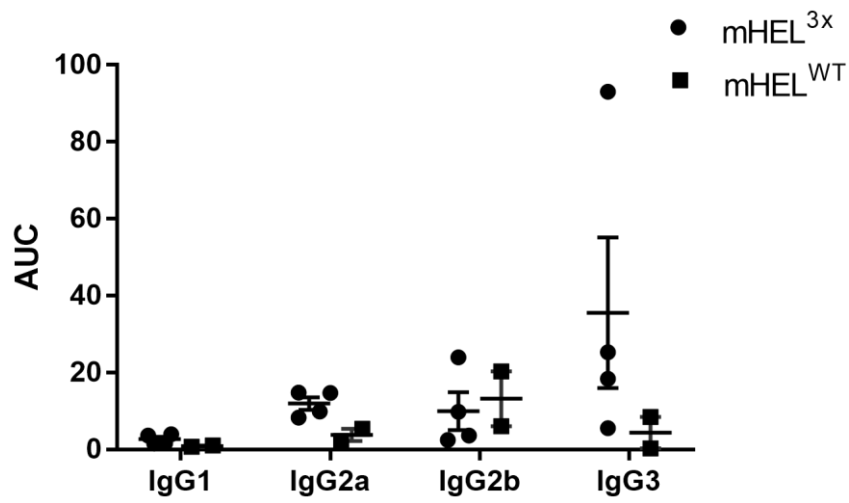


**Figure 36. HEL-specific IgG isotypes distribution in response to mHEL<sup>WT</sup> or mHEL<sup>3x</sup> allografts in BL/6 recipients.** Sera obtained from mHEL<sup>WT</sup> (grey) or mHEL<sup>3x</sup> (black) graft recipients at day 100 post transplantation were tested for the presence of class switched IgG isotypes. Plates were coated with HEL<sup>WT</sup>, and serum IgG was detected by IgG isotype-specific antibodies (mHEL<sup>3x</sup> n=4; mHEL<sup>WT</sup> n=2). Data represents mean  $\pm$  SEM of O.D. values at 450nm converted into area under the curve as described in the methods section. Two-tailed Mann-Whitney test.

## 5.4 Discussion

While the histopathological diagnosis of cellular cardiac rejection - interstitial lymphocytic infiltration that is associated with myocyte injury [252] - is well established; consensus on the histopathological features that constitute cardiac AMR has only recently been achieved, with diagnosis still based on standardized, but arbitrary, histopathologic grading criteria [113]. This deliberation in definitions partly reflects that the described parameters, such as swollen endothelial cells, dilated vessels, and interstitial oedema) are neither sensitive nor specific. In addition, some of the diagnostic features may only be observed in severe AMR (e.g., interstitial haemorrhage, platelet deposition, and local coagulation). Therefore, controversy persists on whether intervention is required for patients who develop DSA but with no apparent graft dysfunction [107]. In this chapter, a transplant model utilizing donor hearts with minor histocompatibility disparity to recipient was used to investigate the role of affinity matured antibodies in the progression of chronic rejection.

In the first described heart transplant model, the  $SW_{HEL}$  strain was used as a recipient for  $mHEL^{WT}$  or  $mHEL^{3x}$  expressing heart grafts. The  $SW_{HEL}$  mice comprises a large population of HEL-specific B cells that once activated are able of undergoing class-switch recombination and somatic hypermutation [273]. The  $SW_{HEL}$  mouse strain was maintained on C57BL/6 background which is known to be a low responder to HEL antigen [326], because processed HEL peptides are poorly recognised by endogenous CD4 T cells in C57BL/6 mice [339]. It is common practice to deliver HEL in combination with an adjuvant [340], or after coupling to xenogeneic RBCs [306] to enhance the T-dependent antibody response. In this model, monoclonal populations of transgenic HEL-specific CD4 T cells 'TCR7' were delivered to some  $mHEL^{3x}$  recipients in an attempt to improve the HEL-specific humoral response. My Initial hypothesis was that the initially low affinity for  $mHEL^{3x}$ -expressing heart allografts would prevent acute rejection, but that chronic rejection would still occur as a consequence of  $SW_{HEL}$  B cell-mediated affinity maturation; in contrast,  $mHEL^{WT}$  hearts (expressing high affinity antigen) would be rejected acutely. Instead, heart grafts expressing  $mHEL^{WT}$  or  $mHEL^{3x}$  antigens did not reject. In addition, histological assessment showed no significant development of vascular lesions when compared to naïve unmodified hearts obtained from  $mHEL^{WT}$  mice. The  $SW_{HEL}$  recipients developed long-lasting  $HEL^{WT}$ -specific antibodies which persisted at high titers up to the day of explant. However, allografts were negative for complement deposition and demonstrated mild histopathological changes (e.g., minimal

inflammatory cell infiltrates with no parenchymal damage). Competitive ELISA did not reveal efficient affinity maturation towards HEL<sup>3x</sup> antigen in serum sampled at week 14 from mHEL<sup>3x</sup> graft recipients. Screening for anti-HEL isotypes demonstrated the generation of complement-fixing IgG isotypes, albeit their precise concentration and their relative abundance to one another were not estimated. This is because the ratio of HRP-conjugate bound to the secondary antibody may vary among the four different isotype-specific antibodies, and therefore affecting the intensity of the developed color and optical density measurements. The lack of allograft C4d deposition, despite a demonstrable alloantibody response, has been previously described for non MHC class I antibodies (e.g., male specific antigen H-Y) [341]. It has been speculated that the lack of complement deposition may reflect a relatively low avidity of the alloantibody for its target antigen on the allograft endothelium [342], [343]. The comparable levels of splenic GC activity in unmodified SW<sub>HEL</sub> recipients or those receiving TCR7 CD4 T cells may indicate that the adoptive transfer of CD4 T cells in immunocompetent recipient resulted in short persistence of the adoptively transferred T-cells in vivo.

The scratch-wound assay was performed to investigate whether serum containing anti-HEL antibodies on mHEL<sup>WT</sup> and mHEL<sup>3x</sup> directly impacted upon endothelial cells (i.e. in absence of complement). However, these experiments were eventually abandoned due to multiple contamination outbreaks following the isolation of primary endothelial cells from donor hearts. Thus, utilizing SW<sub>HEL</sub> mice as recipients to mHEL-expressing heart grafts did not ultimately permit in depth examination of the role of GC-mediated affinity maturation in progression of allograft vasculopathy. If anything, the sparse LLPCs deposition in the bone marrow and the absence of affinity maturation towards HEL<sup>3x</sup> may indicate that the HEL-specific B cell response that was observed in these recipients was predominantly mediated by an extrafollicular response.

In the modified heart transplant model, mHEL<sup>WT</sup> and mHEL<sup>3x</sup> expressing grafts were transplanted into BL/6 recipients. Limited numbers of *Rag2*<sup>-/-</sup>.SW<sub>HEL</sub> B cells were adoptively transferred on the day of transplantation to mirror the low precursor frequencies that are typically seen in primary antibody responses. In previously published work by Brink's group, the approach of transferring SW<sub>HEL</sub> B cells into BL/6 recipients challenged with sRBC-HEL<sup>3x</sup>

proved to be successful at generating affinity matured anti-HEL<sup>3x</sup> antibodies 2 weeks after challenge even without the delivery of TCR7 CD4 T cells [306], [319].

BL/6 recipients were culled 100 days after transplantation as it would be impractically long experiment. Grafts obtained from BL/6 recipients of mHEL<sup>WT</sup> donors and 10<sup>5</sup> *Rag2*<sup>-/-</sup>.SW<sub>HEL</sub> B cells demonstrated CAV development and more prominent inflammatory interstitial infiltrates than that observed in mHEL<sup>3x</sup> allografts. Both mHEL<sup>WT</sup> and mHEL<sup>3x</sup>-expressing allografts displayed no signs of AMR (intact parenchyma and no intravascular macrophage accumulation). In addition, allografts retrieved from either mHEL<sup>WT</sup> or mHEL<sup>3x</sup> donors were negative for C4d deposition. Spleens obtained from BL/6 recipients of mHEL<sup>WT</sup> or mHEL<sup>3x</sup> expressing allografts demonstrated similar levels of HEL-specific GC activity to one another. Despite the apparent HEL-specific GC development, recipients of mHEL<sup>WT</sup> or mHEL<sup>3x</sup> grafts generated considerable class-switched anti-HEL antibody titer at week 2 but the response was not sustained over the time course of transplantation (at week 14). In addition, recipients of mHEL<sup>WT</sup> and mHEL<sup>3x</sup> grafts demonstrated low frequencies of HEL-specific LLPCs deposition in the bone marrow.

One probable reason for the apparent lack of GC output in the various models tested in this chapter is that the endogenous HEL-specific CD4 T cells did not support an anti-HEL GC response. Such an assumption could have been tested by attempting to characterize this population for T<sub>FH</sub> cell differentiation and activity – for example, by flow cytometric characterization of CXCR5 / PD1 surface phenotype. These were not performed, because of the difficulty in identifying the HEL-specific CD4 T cell population within the endogenous C57BL/6 CD4 T cell repertoire. Chan et al. [306], [344] reported that BCR affinity to the target antigen can affect the expansion of the extrafollicular plasma cells generated in a T-dependent antibody response. The study reported that BCRs of higher affinity to the antigen would preferentially undergo rapid expansion and elicit strong antibody titer during the extrafollicular phase of the response. This observation may partly explain the relatively strong anti-HEL<sup>WT</sup> titers generated at week 2, when compared to the week 14 response, in recipients of mHEL<sup>WT</sup> grafts – that the initial high affinity of the HEL-specific B cells for the HEL<sup>WT</sup> antigen promoted strong short-lived extrafollicular responses, at the expense of the subsequent GC response. However, this observation fails to explain why GC activity was not observed in recipients of HEL<sup>3x</sup>-expressing heart allografts.

An interesting observation was that vascular lesions were only apparent in mHEL<sup>WT</sup> donors. The fact that BL/6 recipients received identical treatment (i.e., delivery of the same number and phenotype of B cells) but harbored allografts with minimal non-MHC mismatched antigen suggests a correlation between antibody binding strength and CAV progression. This assumption is based on the transfer of the monoclonal population of *Rag2*<sup>-/-</sup> SW<sub>HEL</sub> B cells which generates antibodies that are of high affinity to HEL<sup>WT</sup> but of low affinity to HEL<sup>3x</sup>. However, this hypothesis was not formally justified. This is because the model did not permit further characterization of affinity maturation in mHEL<sup>3x</sup> recipients by BLI due to the low anti-HEL<sup>3x</sup> antibody titer, and the inability to perform endothelial cells activation/migration assays due to frequent contamination.

Although not MHC-related, the choice of HEL antigen as a model for investigating donor-specific antibodies was based on number of potential advantages. For instance, the availability of two well-characterised antigen variants have enabled different research groups to investigate the cues governing the early decisions by B cells during T-dependent humoral response [306], [336], [345]. The ability of non-MHC antibodies, such as anti-endothelial cell antibodies, to cause endothelial dysfunction and, ultimately, allograft vasculopathy, remains controversial (reviewed [346]). Some studies reported that non-HLA antibodies do not cause complement deposition [347]; others have reported their capability to induce endothelial cells activation and showed that this activation correlated with graft outcome [95]. Thus the presence of non-HLA antibodies in non-sensitized patients may be a risk factor for subsequent CAV development [348]. However, the exact contribution of non-MHC endothelial cell antibodies on graft outcome remains difficult to achieve due to the lack of knowledge of the variable antigenic specificities.

## Chapter 6: Characterising the humoral alloresponse mediated by 'un-linked' helper CD4 T cells.

## 6.1 Introduction

In chapter 3, adoptive transfer of a TCR-transgenic, monoclonal population of CD4 T cells (i.e., TCR75) was used to induce chronic AMR and to develop MHC class I alloantibodies in T cell-deficient recipients. However, in the clinical setting, recipients will harbor memory CD4 T cells of other specificities. Memory CD4 T cells specific for one antigen have been shown to be capable of activating B cells that are specific for another antigen via an “un-linked” recognition pathway (detailed in 1.7.4) [248]. However, this pathway requires that both the ‘helper antigen’ recognised by memory CD4 T cells and the BCR-specific antigen are co-expressed on the same donor cell (figure 37) [248].

Previous work in our lab has shown that un-linked help provided by **naïve** T cells to allospecific B cells elicited short-lived anti-MHC class I antibody responses and was associated with the development of minimal CAV in donor heart grafts [248]. In contrast, delivery of help from un-linked **memory** T cells elicited long-lived alloantibody responses. In addition, heart graft recipients reconstituted with un-linked memory T cells resisted CD40L co-stimulation blockage therapy, and donor grafts developed relatively more severe vasculopathy than observed in recipients reconstituted with naïve CD4 T cells [248]. This presumably reflects the lower activation threshold required by memory T cells to provide help to allospecific B cells [349], which increases their resistance to immunosuppression. Thus, memory T cell responses are thought to be a major challenge in clinical transplantation (recently reviewed [350]).

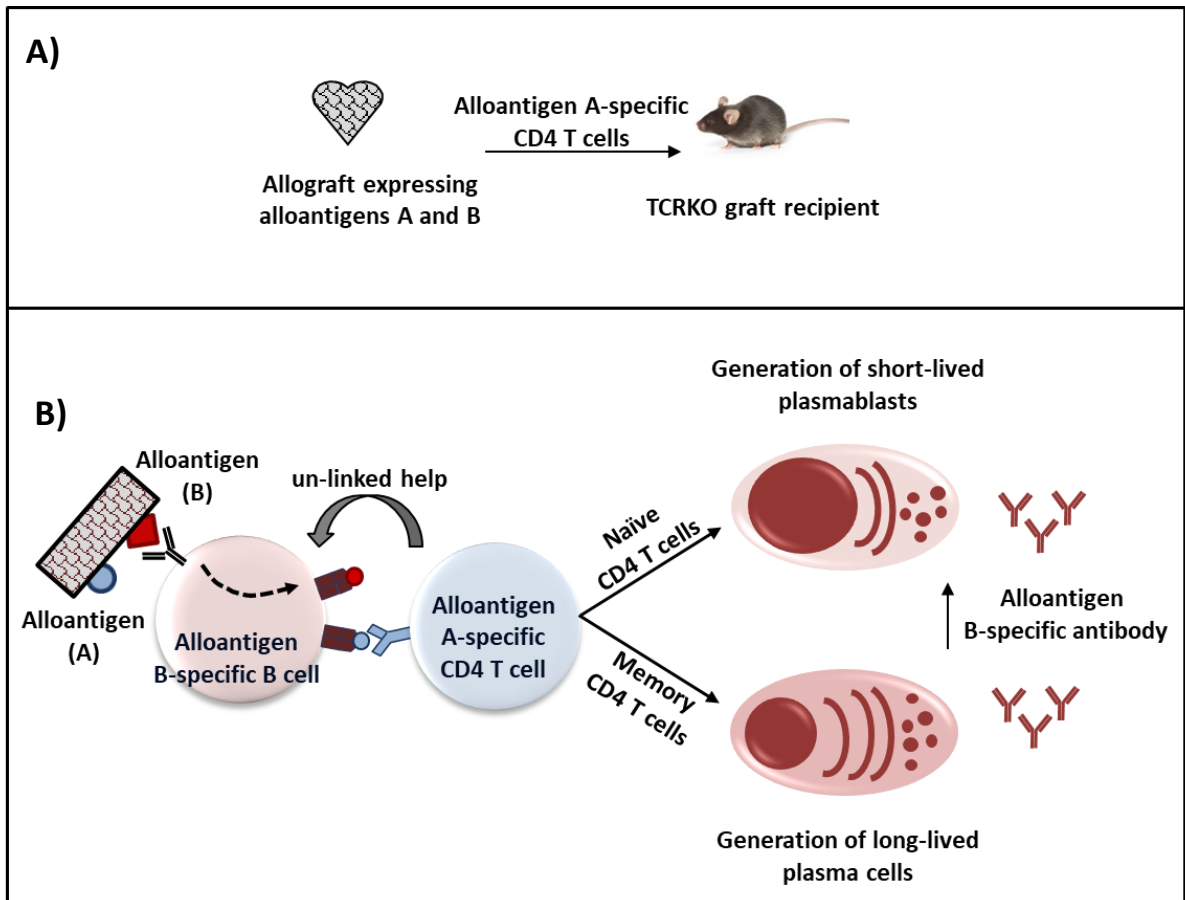


**Figure 37. Simplified diagram of proposed un-linked recognition pathway in murine heart transplant model.** A) heart donor expressing two alloantigens (namely A and B) was transplanted in recipient deficient for T cells but retain a population of B cells that is specific to B alloantigen. Graft recipients were reconstituted with monoclonal population of CD4 T cells that are specific to alloantigen A peptide ‘helper antigen’. B): Alloantigen B expressed on the allograft (represented by red square) is recognized by BCRs on the surface of alloantigen B-specific B cells. Upon alloantigen B binding and uptake by B cells, alloantigen A (represented by blue circle) is also internalized simultaneously by the same B cell. Alloantigen A is then processed and presented on the B cell surface in the context of MHC class II. Cognate interaction between presented alloantigen A peptide and TCR on alloantigen A-specific CD4 T cells can promote B cell activation in “un-linked” manner to produce antibodies that are specific to alloantigen B. Activated B cells can generate short-lived alloantigen B-specific antibody response if activated by naïve CD4 T cells. Long-lived alloantigen B-specific antibody response is generated if B cells were activated by memory CD4 T cells.

## 6.2 Aims

To characterise the alloantibody response generated when help is provided by naïve and memory CD4 T cells responding to 'unlinked' alloantigen minor antigen, and whether the outcome of GC response resembles that of conventional GCs.

## 6.3 Results

### 6.3.1 Development of murine un-linked B cell activation model

Donor hearts from BL/6 mHEL<sup>WT</sup>-K<sup>d</sup> or mHEL<sup>3x</sup>-K<sup>d</sup> (i.e., co-expressing membrane-bound HEL<sup>WT</sup> or HEL<sup>3x</sup> along side MHC class-I H-2K<sup>d</sup> antigen) were transplanted into *Rag2*<sup>-/-</sup> SW<sub>HEL</sub> recipients (devoid of T cells but retaining a monoclonal HEL-specific B cell population). Recipients were reconstituted with either naïve or memory 10<sup>3</sup> TCR75 CD4 T cells; thus providing 'un-linked' help to the *Rag2*<sup>-/-</sup> SW<sub>HEL</sub> B cell population (figure 38). Generation of memory CD4 T cell responses requires an intact B cell compartment [351]. Therefore, to isolate pure populations of primed TCR75 T cells, chimeric *Rag2*<sup>-/-</sup> SW<sub>HEL</sub>.TCR75 mice were generated to provide a monoclonal population of antigen-specific CD4 T cells (described in the methods section 2.2.5). Briefly, memory TCR75 CD4 T cells were generated by immunizing chimeric *Rag2*<sup>-/-</sup> SW<sub>HEL</sub>.TCR75 mice with K<sup>d</sup>-CFA. One week after the second challenge, spleens were collected and CD4 T cells isolated by MACS purification. The number of CD62<sup>lo</sup> CD44<sup>hi</sup> CD4<sup>+</sup> T cells was determined by flow cytometry Trucount™ analysis (figure 39A). Because the CD4 T cells were isolated relatively early after the second challenge, isolated cells may comprise both effector and early memory CD4 T cells. Thus, the isolated CD4 T cell population will be termed early memory CD4 T cells.

As control, *Rag2*<sup>-/-</sup> recipients (that lack both B and T cells) were reconstituted with naïve 10<sup>3</sup> TCR75 CD4 T cells and challenged with mHEL<sup>WT</sup>-K<sup>d</sup> heart grafts. Previous work in our lab confirmed that delivery of naïve or memory CD4 T cells into *Rag2*<sup>-/-</sup> graft recipients generated equivalent levels of luminal stenosis. This finding indicates that vascular disease development is less likely to be effected by the phenotype of delivered CD4 T cells [248]. Thus, in *Rag2*<sup>-/-</sup>.SW<sub>HEL</sub> recipients reconstituted with early memory CD4 T cells, challenge with HEL<sup>WT</sup> and HEL<sup>3x</sup> expressing donor hearts will act as internal controls to one another. Tail bleeds were sampled, and grafts assessed on a weekly basis up to the pre-determined day of experiment termination.

	Donor	Recipient	Transferred CD4 T cells	Replicates
<b>Group 1</b>	mHEL <sup>WT</sup> .K <sup>d</sup>	Rag2 <sup>-/-</sup> .SW <sub>HEL</sub>	10 <sup>3</sup> TCR75 (naïve)	n = 4
<b>Group 2</b>	mHEL <sup>3x</sup> .K <sup>d</sup>	Rag2 <sup>-/-</sup> .SW <sub>HEL</sub>	10 <sup>3</sup> TCR75 (naïve)	n = 3
<b>Group 3</b>	mHEL <sup>WT</sup> .K <sup>d</sup>	Rag2 <sup>-/-</sup> .SW <sub>HEL</sub>	10 <sup>3</sup> TCR75 (memory)	n = 3
<b>Group 4</b>	mHEL <sup>3x</sup> .K <sup>d</sup>	Rag2 <sup>-/-</sup> .SW <sub>HEL</sub>	10 <sup>3</sup> TCR75 (memory)	n = 3
<b>Control</b>	mHEL <sup>WT</sup> .K <sup>d</sup>	Rag2 <sup>-/-</sup>	10 <sup>3</sup> TCR75 (naïve)	n = 3

Experiment terminated at week 14 (control group)  
 Experiment terminated at week 8 (naïve CD4 reconstitution)  
 Experiment terminated at week 5 (memory CD4 reconstitution)

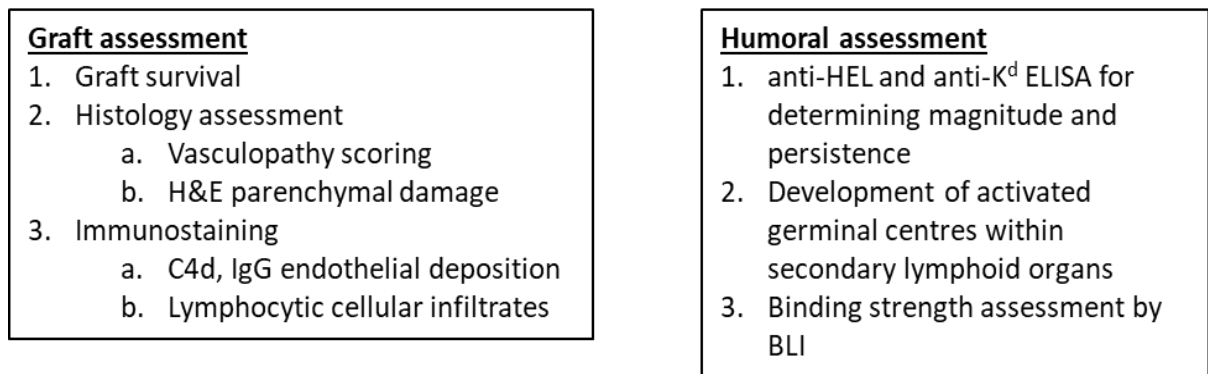


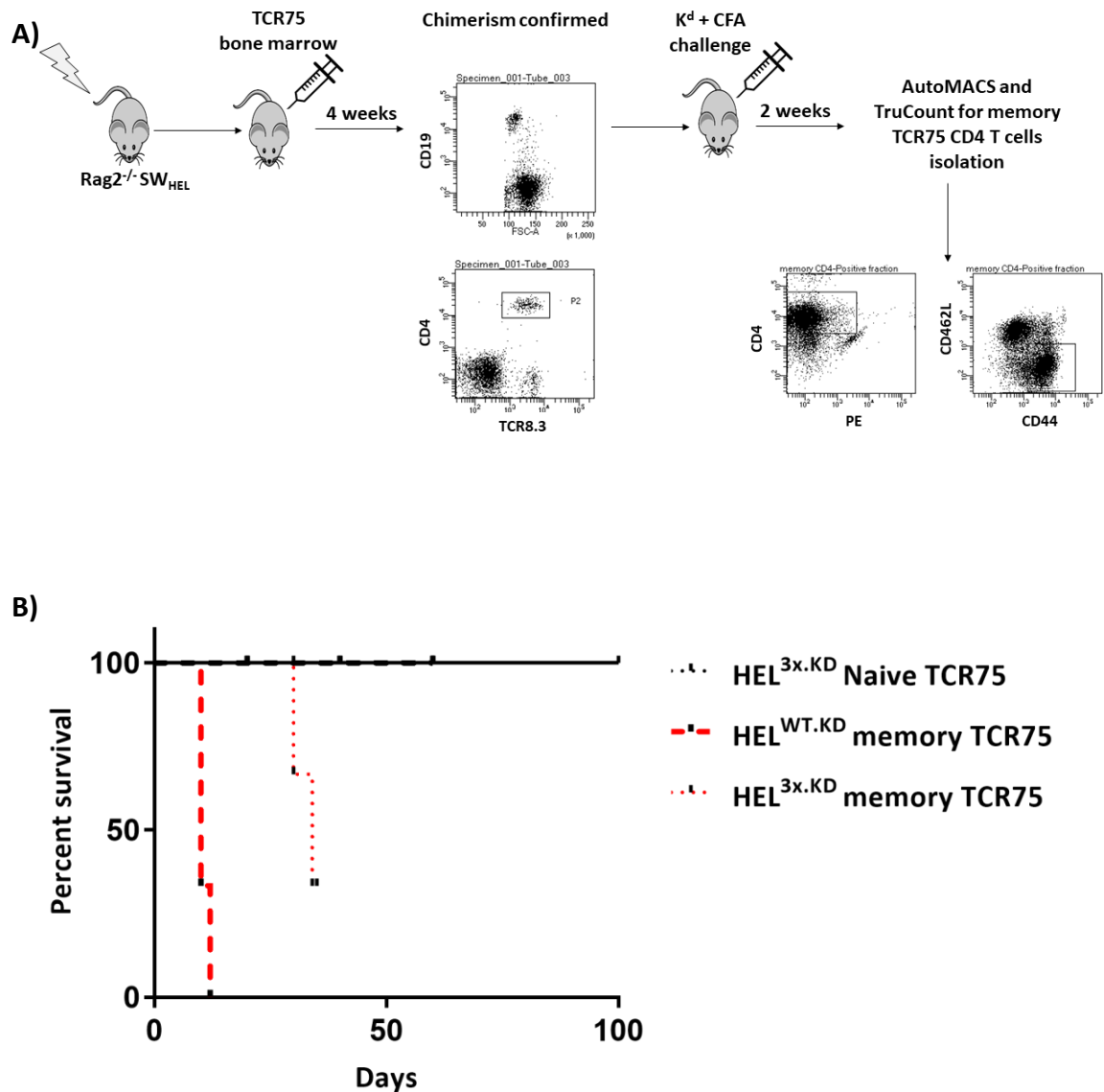
**Figure 38. Schematic presentation of study plan of humoral response triggered by un-linked CD4 T cell help.**

### 6.3.2 Delivery of early memory (but not naïve) CD4 T cells with specificity for second graft alloantigen mediated rapid graft rejection and graft parenchymal damage

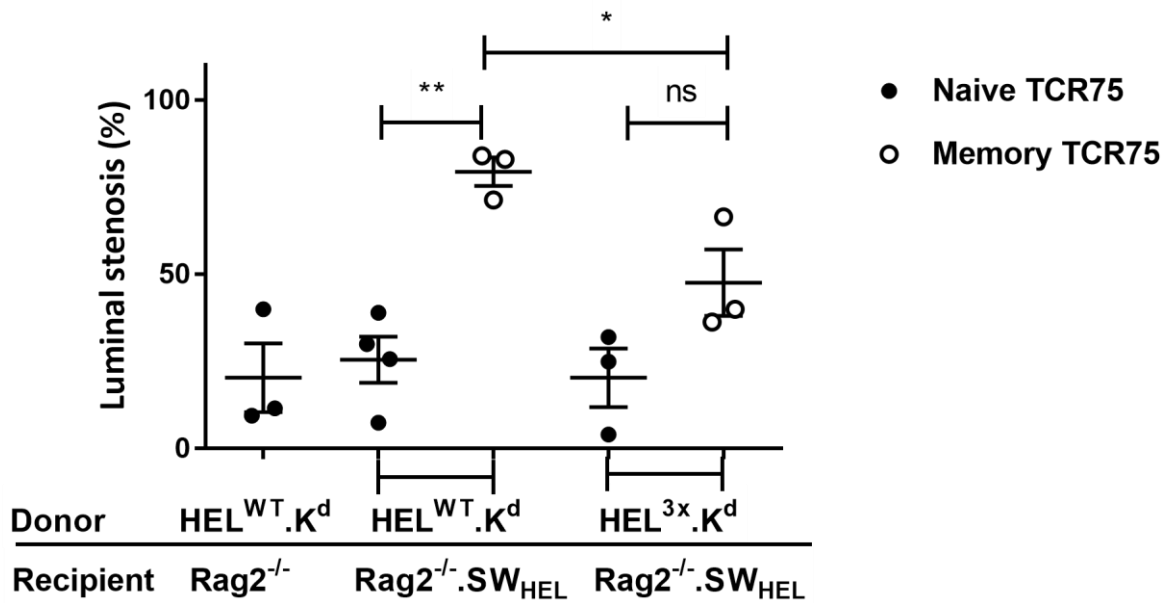
Heart grafts obtained from control *Rag2*<sup>-/-</sup> recipients (devoid of T and B cells) survived long term until the day of experiment termination (day 100) (figure 39B). Similarly, recipients of both mHEL<sup>WT</sup>.K<sup>d</sup> and mHEL<sup>3x</sup>.K<sup>d</sup> heart grafts reconstituted with **naïve** TCR75 CD4 T cells did not reject and continued to beat until the day of experiment termination (week 8); except for one recipient of mHEL<sup>3x</sup>.K<sup>d</sup> heart which was found dead on day 50. The graft obtained from the dead recipient appeared macroscopically to be healthy, suggesting against rejection. In addition, both control *Rag2*<sup>-/-</sup> and experimental *Rag2*<sup>-/-</sup> SW<sub>HEL</sub> recipients of either mHEL<sup>WT</sup>.K<sup>d</sup> or mHEL<sup>3x</sup>.K<sup>d</sup> donor grafts that were reconstituted with **naïve** TCR75 CD4 T cells developed CAV at comparable levels (20 ± 9, 25 ± 5, and 20 ± 3 respectively; mean ± SEM) (figure 40).

In contrast, all recipients of mHEL<sup>WT</sup>.K<sup>d</sup> and two out of three mHEL<sup>3x</sup>.K<sup>d</sup> heart grafts reconstituted with **early memory** TCR75 CD4 T cells rejected at relatively earlier time points (MST, 10 and 34 days, respectively) (figure 39B). Reconstitution with **early memory** TCR75 CD4 T cells in mHEL<sup>WT</sup>.K<sup>d</sup> recipients resulted in pronounced vasculopathy development (79 ± 4% luminal stenosis; mean ± SEM) (figure 40). Recipients of mHEL<sup>3x</sup>.K<sup>d</sup> grafts reconstituted with early memory TCR75 CD4 T cells developed less severe vasculopathy (47 ± 9% luminal stenosis; mean ± SEM), which was nevertheless greater than that observed in the mHEL<sup>3x</sup>.K<sup>d</sup> allografts transplanted in recipient group reconstituted with naïve TCR75 CD4 T cells, although this difference did not reach statistical significance (figure 40).

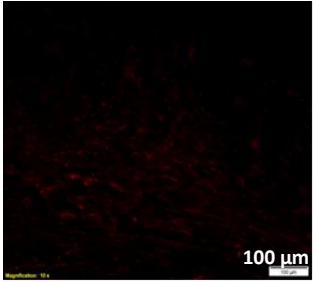
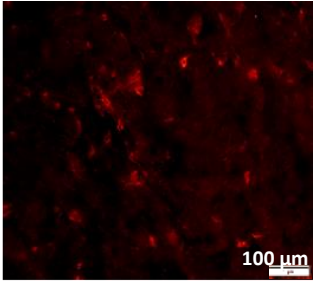
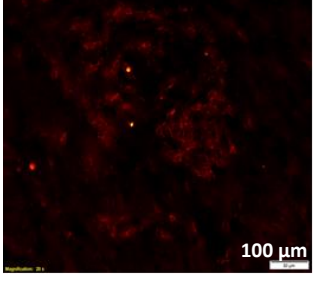
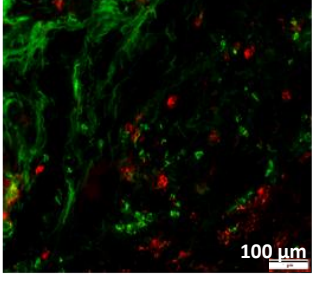
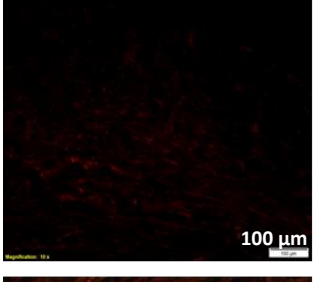
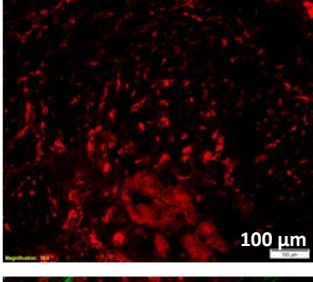
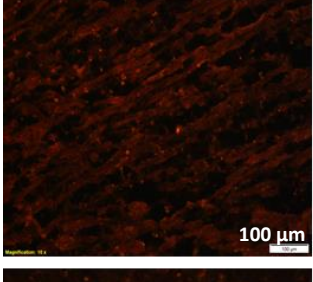
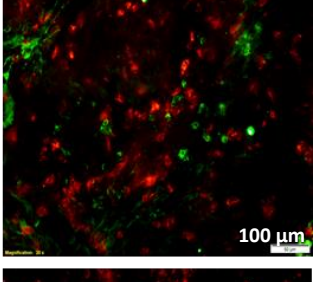
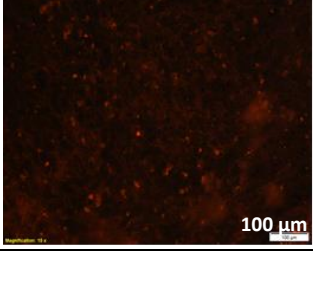
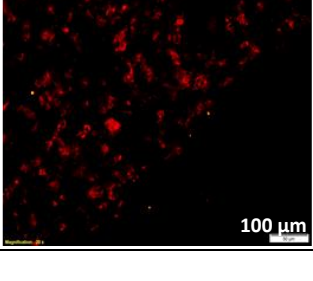
All grafts retrieved from recipients of naïve or early memory CD4 T cells were negative for C4d deposition by immunofluorescence staining, and contained few T and B cell infiltrates (figure 41). CD4 T cells were not confined to a certain locus, and were possibly more prominent in recipients of early memory CD4 T cells. However, the numbers of infiltrating CD4 T cells were not formally enumerated.



**Figure 39. Allograft rejection kinetics induced by un-linked CD4 T cell help signals.** A) Chimeric *Rag2*<sup>-/-</sup>.SW<sub>HEL</sub>. TCR75 mice were challenged twice one week apart with K<sup>d</sup> protein emulsified in CFA intraperitoneally. After the second immunization, CD4 T cells were purified by autoMACs using anti-CD4 beads, and numbers of early memory CD4 T cells were labelled with antibodies specific to CD44 and CD62L and frequencies were determined by TruCount flow cytometry. B) Un-linked help delivered by early memory CD4 T cells mediated rapid and accelerated allograft rejection as opposed to the delivery of naïve un-linked CD4 T cells.



**Figure 40. Development of allograft vasculopathy in Rag2<sup>-/-</sup>.SW<sub>HEL</sub> recipients reconstituted with naïve or memory TCR75 CD4 T cells.** Recipients of memory CD4 T cells demonstrated increased CAV development in mHEL<sup>WT</sup>.K<sup>d</sup> recipients (n=3) and mHEL<sup>3x</sup>.K<sup>d</sup> recipients (n=3). Un-linked helper signals provided by naïve CD4 T cells did not contribute to CAV development in both mHEL<sup>WT</sup>.K<sup>d</sup> (n=4) and mHEL<sup>3x</sup>.K<sup>d</sup> recipients (n=3) and was similar to the degree developed in the control Rag2<sup>-/-</sup> recipient group (n=3). Two-tailed Mann-Whitney test, \*P=0.03 and \*\*P=0.0015, ns: non-significant.

Donor/recipient (T cell phenotype)	C4d	CD4/B220
mHEL <sup>WT</sup> .K <sup>d</sup> / Rag2 <sup>-/-</sup> (naive)		
mHEL <sup>WT</sup> .K <sup>d</sup> / Rag2 <sup>-/-</sup> SW <sub>HEL</sub> (naive)		
mHEL <sup>3x</sup> .K <sup>d</sup> / Rag2 <sup>-/-</sup> SW <sub>HEL</sub> (naive)		
mHEL <sup>WT</sup> .K <sup>d</sup> / Rag2 <sup>-/-</sup> SW <sub>HEL</sub> (early memory)		
mHEL <sup>3x</sup> .K <sup>d</sup> / Rag2 <sup>-/-</sup> SW <sub>HEL</sub> (early memory)		

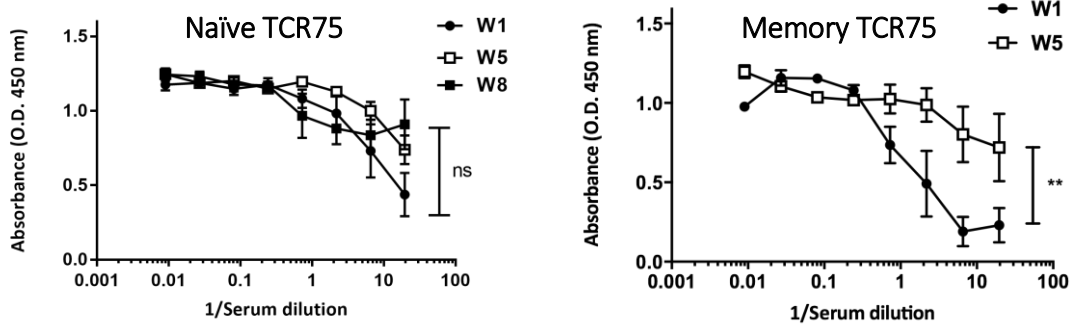
**Figure 41. Immunofluorescence staining of sections obtained from donor hearts stained for C4d and the lymphocyte CD4 T cells and B cells markers.** All donor grafts were negative for the complement split product C4d (left column) as demonstrated by immunofluorescence staining. Few CD4 T cells infiltrates were detected and the lymphocytes were not confined to a certain locus (right column). CD4 T cells were detected with secondary SA-TRITC (red), B cells were detected with anti-CD19-FITC antibody (green).

### 6.3.4 B cells activated via un-linked help by early memory TCR75 CD4 T cells elicit persistent humoral response

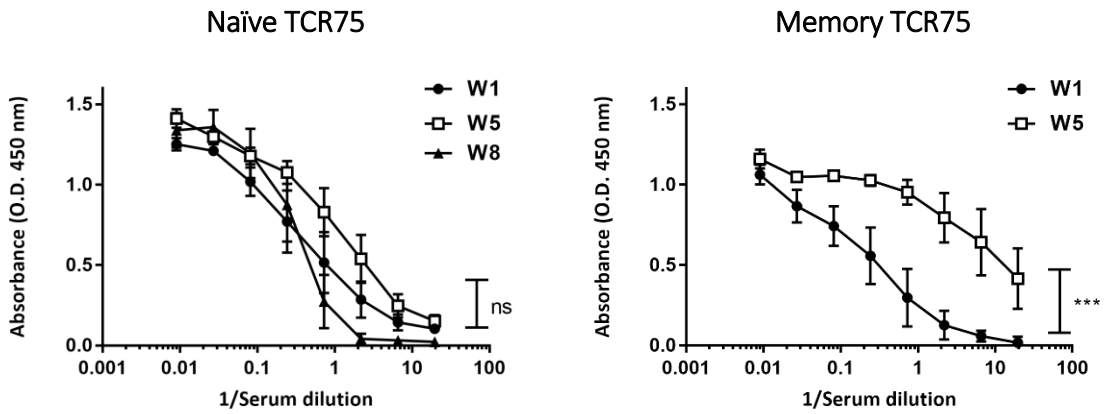
*Rag2*<sup>-/-</sup> SW<sub>HEL</sub> recipients of mHEL<sup>WT</sup>.K<sup>d</sup> or mHEL<sup>3x</sup>.K<sup>d</sup> heart grafts reconstituted with **naïve** TCR75 CD4 T cells elicited strong class-switched anti-HEL responses against HEL<sup>WT</sup> or HEL<sup>3x</sup>, respectively, that persisted for up to 8 weeks (figure 42A, B *left*), but that were broadly similar in magnitude at early and late time points. In contrast, mHEL<sup>WT</sup>.K<sup>d</sup> and mHEL<sup>3x</sup>.K<sup>d</sup> recipients reconstituted with early **memory** TCR75 CD4 T cells elicited relatively stronger anti-HEL IgG response at week 5 (experiment termination time point for early memory CD4 T cells group) than that observed at week 1 and was more significant in recipients of mHEL<sup>3x</sup>.K<sup>d</sup> allografts (figure 42A, B *right*). This observation reflects a continual and ongoing humoral response as evidenced by the increase in anti-HEL IgG antibody titration curve over the time course of the response. As expected, no anti-K<sup>d</sup> alloantibody was generated in any of the *Rag2*<sup>-/-</sup> SW<sub>HEL</sub> recipients (that contain a monoclonal population of HEL-specific B cells only), and no anti-HEL nor anti-K<sup>d</sup> responses developed by the *Rag2*<sup>-/-</sup> control group (figure 43A). To determine whether, in the *Rag2*<sup>-/-</sup> SW<sub>HEL</sub> recipient group that were reconstituted with memory TCR75 CD4 T cells and challenged with mHEL<sup>3x</sup>.K<sup>d</sup> heart allografts, the augmentation in the alloantibody response over time specifically targeted the HEL<sup>3x</sup> antigen, sera sampled from week 1 and week 5 were compared for binding to HEL<sup>WT</sup> or HEL<sup>3x</sup> proteins in ELISA (figure 42C). Antibody titration curves were expressed as the percentage of positive control serum (that is HyHEL-10 for anti-mHEL<sup>WT</sup> coated plates, or anti-HEL<sup>3x</sup> hyperimmune serum for plates coated with HEL<sup>3x</sup>) and antibody titers were displayed as area under the curve (AUC). This revealed that the anti-HEL antibody generated at week 1 bound to a similar extent to both HEL<sup>WT</sup> and HEL<sup>3x</sup> coated plates. However, at week 5 the signal obtained from plates coated with HEL<sup>3x</sup> antigen was significantly higher than that coated with HEL<sup>WT</sup> (figure 43C, right). Similarly, serum obtained from HEL<sup>WT</sup> recipients reconstituted with memory TCR75 CD4 T cells bound more strongly at week 5 to the HEL<sup>WT</sup> target, whereas binding of the same sera to the HEL<sup>3x</sup> target was minimal. These observations indicate that the increase in antibody titers at week 5 in recipients of early memory TCR75 T cells and HEL<sup>WT</sup> or HEL<sup>3x</sup> grafts is indeed antigen-specific, and in doing so are strongly suggestive that affinity maturation has occurred towards the HEL<sup>3x</sup> antigen in the recipient group challenged with mHEL<sup>3x</sup>.K<sup>d</sup> heart allografts.

The off-rate dissociation constants were next determined for serum samples obtained from heart recipients using BLI. Because the concentration of relevant anti-HEL antibody is unknown in the serum samples, only off-rate constant, which is concentration-independent, can be reliably analysed to provide partial information on affinity status. The off-rate measures the dissociation of formed complex between a ligand and a binding site, and a small off-rate value is often associated with stronger binding [284]. It is established that low off-rate is more relevant to antibody affinity, and unlike on-rate, it cannot be compensated by increased concentrations [284]. Serum sampled from mHEL<sup>3x</sup>.K<sup>d</sup> heart graft recipients reconstituted with **naïve** TCR75 CD4 T cells demonstrated an unpredicted pattern (figure 43). The humoral response at week 1 generated class switched antibodies with lower off-rates compared to that obtained at week 8 (time point of experiment termination), indicating that the initial wave of generated anti-HEL<sup>3x</sup> antibodies had stronger binding than those generated at later time points. On the other hand, off-rates were similar at both early and late time points in recipients of **early memory** CD4 T cells. This binding pattern was replicated in recipients of naïve and early memory CD4 T cells and mHEL<sup>WT</sup>.K<sup>d</sup> heart grafts, in that no affinity maturation towards HEL<sup>WT</sup> antigen was observed in either group over the time course of transplantation. However, it is of importance to stress that for some samples, the calculated *off*-rate values (figure 43B) were based on sensorgams obtained from one serum dilution (i.e., 1:20). This is because when the serum was further diluted (1:40) the association curve was hardly noticeable, making model curve fitting and global analysis invalid (figure 43C and D,). According to ForteBio® BLI manual, at least 5% of antibody/ligand dissociation should occur in order to obtain accurate analysis. Repeating the experiment with more concentrated serum samples was hampered due to the limited amount of remaining test serum.

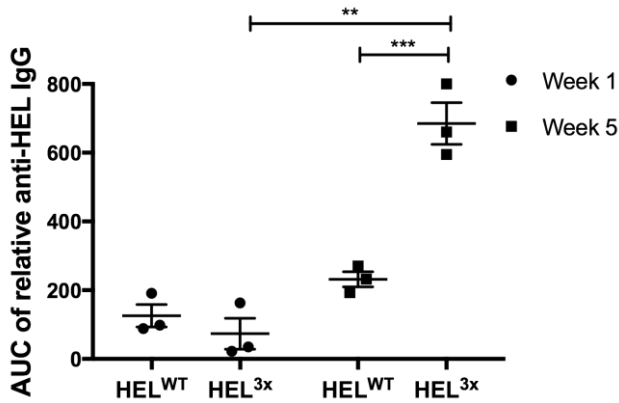
A) HEL<sup>WT</sup>.K<sup>d</sup> donor (plate coated with HEL<sup>WT</sup>)



B) HEL<sup>3x</sup>.K<sup>d</sup> donor (plate coated with HEL<sup>3x</sup>)



C) mHEL<sup>3x</sup>.K<sup>d</sup> donor + memory TCR75



mHEL<sup>WT</sup>.K<sup>d</sup> donor + memory TCR75

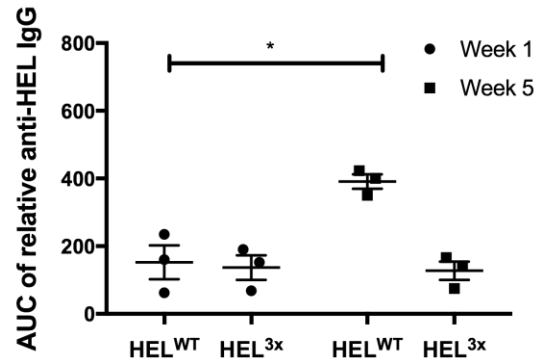


**Figure 42. Humoral responses against mHEL<sup>WT</sup>.K<sup>d</sup> and mHEL<sup>3x</sup>.K<sup>d</sup> graft recipients reconstituted with naïve or early memory CD4 T cells.** Serum samples obtained from recipients of HEL<sup>WT</sup>.K<sup>d</sup> grafts (A), or HEL<sup>3x</sup>.K<sup>d</sup> grafts (B) at weeks 1, 5, and 8 from recipients receiving naïve CD4 T cells, or at weeks 1 and 5 of recipients of early memory CD4 T cells were analyzed by ELISA. Data points represent the average of O.D. absorbance of replicates of the same dilution after subtracting O.D. measures of negative control (naïve *Rag2*<sup>-/-</sup> SW<sub>HEL</sub> serum), ANOVA was calculated as the means of the two groups at each dilution point, ns: non-significant, \*\*\**P*=0.0008. C) area under the curve (AUC) of anti-HEL IgG at weeks 1 and 5 in mHEL<sup>3x</sup>.K<sup>d</sup> recipients (left) or mHEL<sup>WT</sup>.K<sup>d</sup> (right) reconstituted with early memory TCR75 CD4 T cells. Each sample obtained from either week 1 or 5 was tested for binding HEL<sup>WT</sup> or HEL<sup>3x</sup> coated wells in parallel ELISAs. Data displayed as mean ± SEM; Mann-Whitney test, unpaired, two-tailed \**P*= 0.02 (n= 3 in all groups).

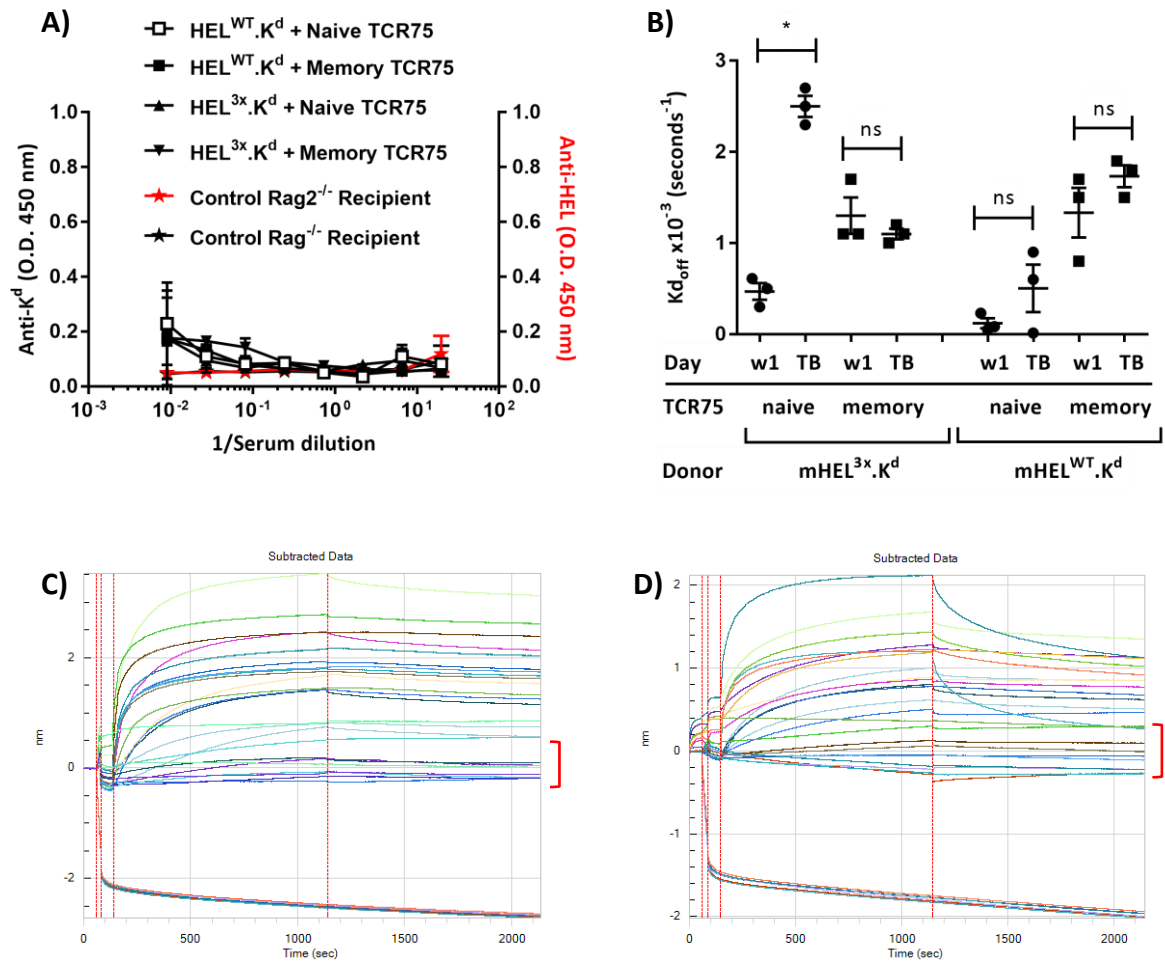


**Figure 43. Characterizing antibody specificity and off-rate of IgG sera obtained from *Rag2*<sup>-/-</sup> SW<sub>HEL</sub> recipients of mHEL<sup>3x</sup>.K<sup>d</sup> or mHEL<sup>WT</sup>.K<sup>d</sup> hearts.** A) ELISA on serum samples obtained from *Rag2*<sup>-/-</sup>.SW<sub>HEL</sub> recipients of heart allografts and naïve or early memory CD4 T cells did not generate anti-K<sup>d</sup> antibodies. Control *Rag2*<sup>-/-</sup> recipients of heart allografts reconstituted with naïve CD4 T cells did not develop anti-K<sup>d</sup> nor anti-HEL antibodies. B) Sera obtained from week 1 (w1) or terminal bleed (TB) were tested for binding kinetics to biotinylated HEL<sup>3x</sup> or HEL<sup>WT</sup> loaded at the tip of streptavidin biosensor. Recipients of mHEL<sup>3x</sup>.K<sup>d</sup> grafts showed lower off-rates at week 1 than that observed from terminal bleed in the group receiving naïve TCR75 CD4 T cells. However, when early memory CD4 T cells were delivered, sera obtained from either an early or late time points demonstrated similar off-rates. A similar pattern was observed in recipients of mHEL<sup>WT</sup>.K<sup>d</sup> allografts; however, when reconstituted with naïve TCR75 CD4 T cells, off-rates between week 1 and TB did not reach statistical significance (n=3 in all groups). Data displayed as mean ± SEM; Mann-Whitney two-tailed, \*P=0.01, ns: non-significant. C) representative binding sensorgrams for serum IgG obtained from recipients of naïve or memory CD4 T cells and their interaction with HEL<sup>WT</sup> or (D) HEL<sup>3x</sup> proteins. Serum samples with low association curves are marked by red curve.

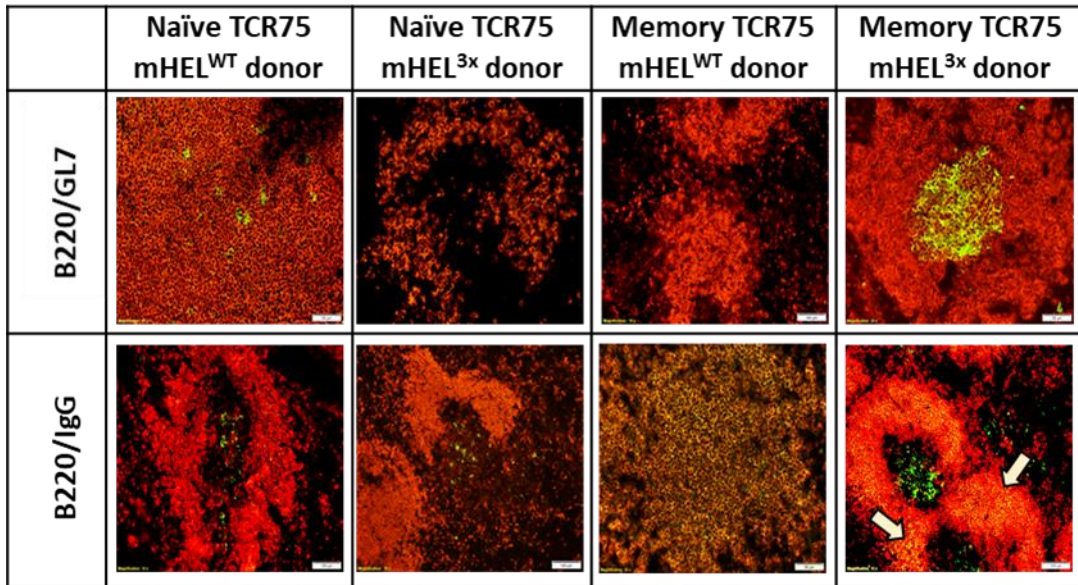
### 6.3.5 GCs establishment via unlinked-help provided from early memory but not naïve CD4 T cells

Analysis of splenic cryostat sections retrieved 8 weeks post-transplantation from recipients of **naïve** TCR75 CD4 T cells did not reveal GC activity, in that B cell follicular areas did not stain for GL7 expression (figure 44A, top). GC activity was similarly absent in week 5 splenic sections obtained from recipients of HEL<sup>WT</sup> grafts that were reconstituted with early **memory** TCR75 CD4 T cells. In contrast, late splenic GC activity was readily detectable in the recipients of HEL<sup>3x</sup> grafts that were reconstituted with early **memory** TCR75 CD4 T cells (figure 44B). These GCs also stained positive for CD4 T cells, and given that helper function can only be provided by the adoptively-transferred, monoclonal TCR75 CD4 T cell population in this model, this suggests that the TCR75 CD4 T cells are acting as T<sub>FH</sub> cells to sustain the GC response (figure 44C).

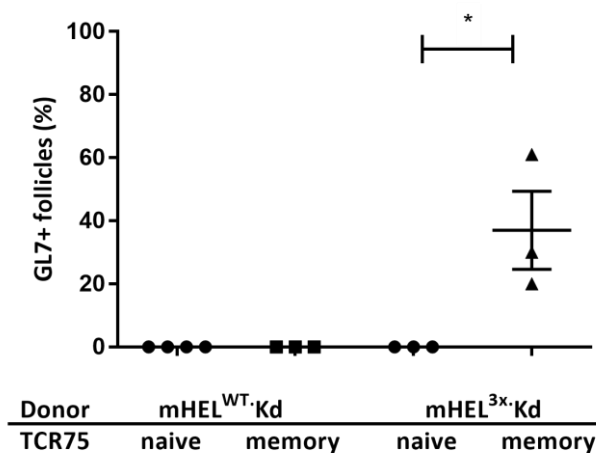
Spleen frozen sections were also stained with anti-mouse IgG to visualize class-switched B cells (figure 44A, bottom). Only spleens retrieved from recipients of HEL<sup>3x</sup> grafts and reconstituted early **memory** TCR75 CD4 T cells demonstrated abundant class-switched B cells within B cell follicles, with some also located in the extrafollicular areas. Spleens obtained from the other groups (those reconstituted with **naïve** TCR75 CD4 T cells or early **memory** TCR75 CD4 T cells and HEL<sup>WT</sup> grafts) demonstrated scarce IgG+ B cells.

Interestingly, the number of class-switched HEL-specific B cells in spleens obtained from recipients of **naïve** or early **memory** TCR75 CD4 T cells demonstrated comparable numbers in HEL-coated ELISA plates. (figure 45). On the other hand, HEL-specific LLPCs deposition in the bone marrow was only evident in recipients of early **memory** TCR75 CD4 T cells.

A)



B)



C)

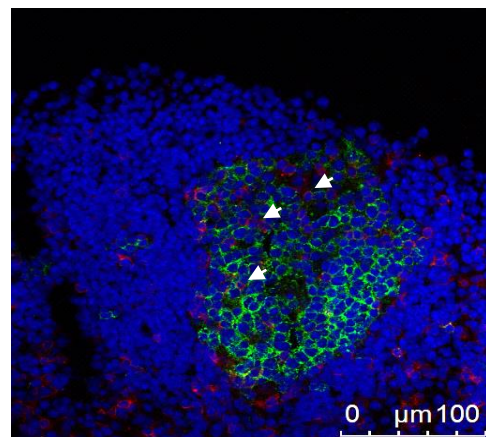


**Figure 44. Naïve un-unlinked CD4 T cells help provide exclusive extrafollicular humoral response.** A) top: Immunofluorescence of splenic frozen sections obtained from Rag2<sup>-/-</sup> SW<sub>HEL</sub> recipients stained for GC activation markers (B220+ (red) and GL7+ (green)). Bottom: Localization of IgG class-switched B cells in relation to follicle was performed to visualize extrafollicular foci (B220+ (red) and IgG+ (green)). Arrows denote IgG+ B cells localised within the follicle. Scale bar is equivalent to 50μm. B) The percentage of GC activation was only apparent in mHEL<sup>3x</sup>.K<sup>d</sup> recipients reconstituted with early memory CD4 T cells (n=3 in all groups). Data presented as mean ± SEM; Mann-Whitney test unpaired, two-tailed, \*P < 0.05. C) Representative confocal image from spleen obtained from mHEL<sup>3x</sup>.K<sup>d</sup> recipient reconstituted with early memory CD4 T cells demonstrating the colocalization of CD4 T cells (red) within a population of GL7 expressing cells (green) in a B cell follicle (DAPI, blue).

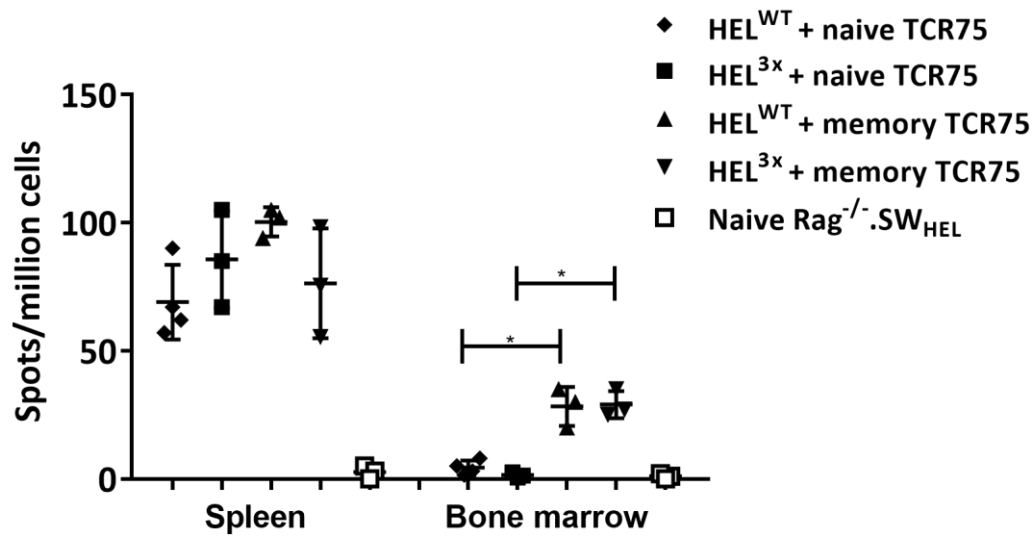


**Figure 45. HEL-coated elispot plates demonstrated HEL-specific B cell IgG class switching following un-linked CD4 T cell activation.** Both naïve and early memory TCR75 CD4 T cells mediated HEL-specific B cell class switching into IgG<sup>pos</sup> HEL-specific B cells in spleens obtained from HEL<sup>WT</sup> or HEL<sup>3x</sup> graft recipients. The number of generated bone marrow LLPCs was higher in recipients of early memory TCR75 CD4 T cells. Data displayed as mean  $\pm$  SD (n=3 in all groups except for HEL<sup>WT</sup> + naïve TCR75 (n=4)); Mann-Whitney, two-tailed, \* $P < 0.005$ .

## 6.4 Discussion:

CD4 T cells can activate different subsets of immune cells via cognate (i.e., TCR-dependent) and non-cognate interactions (i.e., toll-like receptor ligands or cytokines). In addition, several studies have reported sequence homology between CMV and human-HLA class I, implying that cross reactive CMV-specific memory CD4 T cells may provide help for generating humoral alloreactivity to HLA-allospecific B cells [352], [353]. An additional level of complexity was revealed when exploring the nature of cognate interactions between helper CD4 T cells and B cells of disparate antigen specificities in the context of transplantation [248]. The implications of this un-linked recognition are not only limited to transplant immunology but may extend to other pathological immune scenarios such as autoimmunity, and help improve our current understanding of the cues governing B cells activation and fate.

Previous work in our lab demonstrated that a humoral response triggered by unlinked CD4 T cell activation is more potent and long-lived when help was provided by memory, rather than naïve, CD4 T cells; however, the exact mechanism underlying this distinction was not investigated [248]. This observation is widely accepted for conventional cognate B cell/T cell interactions, where memory CD4 T cells accelerate B cell responses in a manner less dependent on co-stimulatory molecules, and with requirement for fewer CD4 T cells [354]. However, in these models, T cell memory was generally examined in the context of recall memory B cell responses. My work differed, in that the responding allospecific B cell population was antigen-unexperienced. We employed the recipient strain, *Rag2*<sup>-/-</sup> SW<sub>HEL</sub>, which is devoid of T cells but retains Ig-knockin HEL-specific B cells [319]. The recipient strain was transplanted with heart grafts expressing high affinity (HEL<sup>WT</sup>) or low affinity (HEL<sup>3x</sup>) antigen, which was co-expressed alongside MHC class I (H2-K<sup>d</sup>). Recipients were reconstituted with either **naïve** or early **memory** TCR75 CD4 T cells for the provision of un-linked help due to their recognition of K<sup>d</sup> peptide presented by MHC class II I-A<sup>b</sup> on the surface of SW<sub>HEL</sub> B cells. In this chapter, previous findings were extended to investigate whether B cells activated via un-linked help underwent affinity maturation as part of a conventional GC response.

Both HEL<sup>WT</sup> and HEL<sup>3x</sup> heart grafts transplanted in recipients of **naïve** CD4 T cells survived long-term (up to day 100). On the other hand, recipients of early **memory** CD4 T cells displayed dichotomous survival times and CAV development based on differences in donor tissue phenotype. HEL<sup>WT</sup> allografts were rejected more rapidly and displayed significant

greater luminal stenosis, whereas HEL<sup>3x</sup> allografts rejected more slowly and with a reduction in severity of allograft vasculopathy.

Serum obtained from recipients reconstituted with **naïve** CD4 T cells displayed consistent anti-HEL<sup>3x</sup> levels at weeks 1, 5, 8. In addition, LLPCs deposition in the bone marrow did not occur, and serum obtained from these recipients generated, if anything, lower off-rate (stronger binding) anti-HEL antibodies at week 1 as opposed to that at week 5. Initially high affinity responses that do not then mature have been reported previously [307] [355], [356], although the mechanisms are not fully understood. Nevertheless when combined with the absence of obvious splenic germinal centre activity, these experiments strongly suggest that the anti-HEL response observed when mice were reconstituted with naïve TCR75 CD4 T cells was limited to extrafollicular foci only. The generation of long-lived extrafollicular responses has been previously reported in a rat model of T-independent antibody response against NP-Ficoll and dsRNA, which elicited class-switched IgG that persisted in the serum up to day 182 post-immunisation, and in the complete absence of plasma cells in the BM [357]. An exclusively extrafollicular response to T-dependent antigen has also been reported in the context of heightened engagement of CD40 signals, and was sustained for 21 days [358]. In the model presented in this chapter, the persistent and steady anti-HEL antibody titers observed in recipients reconstituted with **naïve** CD4 T cells is possibly a consequence of the unusual B cell compartment in the *Rag2*<sup>-/-</sup> SW<sub>HEL</sub> strain. It consists exclusively of Ig-knockin HEL-specific B cells, at a much greater frequency than the endogenous HEL-specific B cell population present in a wild-type C57BL/6 mouse. Such a high precursor frequency of antigen-specific B cells may profoundly influence the magnitude and kinetics of the subsequent humoral response.

In those recipients reconstituted with memory CD4 T cells, the difference in rejection kinetics and severity of CAV following transplantation with HEL<sup>WT</sup> and HEL<sup>3x</sup> grafts was the most intriguing finding, and is likely a consequence of the humoral response generated against the high affinity HEL<sup>WT</sup> antigen, rather than an autonomous function of the memory CD4 T cells. In these strain combinations, the helper T cell population (memory TCR75 CD4 T cells) and the target H-2K<sup>d</sup> antigen are unchanged – the only difference is the nature of the HEL antigen. In support, immunofluorescence staining for CD4 T cells and B cells was not suggestive of cellular rejection, although thorough histological assessment of donor grafts was not performed, because grafts were often retrieved having rejected several weeks earlier and were often only fibrotic remnants.

The development of a GC response in recipients reconstituted with memory TCR75 CD4 T cells and challenged with a mHEL<sup>3x</sup>.K<sup>d</sup> heart graft was striking, and not present in the other experimental groups. Confocal imaging confirmed localisation of the transferred TCR75 CD4 T cells within the GC structure (figure 45C), suggesting that the TCR75 CD4 T cells were providing T<sub>FH</sub> cell function for maintaining an anti-HEL GC response. In support the GC response was associated with deposition of significant numbers of HEL<sup>3x</sup>-specific LLPCs in the bone marrow.

Surprisingly, no GCs were detected in recipients of HEL<sup>WT</sup>-expressing grafts reconstituted with **early memory** CD4 T cells. This discrepancy is perhaps due to the rapid antibody-mediated rejection of the mHEL<sup>WT</sup>.K<sup>d</sup> grafts (MST = 10). All grafts were fibrous upon retrieval and it is likely that alloantigen (either the HEL antigen for B cell recognition, or the K<sup>d</sup> antigen for indirect-pathway CD4 T cell recognition) was no longer being presented in the recipient. This would curtail the GC response – ongoing delivery of help from the T<sub>FH</sub> cell population is required for its maintenance [359]. The fact that recipients of **memory** CD4 T cells demonstrated LLPCs deposition in the BM (as opposed to the parallel group reconstituted with naïve CD4 T cells) suggests that the humoral response generated in those recipients was GC-driven. To directly confirm this assumption, spleens would have been investigated for B cells with GC phenotype at an earlier time point (e.g., day 14); unfortunately however, this was not performed. Attempts of staining recipient spleens for APCs and K<sup>d</sup> antigen were not successful.

What role does the germinal centre response play in rejection of the Hel3x grafts in mice reconstituted with memory TCR75 CD4 T cells? Given that recipients reconstituted with naïve TCR75 CD4 T cells did not reject their grafts, whereas HEL3x WT grafts were rapidly rejected in those recipients reconstituted with memory TCR75 CD4 T cells, it seems likely that the GC response was critical for rejection of the HEL<sup>3x</sup> graft, principally because it resulted in generation of mutated anti-HEL antibody with increasing affinity. In this respect, although the BLI experiments were inconclusive, comparison of the relative binding of test sera at late time points to the HEL<sup>WT</sup> and HEL<sup>3x</sup> antigens is strongly suggestive that affinity maturation had occurred to the HEL<sup>3x</sup> variant. An alternative explanation is that memory TCR75 CD4 T cells developed cytotoxic killing function and effected rejection autonomously, without involvement of alloantibody. Certainly, the donor grafts in these experiments theoretically expressed the appropriate I-A<sup>b</sup>/K<sup>d</sup> peptide complex for cognate interaction with TCR75 CD4 T cells, and Brennan and colleagues have reported that TCR75 CD4 T cells can

effect graft rejection autonomously, if present in large enough numbers [360]. This however, does not explain the observation that delivery of the same memory CD4 T cell population resulted in rapid rejection in **HEL<sup>WT</sup>**- expressing grafts, but not in **HEL<sup>3x</sup>**-expressing grafts. One approach to confirm an obligate role for the GC response in rejection of the BL/6.K<sup>d</sup>.HEL<sup>3x</sup> grafts would have been to incorporate the SAP<sup>-/-</sup>.TCR75 CD4 T cell strain as employed in the initial model of chronic AMR, but this was not possible due to time constraints.

This raises the intriguing question how the memory K<sup>d</sup>-specific TCR75 CD4 T cells are apparently providing help for an effective GC response against the HEL antigen; one moreover that sustains SHM and effective selection of mutated SW<sub>HEL</sub> clone with higher affinity for the HEL antigen. Typically, mutated B cells with higher affinity are thought to outcompete lower affinity clones, because they capture more target antigen as a result of BCR-mediated internalisation. This leads to presentation of higher concentrations of processed peptide and enables the B cell to receive essential survival signals from the limiting numbers of T<sub>FH</sub> cells within the GC. Thus, the crux of this selection process is that the delivery of CD4 T cell help is calibrated against the affinity of the B cell for target antigen. The provision of help from the K<sup>d</sup> reactive CD4 T cell to the HEL-specific B cell would appear to contradict this principle. However, our earlier work has demonstrated that unlinked help occurs because, as well as target antigen, the B cell internalises additional 'helper' antigens from the donor cell. These are processed and presented, such that CD4 T cells with exclusive specificity for these helper antigens can provide help for class-switched responses against the target antigen. Thus one possibility is that those mutated SW<sub>HEL</sub> B cells with highest affinity for HEL target also internalise more H-2K<sup>d</sup> alloantigen from the donor cell and outcompete other clones by presenting greater quantities of H-2K<sup>d</sup> peptide to the TCR75 T<sub>FH</sub> cells.

Taken together, the relevance of this unique recognition pathway to clinical transplantation can be apparent in patients with memory T cells generated as a response to viral or previous exposure to MHC antigens or non-MHC antigens. Although naive CD4 T cell activation can be efficiently controlled by current immunosuppression therapies [361], memory CD4 T cells are proven to be more resistant [362]. In addition, the contribution of memory unlinked CD4 T cells in the formation of GC-like structures may be considered as a risk factor for the development of self-reactive antibodies due to the lack of proper BCR selection measures. Investigating this aspect may be of particular interest in the fields of clinical transplantation and autoimmune diseases.



## Chapter 7: Overall discussion and future plan

Transplant failure is a multifactorial process and the role of the adaptive immune system in recognising donor alloantigens has long been recognised as a critical contributor for graft rejection. Generated donor-specific alloantibodies are capable of activating complement and donor graft endothelial cells. Activated endothelium express pro-inflammatory receptors which in turn recruit effector cells (e.g., macrophage, NK cells). Graft infiltration with activated effector cells can contribute to graft damage [113]. It is now established that DSAs represent a barrier to transplantation, and sensitised patients have very low transplant rates [87]. Hyperacute AMR has become of less significance with the availability of cross-matching tests. Although a practical definition for acute and chronic AMR is available for kidney allografts, a well-established definition for chronic heart AMR has not yet been achieved.

The overall objective of work described in this thesis is to improve the current understanding of how allospecific B cells contribute to AMR by using murine heart transplant models. The product of work discussed in this thesis included the development of a murine transplant model of AMR adopting similar histological criteria to that observed clinically. The developed model consisted of total MHC class I mismatched heart transplantation into T cell deficient recipients, and T cell help was compensated by the delivery of varying numbers of allospecific monoclonal CD4 T cells capable of recognising donor MHC class I via the indirect pathway (detailed in chapter 3). The described model can be a useful tool for future studies aiming at understanding the mechanisms and signalling pathways involved in the progression of humoral alloimmunity. The model can also be used to explore potential therapeutic targets to ameliorate chronic AMR. Several noteworthy findings arose utilising this model. First, humoral response elicited exclusively by strong T-cell dependent extrafollicular response can contribute to acute graft failure. On the other hand, chronic graft rejection mediated by DSAs in the absence of the cellular arm of the immune response appears to be dependent on GC development. How the pathogenesis of acute humoral response differs from that induced by chronic humoral response, and to what extent does prolonged exposure of MHC-specific antibodies contribute to CAV development remains largely unknown. However, initial findings from this thesis suggest that prolonged antibody production principally by the deposition of LLPCs in the bone marrow following GC development contributes to AMR development. This was supported by replicating the MHC class I mismatched AMR model in recipients reconstituted with SAP<sup>-/-</sup> CD4 T cells, which are incapable of differentiating into T<sub>FH</sub>s. Transfer of defective T<sub>FH</sub> cells resulted in abrogating the

continuous production of alloantibodies and the absence of splenic GC structures and LLPCs deposition in the bone marrow. Heart grafts obtained from this group were free from chronic AMR manifestations described in the paralleled wild type group and remained healthy with minimal CAV development.

The second observation was that the frequency of endogenous allogenic CD4 T cells can have a direct impact on the size and antibody production pathway. The delivery of higher CD4 T cell frequencies (in respect to endogenous allospecific B cells) resulted in rapid humoral response. The strong response was reflected by the generation of strong allospecific antibody response at a threshold sufficient to elicit acute rejection even in the absence of GC structures (i.e., acute model reconstituted with SAP<sup>-/-</sup> CD4 T cells). An adoptive transfer model further supported this hypothesis where CFA-HEL immunised mice were subjected to the delivery of variable ratios of HEL-specific CD4 and HEL-specific B cells (detailed in chapter 4). In this experiment, it was clear that delivery of high frequencies of antigen-specific CD4 T cells as opposed to antigen-specific B cells favoured rapid B cells differentiation into plasmablasts. The response was also associated with the generation of strong antibody response that was mainly extrafollicular in nature following one week of cells transfer. Mature GC structures were not evident at this time point and instead few GL7<sup>+</sup> B cells were scattered within splenic B cell follicles. On the other hand, the co-transfer of high frequencies of HEL-specific B cells and limited numbers of HEL-specific CD4 T cells resulted in a weak extrafollicular response at week one as evident by the low anti-HEL antibody titers. However, by week 3 this group developed the strongest GC response as demonstrated by flow cytometry and immunofluorescence staining of spleen frozen sections.

Initial findings obtained from this thesis described a correlation between pathogenic changes on heart allografts and DSAs. It hypothesized that during the time course of chronic rejection, allontibodies undergo affinity maturation towards donor graft alloantigens. To explore this hypothesis, HEL-expressing donor grafts were utilised to enable the investigation of humoral response against antigens of known affinities in the context of transplantation. Two strains (BL/6.HEL<sup>WT</sup> and BL/6.HEL<sup>3x</sup>) were used as donors to BL/6 recipients in order to limit the disparity between donors and recipients to a single defined antigen. In addition, graft recipients received equivalent numbers of *Rag2*<sup>-/-</sup> SW<sub>HEL</sub> B cells (detailed in chapter 5).

The advantage of using the HEL system is to facilitate the investigation of the humoral response elicited by SW<sub>HEL</sub> B cells which retain high affinity towards HEL<sup>WT</sup> antigen, but lower affinity towards HEL<sup>3x</sup> antigen; thereby allowing the ability to compare and contrast the outcomes of antibody affinity towards donor antigens over the time course of transplantation. Although the HEL protein was linked to MHC class I cytoplasmic tail, generated antibodies did not seem to contribute to graft rejection, in that all donor hearts were still beating upon experiment termination. Regardless, few interesting observations were noted. For instance, the disparity in the humoral response between the two groups was mostly manifested in CAV development. In recipients of HEL<sup>WT</sup> expressing hearts, the affinity of SW<sub>HEL</sub> BCRs to the HEL<sup>WT</sup> antigen was initially high. Although generated anti-HEL antibody did not contribute to graft rejection, mHEL<sup>WT</sup> donor hearts developed statistically significant CAV in comparison to mHEL<sup>3x</sup> donor grafts which remained free from CAV. Another interesting observation was that although recipients of HEL<sup>WT</sup> or HEL<sup>3x</sup> heart allografts developed equivalent splenic GC activity, the output of HEL-specific LLPCs in the bone marrow was poor. This was reflected by the magnitude of generated anti-HEL antibodies over the course of transplantation, especially in HEL<sup>3x</sup> recipients. The low T-dependent antibody responses against HEL in BL/6 background hosts can be attributed to the low immunogenicity of HEL protein peptides recognised by endogenous C57BL/6 CD4 T cells [326]. To increase immunogenicity, the HEL antigen was coupled to an antigenic carrier from a different species (i.e., sRBCs) [319]. Nevertheless, observations in BL/6 recipients of mHEL expressing grafts described in this work support the crucial role of LLPCs in the maintenance of alloantibody titres and their possible correlation with AMR progression. Number of studies have highlighted that memory B cells continue to generate, and those at later time points are likely to be driven from GC precursors that are of higher affinities [363]. Similarly, LLPCs generated at later time points are more likely to outcompete and displace those LLPCs generated during an earlier time point of the response due to limited bone marrow niches [311]. The slow process of high affinity LLPCs generation is of particular relevance for transplantation as discussed earlier and is thought to underpin the progressive formation of CAV. In addition, the generation of LLPCs and memory B cells after GC establishment in graft recipients carries substantial challenge because both cells are responsible for the release of long-lasting alloantibodies.

Although current AMR management strategies include plasmapheresis and intravenous immunoglobulin treatment to reduce anti-DSA titer, the source of antibodies (i.e., LLPCs) are less likely to be influenced and are difficult to deplete because their surface markers are downregulated (e.g., CD20) [11]. Last but not least, the results described using the HEL-transplant system agrees with published literature on the role of non-MHC alloantibodies (such the endothelial angiotensin type 1 receptor (AT1R) antibody as being a risk factor in donor HLA-antibody negative patients [364]. However, it is necessary to stress that controversy occur [365], making the conclusion of to what extent do non-MHC alloantibodies can be considered as a risk factor not clearly determined and requires more research and cohort study analyses [366].

A great deal of investigation has been performed with the aim of understanding the role of T<sub>FH</sub> cells in the context of solid organ transplantation for the identification of key targets that may intervene with T<sub>FH</sub>-B cell interaction to prevent AMR development at its earliest stages (reviewed [251], [252], [367]). In previous experiments performed by our group, it was shown that alloantibody responses triggered by memory un-linked CD4 T cell help resulted in CAV development and strong humoral response [248]. In addition, delivery of memory CD4 T cells in *Rag2*<sup>-/-</sup> recipients of mismatched heart grafts did not result in graft rejection, indicating that the changes were the absolute outcome of collaborative humoral response and not due to bystander memory CD4 T cells [248]. This novel B cell activation pathway was further investigated in this thesis to determine whether unlinked memory CD4 T cells can seed GC reaction and generate secondary B cell follicles. In order to explore this hypothesis, work in this thesis employed recipients that are deficient in T cells yet retain a transgenic population of B cells that are specific to HEL<sup>WT</sup> antigen (*Rag2*<sup>-/-</sup> SW<sub>HEL</sub>) [detailed in chapter 6]. Recipients were transplanted with heart grafts co-expressing H2-K<sup>d</sup> and either HEL<sup>WT</sup> or HEL<sup>3x</sup>. Monoclonal populations of naïve or memory CD4 T cells that are specific to the H2-K<sup>d</sup> peptide antigen presented in the context of I-A<sup>b</sup> (TCR75 T cells) were delivered to the graft recipients. Delivery of early memory but not naïve CD4 T cells resulted in the generation of GC structures, and CD4 T cells differentiated into T<sub>FHs</sub> as apparent by their microanatomical localisation in immunofluorescence photomicrographs of splenic GCs. The magnitude of the humoral response between recipients (of either HEL<sup>WT</sup> or HEL<sup>3x</sup>) of naïve or memory CD4 T cells differed in their magnitude. Although recipients of naïve CD4 T cells showed HEL-specific antibodies that persisted up to week 8, antibody titers were similar to those

observed at week 1, possibly reflecting that the response was not continuous but rather due to HEL-antibody retention following the original response which persisted due to the nature of the global humoral response in transgenic *Rag2*<sup>-/-</sup> SW<sub>HEL</sub> recipients. On the other hand, heart recipients reconstituted with memory CD4 T cells demonstrated significant increase in HEL-specific antibody titers following 5 weeks of transplantation as opposed to that at week 1, reflecting an ongoing generation of anti-HEL<sup>3x</sup> antibodies as evident by the increased antibody titers.

Among the two recipient groups reconstituted with memory CD4 T cells, only those transplanted with HEL<sup>WT</sup> grafts have rejected acutely and with significant CAV development. On the other hand, recipients of grafts expressing HEL<sup>3x</sup> antigen had slower rejection kinetics, and the level of CAV development was lower than that observed in the paralleled group reconstituted with naïve CD4 T cells. This observation suggests that both rapid graft failure and level of CAV development were the outcome of the original high affinity between SW<sub>HEL</sub> B cells and HEL<sup>WT</sup> antigen. The consequences of these findings indicate that it is possible for memory CD4 T cells generated during a former immune response to a defined “helper” antigen to activate naïve B cells with BCR of different specificity and can result in potent humoral response.

Thus far, work described in this thesis explored various aspects of the humoral response in murine heart transplant models. Findings obtained from this thesis further confirmed the complexity of the humoral response generated following solid organ transplantation. The results also provide evidence for the crucial role of GCs in the contribution of long-lasting alloantibody generation. Interesting observations and questions also arose from this thesis and can be a subject for future work, some of which are briefly described below.

## Recommendations and future plans

### 1. For specific in vivo allospecific B cells depletion

After optimising dosage and frequency, MHC-class I tetramer-toxin conjugates can be used as an in vivo approach for the specific depletion of allospecific B cells. This approach would enable the exploration of whether targeting allospecific B cells at different time points affect the graft outcome. For instance, to what extent does depletion of endogenous, plasmablasts, or memory B cells can be affective at prolonging graft survival or reduce CAV development.

### 2. Investigating the molecular cues governing un-linked memory CD4 T cells differentiation to T<sub>FHs</sub>

Investigating the molecular cues governing unlinked T<sub>FH</sub> cells differentiation would be of importance. RNA profiling technology offers the advantage of viewing genes that are currently being transcribed by a cell. Therefore, unlinked T<sub>FH</sub> CD4 T cells can be induced by designed transgenic mice donor/recipient combinations. Unlinked T<sub>FH</sub> CD4 T cells can then be FACS sorted by gating on congenic or T<sub>FH</sub> CD4 T cells markers. In addition, naïve, and conventional central or effector memory CD4 T cells can be generated and sorted to provide a comprehensive comparison. Following T<sub>FH</sub> CD4 T cells isolation, mRNA profiling for select array of genes and levels of up/down-regulation may provide initial insight on the discrimination between molecular mechanisms corresponding to such differentiation states.

## References

- [1] H. Azuma and N. L. Tilney, "Chronic graft rejection," *Curr. Opin. Immunol.*, vol. 6, no. 5, pp. 770–776, Jan. 1994.
- [2] J. Stehlik *et al.*, "The Registry of the International Society for Heart and Lung Transplantation: twenty-seventh official adult heart transplant report--2010.," *J. Heart Lung Transplant.*, vol. 29, no. 10, pp. 1089–1093, Oct. 2010.
- [3] S. Stewart *et al.*, "Revision of the 1990 working formulation for the standardization of nomenclature in the diagnosis of heart rejection.," *J. Heart Lung Transplant.*, vol. 24, no. 11, pp. 1710–20, Nov. 2005.
- [4] T. Hussain *et al.*, "Positive pretransplantation cytomegalovirus serology is a risk factor for cardiac allograft vasculopathy in children.," *Circulation*, vol. 115, no. 13, pp. 1798–805, Apr. 2007.
- [5] J. P. Costello, T. Mohanakumar, and D. S. Nath, "Mechanisms of chronic cardiac allograft rejection.," *Texas Hear. Inst. J.*, vol. 40, no. 4, pp. 395–9, 2013.
- [6] J. L. Gowans, D. D. McGREGOR, and D. M. Cowen, "Initiation of immune responses by small lymphocytes.," *Nature*, vol. 196, pp. 651–655, 1962.
- [7] P. B. Medawar, "The behaviour and fate of skin autografts and skin homografts in rabbits: A report to the War Wounds Committee of the Medical Research Council.," *J. Anat.*, vol. 78, no. Pt 5, pp. 176–199, 1944.
- [8] H. Auchincloss and D. H. Sachs, "Xenogeneic transplantation.," *Annu. Rev. Immunol.*, vol. 16, pp. 433–70, Jan. 1998.
- [9] A. Schilling, W. Land, E. Pratschke, K. Pielsticker, and W. Brendel, "Dominant role of complement in the hyperacute xenograft rejection reaction," *Surg. Gynecol. Obstet.*, vol. 142, no. 1, pp. 29–32, 1976.
- [10] C. B. Drachenberg *et al.*, "Banff schema for grading pancreas allograft rejection: Working proposal by a Multi-Disciplinary International Consensus Panel," *Am. J. Transplant.*, vol. 8, no. 6, pp. 1237–1249, 2008.

- [11] M. M. Colvin *et al.*, "Antibody-Mediated Rejection in Cardiac Transplantation: Emerging Knowledge in Diagnosis and Management," *Circulation*, vol. 131, no. 18, pp. 1608–1639, May 2015.
- [12] K. A. Andreoni, K. L. Brayman, M. K. Guidinger, C. M. Sommers, and R. S. Sung, "Kidney and Pancreas Transplantation in the United States, 1996-2005," *Am. J. Transplant.*, vol. 7, no. s1, pp. 1359–1375, May 2007.
- [13] R. B. Colvin and R. N. Smith, "Antibody-mediated organ-allograft rejection.," *Nat. Rev. Immunol.*, vol. 5, no. 10, pp. 807–817, 2005.
- [14] N. Nair, T. Ball, P. A. Uber, and M. R. Mehra, "Current and future challenges in therapy for antibody-mediated rejection.," *J. Heart Lung Transplant.*, vol. 30, no. 6, pp. 612–7, Jun. 2011.
- [15] H. R. Colten, "Expression of the MHC class III genes.," *Philos. Trans. R. Soc. Lond. B. Biol. Sci.*, vol. 306, no. 1129, pp. 355–66, Sep. 1984.
- [16] M. Steinmetz and L. Hood, "Genes of the major histocompatibility complex in mouse and man," *Science (80-. )*, vol. 222, pp. 727–734, Nov. 1983.
- [17] J. W. Fabre, "Regulation of MHC expression," *Immunol. Lett.*, vol. 29, no. 1–2, pp. 3–8, Jul. 1991.
- [18] M. Wieczorek *et al.*, "Major Histocompatibility Complex (MHC) Class I and MHC Class II Proteins: Conformational Plasticity in Antigen Presentation.," *Front. Immunol.*, vol. 8, p. 292, 2017.
- [19] K. S. Kobayashi and P. J. van den Elsen, "NLRC5: a key regulator of MHC class I-dependent immune responses," *Nat. Rev. Immunol.*, vol. 12, no. 12, pp. 813–820, Nov. 2012.
- [20] S. Jung *et al.*, "In vivo depletion of CD11c+ dendritic cells abrogates priming of CD8+ T cells by exogenous cell-associated antigens.," *Immunity*, vol. 17, no. 2, pp. 211–20, Aug. 2002.
- [21] J. A. Trapani and M. J. Smyth, "Functional significance of the perforin/granzyme cell

- death pathway,” *Nature Reviews Immunology*, vol. 2, no. 10. Nature Publishing Group, pp. 735–747, 01-Oct-2002.
- [22] G. F. Gao *et al.*, “Crystal structure of the complex between human CD8 $\alpha\alpha$  and HLA-A2,” *Nature*, vol. 387, no. 6633, pp. 630–634, Jun. 1997.
- [23] P. S. Kern *et al.*, “Structural basis of CD8 coreceptor function revealed by crystallographic analysis of a murine CD8 $\alpha\alpha$  ectodomain fragment in complex with H-2Kb,” *Immunity*, vol. 9, no. 4, pp. 519–30, Oct. 1998.
- [24] J. J. Obar and L. Lefrançois, “Memory CD8+ T cell differentiation,” *Ann. N. Y. Acad. Sci.*, vol. 1183, pp. 251–66, Jan. 2010.
- [25] A. Thielens, E. Vivier, and F. Romagné, “NK cell MHC class I specific receptors (KIR): from biology to clinical intervention,” *Curr. Opin. Immunol.*, vol. 24, no. 2, pp. 239–245, Apr. 2012.
- [26] V. Kumar and M. E. McNerney, “A new self: MHC-class-I-independent Natural-killer-cell self-tolerance,” *Nat. Rev. Immunol.*, vol. 5, no. 5, pp. 363–374, May 2005.
- [27] C. S. K. Leung, “Endogenous antigen presentation of MHC class II epitopes through non-autophagic pathways,” *Frontiers in Immunology*, vol. 6, no. SEP. 2015.
- [28] S. D. Miller, D. M. Turley, and J. R. Podojil, “Antigen-specific tolerance strategies for the prevention and treatment of autoimmune disease,” *Nat. Rev. Immunol.*, vol. 7, no. 9, pp. 665–677, Sep. 2007.
- [29] Q.-J. Li *et al.*, “CD4 enhances T cell sensitivity to antigen by coordinating Lck accumulation at the immunological synapse,” *Nat. Immunol.*, vol. 5, no. 8, pp. 791–799, Aug. 2004.
- [30] M. D. Vu, M. R. Clarkson, H. Yagita, L. A. Turka, M. H. Sayegh, and X. C. Li, “Critical, but Conditional, Role of OX40 in Memory T Cell-Mediated Rejection,” *J. Immunol.*, vol. 176, no. 3, pp. 1394–1401, 2006.
- [31] A. M. Workman, A. K. Jacobs, A. J. Vogel, S. Condon, and D. M. Brown, “Inflammation Enhances IL-2 Driven Differentiation of Cytolytic CD4 T Cells,” *PLoS One*, vol. 9, no. 2,

p. e89010, Feb. 2014.

- [32] S. Saito, S. Ota, E. Yamada, H. Inoko, and M. Ota, "Allele frequencies and haplotypic associations defined by allelic DNA typing at HLA class I and class II loci in the Japanese population.," *Tissue Antigens*, vol. 56, no. 6, pp. 522–9, Dec. 2000.
- [33] P. Parham *et al.*, "Diversity of class I HLA molecules: functional and evolutionary interactions with T cells.," *Cold Spring Harb. Symp. Quant. Biol.*, vol. 54 Pt 1, pp. 529–43, 1989.
- [34] K. Murphy, *Garland Science - Janeway's Immunobiology, Eighth Edition Resources*. 2012.
- [35] T. M. Williams, "Human leukocyte antigen gene polymorphism and the histocompatibility laboratory.," *J. Mol. Diagn.*, vol. 3, no. 3, pp. 98–104, 2001.
- [36] A. A. Zachary and M. S. Leffell, "HLA Mismatching Strategies for Solid Organ Transplantation - A Balancing Act.," *Front. Immunol.*, vol. 7, p. 575, 2016.
- [37] P. I. Terasaki, Y. Cho, S. Takemoto, M. Cecka, and D. Gjertson, "Twenty-year follow-up on the effect of HLA matching on kidney transplant survival and prediction of future twenty-year survival.," *Transplant. Proc.*, vol. 28, no. 3, pp. 1144–5, Jun. 1996.
- [38] S. Bahram, M. Bresnahan, D. E. Geraghty, and T. Spies, "A second lineage of mammalian major histocompatibility complex class I genes.," *Proc. Natl. Acad. Sci. U. S. A.*, vol. 91, no. 14, pp. 6259–63, Jul. 1994.
- [39] M. E. McNerney *et al.*, "Role of natural killer cell subsets in cardiac allograft rejection.," *Am. J. Transplant*, vol. 6, no. 15, pp. 505–513, 2006.
- [40] B. Suárez-Álvarez, A. López-Vázquez, J. M. Baltar, F. Ortega, and C. López-Larrea, "Potential Role of NKG2D and Its Ligands in Organ Transplantation: New Target for Immunointervention," *Am. J. Transplant.*, vol. 9, no. 2, pp. 251–257, Feb. 2009.
- [41] P. Li, S. T. Willie, S. Bauer, D. L. Morris, T. Spies, and R. K. Strong, "Crystal structure of the MHC class I homolog MIC-A, a gammadelta T cell ligand.," *Immunity*, vol. 10, no. 5, pp. 577–84, May 1999.

- [42] V. Groh, A. Steinle, S. Bauer, and T. Spies, "Recognition of stress-induced MHC molecules by intestinal epithelial gammadelta T cells.," *Science*, vol. 279, no. 5357, pp. 1737–40, Mar. 1998.
- [43] N. W. Zwirner, K. Dole, and P. Stastny, "Differential surface expression of MICA by endothelial cells, fibroblasts, keratinocytes, and monocytes.," *Hum. Immunol.*, vol. 60, no. 4, pp. 323–30, Apr. 1999.
- [44] L. L. Molinero, C. I. Domaica, M. B. Fuertes, M. V. Girart, L. E. Rossi, and N. W. Zwirner, "Intracellular Expression of MICA in Activated CD4 T Lymphocytes and Protection from NK Cell-Mediated MICA-Dependent Cytotoxicity," *Hum. Immunol.*, vol. 67, no. 3, pp. 170–182, Mar. 2006.
- [45] S. Sumitran-Holgersson, H. E. Wilczek, J. Holgersson, and K. Söderström, "Identification of the nonclassical HLA molecules, mica, as targets for humoral immunity associated with irreversible rejection of kidney allografts.," *Transplantation*, vol. 74, no. 2, pp. 268–77, Jul. 2002.
- [46] B. Suárez-Álvarez *et al.*, "The Relationship of Anti-MICA Antibodies and MICA Expression with Heart Allograft Rejection," *Am. J. Transplant.*, vol. 7, no. 7, pp. 1842–1848, Jul. 2007.
- [47] Y. Zou, F. Mirbaha, A. Lazaro, Y. Zhang, B. Lavingia, and P. Stastny, "MICA is a target for complement-dependent cytotoxicity with mouse monoclonal antibodies and human alloantibodies.," *Hum. Immunol.*, vol. 63, no. 1, pp. 30–9, Jan. 2002.
- [48] K. Mizutani *et al.*, "Serial Ten-Year Follow-Up of HLA and MICA Antibody Production Prior to Kidney Graft Failure," *Am. J. Transplant.*, vol. 5, no. 9, pp. 2265–2272, Sep. 2005.
- [49] N. W. Zwirner, C. Y. Marcos, F. Mirbaha, Y. Zou, and P. Stastny, "Identification of MICA as a new polymorphic alloantigen recognized by antibodies in sera of organ transplant recipients.," *Hum. Immunol.*, vol. 61, no. 9, pp. 917–24, Sep. 2000.
- [50] Y. Zou and P. Stastny, "The role of major histocompatibility complex class I chain-related gene A antibodies in organ transplantation.," *Curr. Opin. Organ Transplant.*,

vol. 14, no. 4, pp. 414–8, Aug. 2009.

- [51] E. D. Thomas *et al.*, “Bone-Marrow Transplantation,” *N. Engl. J. Med.*, vol. 292, no. 16, pp. 832–843, Apr. 1975.
- [52] E. GOULMY, A. TERMIJTELEN, B. A. BRADLEY, and J. J. VAN ROOD, “Y-antigen killing by T cells of women is restricted by HLA,” *Nature*, vol. 266, no. 5602, pp. 544–545, Apr. 1977.
- [53] E. Ingulli, “Mechanism of cellular rejection in transplantation,” *Pediatr. Nephrol.*, vol. 25, no. 1, pp. 61–74, Jan. 2010.
- [54] Y. Akatsuka *et al.*, “Identification of a Polymorphic Gene, BCL2A1, Encoding Two Novel Hematopoietic Lineage-specific Minor Histocompatibility Antigens,” *J. Exp. Med.*, vol. 197, no. 11, pp. 1489–1500, Jun. 2003.
- [55] E. Simpson, D. Scott, and P. Chandler, “THE MALE-SPECIFIC HISTOCOMPATIBILITY ANTIGEN, H-Y:A History of Transplantation, Immune Response Genes, Sex Determination and Expression Cloning,” *Annu. Rev. Immunol.*, vol. 15, no. 1, pp. 39–61, Apr. 1997.
- [56] E. Spierings *et al.*, “Identification of HLA class II-restricted H-Y-specific T-helper epitope evoking CD4+ T-helper cells in H-Y-mismatched transplantation,” *Lancet*, vol. 362, no. 9384, pp. 610–615, Aug. 2003.
- [57] E. Spierings, “Minor histocompatibility antigens: past, present, and future,” *Tissue Antigens*, vol. 84, no. 4, pp. 374–360, Oct. 2014.
- [58] A. Heinold *et al.*, “Role of Minor Histocompatibility Antigens in Renal Transplantation,” *Am. J. Transplant.*, vol. 8, no. 1, pp. 95–102, Dec. 2007.
- [59] M. P. Dierselhuis *et al.*, “Minor H antigen matches and mismatches are equally distributed among recipients with or without complications after HLA identical sibling renal transplantation,” *Tissue Antigens*, vol. 82, no. 5, pp. 312–316, Nov. 2013.
- [60] A. Gratwohl, B. Döhler, M. Stern, and G. Opelz, “H-Y as a minor histocompatibility antigen in kidney transplantation: a retrospective cohort study,” *Lancet*, vol. 372, no.

9632, pp. 49–53, Jul. 2008.

- [61] H. A. Erlich, G. Opelz, and J. Hansen, "HLA DNA typing and transplantation.," *Immunity*, vol. 14, no. 4, pp. 347–56, Apr. 2001.
- [62] D. S. Gould and H. Auchincloss, "Direct and indirect recognition: the role of MHC antigens in graft rejection.," *Immunol. Today*, vol. 20, no. 2, pp. 77–82, Feb. 1999.
- [63] V. Steimle, C. A. Siegrist, A. Mottet, B. Lisowska-Grospierre, and B. Mach, "Regulation of MHC class II expression by interferon-gamma mediated by the transactivator gene CIITA.," *Science*, vol. 265, no. 5168, pp. 106–9, Jul. 1994.
- [64] N. J. Rogers and R. I. Lechler, "Allorecognition.," *Am. J. Transplant*, vol. 1, no. 2, pp. 97–102, Jul. 2001.
- [65] T. Ueno *et al.*, "Divergent role of donor dendritic cells in rejection versus tolerance of allografts.," *J. Am. Soc. Nephrol.*, vol. 20, no. 3, pp. 535–44, Mar. 2009.
- [66] R. I. Lechler and J. R. Batchelor, "Immunogenicity of retransplanted rat kidney allografts. Effect of inducing chimerism in the first recipient and quantitative studies on immunosuppression of the second recipient.," *J. Exp. Med.*, vol. 156, no. 6, pp. 1835–41, Dec. 1982.
- [67] R. I. Lechler and J. R. Batchelor, "Restoration of immunogenicity to passenger cell-depleted kidney allografts by the addition of donor strain dendritic cells.," *J. Exp. Med.*, vol. 155, no. 1, pp. 31–41, Jan. 1982.
- [68] T. M. Conlon *et al.*, "Germinal center alloantibody responses are mediated exclusively by indirect-pathway CD4 T follicular helper cells.," *J. Immunol.*, vol. 188, no. 6, pp. 2643–52, Mar. 2012.
- [69] O. B. Herrera *et al.*, "A Novel Pathway of Alloantigen Presentation by Dendritic Cells," *J. Immunol.*, vol. 173, no. 8, pp. 4828–4837, Oct. 2004.
- [70] P. N. Rocha, T. J. Plumb, S. D. Crowley, and T. M. Coffman, "Effector mechanisms in transplant rejection," *Immunological Reviews*, vol. 196, pp. 51–64, 2003.
- [71] T. B. Strom, N. L. Tilney, C. B. Carpenter, and G. J. Busch, "Identity and cytotoxic

- capacity of cells infiltrating renal allografts.," *N. Engl. J. Med.*, vol. 292, no. 24, pp. 1257–1263, 1975.
- [72] A. S. Rosenberg, T. Mizuochi, S. O. Sharrow, and A. Singer, "Phenotype, specificity, and function of T cell subsets and T cell interactions involved in skin allograft rejection," *J Exp Med*, vol. 165, no. 5, pp. 1296–1315, 1987.
- [73] J. P. Ridge, F. Di Rosa, and P. Matzinger, "A conditioned dendritic cell can be a temporal bridge between a CD4+ T-helper and a T-killer cell," *Nature*, vol. 393, no. 6684, pp. 474–478, 1998.
- [74] D. Kreisel *et al.*, "Mouse vascular endothelium activates CD8+ T lymphocytes in a B7-dependent fashion.," *J. Immunol.*, vol. 169, no. 11, pp. 6154–61, 2002.
- [75] G. Behrens *et al.*, "Helper T cells, dendritic cells and CTL Immunity," *Immunol. Cell Biol.*, vol. 82, no. 1, pp. 84–90, Feb. 2004.
- [76] C. M. Smith *et al.*, "Cognate CD4+ T cell licensing of dendritic cells in CD8+ T cell immunity," *Nat. Immunol.*, 2004.
- [77] S. J. F. Harper *et al.*, "CD8 T-cell recognition of acquired alloantigen promotes acute allograft rejection.," *Proc. Natl. Acad. Sci. U. S. A.*, vol. 112, no. 41, pp. 12788–93, Oct. 2015.
- [78] J. M. Ali, E. M. Bolton, J. A. Bradley, and G. J. Pettigrew, "Allorecognition pathways in transplant rejection and tolerance.," in *Transplantation*, 2013, vol. 96, no. 8, pp. 681–8.
- [79] A. Valujskikh, O. Lantz, S. Celli, P. Matzinger, and P. S. Heeger, "Cross-primed CD8+T cells mediate graft rejection via a distinct effector pathway," *Nat. Immunol.*, vol. 3, no. 9, pp. 844–851, 2002.
- [80] H. Auchincloss, R. Lee, S. Shea, J. S. Markowitz, M. J. Grusby, and L. H. Glimcher, "The role of 'indirect' recognition in initiating rejection of skin grafts from major histocompatibility complex class II-deficient mice.," *Proc. Natl. Acad. Sci. U. S. A.*, vol. 90, no. 8, pp. 3373–3377, 1993.

- [81] I. A. Popov, E. V Fedoseyeva, P. L. Orr, M. R. Garovoy, and G. Benichou, "Direct evidence for in vivo induction of CD8+ cytotoxic T cells directed to donor MHC class I peptides following mouse allotransplantation," *Transplantation*, vol. 60, no. 12, pp. 1621–1624, 1995.
- [82] J. Marino, J. Paster, and G. Benichou, "Allorecognition by T lymphocytes and allograft rejection," *Frontiers in Immunology*, vol. 7, no. DEC. 2016.
- [83] M. J. Weiss, J. C. Madsen, B. R. Rosengard, and J. S. Allan, "Mechanisms of chronic rejection in cardiothoracic transplantation.," *Front. Biosci.*, vol. 13, pp. 2980–8, Jan. 2008.
- [84] R. D. Taylor DO, Yowell RL, Kfoury AG, Hammond EH, "Allograft coronary artery disease: clinical correlations with circulating anti-HLA antibodies and the immunohistopathologic pattern of vascular rej... - PubMed - NCBI," *J Hear. Lung Transpl. ,* vol. 19, no. 6, pp. 518–21, 2000.
- [85] M. R. Costanzo *et al.*, "The International Society of Heart and Lung Transplantation Guidelines for the care of heart transplant recipients," *J. Hear. Lung Transplant.*, vol. 29, no. 8, pp. 914–956, Aug. 2010.
- [86] J. E. Worthington, S. Martin, D. M. Al-Husseini, P. A. Dyer, and R. W. G. Johnson, "Posttransplantation production of donor HLA-specific antibodies as a predictor of renal transplant outcome1," *Transplantation*, vol. 75, no. 7, pp. 1034–1040, Apr. 2003.
- [87] J. D. Smith *et al.*, "De novo donor HLA-specific antibodies after heart transplantation are an independent predictor of poor patient survival," *Am. J. Transplant.*, vol. 11, no. 2, pp. 312–319, 2011.
- [88] I.-S. A. Ntokou *et al.*, "Long-term follow up for anti-HLA donor specific antibodies postrenal transplantation: high immunogenicity of HLA class II graft molecules," *Transpl. Int.*, vol. 24, no. 11, pp. 1084–1093, Nov. 2011.
- [89] P. I. Terasaki, M. Ozawa, and R. Castro, "Four-year Follow-up of a Prospective Trial of HLA and MICA Antibodies on Kidney Graft Survival," *Am. J. Transplant.*, vol. 7, no. 2,

pp. 408–415, Feb. 2007.

- [90] J. Le Pavec *et al.*, “De-novo donor-specific anti-HLA antibodies 30 days after lung transplantation are associated with a worse outcome,” *J. Hear. Lung Transplant.*, vol. 35, no. 9, pp. 1067–1077, Sep. 2016.
- [91] M. Willicombe *et al.*, “De Novo DQ Donor-Specific Antibodies Are Associated With a Significant Risk of Antibody-Mediated Rejection and Transplant Glomerulopathy,” *Transplant. J.*, vol. 94, no. 2, pp. 172–177, Jul. 2012.
- [92] E. C. Jolly *et al.*, “Preformed Donor HLA-DP-Specific Antibodies Mediate Acute and Chronic Antibody-Mediated Rejection Following Renal Transplantation,” *Am. J. Transplant.*, vol. 12, no. 10, pp. 2845–2848, Oct. 2012.
- [93] A. Loupy *et al.*, “Complement-Binding Anti-HLA Antibodies and Kidney-Allograft Survival,” *N. Engl. J. Med.*, vol. 369, no. 13, pp. 1215–1226, Sep. 2013.
- [94] Y. Zou *et al.*, “Detection of Anti-MICA Antibodies in Patients Awaiting Kidney Transplantation, during the Post-transplant Course, and in Eluates from Rejected Kidney Allografts by Luminex Flow Cytometry,” *Hum. Immunol.*, vol. 67, no. 3, pp. 230–237, Mar. 2006.
- [95] G. D. Wu *et al.*, “Vascular endothelial cell apoptosis induced by anti-donor non-MHC antibodies: a possible injury pathway contributing to chronic allograft rejection,” *J. Heart Lung Transplant.*, vol. 21, no. 11, pp. 1174–87, Nov. 2002.
- [96] B. Mahesh, H.-S. Leong, K. S. Nair, A. McCormack, P. Sarathchandra, and M. L. Rose, “Autoimmunity to vimentin potentiates graft vasculopathy in murine cardiac allografts,” *Transplantation*, vol. 90, no. 1, pp. 4–13, Jul. 2010.
- [97] Q. Zhang *et al.*, “HLA and MICA: Targets of Antibody-Mediated Rejection in Heart Transplantation,” *Transplantation*, vol. 91, no. 10, pp. 1153–1158, May 2011.
- [98] M. J. Dunn, S. J. Crisp, M. L. Rose, P. M. Taylor, and M. H. Yacoub, “Anti-endothelial antibodies and coronary artery disease after cardiac transplantation,” *Lancet (London, England)*, vol. 339, no. 8809, pp. 1566–70, Jun. 1992.

- [99] P. I. Terasaki and J. Cai, "Human Leukocyte Antigen Antibodies and Chronic Rejection: From Association to Causation," *Transplantation*, vol. 86, no. 3, pp. 377–383, Aug. 2008.
- [100] A. Herskowitz *et al.*, "Arteriolar vasculitis on endomyocardial biopsy: a histologic predictor of poor outcome in cyclosporine-treated heart transplant recipients.," *J. Heart Transplant.*, vol. 6, no. 3, pp. 127–36, Jan. 1987.
- [101] E. H. Hammond *et al.*, "Vascular (humoral) rejection in heart transplantation: pathologic observations and clinical implications.," *J. Heart Transplant.*, vol. 8, no. 6, pp. 430–43, Jan. 1989.
- [102] N. M. Fine *et al.*, "The role of donor-specific antibodies in acute cardiac allograft dysfunction in the absence of cellular rejection.," *Transplantation*, vol. 98, no. 2, pp. 229–38, Jul. 2014.
- [103] A. Loupy *et al.*, "Outcome of subclinical antibody-mediated rejection in kidney transplant recipients with preformed donor-specific antibodies," *Am. J. Transplant.*, vol. 9, no. 11, pp. 2561–2570, 2009.
- [104] S. Redpath, T. Michaelsen, I. Sandlie, and M. R. Clark, "Activation of complement by human IgG1 and human IgG3 antibodies against the human leucocyte antigen CD52.," *Immunology*, vol. 93, no. 4, pp. 595–600, Apr. 1998.
- [105] B. A. Wasowska, "Mechanisms involved in antibody- and complement-mediated allograft rejection.," *Immunol. Res.*, vol. 47, no. 1–3, pp. 25–44, Jul. 2010.
- [106] A. Loupy *et al.*, "Complement-Binding Anti-HLA Antibodies and Kidney-Allograft Survival," *N. Engl. J. Med.*, vol. 369, no. 13, pp. 1215–1226, Sep. 2013.
- [107] K. a. Thomas, N. M. Valenzuela, and E. F. Reed, "The perfect storm: HLA antibodies, complement, FcγRs, and endothelium in transplant rejection," *Trends Mol. Med.*, vol. 21, no. 5, pp. 319–329, 2015.
- [108] K. Murata, W. M. Baldwin, and III, "Mechanisms of complement activation, C4d deposition, and their contribution to the pathogenesis of antibody-mediated rejection.," *Transplant. Rev. (Orlando).*, vol. 23, no. 3, pp. 139–50, Jul. 2009.

- [109] T. Monsinjon, P. Gasque, P. Chan, A. Ischenko, J. J. Brady, and M. C. Fontaine, "Regulation by complement C3a and C5a anaphylatoxins of cytokine production in human umbilical vein endothelial cells.," *FASEB J.*, vol. 17, no. 9, pp. 1003–14, Jun. 2003.
- [110] S. Saadi and J. L. Platt, "Humoral rejection and endothelial cell activation, 2001.," *Xenotransplantation*, vol. 9, no. 4, pp. 239–41, Jul. 2002.
- [111] I. U. Schraufstatter, K. Trieu, L. Sikora, P. Sriramarao, and R. DiScipio, "Complement c3a and c5a induce different signal transduction cascades in endothelial cells.," *J. Immunol.*, vol. 169, no. 4, pp. 2102–10, Aug. 2002.
- [112] R. Snyderman, M. C. Pike, D. McCarley, and L. Lang, "Quantification of mouse macrophage chemotaxis in vitro: role of C5 for the production of chemotactic activity.," *Infect. Immun.*, vol. 11, no. 3, pp. 488–92, Mar. 1975.
- [113] M. M. Colvin *et al.*, *Antibody-Mediated Rejection in Cardiac Transplantation: Emerging Knowledge in Diagnosis and Management: A Scientific Statement From the American Heart Association*. 2015.
- [114] W. M. Baldwin, M. K. Halushka, A. Valujskikh, and R. L. Fairchild, "B cells in cardiac transplants: From clinical questions to experimental models," *Semin. Immunol.*, vol. 24, no. 2, pp. 122–130, Apr. 2012.
- [115] J. S. Pober, M. S. Kluger, and J. S. Schechner, "Human endothelial cell presentation of antigen and the homing of memory/effector T cells to skin.," *Ann. N. Y. Acad. Sci.*, vol. 941, pp. 12–25, 2001.
- [116] J. M. Cook-Mills and T. L. Deem, "Active participation of endothelial cells in inflammation.," *J. Leukoc. Biol.*, vol. 77, no. 4, pp. 487–95, Apr. 2005.
- [117] M. D. Filippi, "Mechanism of Diapedesis: Importance of the Transcellular Route," in *Advances in Immunology*, vol. 129, 2016, pp. 25–53.
- [118] Y. Sakai and M. Kobayashi, "Lymphocyte 'homing' and chronic inflammation," *Pathology International*, vol. 65, no. 7, pp. 344–354, 2015.

- [119] M. Schnoor, "Endothelial Actin-Binding Proteins and Actin Dynamics in Leukocyte Transendothelial Migration," *J. Immunol.*, vol. 194, no. 8, pp. 3535–3541, 2015.
- [120] S. Nourshargh and R. Alon, "Leukocyte Migration into Inflamed Tissues," *Immunity*, vol. 41, no. 5, pp. 694–707, 2014.
- [121] R. S. Al-Lamki, J. R. Bradley, and J. S. Pober, "Endothelial cells in allograft rejection," *Transplantation*, vol. 86, no. 10, pp. 1340–1348, 2008.
- [122] M. Yamakuchi *et al.*, "Antibody to human leukocyte antigen triggers endothelial exocytosis," *Proc. Natl. Acad. Sci. U. S. A.*, vol. 104, no. 4, pp. 1301–1306, 2007.
- [123] C. N. Morrell *et al.*, "In vivo platelet-endothelial cell interactions in response to major histocompatibility complex alloantibody," *Circ. Res.*, vol. 102, no. 7, pp. 777–785, 2008.
- [124] P. E. Harris, H. Bian, and E. F. Reed, "Induction of high affinity fibroblast growth factor receptor expression and proliferation in human endothelial cells by anti-HLA antibodies: a possible mechanism for transplant atherosclerosis," *J. Immunol.*, vol. 159, no. 11, pp. 5697–704, Dec. 1997.
- [125] P. T. Jindra, Y.-P. Jin, R. Jacamo, E. Rozengurt, and E. F. Reed, "MHC class I and integrin ligation induce ERK activation via an mTORC2-dependent pathway," *Biochem. Biophys. Res. Commun.*, vol. 369, no. 2, pp. 781–7, May 2008.
- [126] F. Li, M. E. Atz, and E. F. Reed, "Human leukocyte antigen antibodies in chronic transplant vasculopathy-mechanisms and pathways," *Current Opinion in Immunology*, vol. 21, no. 5, pp. 557–562, 2009.
- [127] M. J. Hickey, N. M. Valenzuela, and E. F. Reed, "Alloantibody Generation and Effector Function Following Sensitization to Human Leukocyte Antigen," *Front. Immunol.*, vol. 7, p. 30, 2016.
- [128] M. Tible *et al.*, "Pathologic classification of antibody-mediated rejection correlates with donor-specific antibodies and endothelial cell activation," *J. Hear. Lung Transplant.*, vol. 32, no. 8, pp. 769–776, Aug. 2013.

- [129] A. M. Miltenburg, M. E. Meijer-Paape, J. J. Weening, M. R. Daha, L. A. van Es, and F. J. van der Woude, "Induction of antibody-dependent cellular cytotoxicity against endothelial cells by renal transplantation.," *Transplantation*, vol. 48, no. 4, pp. 681–8, Oct. 1989.
- [130] T. Castro-Dopico and M. R. Clatworthy, "Fcγ Receptors in Solid Organ Transplantation," *Curr. Transplant. Reports*, vol. 3, no. 4, pp. 284–293, 2016.
- [131] T. Hirohashi *et al.*, "A novel pathway of chronic allograft rejection mediated by NK cells and alloantibody.," *Am. J. Transplant*, vol. 12, no. 2, pp. 313–21, Feb. 2012.
- [132] T. Hirohashi *et al.*, "Complement Independent Antibody-Mediated Endarteritis and Transplant Arteriopathy in Mice."
- [133] G. W. Wu *et al.*, "Asymptomatic antibody-mediated rejection after heart transplantation predicts poor outcomes.," *J. Heart Lung Transplant.*, vol. 28, no. 5, pp. 417–22, May 2009.
- [134] "Utility of Histologic Parameters in Screening for Antibody-Mediated Rejection of the Cardiac Allograft: A Study of 3,170 Biopsies," *J. Hear. Lung Transplant.*, vol. 24, no. 12, pp. 2015–2021, Dec. 2005.
- [135] H. Regele *et al.*, "Capillary deposition of complement split product C4d in renal allografts is associated with basement membrane injury in peritubular and glomerular capillaries: a contribution of humoral immunity to chronic allograft rejection.," *J. Am. Soc. Nephrol.*, vol. 13, no. 9, pp. 2371–80, Sep. 2002.
- [136] A. Jaramillo, C. R. Smith, T. Maruyama, L. Zhang, G. A. Patterson, and T. Mohanakumar, "Anti-HLA class I antibody binding to airway epithelial cells induces production of fibrogenic growth factors and apoptotic cell death: a possible mechanism for bronchiolitis obliterans syndrome.," *Hum. Immunol.*, vol. 64, no. 5, pp. 521–9, May 2003.
- [137] B. Leendert, Paul. Hallgrimus, "Chronic transplant rejection: Magnitude of the problem and pathogenetic mechanisms," *Transplant. Rev.*, vol. 7, no. 2, pp. 96–113, Apr. 1993.

- [138] J. M. de la Torre Hernandez *et al.*, "Virtual Histology Intravascular Ultrasound Assessment of Cardiac Allograft Vasculopathy From 1 to 20 Years After Heart Transplantation," *J. Hear. Lung Transplant.*, vol. 28, no. 2, pp. 156–162, Feb. 2009.
- [139] L. G. Hidalgo *et al.*, "NK cell transcripts and NK cells in kidney biopsies from patients with donor-specific antibodies: evidence for NK cell involvement in antibody-mediated rejection.," *Am. J. Transplant*, vol. 10, no. 8, pp. 1812–22, Aug. 2010.
- [140] T. S. Loy *et al.*, "Immunostaining of cardiac biopsy specimens in the diagnosis of acute vascular (humoral) rejection: a control study.," *J. Heart Lung Transplant.*, vol. 12, no. 5, pp. 736–40, Jan. 1993.
- [141] M. A. Lones, L. S. Czer, A. Trento, D. Harasty, J. M. Miller, and M. C. Fishbein, "Clinical-pathologic features of humoral rejection in cardiac allografts: a study in 81 consecutive patients.," *J. Heart Lung Transplant.*, vol. 14, no. 1 Pt 1, pp. 151–62, Jan. 1995.
- [142] J. D. Christie *et al.*, "The Registry of the International Society for Heart and Lung Transplantation: twenty-seventh official adult lung and heart-lung transplant report--2010.," *J. Heart Lung Transplant.*, vol. 29, no. 10, pp. 1104–18, Oct. 2010.
- [143] A. Seki and M. C. Fishbein, "Predicting the development of cardiac allograft vasculopathy.," *Cardiovasc. Pathol.*, vol. 23, no. 5, pp. 253–60, Jan. 2014.
- [144] J. L. Hillebrands, F. A. Klatter, B. M. van den Hurk, E. R. Popa, P. Nieuwenhuis, and J. Rozing, "Origin of neointimal endothelium and alpha-actin-positive smooth muscle cells in transplant arteriosclerosis.," *J. Clin. Invest.*, vol. 107, no. 11, pp. 1411–22, Jun. 2001.
- [145] J.-L. Hillebrands, F. A. Klatter, and J. Rozing, "Origin of Vascular Smooth Muscle Cells and the Role of Circulating Stem Cells in Transplant Arteriosclerosis," *Arterioscler. Thromb. Vasc. Biol.*, vol. 23, no. 3, pp. 380–387, Mar. 2003.
- [146] G. J. Berry *et al.*, "The 2013 International Society for Heart and Lung Transplantation Working Formulation for the standardization of nomenclature in the pathologic diagnosis of antibody-mediated rejection in heart transplantation," *J. Hear. Lung*

*Transplant.*, vol. 32, no. 12, pp. 1147–1162, Dec. 2013.

- [147] P. J. Michaels *et al.*, “Humoral rejection in cardiac transplantation: risk factors, hemodynamic consequences and relationship to transplant coronary artery disease.,” *J. Heart Lung Transplant.*, vol. 22, no. 1, pp. 58–69, Jan. 2003.
- [148] E. H. Hammond *et al.*, “Vascular rejection in cardiac transplantation: Histologic, immunopathologic, and ultrastructural features.,” *Cardiovasc. Pathol.*, vol. 2, no. 1, pp. 21–34, Jan. 1993.
- [149] R. N. Smith *et al.*, “C4d deposition in cardiac allografts correlates with alloantibody.,” *J. Heart Lung Transplant.*, vol. 24, no. 9, pp. 1202–10, Sep. 2005.
- [150] T. M. Behr *et al.*, “Detection of humoral rejection in human cardiac allografts by assessing the capillary deposition of complement fragment C4d in endomyocardial biopsies.,” *J. Heart Lung Transplant.*, vol. 18, no. 9, pp. 904–12, Sep. 1999.
- [151] E. F. Reed, B. Hong, E. Ho, P. E. Harris, J. Weinberger, and N. Suci-Foca, “Monitoring of soluble HLA alloantigens and anti-HLA antibodies identifies heart allograft recipients at risk of transplant-associated coronary artery disease.,” *Transplantation*, vol. 61, no. 4, pp. 566–72, Feb. 1996.
- [152] N. Singh, J. Pirsch, and M. Samaniego, “Antibody-mediated rejection: treatment alternatives and outcomes,” *Transplant. Rev.*, vol. 23, no. 1, pp. 34–46, 2009.
- [153] M. C. Dalakas, “Mechanisms of action of IVIg and therapeutic considerations in the treatment of acute and chronic demyelinating neuropathies.,” *Neurology*, vol. 59, no. 12 Suppl 6, pp. S13-21, Dec. 2002.
- [154] A. K. Gopal and O. W. Press, “Clinical applications of anti-CD20 antibodies.,” *J. Lab. Clin. Med.*, vol. 134, no. 5, pp. 445–50, Nov. 1999.
- [155] M. R. Costanzo-Nordin *et al.*, “Prospective randomized trial of OKT3- versus horse antithymocyte globulin-based immunosuppressive prophylaxis in heart transplantation.,” *J. Heart Transplant.*, vol. 9, no. 3 Pt 2, pp. 306–15, 1990.
- [156] J. E. Locke *et al.*, “The Utility of Splenectomy as Rescue Treatment for Severe Acute

Antibody Mediated Rejection," *Am. J. Transplant.*, vol. 7, no. 4, pp. 842–846, Apr. 2007.

- [157] J. W. Alexander *et al.*, "The late adverse effect of splenectomy on patient survival following cadaveric renal transplantation," *Transplantation*, vol. 37, no. 5, pp. 467–70, May 1984.
- [158] M. D. Stegall *et al.*, "Terminal complement inhibition decreases antibody-mediated rejection in sensitized renal transplant recipients," *Am. J. Transplant.*, vol. 11, no. 11, pp. 2405–2413, 2011.
- [159] B. Meiser *et al.*, "ISHLT Guidelines for the Care of Heart Transplant Recipients The international society of heart and lung transplantation guidelines for the care of heart transplant recipients Task Force 2: Immunosuppression and Rejection Topic 1: Rejection Surveillance," 2010.
- [160] J. Lindenfeld *et al.*, "Drug Therapy in the Heart Transplant Recipient: Part I: Cardiac Rejection and Immunosuppressive Drugs," *Circulation*, vol. 110, no. 24, pp. 3734–3740, Dec. 2004.
- [161] M. A. Mohamed *et al.*, "Post-transplant DSA monitoring may predict antibody-mediated rejection in sensitized kidney transplant recipients.," *Clin. Transpl.*, pp. 389–94, 2011.
- [162] M. A. Swartz and A. W. Lund, "Lymphatic and interstitial flow in the tumour microenvironment: linking mechanobiology with immunity," *Nat. Rev. Cancer*, vol. 12, no. 3, pp. 210–219, Feb. 2012.
- [163] U. H. von Andrian and T. R. Mempel, "Homing and cellular traffic in lymph nodes.," *Nat. Rev. Immunol.*, vol. 3, no. 11, pp. 867–78, Nov. 2003.
- [164] N. S. De Silva and U. Klein, "Dynamics of B cells in germinal centres," *Nat. Rev. Immunol.*, vol. 15, no. 3, pp. 137–148, 2015.
- [165] J. E. Gretz, A. O. Anderson, and S. Shaw, "Cords, channels, corridors and conduits: critical architectural elements facilitating cell interactions in the lymph node cortex.," *Immunol. Rev.*, vol. 156, pp. 11–24, Apr. 1997.

- [166] J. G. Cyster, "Chemokines, sphingosine-1-phosphate, and cell migration in secondary lymphoid organs.," *Annu. Rev. Immunol.*, vol. 23, pp. 127–59, Jan. 2005.
- [167] V. T. MARCHESI and J. L. GOWANS, "THE MIGRATION OF LYMPHOCYTES THROUGH THE ENDOTHELIUM OF VENULES IN LYMPH NODES: AN ELECTRON MICROSCOPE STUDY.," *Proc. R. Soc. London. Ser. B, Biol. Sci.*, vol. 159, pp. 283–90, Jan. 1964.
- [168] M. Miyasaka and T. Tanaka, "Lymphocyte trafficking across high endothelial venules: dogmas and enigmas," *Nat. Rev. Immunol.*, vol. 4, no. 5, pp. 360–370, May 2004.
- [169] S. D. Rosen, "Ligands for L-selectin: homing, inflammation, and beyond.," *Annu. Rev. Immunol.*, vol. 22, pp. 129–56, Jan. 2004.
- [170] M. Bajénoff *et al.*, "Stromal cell networks regulate lymphocyte entry, migration, and territoriality in lymph nodes.," *Immunity*, vol. 25, no. 6, pp. 989–1001, Dec. 2006.
- [171] R. Förster, A. C. Davalos-Misslitz, and A. Rot, "CCR7 and its ligands: balancing immunity and tolerance," *Nat. Rev. Immunol.*, vol. 8, no. 5, pp. 362–371, May 2008.
- [172] S. N. Mueller and R. N. Germain, "Stromal cell contributions to the homeostasis and functionality of the immune system.," *Nat. Rev. Immunol.*, vol. 9, no. 9, pp. 618–29, Sep. 2009.
- [173] H. Saito, Y. Yokoi, S. Watanabe, J. Tajima, H. Kuroda, and T. Namihisa, "Reticular meshwork of the spleen in rats studied by electron microscopy.," *Am. J. Anat.*, vol. 181, no. 3, pp. 235–52, Mar. 1988.
- [174] R. E. Mebius and G. Kraal, "Structure and function of the spleen.," *Nat. Rev. Immunol.*, vol. 5, no. 8, pp. 606–16, Aug. 2005.
- [175] M. F. Cesta, "Normal structure, function, and histology of the spleen.," *Toxicol. Pathol.*, vol. 34, no. 5, pp. 455–65, Jan. 2006.
- [176] G. Kraal, "Cells in the marginal zone of the spleen.," *Int. Rev. Cytol.*, vol. 132, pp. 31–74, Jan. 1992.
- [177] A. M. Oliver, F. Martin, G. L. Gartland, R. H. Carter, and J. F. Kearney, "Marginal zone B cells exhibit unique activation, proliferative and immunoglobulin secretory

- responses.," *Eur. J. Immunol.*, vol. 27, no. 9, pp. 2366–74, Sep. 1997.
- [178] H. Song and J. Cerny, "Functional Heterogeneity of Marginal Zone B Cells Revealed by Their Ability to Generate Both Early Antibody-forming Cells and Germinal Centers with Hypermutation and Memory in Response to a T-dependent Antigen," *J. Exp. Med.*, vol. 198, no. 12, pp. 1923–1935, Dec. 2003.
- [179] T. V. Obukhanych and M. C. Nussenzweig, "T-independent type II immune responses generate memory B cells.," *J. Exp. Med.*, vol. 203, no. 2, pp. 305–10, Feb. 2006.
- [180] B. Nutt, Stephen L. Kee, "The Transcriptional Regulation of B Cell Lineage Commitment," *Immunity*, vol. 26, no. 6, pp. 715–725, Jun. 2007.
- [181] T. L. Rothstein, D. O. Griffin, N. E. Holodick, T. D. Quach, and H. Kaku, "Human B-1 cells take the stage," *Ann. N. Y. Acad. Sci.*, vol. 1285, no. 1, pp. 97–114, 2013.
- [182] R. S. Davis, "FCRL regulation in innate-like B cells.," *Ann. N. Y. Acad. Sci.*, vol. 1362, no. 1, pp. 110–6, Dec. 2015.
- [183] L. D. Wang and M. R. Clark, "B-cell antigen-receptor signalling in lymphocyte development.," *Immunology*, vol. 110, no. 4, pp. 411–20, Dec. 2003.
- [184] J. Dal Porto, JM. Gauld, SB. Merrell, KT. Mills, D. Paugh-Bernard, AE, Cambier, "B cell antigen receptor signaling 101," *Mol. Immunol.*, vol. 41, no. 6–7, pp. 599–613, Jul. 2004.
- [185] C. C. Goodnow, C. G. Vinuesa, K. L. Randall, F. Mackay, and R. Brink, "Control systems and decision making for antibody production.," *Nat. Immunol.*, vol. 11, no. 8, pp. 681–688, 2010.
- [186] F. Borriello *et al.*, "B7-1 and B7-2 have overlapping, critical roles in immunoglobulin class switching and germinal center formation.," *Immunity*, vol. 6, no. 3, pp. 303–13, Mar. 1997.
- [187] S. E. Ferguson, S. Han, G. Kelsoe, and C. B. Thompson, "CD28 is required for germinal center formation.," *J. Immunol.*, vol. 156, no. 12, pp. 4576–81, Jun. 1996.
- [188] J. M. Lumsden, J. A. Williams, and R. J. Hodes, "Differential requirements for

- expression of CD80/86 and CD40 on B cells for T-dependent antibody responses in vivo.," *J. Immunol.*, vol. 170, no. 2, pp. 781–7, Jan. 2003.
- [189] Y. J. Liu, D. E. Joshua, G. T. Williams, C. A. Smith, J. Gordon, and I. C. MacLennan, "Mechanism of antigen-driven selection in germinal centres.," *Nature*, vol. 342, no. 6252, pp. 929–31, Jan. 1989.
- [190] C. G. Vinuesa, S. G. Tangye, B. Moser, and C. R. Mackay, "Follicular B helper T cells in antibody responses and autoimmunity.," *Nat. Rev. Immunol.*, vol. 5, no. November 2005, pp. 853–865, 2005.
- [191] J.-P. Girard, C. Moussion, and R. Förster, "HEVs, lymphatics and homeostatic immune cell trafficking in lymph nodes.," *Nat. Rev. Immunol.*, vol. 12, no. 11, pp. 762–73, Nov. 2012.
- [192] D. C. Hargreaves *et al.*, "A coordinated change in chemokine responsiveness guides plasma cell movements.," *J. Exp. Med.*, vol. 194, no. 1, pp. 45–56, Jul. 2001.
- [193] K. Reif *et al.*, "Balanced responsiveness to chemoattractants from adjacent zones determines B-cell position.," *Nature*, vol. 416, no. 6876, pp. 94–99, Mar. 2002.
- [194] I. C. M. MacLennan *et al.*, "Extrafollicular antibody responses," *Immunol. Rev.*, vol. 194, no. 1, pp. 8–18, Aug. 2003.
- [195] D. Gatto, D. Paus, A. Basten, C. R. Mackay, and R. Brink, "Guidance of B Cells by the Orphan G Protein-Coupled Receptor EBI2 Shapes Humoral Immune Responses," *Immunity*, vol. 31, no. 2, pp. 259–269, 2009.
- [196] S. A. Luther, I. Maillard, F. Luthi, L. Scarpellino, H. Diggelmann, and H. Acha-Orbea, "Early neutralizing antibody response against mouse mammary tumor virus: critical role of viral infection and superantigen-reactive T cells.," *J. Immunol.*, vol. 159, no. 6, pp. 2807–14, Sep. 1997.
- [197] A. Cerutti, M. Cols, and I. Puga, "Marginal zone B cells: virtues of innate-like antibody-producing lymphocytes.," *Nat. Rev. Immunol.*, vol. 13, no. 2, pp. 118–32, 2013.
- [198] K. G. Smith, T. D. Hewitson, G. J. Nossal, and D. M. Tarlinton, "The phenotype and fate

- of the antibody-forming cells of the splenic foci,” *Eur. J. Immunol.*, vol. 26, no. 2, pp. 444–8, Feb. 1996.
- [199] H. Toyama *et al.*, “Memory B cells without somatic hypermutation are generated from Bcl6-deficient B cells,” *Immunity*, vol. 17, no. 3, pp. 329–39, Sep. 2002.
- [200] J. J. Taylor, K. A. Pape, and M. K. Jenkins, “A germinal center-independent pathway generates unswitched memory B cells early in the primary response,” *J. Exp. Med.*, vol. 209, no. 3, pp. 597–606, Mar. 2012.
- [201] A. Inamine *et al.*, “Two waves of memory B-cell generation in the primary immune response,” *Int. Immunol.*, vol. 17, no. 5, pp. 581–589, May 2005.
- [202] M. J. Miller, S. H. Wei, I. Parker, and M. D. Cahalan, “Two-photon imaging of lymphocyte motility and antigen response in intact lymph node,” *Science*, vol. 296, no. 5574, pp. 1869–73, Jun. 2002.
- [203] T. Okada and J. G. Cyster, “B cell migration and interactions in the early phase of antibody responses,” *Curr. Opin. Immunol.*, vol. 18, no. 3, pp. 278–85, Jun. 2006.
- [204] S. Crotty, E. N. Kersh, J. Cannons, P. L. Schwartzberg, and R. Ahmed, “SAP is required for generating long-term humoral immunity,” *Nature*, vol. 421, no. 6920, pp. 282–7, Jan. 2003.
- [205] H. Qi, J. L. Cannons, F. Klauschen, P. L. Schwartzberg, and R. N. Germain, “SAP-controlled T-B cell interactions underlie germinal centre formation,” *Nature*, vol. 455, no. 7214, pp. 764–9, Oct. 2008.
- [206] I. C. M. MacLennan, “Germinal Centers,” *Annu. Rev. Immunol.*, vol. 12, no. 1, pp. 117–139, Apr. 1994.
- [207] C. S. Ma, E. K. Deenick, M. Batten, and S. G. Tangye, “The origins, function, and regulation of T follicular helper cells,” *J. Exp. Med.*, vol. 209, no. 7, pp. 1241–53, Jul. 2012.
- [208] A. Garin *et al.*, “Toll-like receptor 4 signaling by follicular dendritic cells is pivotal for germinal center onset and affinity maturation,” *Immunity*, vol. 33, no. 1, pp. 84–95,

Jul. 2010.

- [209] Y. Wu, M. E. M. El Shikh, R. M. El Sayed, A. M. Best, A. K. Szakal, and J. G. Tew, "IL-6 produced by immune complex-activated follicular dendritic cells promotes germinal center reactions, IgG responses and somatic hypermutation.," *Int. Immunol.*, vol. 21, no. 6, pp. 745–56, Jun. 2009.
- [210] G. D. Victora and M. C. Nussenzweig, "Germinal Centers," Mar. 2012.
- [211] S. M. Ranuncolo *et al.*, "Bcl-6 mediates the germinal center B cell phenotype and lymphomagenesis through transcriptional repression of the DNA-damage sensor ATR," *Nat. Immunol.*, vol. 8, no. 7, pp. 705–714, 2007.
- [212] R. T. Phan and R. Dalla-Favera, "The BCL6 proto-oncogene suppresses p53 expression in germinal-centre B cells," *Nature*, vol. 432, no. 7017, pp. 635–639, 2004.
- [213] R. T. Phan, M. Saito, K. Basso, H. Niu, and R. Dalla-Favera, "BCL6 interacts with the transcription factor Miz-1 to suppress the cyclin-dependent kinase inhibitor p21 and cell cycle arrest in germinal center B cells," *Nat. Immunol.*, vol. 6, no. 10, pp. 1054–1060, 2005.
- [214] R. L. Flynn and L. Zou, "ATR: A master conductor of cellular responses to DNA replication stress," *Trends in Biochemical Sciences*, vol. 36, no. 3. pp. 133–140, 2011.
- [215] C. G. Vinuesa, M. A. Linterman, C. C. Goodnow, and K. L. Randall, "T cells and follicular dendritic cells in germinal center B-cell formation and selection," *Immunological Reviews*, vol. 237, no. 1. pp. 72–89, 2010.
- [216] D. Zotos and D. M. Tarlinton, "Structure and function of lymphoid tissues Determining germinal centre B cell fate," 2012.
- [217] M. J. Shlomchik, A. Marshak-Rothstein, C. B. Wolfowicz, T. L. Rothstein, and M. G. Weigert, "The role of clonal selection and somatic mutation in autoimmunity.," *Nature*, vol. 328, no. 6133, pp. 805–11, Jan. 1987.
- [218] G. D. Victora and M. C. Nussenzweig, "Germinal centers.," *Annu. Rev. Immunol.*, vol. 30, pp. 429–57, Jan. 2012.

- [219] F. D. Batista, D. Iber, and M. S. Neuberger, "B cells acquire antigen from target cells after synapse formation.," *Nature*, vol. 411, no. 6836, pp. 489–94, May 2001.
- [220] F. D. Batista *et al.*, "The role of integrins and coreceptors in refining thresholds for B-cell responses.," *Immunol. Rev.*, vol. 218, pp. 197–213, Aug. 2007.
- [221] M. E. Meyer-Hermann, P. K. Maini, and D. Iber, "An analysis of B cell selection mechanisms in germinal centers.," *Math. Med. Biol.*, vol. 23, no. 3, pp. 255–77, Sep. 2006.
- [222] D. M. Tarlinton, "Evolution in miniature: selection, survival and distribution of antigen reactive cells in the germinal centre.," *Immunol. Cell Biol.*, vol. 86, no. 2, pp. 133–138, Jan. 2008.
- [223] A. D. Gitlin, Z. Shulman, and M. C. Nussenzweig, "Clonal selection in the germinal centre by regulated proliferation and hypermutation.," *Nature*, vol. 509, p. 637–, 2014.
- [224] J. Ersching *et al.*, "Germinal Center Selection and Affinity Maturation Require Dynamic Regulation of mTORC1 Kinase.," *Immunity*, vol. 46, no. 6, p. 1045–1058.e6, 2017.
- [225] M. Muramatsu, K. Kinoshita, S. Fagarasan, S. Yamada, Y. Shinkai, and T. Honjo, "Class switch recombination and hypermutation require activation-induced cytidine deaminase (AID), a potential RNA editing enzyme.," *Cell*, vol. 102, no. 5, pp. 553–63, Sep. 2000.
- [226] H. Shan, M. Shlomchik, and M. Weigert, "Heavy-chain class switch does not terminate somatic mutation.," *J. Exp. Med.*, vol. 172, no. 2, pp. 531–6, Aug. 1990.
- [227] F. Mackay and P. Schneider, "Cracking the BAFF code.," *Nat. Rev. Immunol.*, vol. 9, no. 7, pp. 491–502, Jul. 2009.
- [228] A. E. Hauser *et al.*, "Chemotactic responsiveness toward ligands for CXCR3 and CXCR4 is regulated on plasma blasts during the time course of a memory immune response.," *J. Immunol.*, vol. 169, no. 3, pp. 1277–82, Aug. 2002.
- [229] D. J. DiLillo *et al.*, "Maintenance of long-lived plasma cells and serological memory despite mature and memory B cell depletion during CD20 immunotherapy in mice.," *J.*

*Immunol.*, vol. 180, no. 1, pp. 361–71, Jan. 2008.

- [230] U. Klein *et al.*, “Transcription factor IRF4 controls plasma cell differentiation and class-switch recombination.,” *Nat. Immunol.*, vol. 7, no. 7, pp. 773–82, Jul. 2006.
- [231] R. Sciammas, A. L. Shaffer, J. H. Schatz, H. Zhao, L. M. Staudt, and H. Singh, “Graded expression of interferon regulatory factor-4 coordinates isotype switching with plasma cell differentiation.,” *Immunity*, vol. 25, no. 2, pp. 225–36, Aug. 2006.
- [232] J. MITCHELL and A. ABBOT, “Ultrastructure of the Antigen-retaining Reticulum of Lymph Node Follicles as shown by High-resolution Autoradiography,” *Nature*, vol. 208, no. 5009, pp. 500–502, Oct. 1965.
- [233] R. J. Johnston *et al.*, “Bcl6 and Blimp-1 are reciprocal and antagonistic regulators of T follicular helper cell differentiation.,” *Science*, vol. 325, no. 5943, pp. 1006–10, Aug. 2009.
- [234] R. I. Nurieva *et al.*, “Bcl6 mediates the development of T follicular helper cells.,” *Science*, vol. 325, no. 5943, pp. 1001–5, Aug. 2009.
- [235] D. Yu *et al.*, “The transcriptional repressor Bcl-6 directs T follicular helper cell lineage commitment.,” *Immunity*, vol. 31, no. 3, pp. 457–68, Sep. 2009.
- [236] G. M. Jogdand, S. Mohanty, and S. Devadas, “Regulators of Tfh cell differentiation,” *Frontiers in Immunology*, vol. 7, no. NOV. 2016.
- [237] S. Crotty, “T follicular helper cell differentiation, function, and roles in disease,” *Immunity*, vol. 41, no. 4, pp. 529–542, 2014.
- [238] R. Goenka *et al.*, “Cutting Edge: Dendritic Cell-Restricted Antigen Presentation Initiates the Follicular Helper T Cell Program but Cannot Complete Ultimate Effector Differentiation,” *J. Immunol.*, vol. 187, no. 3, pp. 1091–1095, 2011.
- [239] N. J. Tubo *et al.*, “Single naive CD4+ T cells from a diverse repertoire produce different effector cell types during infection,” *Cell*, vol. 153, no. 4, pp. 785–796, 2013.
- [240] J. P. Weber *et al.*, “ICOS maintains the T follicular helper cell phenotype by down-regulating Krüppel-like factor 2,” *J. Exp. Med.*, vol. 212, no. 2, pp. 217–233, 2015.

- [241] R. I. Nurieva *et al.*, "Generation of T Follicular Helper Cells Is Mediated by Interleukin-21 but Independent of T Helper 1, 2, or 17 Cell Lineages," *Immunity*, vol. 29, no. 1, pp. 138–149, 2008.
- [242] E. K. Deenick *et al.*, "Follicular Helper T Cell Differentiation Requires Continuous Antigen Presentation that Is Independent of Unique B Cell Signaling," *Immunity*, vol. 33, no. 2, pp. 241–253, 2010.
- [243] S. Crotty, "Follicular helper CD4 T cells (TFH)," *Annu. Rev. Immunol.*, vol. 29, pp. 621–63, 2011.
- [244] S. Hannedouche *et al.*, "Oxysterols direct immune cell migration via EBI2," *Nature*, vol. 475, no. 7357, pp. 524–527, 2011.
- [245] Z. Shulman *et al.*, "T follicular helper cell dynamics in germinal centers.," *Science*, vol. 341, no. 6146, pp. 673–7, 2013.
- [246] S. Crotty, R. J. Johnston, and S. P. Schoenberger, "Effectors and memories: Bcl-6 and Blimp-1 in T and B lymphocyte differentiation.," *Nat. Immunol.*, vol. 11, no. 2, pp. 114–120, 2010.
- [247] S. L. Nutt, P. D. Hodgkin, D. M. Tarlinton, and L. M. Corcoran, "The generation of antibody-secreting plasma cells," *Nat. Rev. Immunol.*, vol. 15, no. 3, pp. 160–171, Feb. 2015.
- [248] T. M. Conlon *et al.*, "Unlinked memory helper responses promote long-lasting humoral alloimmunity.," *J. Immunol.*, vol. 189, no. 12, pp. 5703–12, Dec. 2012.
- [249] I. Kaczmarek *et al.*, "Donor-specific HLA alloantibodies: long-term impact on cardiac allograft vasculopathy and mortality after heart transplant.," *Exp. Clin. Transplant.*, vol. 6, no. 3, pp. 229–35, Sep. 2008.
- [250] A. G. Kfoury *et al.*, "Impact of Repetitive Episodes of Antibody-mediated or Cellular Rejection on Cardiovascular Mortality in Cardiac Transplant Recipients: Defining Rejection Patterns," *J. Hear. Lung Transplant.*, vol. 25, no. 11, pp. 1277–1282, Nov. 2006.

- [251] G. D. Walters and C. G. Vinuesa, "T Follicular Helper Cells in Transplantation.," *Transplantation*, vol. 100, no. 8, pp. 1650–5, Aug. 2016.
- [252] C. C. Baan, G. N. de Graav, and K. Boer, "T Follicular Helper Cells in Transplantation: The Target to Attenuate Antibody-Mediated Allogeneic Responses?," *Curr. Transplant. reports*, vol. 1, no. 3, pp. 166–172, Jan. 2014.
- [253] J. L. Halliley *et al.*, "Long-Lived Plasma Cells Are Contained within the CD19–CD38hiCD138+ Subset in Human Bone Marrow," *Immunity*, vol. 43, no. 1, pp. 132–145, 2015.
- [254] D. J. DiLillo *et al.*, "B lymphocytes differentially influence acute and chronic allograft rejection in mice.," *J. Immunol.*, vol. 186, no. 4, pp. 2643–54, Feb. 2011.
- [255] B.-Z. Katz and Y. Herishanu, "Therapeutic targeting of CD19 in hematological malignancies: past, present, future and beyond," *Leuk. Lymphoma*, vol. 55, no. 5, pp. 999–1006, 2014.
- [256] T. F. Tedder, "CD19: A promising B cell target for rheumatoid arthritis," *Nature Reviews Rheumatology*, vol. 5, no. 10, pp. 572–577, 2009.
- [257] B. Sadaka, R. R. Alloway, and E. S. Woodle, "Management of Antibody-Mediated Rejection in Transplantation," *Surg. Clin. North Am.*, vol. 93, no. 6, pp. 1451–1466, Dec. 2013.
- [258] L. J. May *et al.*, "HLA desensitization with bortezomib in a highly sensitized pediatric patient," *Pediatr. Transplant.*, vol. 18, no. 8, pp. E280–E282, Dec. 2014.
- [259] J. Patel, M. Everly, D. Chang, M. Kittleson, E. Reed, and J. Kobashigawa, "Reduction of alloantibodies via proteasome inhibition in cardiac transplantation," *J. Hear. Lung Transplant.*, vol. 30, no. 12, pp. 1320–1326, Dec. 2011.
- [260] W. R. Morrow *et al.*, "Rapid Reduction in Donor-Specific Anti-Human Leukocyte Antigen Antibodies and Reversal of Antibody-Mediated Rejection With Bortezomib in Pediatric Heart Transplant Patients," *Transplantation*, vol. 93, no. 3, pp. 319–324, Feb. 2012.

- [261] R. Kim, M. Emi, K. Tanabe, and S. Murakami, "Role of the unfolded protein response in cell death," *Apoptosis*, vol. 11, no. 1, pp. 5–13, Jan. 2006.
- [262] R. Sberro-Soussan, J. Zuberl, C. Suberbielle-Boissel, and C. Legendre, "Bortezomib alone fails to decrease donor specific anti-HLA antibodies: even after one year post-treatment.," *Clin. Transpl.*, pp. 409–14, 2010.
- [263] R. Sberro-Soussan *et al.*, "Bortezomib as the Sole Post-Renal Transplantation Desensitization Agent Does Not Decrease Donor-Specific Anti-HLA Antibodies," *Am. J. Transplant.*, vol. 10, no. 3, pp. 681–686, Mar. 2010.
- [264] D. K. Perry *et al.*, "Proteasome Inhibition Causes Apoptosis of Normal Human Plasma Cells Preventing Alloantibody Production," *Am. J. Transplant.*, vol. 9, no. 1, pp. 201–209, Oct. 2008.
- [265] M. J. Everly *et al.*, "Bortezomib Provides Effective Therapy for Antibody- and Cell-Mediated Acute Rejection," *Transplantation*, vol. 86, no. 12, pp. 1754–1761, Dec. 2008.
- [266] R. Apps, Z. Meng, G. Q. Del Prete, J. D. Lifson, M. Zhou, and M. Carrington, "Relative Expression Levels of the HLA Class-I Proteins in Normal and HIV-Infected Cells," *J. Immunol.*, vol. 194, no. 8, pp. 3594–3600, 2015.
- [267] C. F. Bryan *et al.*, "Sharing kidneys across donor-service area boundaries with sensitized candidates can be influenced by HLA C," *Clin. Transplant.*, vol. 24, no. 1, pp. 56–61, 2010.
- [268] S. Daga *et al.*, "Direct quantitative measurement of the kinetics of HLA-specific antibody interactions with isolated HLA proteins," *Human Immunology*, 2017.
- [269] F. Kushihata, J. Watanabe, A. Mulder, F. Claas, and J. C. Scornik, "Human leukocyte antigen antibodies and human complement activation: role of IgG subclass, specificity, and cytotoxic potential.," *Transplantation*, vol. 78, no. 7, pp. 995–1001, 2004.
- [270] J. W. Oldfather, C. B. Anderson, D. L. Phelan, D. E. Cross, A. M. Luger, and G. E. Rodey, "Prediction of crossmatch outcome in highly sensitized dialysis patients based on the identification of serum HLA antibodies.," *Transplantation*, vol. 42, no. 3, pp. 267–70,

Sep. 1986.

- [271] F. L. Delmonico *et al.*, “New approaches to donor crossmatching and successful transplantation of highly sensitized patients.,” *Transplantation*, vol. 36, no. 6, pp. 629–33, Dec. 1983.
- [272] K. Honjo, X. Y. Xu, and R. P. Bucy, “Heterogeneity of T cell clones specific for a single indirect alloantigenic epitope (I-Ab/H-2Kd54-68) that mediate transplant rejection.,” *Transplantation*, vol. 70, no. 10, pp. 1516–24, Nov. 2000.
- [273] T. G. Phan *et al.*, “B cell receptor-independent stimuli trigger immunoglobulin (Ig) class switch recombination and production of IgG autoantibodies by anergic self-reactive B cells.,” *J. Exp. Med.*, vol. 197, no. 7, pp. 845–60, Apr. 2003.
- [274] S. B. Hartley, J. Crosbie, R. Brink, A. B. Kantor, A. Basten, and C. C. Goodnow, “Elimination from peripheral lymphoid tissues of self-reactive B lymphocytes recognizing membrane-bound antigens.,” *Nature*, vol. 353, no. 6346, pp. 765–9, Oct. 1991.
- [275] M. Neighbors, S. B. Hartley, X. Xu, A. G. Castro, D. M. Bouley, and A. O’Garra, “Breakpoints in immunoregulation required for Th1 cells to induce diabetes,” *Eur. J. Immunol.*, vol. 36, no. 9, pp. 2315–2323, 2006.
- [276] R. J. Corry, H. J. Winn, and P. S. Russell, “Primarily vascularized allografts of hearts in mice. The role of H-2D, H-2K, and non-H-2 antigens in rejection.,” *Transplantation*, vol. 16, no. 4, pp. 343–50, Oct. 1973.
- [277] D. Homann, L. Teyton, and M. B. Oldstone, “Differential regulation of antiviral T-cell immunity results in stable CD8+ but declining CD4+ T-cell memory.,” *Nat. Med.*, vol. 7, no. 8, pp. 913–919, 2001.
- [278] S. M. Kaech, E. J. Wherry, and R. Ahmed, “VACCINES: EFFECTOR AND MEMORY T-CELL DIFFERENTIATION: IMPLICATIONS FOR VACCINE DEVELOPMENT,” *Nat. Rev. Immunol.*, vol. 2, no. 4, pp. 251–262, 2002.
- [279] J. Chen *et al.*, “Reversing endogenous alloreactive B cell GC responses with anti-CD154 or CTLA-4Ig,” *Am. J. Transplant.*, 2013.

- [280] B. J. Holmes *et al.*, "Anti-pig antibody levels in naïve baboons and cynomolgus monkeys.," *Xenotransplantation*, vol. 9, no. 2, pp. 135–47, Mar. 2002.
- [281] N. B. Shah and T. M. Duncan, "Bio-layer interferometry for measuring kinetics of protein-protein interactions and allosteric ligand effects.," *J. Vis. Exp.*, no. 84, p. e51383, 2014.
- [282] R. Petersen, "Strategies Using Bio-Layer Interferometry Biosensor Technology for Vaccine Research and Development," *Biosensors*, vol. 7, no. 4, p. 49, Oct. 2017.
- [283] M. Nirschl, F. Reuter, and J. Vörös, "Review of Transducer Principles for Label-Free Biomolecular Interaction Analysis," *Biosensors*, vol. 1, no. 4, pp. 70–92, Jul. 2011.
- [284] F. Ylera, S. Harth, D. Waldherr, C. Frisch, and A. Knappik, "Off-rate screening for selection of high-affinity anti-drug antibodies.," *Anal. Biochem.*, vol. 441, no. 2, pp. 208–13, Oct. 2013.
- [285] K. Honjo, X. Yan Xu, J. A. Kapp, and R. P. Bucy, "Evidence for cooperativity in the rejection of cardiac grafts mediated by CD4 TCR Tg T cells specific for a defined allopeptide.," *Am. J. Transplant*, vol. 4, no. 11, pp. 1762–8, Nov. 2004.
- [286] T. A. Schwickert *et al.*, "A dynamic T cell-limited checkpoint regulates affinity-dependent B cell entry into the germinal center.," *J. Exp. Med.*, vol. 208, no. 6, pp. 1243–52, Jun. 2011.
- [287] C. D'rije *et al.*, "Early Versus Late Acute Antibody-Mediated Rejection in Renal Transplant Recipients," *Transplant. J.*, vol. 96, no. 1, pp. 79–84, Jul. 2013.
- [288] W. W. Hancock, R. Buelow, M. H. Sayegh, and L. A. Turka, "Antibody-induced transplant arteriosclerosis is prevented by graft expression of anti-oxidant and anti-apoptotic genes," *Nat. Med.*, vol. 4, no. 12, pp. 1392–1396, 1998.
- [289] B. A. Wasowska *et al.*, "Passive transfer of alloantibodies restores acute cardiac rejection in IgKO mice.," *Transplantation*, vol. 71, no. 6, pp. 727–36, Mar. 2001.
- [290] S. Rahimi, Z. Qian, J. Layton, K. Fox-Talbot, W. M. Baldwin, and B. A. Wasowska, "Non-Complement- and Complement-Activating Antibodies Synergize to Cause Rejection of

Cardiac Allografts," *Am. J. Transplant.*, vol. 4, no. 3, pp. 326–334, 2004.

- [291] T. Nozaki *et al.*, "Antibody-mediated rejection of cardiac allografts in CCR5-deficient recipients.," *J. Immunol.*, vol. 179, no. 8, pp. 5238–45, Oct. 2007.
- [292] T. S. Win and G. J. Pettigrew, "Humoral autoimmunity and transplant vasculopathy: when allo is not enough.," *Transplantation*, vol. 90, no. 2, pp. 113–120, 2010.
- [293] T. S. Win *et al.*, "Donor CD4 T cells contribute to cardiac allograft vasculopathy by providing help for autoantibody production.," *Circ. Heart Fail.*, vol. 2, pp. 361–369, 2009.
- [294] J. Kwun *et al.*, "Patterns of de novo allo B cells and antibody formation in chronic cardiac allograft rejection after alemtuzumab treatment.," *Am. J. Transplant*, vol. 12, no. 10, pp. 2641–51, Oct. 2012.
- [295] H. Wang *et al.*, "Inhibition of Terminal Complement Components in Presensitized Transplant Recipients Prevents Antibody-Mediated Rejection Leading to Long-Term Graft Survival and Accommodation," *J. Immunol.*, vol. 179, no. 7, pp. 4451–4463, 2007.
- [296] P. S. Russell, C. M. Chase, H. J. Winn, and R. B. Colvin, "Coronary atherosclerosis in transplanted mouse hearts. II. Importance of humoral immunity.," *J. Immunol.*, vol. 152, no. 10, 1994.
- [297] P. S. Russell, C. M. Chase, H. J. Winn, and R. B. Colvin, "Coronary atherosclerosis in transplanted mouse hearts. II. Importance of humoral immunity.," *J. Immunol.*, vol. 152, no. 10, 1994.
- [298] M. Chhabra, J. Alsughayyir, S. Qureshi, and et al., "Germinal Center Alloantibody Responses Mediate Progression of Chronic Allograft Injury," *Submitted*, 2017.
- [299] M. Haas *et al.*, "Banff 2013 Meeting Report: Inclusion of C4d-Negative Antibody-Mediated Rejection and Antibody-Associated Arterial Lesions," *Am. J. Transplant.*, vol. 14, no. 2, pp. 272–283, Feb. 2014.
- [300] J. L. Cannons *et al.*, "Optimal germinal center responses require a multistage T cell:B

- cell adhesion process involving integrins, SLAM-associated protein, and CD84.," *Immunity*, vol. 32, no. 2, pp. 253–65, Feb. 2010.
- [301] R. N. Mitchell, "Graft vascular disease: immune response meets the vessel wall.," *Annu. Rev. Pathol.*, vol. 4, pp. 19–47, Jan. 2009.
- [302] P. T. Jindra, Y.-P. Jin, E. Rozengurt, and E. F. Reed, "HLA class I antibody-mediated endothelial cell proliferation via the mTOR pathway.," *J. Immunol.*, vol. 180, no. 4, pp. 2357–66, Feb. 2008.
- [303] F. Li, X. Zhang, Y.-P. Jin, A. Mulder, and E. F. Reed, "Antibody ligation of human leukocyte antigen class I molecules stimulates migration and proliferation of smooth muscle cells in a focal adhesion kinase-dependent manner.," *Hum. Immunol.*, vol. 72, no. 12, pp. 1150–9, Dec. 2011.
- [304] N. M. Valenzuela, J. T. McNamara, and E. F. Reed, "Antibody-mediated graft injury: complement-dependent and complement-independent mechanisms.," *Curr. Opin. Organ Transplant.*, vol. 19, no. 1, pp. 33–40, Feb. 2014.
- [305] Y.-P. Jin *et al.*, "Anti-HLA class I antibody-mediated activation of the PI3K/Akt signaling pathway and induction of Bcl-2 and Bcl-xL expression in endothelial cells.," *Hum. Immunol.*, vol. 65, no. 4, pp. 291–302, Apr. 2004.
- [306] D. Paus, T. G. Phan, T. D. Chan, S. Gardam, A. Basten, and R. Brink, "Antigen recognition strength regulates the choice between extrafollicular plasma cell and germinal center B cell differentiation.," *J. Exp. Med.*, vol. 203, no. 4, pp. 1081–91, Apr. 2006.
- [307] R. Di Niro *et al.*, "Salmonella Infection Drives Promiscuous B Cell Activation Followed by Extrafollicular Affinity Maturation.," *Immunity*, vol. 43, no. 1, pp. 120–31, Jul. 2015.
- [308] S. a Camacho, M. H. Kosco-Vilbois, and C. Berek, "The dynamic structure of the germinal center," *Immunol Today*, vol. 19, no. 11, pp. 511–514, 1998.
- [309] J. S. Moreira and J. Faro, "Modelling Two Possible Mechanisms for the Regulation of the Germinal Center Dynamics," *J. Immunol.*, vol. 177, no. 6, pp. 3705–3710, 2006.

- [310] K. G. C. Smith, A. Light, G. J. V. Nossal, and D. M. Tarlinton, "The extent of affinity maturation differs between the memory and antibody-forming cell compartments in the primary immune response," *EMBO J.*, vol. 16, no. 11, pp. 2996–3006, 1997.
- [311] D. M. Sze, K. M. Toellner, C. García de Vinuesa, D. R. Taylor, and I. C. MacLennan, "Intrinsic constraint on plasmablast growth and extrinsic limits of plasma cell survival," *J. Exp. Med.*, vol. 192, no. 6, pp. 813–821, 2000.
- [312] E. J. Kim *et al.*, "Costimulation Blockade Alters Germinal Center Responses and Prevents Antibody-Mediated Rejection," *Am. J. Transplant.*, vol. 14, no. 1, pp. 59–69, Jan. 2014.
- [313] D. Jane-Wit *et al.*, "Alloantibody and complement promote T cell-mediated cardiac allograft vasculopathy through noncanonical nuclear factor- $\kappa$ B signaling in endothelial Cells," *Circulation*, vol. 128, no. 23, pp. 2504–2516, 2013.
- [314] F. M. A. Naemi, V. Carter, J. A. Kirby, and S. Ali, "Anti-donor HLA class I antibodies: Pathways to endothelial cell activation and cell-mediated allograft rejection," *Transplantation*, vol. 96, no. 3, pp. 258–266, 2013.
- [315] N. M. Valenzuela and E. F. Reed, "The link between major histocompatibility complex antibodies and cell proliferation," *Transplantation Reviews*, vol. 25, no. 4, pp. 154–166, 2011.
- [316] M. J. Everly *et al.*, "Reducing De Novo Donor-Specific Antibody Levels during Acute Rejection Diminishes Renal Allograft Loss," *Am. J. Transplant.*, vol. 9, no. 5, pp. 1063–1071, May 2009.
- [317] S. Preite *et al.*, "Somatic mutations and affinity maturation are impaired by excessive numbers of T follicular helper cells and restored by Treg cells or memory T cells.," *Eur. J. Immunol.*, vol. 45, no. 11, pp. 3010–21, Nov. 2015.
- [318] A. Pratama and C. G. Vinuesa, "Control of TFH cell numbers: why and how?," *Immunol. Cell Biol.*, vol. 92, no. 1, pp. 40–48, Jan. 2014.
- [319] R. Brink, T. G. Phan, D. Paus, and T. D. Chan, "Visualizing the effects of antigen affinity on T-dependent B-cell differentiation," *Immunol. Cell Biol.*, vol. 86, no. 1, pp. 31–39,

Nov. 2007.

- [320] S. B. Hartley *et al.*, "Elimination of self-reactive B lymphocytes proceeds in two stages: arrested development and cell death.," *Cell*, vol. 72, no. 3, pp. 325–35, Feb. 1993.
- [321] D. Nemazee and K. A. Hogquist, "Antigen receptor selection by editing or downregulation of V(D)J recombination.," *Curr. Opin. Immunol.*, vol. 15, no. 2, pp. 182–9, Apr. 2003.
- [322] R. Brink *et al.*, "The SWHEL System for High-Resolution Analysis of In Vivo Antigen-Specific T-Dependent B Cell Responses," in *Methods in molecular biology (Clifton, N.J.)*, vol. 1291, 2015, pp. 103–123.
- [323] I. S. Moreira, P. A. Fernandes, and M. J. Ramos, "Hot spot computational identification: Application to the complex formed between the hen egg white lysozyme (HEL) and the antibody HyHEL-10," *Int. J. Quantum Chem.*, vol. 107, no. 2, pp. 299–310, 2007.
- [324] S. J. Smith-Gill, C. Mainhart, T. B. Lavoie, R. J. Feldmann, W. Drohan, and B. R. Brooks, "A three-dimensional model of an anti-lysozyme antibody," *J. Mol. Biol.*, vol. 194, no. 4, pp. 713–724, 1987.
- [325] S. J. Smith-Gill, A. C. Wilson, M. Potter, E. M. Prager, R. J. Feldmann, and C. R. Mainhart, "Mapping the Antigenic Epitope for a Monoclonal Antibody Against Lysozyme," *J. Immunol.*, vol. 128, no. 1, p. 314, 1982.
- [326] G. Gammon *et al.*, "The choice of T-cell epitopes utilized on a protein antigen depends on multiple factors distant from, as well as at the determinant site.," *Immunol. Rev.*, vol. 98, no. 98, pp. 53–73, 1987.
- [327] T. Okada *et al.*, "Antigen-engaged B cells undergo chemotaxis toward the T zone and form motile conjugates with helper T cells," *PLoS Biol.*, vol. 3, no. 6, pp. 1047–1061, 2005.
- [328] J. M. Smits, H. C. van Houwelingen, J. De Meester, G. G. Persijn, and F. H. Claas, "Analysis of the renal transplant waiting list: application of a parametric competing risk method.," *Transplantation*, vol. 66, no. 9, pp. 1146–53, Nov. 1998.

- [329] H. M. Gebel and R. A. Bray, "HLA Antibody Detection With Solid Phase Assays: Great Expectations or Expectations Too Great?," *Am. J. Transplant.*, vol. 14, no. 9, pp. 1964–1975, Sep. 2014.
- [330] M. Banasik *et al.*, "Long-term follow-up of non-HLA and anti-HLA antibodies: Incidence and importance in renal transplantation," in *Transplantation Proceedings*, 2013, vol. 45, no. 4, pp. 1462–1465.
- [331] H. Cardinal, M. Dieudé, and M.-J. Hébert, "The Emerging Importance of Non-HLA Autoantibodies in Kidney Transplant Complications," *J. Am. Soc. Nephrol.*, vol. 28, no. 2, pp. 400–406, 2017.
- [332] M. Banasik *et al.*, "The influence of non-HLA antibodies directed against angiotensin II type 1 receptor (AT1R) on early renal transplant outcomes.," *Transpl. Int.*, vol. 27, no. 10, pp. 1029–38, 2014.
- [333] R. J. Lynch, I. A. Silva, B. J. Chen, J. D. Punch, M. Cascalho, and J. L. Platt, "Cryptic B cell response to renal transplantation," *Am. J. Transplant.*, vol. 13, no. 7, pp. 1713–1723, 2013.
- [334] K. W. Snape, R. Tjian, C. C. Blake, and D. E. Koshland, "Crystallographic study of the interaction of urea with lysozyme.," *Nature*, vol. 250, no. 464, pp. 295–8, Jul. 1974.
- [335] T. G. Phan *et al.*, "High affinity germinal center B cells are actively selected into the plasma cell compartment," *J. Exp. Med.*, vol. 203, no. 11, pp. 2419–2424, 2006.
- [336] T. D. Chan *et al.*, "Elimination of Germinal-Center-Derived Self-Reactive B Cells Is Governed by the Location and Concentration of Self-Antigen," *Immunity*, vol. 37, no. 5, pp. 893–904, Nov. 2012.
- [337] T. Germann *et al.*, "Interleukin-12 profoundly up-regulates the synthesis of antigen-specific complement-fixing IgG2a, IgG2b and IgG3 antibody subclasses *in vivo*," *Eur. J. Immunol.*, vol. 25, no. 3, pp. 823–829, Mar. 1995.
- [338] M. McHeyzer-Williams, S. Okitsu, N. Wang, and L. McHeyzer-Williams, "Molecular programming of B cell memory," *Nat. Rev. Immunol.*, vol. 12, no. 1, p. 24, Dec. 2011.

- [339] Y. S. Jang, J. A. Mikszta, and B. S. Kim, "T cell epitope recognition involved in the low-responsiveness to a region of hen egg lysozyme (46-61) in C57BL/6 mice," *Mol. Immunol.*, vol. 31, no. 11, pp. 803–812, 1994.
- [340] S. H. Chang *et al.*, "Modification of the Inhibitory Amino Acid for Epitope Peptide Binding onto Major Histocompatibility Complex Class II Molecules Enhances Immunogenicity of the Antigen," *Scand. J. Immunol.*, vol. 59, no. 2, pp. 123–132, 2004.
- [341] S. Uehara, C. M. Chase, L. D. Cornell, J. C. Madsen, P. S. Russell, and R. B. Colvin, "Chronic cardiac transplant arteriopathy in mice: Relationship of alloantibody, C4d deposition and neointimal fibrosis," *Am. J. Transplant.*, vol. 7, no. 1, pp. 57–65, 2007.
- [342] A. R. Tambur *et al.*, "Assessing Antibody Strength: Comparison of MFI, C1q, and Titer Information," *Am. J. Transplant.*, vol. 15, no. 9, pp. 2421–2430, 2015.
- [343] E. K. Ho *et al.*, "Pre- and posttransplantation allosensitization in heart allograft recipients: Major impact of de novo alloantibody production on allograft survival," *Hum. Immunol.*, vol. 72, no. 1, pp. 5–10, 2011.
- [344] A. B. and R. B. Tyani D. Chan, Dominique Gatto, Katherine Wood, Tahra Camidge, "Antigen Affinity Controls Rapid Antigen Affinity Controls Rapid T-Dependent Antibody Production by Driving the Expansion Rather than the Differentiation or Extrafollicular Migration of Early Plasmablasts," vol. 183, pp. 3139–3149, 2009.
- [345] T. G. Phan, S. Gardam, A. Basten, and R. Brink, "Altered migration, recruitment, and somatic hypermutation in the early response of marginal zone B cells to T cell-dependent antigen," *J. Immunol.*, vol. 174, no. 8, pp. 4567–78, Apr. 2005.
- [346] N. M. Valenzuela and E. F. Reed, "Antibodies in transplantation: The effects of HLA and non-HLA antibody binding and mechanisms of injury," *Methods Mol. Biol.*, vol. 1034, pp. 41–70, 2013.
- [347] A. M. Duijvestijn, J. G. Derhaag, and P. J. C. Van Breda Vriesman, "Complement activation by anti-endothelial cell antibodies in MHC-mismatched and MHC-matched heart allograft rejection: Anti-MHC-, but not anti non-MHC alloantibodies are effective in complement activation," *Transpl. Int.*, vol. 13, no. 5, pp. 363–371, 2000.

- [348] J. D. Smith *et al.*, "A reevaluation of the role of IgM Non-HLA antibodies in cardiac transplantation," *Transplantation*, vol. 87, no. 6, pp. 864–871, 2009.
- [349] M. K. L. MacLeod, A. David, A. S. McKee, F. Crawford, J. W. Kappler, and P. Murrack, "Memory CD4 T cells that express CXCR5 provide accelerated help to B cells.," *J. Immunol.*, vol. 186, no. 5, pp. 2889–96, Mar. 2011.
- [350] G. Benichou, B. Gonzalez, J. Marino, K. Ayasoufi, and A. Valujskikh, "Role of Memory T Cells in Allograft Rejection and Tolerance.," *Front. Immunol.*, vol. 8, p. 170, 2017.
- [351] J. K. Whitmire *et al.*, "Requirement of B cells for generating CD4+ T cell memory.," *J Immunol*, vol. 182, no. 4, pp. 1868–1876, 2009.
- [352] C. E. Hall *et al.*, "Sequence homology between HLA-bound cytomegalovirus and human peptides: A potential trigger for alloreactivity," *PLoS One*, vol. 12, no. 8, p. e0178763, Aug. 2017.
- [353] A. S. and C. N. Sarkar A, Chatterjee A, "Characterization of Molecular Mimicry Between UL18 Glycoprotein of Human Cytomegalovirus [HCMV] and Class-I MHC Molecule through Pattern-based Analysis: An In-silico Approach," *J. Heal. Med. informatics*, vol. 7, no. 3, p. 230, 2016.
- [354] M. Rabant #1, V. Gorbacheva, R. Fan, H. Yu, and A. Valujskikh, "CD40-independent help by memory CD4 T cells induces pathogenic alloantibody but does not lead to long-lasting humoral immunity."
- [355] H. P. Roost *et al.*, "Early high-affinity neutralizing anti-viral IgG responses without further overall improvements of affinity.," *Proc. Natl. Acad. Sci. U. S. A.*, vol. 92, no. 5, pp. 1257–61, Feb. 1995.
- [356] M. A. Newman, C. R. Mainhart, C. P. Mallett, T. B. Lavoie, and S. J. Smith-Gill, "Patterns of antibody specificity during the BALB/c immune response to hen eggwhite lysozyme.," *J. Immunol.*, vol. 149, no. 10, pp. 3260–72, Nov. 1992.
- [357] C. L. Swanson, T. J. Wilson, P. Strauch, M. Colonna, R. Pelanda, and R. M. Torres, "Type I IFN enhances follicular B cell contribution to the T cell-independent antibody response.," *J. Exp. Med.*, vol. 207, no. 7, pp. 1485–500, Jul. 2010.

- [358] L. D. Erickson *et al.*, "Short-circuiting long-lived humoral immunity by the heightened engagement of CD40," *J. Clin. Invest.*, vol. 109, no. 5, pp. 613–620, Mar. 2002.
- [359] D. Baumjohann *et al.*, "Persistent Antigen and Germinal Center B Cells Sustain T Follicular Helper Cell Responses and Phenotype," *Immunity*, vol. 38, pp. 596–605, 2013.
- [360] T. V. Brennan *et al.*, "A New T-Cell Receptor Transgenic Model of the CD4+ Direct Pathway: Level of Priming Determines Acute Versus Chronic Rejection," *Transplantation*, vol. 85, no. 2, pp. 247–255, Jan. 2008.
- [361] Q. Zhang, Y. Chen, R. L. Fairchild, P. S. Heeger, and A. Valujskikh, "Lymphoid sequestration of alloreactive memory CD4 T cells promotes cardiac allograft survival.," *J. Immunol. (Baltimore, Md. 1950)*, vol. 176, no. 2, pp. 770–777, 2006.
- [362] Y. Chen, P. S. Heeger, and A. Valujskikh, "In vivo helper functions of alloreactive memory CD4+ T cells remain intact despite donor-specific transfusion and anti-CD40 ligand therapy," *J Immunol*, vol. 172, no. 9, pp. 5456–5466, 2004.
- [363] T. B. Kepler and A. S. Perelson, "Cyclic re-entry of germinal center B cells and the efficiency of affinity maturation," *Immunol. Today*, vol. 14, no. 8, pp. 412–415, 1993.
- [364] N. L. Reinsmoen *et al.*, "Anti-angiotensin type 1 receptor antibodies associated with antibody mediated rejection in donor HLA antibody negative patients," *Transplantation*, vol. 90, no. 12, pp. 1473–1477, 2010.
- [365] Q. Zhang and E. F. Reed, "The importance of non-HLA antibodies in transplantation," *Nature Reviews Nephrology*, vol. 12, no. 8, pp. 484–495, 2016.
- [366] Q. Zhang and E. F. Reed, "Non-MHC antigenic targets of the humoral immune response in transplantation," *Current Opinion in Immunology*, vol. 22, no. 5, pp. 682–688, 2010.
- [367] S. G. Tangye, C. S. Ma, R. Brink, and E. K. Deenick, "The good, the bad and the ugly - TFH cells in human health and disease.," *Nat. Rev. Immunol.*, vol. 13, no. 6, pp. 412–26, 2013.

- [368] T. Do, F. Ho, B. Heidecker, K. Witte, L. Chang, and L. Lerner, "A rapid method for determining dynamic binding capacity of resins for the purification of proteins," *Protein Expr. Purif.*, vol. 60, no. 2, pp. 147–150, 2008.